FSTC-HT-23-766-70

ARMY MATERIEL COMMAND

U.S. ARMY
FOREIGN SCIENCE AND TECHNOLOGY CENTER

STARTING OF AIRCRAFT GAS TURBINE ENGINES

By

M. A. ALABIN
B. M. KATS
YU. A. LITVINOV

SUBJECT COUNTRY: RUSSIA

This document is a rendition of the original foreign text without any analytical or editorial comment.

Approved for public release; distribution unlimited.

UNCLASSIFIED
Security Classification

DOCUMENT CONTROL DATA - R & D

(Security classification of title, body of abstract and indexing annotation must be entered when the overall report is classified)

1. ORIGINATING ACTIVITY (Corporate author) Foreign Science and Technology Center US Army Materiel Command Department of the Army	2a. REPORT SECURITY CLASSIFICATION Unclassified 2b. GROUP

3. REPORT TITLE

Starting of Aircraft Gas Turbine Engines

4. DESCRIPTIVE NOTES (Type of report and inclusive dates)

Translation

5. AUTHOR(S) (First name, middle initial, last name)

M. A. Alabin, B. M. Kats, Yu. A. Litvinov

6. REPORT DATE 12 January 1972	7a. TOTAL NO. OF PAGES 227	7b. NO. OF REFS N/A
8a. CONTRACT OR GRANT NO. b. PROJECT NO. c. T/02301 2301 d. Requester Avn Systems Cmd	9a. ORIGINATOR'S REPORT NUMBER(S) FSTC-HT-23- 766-70 9b. OTHER REPORT NO(S) (Any other numbers that may be assigned this report) K-0571	

10. DISTRIBUTION STATEMENT

Approved for public release; distribution unlimited.

11. SUPPLEMENTARY NOTES	12. SPONSORING MILITARY ACTIVITY US Army Foreign Science and Technology Center

13. ABSTRACT

Examined in this book is the theory of starting aviation gas turbine engines on the ground and in flight. This discussion goes into considerably greater detail than previously published literature on aviation engines. The design principles and operating features of individual components of the starter system and engine accessories during start up are examined, the methods of calculating the starting characteristics of various types of engines on the ground and in flight are set forth and the physical essence of starting processes is explained. The influence of various factors on engine starting reliability is examined in detail.

Chief attention is devoted to investigation of the starting processes of single rotor turbojet engines. Certain features of starting of turboprop and turbojet engines of the two-rotor design are also discussed.

Recommendations on the choice of starter system type for aircraft engines are made on the basis of analyses of power balance of gas turbine engine starting, possible causes of unreliable starting and efficiency of the various starter systems.

Methods of calculating engine parameters in the autorotation and low rpm regimes and engine starting reliability limits in flight are given, which can be used in the testing and operation of gas turbine engines.

DD FORM 1 NOV 68 1473 REPLACES DD FORM 1473, 1 JAN 64, WHICH IS OBSOLETE FOR ARMY USE.

UNCLASSIFIED
Security Classification

14. KEY WORDS	LINK A		LINK B		LINK C	
	ROLE	WT	ROLE	WT	ROLE	WT
Gas turbine engine Aircraft engine Gas turbine starter Engine starter system Turbojet engine Turboprop engine Turbine rotor Turbine design Country Code: Russia Subject Code: 01, 21						

TECHNICAL TRANSLATION

FSTC-HT-23- 766-70

ENGLISH TITLE: Starting of Aircraft Gas Turbine Engines

FOREIGN TITLE: Zaoysj Aviatsionnykh Gazoturbinnykh Dvigatelei

AUTHOR: M. A. Alabin, B. M. Kats, Yu. A. Litvinov

SOURCE: Zapusk Aviatsionnykh Gazoturbinnykh Dvigateley, Russian, "Mashinostroyeniye" Publishing House, 1968, 227 pages

Translated for FSTC by ACSI

NOTICE

Details of illustrations in this document may be better studied on microfiche

STARTING OF AIRCRAFT GAS TURBINE ENGINES

[Book by M. A. Alabin, B. M. Kats, Yu. A. Litvinov; Moscow, Zapusk Aviatsionnykh Gazoturbinnykh Dvigateley, Russian, "Mashinostroyeniye" Publishing House, 1968, 227 pages]

UDC 629.7.036-572/-576.001

ANNOTATION

Examined in this book is the theory of starting aviation gas turbine engines on the ground and in flight. This discussion goes into considerably greater detail than previously published literature on aviation engines. The design principles and operating features of individual components of the starter system and engine accessories during start-up are examined, the methods of calculating the starting characteristics of various types of engines on the ground and in flight are set forth and the physical essence of starting processes is explained. The influence of various factors on engine starting reliability is examined in detail.

Chief attention is devoted to investigation of the starting processes of single-rotor turbojet engines. Certain features of starting of turboprop and turbojet engines of the two-rotor design are also discussed.

Recommendations on the choice of starter system type for aircraft engines are made on the basis of analyses of power balance of gas turbine engine starting, possible causes of unreliable starting and efficiency of the various starter systems.

Methods of calculating engine parameters in the autorotation and low rpm regimes and engine starting reliability limits in flight are given, which can be used in the testing and operation of gas turbine engines.

The book is intended for engineers and technicians in the aviation industry and civil and military aviation. It may also be of use to teachers and students in related aviation courses.

PREFACE

The rapid development of aviation gas turbine engines (GTE) and their extensive adoption necessitate a special study of the characteristics of the engine starting process and improvement of starting equipment. In aviation these characteristics reflect the preparedness of aircraft for flight, and the operation of the components of the starting system has a direct influence on flight safety, engine reliability and service life.

The purpose of this book is to assist the large community of specialists of the aviation industry, military and civil aviation in the design, testing and operation of engine starter systems.

The book consists of three parts.

Part One contains basic information concerning aviation GTE starter systems, analysis of the starting process and classification of starter systems. Examined in the corresponding sections of Part One are the principles of design and operation of the main components of the starter system -- of various types of starters (rotor accelerator units), components of the starting control system, starter fuel system, etc.

Part Two is devoted to the processes of starting GTE on the ground, analytical characteristics of the moments acting on the engine rotor, dynamic equilibrium of rotor during starting process. The influence of various design and operation factors on starting reliability is analyzed and nomograms are included for calculation of the basic parameters of the starting process and starter systems.

Part Three deals with the development of theory and analysis of the physical essence of in-flight starting processes and includes an evaluation of the effect of various factors on GTE starting reliability.

In-flight engine starting processes are examined and their parameters in the low rpm state are analyzed in application to subsonic speeds. Engine parameters in the autorotation mode and the dependence of the mode of autorotation on various factors are analyzed for velocities $M \leq 3$. Many of the graphs are plotted in relative coordinates, and the values of the parameters in the low rpm state are used as 100%.

The diagrams of the starter systems and designs of rotor preaccelerator units, presented in Part One of this book, were borrowed from Soviet and foreign sources.

Some of the sections contain materials generously given the authors by candidate of technical sciences N. F. Dubovkin.

All units of measurement used in this book are given in the MKS [meter-kilogram-second] and MKGSS [Meter-kilogram force-second] systems. The following table may be used as an aid to conversion to the units of the international system IS:

Parameter	Symbol of units of measurement in systems		Ratio of units of measurement
	MKGSS	IS	
Force	kg	N	1 kg = 9.81 N
Mass	$kg \cdot sec^2/m$	kg	1 $kg \cdot sec^2/m$ = 9.81 kg
Pressure	kg/m^2	N/m^2	1 kg/m^2 = 9.81 N/m^2
Torque (moment of force)	kg·m	N·m	1 kg·m = 9.81 N·m
Effort, energy	kg·m	J	1 kg·m = 9.81 J
Moment of inertia (dynamic)	$kg \cdot m \cdot sec^2$	$kg \cdot m^2$	1 $kg \cdot m \cdot sec^2$ = 9.81 $kg \cdot m^2$
Power	kg·m/sec	W	1 kg·m/sec = 9.81 W 1 hp = 735.5 W

The authors express their sincere gratitude to the reviewer -- doctor of technical sciences B. A. Cherkasov, who offered many valuable recommendations for improvement of the manuscript. They will also acknowledge the readers for all critical comments and requests, which should be addressed to "Mashinostroyeniye" Publishing House (Moscow, K-51, Petrovka, 24).

PRINCIPAL SYMBOLS

G_a -- air flow rate through compressor in kg/sec;

G_g -- gas flow rate through turbine in kg/sec;

G_f -- fuel flow rate through engine in kg/hr;

p^* -- total pressure of working medium through engine duct in kg/cm^2;
p - static pressure of working medium through engine duct in kg/cm^2;
π_k^* -- air compression ratio in compressor;

π_t^* -- air compression ratio in turbine;

K_s -- compressor stability factor;

K_{G_f} -- compressor stability factor in terms of fuel flow rate;

η_k^* -- compressor efficiency in terms of stagnation flow parameters;

η_t^* -- turbine efficiency in terms of stagnation flow parameters;

T -- absolute temperature of working medium in engine duct in °K;
N -- power in hp;
M -- torque in kg·m;
J_0 -- polar moment of inertia in $kg \cdot m \cdot sec^2$;

ΔN -- surplus power in hp;
n -- rpm
n_1 -- rpm of engine rotor at ignition of main fuel;

n_f -- final motoring rpm of engine rotor by starter;

n_c -- engine rotor rpm at which the turbine moment is equal to the engine resistance moment;
n_2 -- engine rotor rpm at moment of starter disengagement;

$n_{1.p}$ -- engine rotor rpm in low power state;

H_{ad} -- adiabatic heat drop in kcal/kg;

J -- enthalpy of working medium in kcal/kg;
L_{ad} -- adiabatic work of 1 kg of working medium in kg·m/kg;

R -- gas constant in kg·m/kg·deg;

H_u -- calorific value of fuel in kcal/kg;

c_p -- heat capacity of working medium at constant pressure in kcal/kg·deg;

c_V -- heat capacity of working medium at constant volume in kcal/kg·deg;

C -- absolute velocity of working medium in m/sec;
W -- relative velocity of working medium in m/sec;
V -- flight velocity in km/hour;
F -- cross section area in m^2;
k -- adiabatic index;
m -- mass in $kg \cdot sec^2/m$;
g -- acceleration of gravity in m/sec^2;
M -- Mach number of flight;
H -- flight altitude in meters;
τ_k^* -- ratio of stagnation temperatures of air behind and in front of the compressor;
$\tau_{k.c}^*$ -- ratio of stagnation temperatures at the end of the combustion chamber and at compressor exhaust;
τ_t^* -- ratio of stagnation temperatures in front of and behind engine turbine;
$\tau_{s.s}$ -- duration of starter system operation in sec;
τ_{st} -- starting time (time required for going into the low rpm state) in sec;
σ -- pressure recovery coefficient;

Indices

re -- parameters reduced to MSA [International Standard Atmosphere]
s -- parameters in steady state starter operation modes;
n -- parameters in nonsteady starter operation modes;
lim -- compressor parameters at stability limit;
k -- parameters at compressor exhaust;
g -- parameters at turbine intake;
t -- parameters at turbine exhaust;
c -- parameters at exit of reactive nozzle;
by -- parameters through engine duct with bypass of air from compressor;
a -- axial component of velocity;
ins -- instrument values of parameter;
s.s -- parameters pertaining to starter system.

PART ONE. STARTER SYSTEMS

CHAPTER 1. GENERAL CONCEPTS OF THE STARTING PROCESS

In order to use any engine for its main purpose it is essential to operate it in the state of minimal operating stability. The process of reaching this state, called the low rpm state, also represents engine start-up.

The starting of an aviation gas turbine engine is the unsteady process of accelerating the engine rotor from the motionless state on the ground or from the autorotation state in flight to the low rpm state.

In order to start an engine it is necessary that the working medium be brought up to the state in which the working process can proceed stably. The working process of a gas turbine engine is characterized by continuous combustion of the fuel-air mixture in the combustion chamber.

Stable combustion of the fuel-air mixture is possible only with the continuous entry of the required amount of air into the combustion chamber under some excess pressure. The air is forced into the combustion chamber by a compressor. The power required for rotating the compressor is determined by the equation

$$N_к = \frac{102{,}5 G_a T^*_{in}}{75\eta^*_к}(\pi_к^{*0.286} - 1), \qquad (1.1)$$

where G_a is the amount of air passing through the compressor in kg/sec;

T^*_{in} is the temperature of the air at compressor intake in °K;

π^*_k is compression of air in the compressor;

η^*_k is compressor efficiency.

As seen in equation (1.1), the power required for compressor operation depends on the flow rate of air through the engine, the degree of compression of the air in the compressor and efficiency. Naturally, the greater the flow rate of air through the engine, degree of compression of the air and the lower the efficiency of the compressor, the more power will be required for compressor operation.

The power required for operating the compressor of a specific type of engine is determined by the above-stated parameters under starting conditions. The typical change of air compression in the compressor, air flow rate through the engine and power used for rotating the compressor in the starting regimes is illustrated in Figure 1 in terms of rpm. As seen, progressively more power is required for rotating the compressor in the starting regimes as the rpm increases.

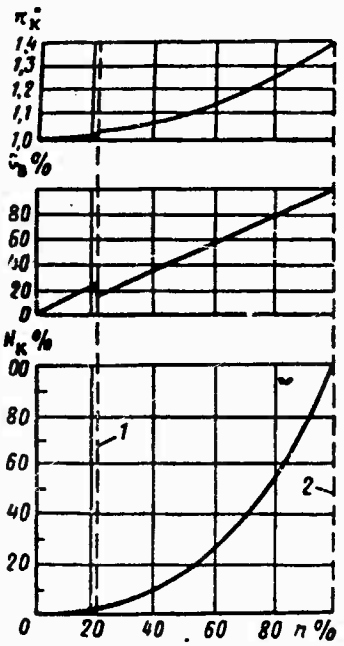

Figure 1. Pressure increase π_k^*, air flow rate G_a through engine and power N_k required for driving compressor as functions of engine rpm in starting regimes:
1 -- moment of fuel ignition;
2 -- low rpm state.

Continuous acceleration of the engine rotor during start-up is possible only when the power of the starter system exceeds the power required for rotating the compressor and overcoming the various types of forces of resistance in the engine. This surplus power provides the required acceleration of the rotating parts of the engine. Acceleration of the engine rotor during the starting process and the time required for attaining the low rpm state depend on the stated power surplus. The amount of surplus power of the starter system should enable the engine to reach the low rpm condition within the time stated by the technical specifications. The amount of power used for accelerating the engine rotor is calculated using the equation

$$N_j = \frac{\pi^2}{900 \cdot 75} J_0 \frac{dn}{d\tau} n, \qquad (1.2)$$

where J_0 is the moment of inertia of rotating parts of the engine in $kg \cdot m \cdot sec^2$;
n is the rpm;
$dn/d\tau$ is rotor acceleration in rpm/sec.

As seen in equation (1.2), the greater the moment of inertia of the rotating parts and the higher the acceleration of the rotor, the greater will be the power required for accelerating the rotor at the same rpm.

Thus, in order to start an engine it is necessary to deliver to its rotor the power required for overcoming the forces of resistance and for accelerating the rotor.

A turbine is used as the power source of a gas turbine engine. The

power developed by a turbine, as we know, is determined by the equation

$$N_t = \frac{117{,}5 G_g T_g^*}{75}\left(1 - \frac{1}{\pi_t^{*0{,}25}}\right)\eta_t^*, \qquad (1.3)$$

where G_g is flow rate of gases through the turbine in kg/sec;

T_g^* is the temperature of the gases in front of the turbine in °K;

π_t^* is the expansion ratio of the gases in the turbine;

η_t^* is turbine efficiency.

The power developed by a turbine depends largely on the temperature of the gases in front of the turbine and the pressure drop acting on the turbine. Figure 2 shows the typical change of temperature of the gases in front of the turbine, expansion ratio of the gases in the turbine and turbine power in terms of rpm in the starting regimes. At the initial starting moment an engine's turbine, as we see, not only produces no power but, on the contrary, requires power in order to rotate. Moreover, even after the turbine goes into active operation (starting in Figure 3 at rpm n_1) power has to be delivered to the engine rotor to ensure the required acceleration until the rpm reaches at least n_2 (Figure 3).

At rpm n_2 the state of autorotation of the rotor of a started engine is established when its turbine develops power sufficient for its own rotation as well as for the rotation of the compressor, engine accessories and for overcoming mechanical losses in the engine.

In order to accelerate the engine rotor to an rpm of at least n_2, as shown in Figure 3, it must be supplied power from a constant power source. This power is provided by different types of starter systems. The moment of disengagement of a starter system after start-up is established so that after shutdown of the preaccelerator unit the turbine alone will be able to run the engine rotor up to the low rpm state within the specified time.

Reliable engine starting is ensured under all operating conditions by the proper combination of starter system, engine design and design of starting systems and automatic equipment. An engine should be started on the first try with the power sources provided without any extra operations after placing the engine control lever in the low rpm position and engaging the starter system.

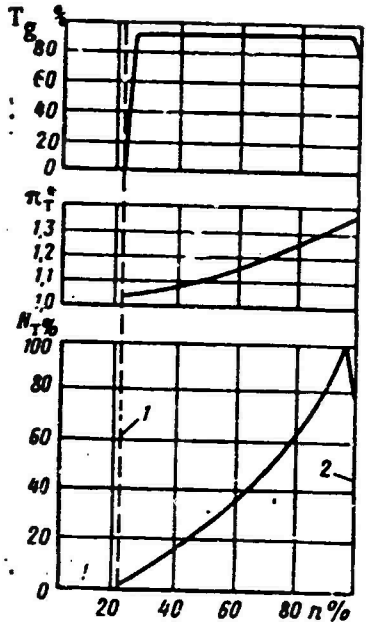

Figure 2. Gas temperature T_g in front of turbine, gas expansion ratio π_t^* in turbine and power N_t developed by turbine in starting regimes as functions of engine rpm: 1 -- moment of fuel mixture ignition; 2 -- low rpm state.

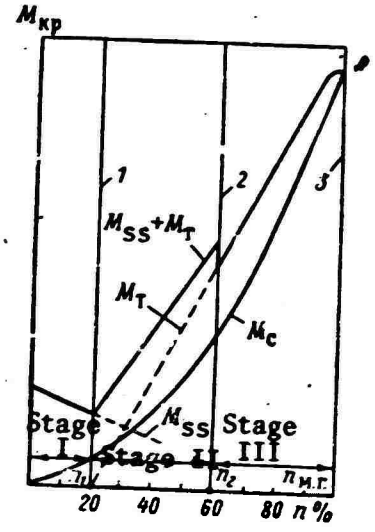

Figure 3. Engine starting stages: M_{ss} -- moment of starter system; M_t -- moment of turbine; M_c -- moment of resistance; 1 -- moment of fuel mixture ignition; 2 -- moment of disengagement of starter system; 3 -- low rpm state.

CHAPTER 2. CLASSIFICATION AND LAYOUT PRINCIPLES OF STARTER SYSTEMS

A special array of units and accessories, installed on the engine and on the aircraft, is required for reliable engine starting. The compliment of such units and accessories together with various types of connective communications comprises the starter system.

The starter system includes assemblies and accessories that ensure preliminary acceleration of the engine rotor; systems for fuel supply and ignition of fuel mixture in combustion chamber; equipment ensuring stable engine operation during starting process; devices that ensure the correct sequence and automation of starter system operation.

The type of starter system is governed by the type of engine rotor preaccelerator unit and type of power source. The following are used most often as preaccelerators: electric starters, turbostarters using the same fuel as the aircraft engines, turbostarters operating on single component liquid fuel, air turbostarters, turbostarters working on solid fuel.

The power sources can be either on-board, installed aboard the aircraft itself, or airfield (ground) power equipment.

The weight and dimensions of the starter system of a given engine depend on the type of starter system selected and the time period within which the engine must be placed in the low rpm state.

Starter systems operating on physically stored energy (electricity or compressed air) are used for starting gas turbine engines with a small rotor inertia and comparatively long time for reaching the low rpm state. Starter systems operating on the heat energy produced by the combustion or decomposition of various types of fuel are used for starting engines with a limited time for attaining the low rpm state.

§1. Electric Starter Systems

Electric starter systems are used extensively for starting various turbojet and turboprop engines because they are simple to control, their starting operations are easily automated, they are reliable, simple and easy to service.

The need to reduce engine starting time necessitates an increase in starter power. The electric starter systems are characterized by substantial weight increase when their power is increased. Therefore these systems are least suitable for fast independent starting of aircraft engines.

Direct current electric starters are used at the present time (Figure 4). The operating principle of such a system is determined by the principle of control of the rate of rotation of the electrostarter during the starting process. Such regulation is essential for ensuring engine rotor acceleration by the starter to rpm n_2 during the starting process.

The rate of rotation of the rotor of the electrostarter is

$$n = \frac{U - I_a(R_a + R_{ad})}{C\Phi}, \qquad (2.1)$$

where U is the voltage on the terminals of the motor;

I_a is armature current;

R_a is armature resistance;

R_{ad} is additional resistance in the armature circuit;

Φ is excitation current;

C is a constant coefficient.

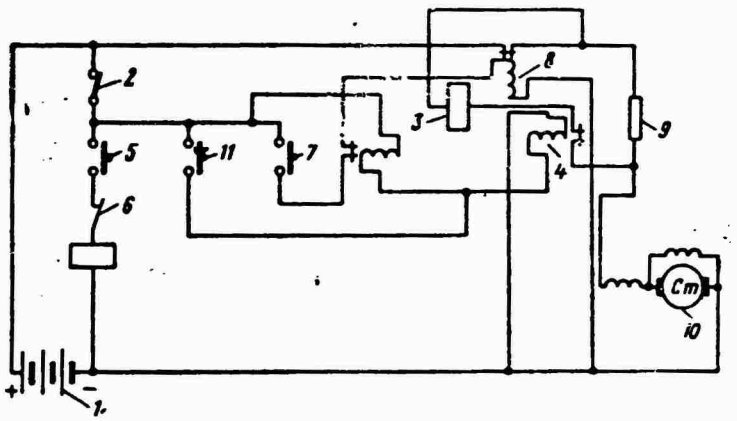

Figure 4. Schematic diagram of electric starter system: 1 -- power source (storage battery); 2 -- switch; 3 -- relay; 4 and 8 -- contactors; 5 -- starter button; 6 -- time relay; 7 -- time relay contact; 9 -- starter resistance; 10 -- starter; 11 -- contact.

As seen in equation (2.1), there are three ways to regulate the rpm of DC motors: 1) add extra resistance to the armature circuit; 2) change the excitation current; 3) change the voltage of the system. The last two of these three control methods are used for high-power electric motors.

Control of the rpm of an electric motor by changing the excitation current is usually employed for parallel excitation motors. When additional resistance is added to the excitation winding the current in it and, consequently the magnetic flux decrease, causing the rpm of the armature of the starter to increase.

Starter systems can be 24-volt with parallel connection of the power sources for the entire time of operation of the systems and staged -- with switching of the power sources during the starting process from parallel connection to series. In the latter case high voltage is applied to the terminals. The step-by-step on switching of electric power sources during engine start-up ensures more efficient utilization of the capacity of the power sources.

The moment of switching of the power sources from parallel connection to series connection is selected with consideration of the character of change of the current load of the batteries during acceleration of the engine and moment of establishment of active engine turbine operation. The switching of the batteries to series connection before the current required by the electric starter decreases to some specific value reduces the resistance in the circuit and consequently adversely affects starting conditions. The time of switching of the batteries is established experimentally for each specific engine.

In the staged type of power source one-half voltage is applied to the electric starter during the period of parallel connection of the batteries, and only after the switchover is accomplished is full voltage applied. Consequently the storage batteries discharge more uniformly during engine start-up than during start-up with a system without battery switching. During starting with switching of the power sources accident situations can arise due to short circuiting of the batteries when improperly connected and during attempts to start an engine with one battery.

High source voltage in electric starter systems increases the power and efficiency of a starter system. This increases the final rpm of the engine rotor by the electric starter and its surplus moments, improves the quality and increases the reliability of engine starting. These starter systems are used extensively for aircraft.

After completing all preparatory operations of ordinary preflight preparation the airfield or on-board power source is connected into the aircraft circuitry for starting.

When switch 2 (Figure 4) is closed power is supplied to the control circuit. Current from storage battery 1 flows through one of the windings of relay 3 and contactor 4. In series connection of these windings only the contacts of relay 3 are closed, and the contacts of contactor 4 remain open, since there is a weak current in its winding. To actuate the starter starter button 5 is closed for 1-2 sec. During this time the current flows through the winding of the solenoid of time relay 6, the armature of which

actuates the timer. The timer mechanism engages contacts 7, which close the winding circuit of contactor 8. The latter triggers and connects the starter to the storage battery through starter resistance 9 on low voltage.

A supply of low voltage to starter 10 is essential in order to avoid sharp impacts between engaging parts. Approximately 2 sec after the beginning of operation of the time relay contacts 11 are closed, providing power to the winding of contactor 4 for its shut-off. Contactor 4 actuates and with its contacts and series winding of relay 3 shunts starter resistance 9, which causes a sudden increase in current in the starter circuit and corresponding increase in torque.

The rpm of the motor increases rapidly. At the same time, contacts 11, after closing, shunt the parallel winding of relay 3, but its contacts remain in the closed position because of the series winding. After the engine turbine begins to operate, the rpm of the engine rotor increases rapidly. The current in the starter circuit, due to an increase in counter emf, drops to the level at which the winding of relay 3 cannot hold the contacts closed. The latter are opened, thereby shutting off the winding of the contactor. The contacts of the contactor open and disconnect the starter from the storage battery. Some time after starter disengagement all contacts of the time relay return to the initial position.

The character of change of engine rpm and starter parameters during starting is illustrated in Figure 5. At point 0 low voltage is applied to the starter through the starter resistance, whereupon the backlash in the gears from the starter to the engine rotor is selected. The starter resistance is shunted at point A and acceleration of the engine begins. As starter rpm increases, the current in the circuit decreases because of the increasing counter emf and the voltage on the starter terminals increases. At point B the power sources are connected in series and high voltage is applied to the starter. The starter rpm increases, the current in the circuit decreases and the voltage on the starter continues to increase. After removal of the load from the starter's shaft, after its disengagement, starter rpm abruptly increases and the current drops, and when the current in the starter circuit reaches 100 ± 10 a, the starter is switched off.

The electrical diagram of a starter system with a generator starter and the approximate oscillogram of the current it uses in one starting cycle are illustrated in Figure 6.

The power source of electric starter systems is either a set of different types of storage batteries or an on-board or airfield turbogenerator, driving a DC generator. The turbogenerator is more reliable and suitable as an on-board power source compared to storage batteries. One such system -- TG-16 on-board turbogenerator, used for starting turboprop engines on An-24 and Il-18 passenger liners, is illustrated in Figure 7.

The TG-16 is an independent unit consisting of a GTD-16 gas turbine engine, reducer with fan, GS-24A DC generator and systems that provide for the starting and operation of the unit. It is equipped with an automatic

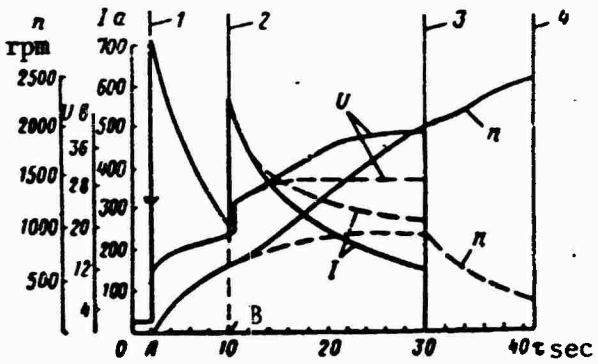

Figure 5. Change of engine and electric starter parameters during start-up and acceleration: n -- engine rotor rpm; I -- current in starter circuit; U -- voltage on starter terminals during start-up (continuous curve) and during acceleration (broken curve); 1 -- starter turn-on; 2 -- switching of batteries; 3 -- starter shut-off; 4 -- low rpm regime.

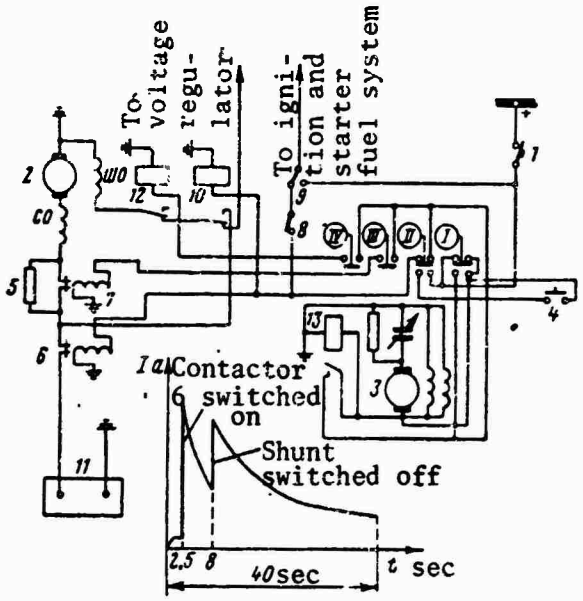

Figure 6. Schematic diagram of electric starter system with GSR-ST generator starter and oscillogram of current consumed by it during starting process: 1 -- AZS [Avtomat zashchity seti; Circuit breaker] of power circuit; 2 -- generator-starter; 3 -- timer motor; 4 -- starter button; 5 -- starter resistance; 6 and 7 -- contactors; 8 -- cold cranking switch; 9 -- "in-flight start" switch; 10, 12 and 13 -- relays; 11 -- storage battery.

starter system. The working rpm of the unit is maintained automatically by a TNR-3R governor and maximum rpm is limited by a TsD-3A-10 centrifugal sensor.

Figure 7. General view of TG-16 turbogenerator.

The specifications of the TG-16 unit are: length 1,573 mm, width 640 mm, height 640 mm, voltage up to 60 V, steady current at 60 V up to 1,000 a, nominal power output 60 kW.

§2. Starter Systems with Turbocompressor Starter

A turbocompressor starter is a small gas turbine engine possessing all the accessories and systems required for operating an ordinary gas turbine engine. These turbostarters are themselves usually started by a direct action electric starter, and then, after reaching the working regime, crank the rotor of the engine being started with the surplus power developed by the turbine of the turbostarter. Turbostarters usually have a centrifugal compressor, driven by a single-stage turbine, and differ with respect to the type and shape of combustion chamber, method of transmitting power to the engine rotor, and dimensions and characteristics.

The schematic diagram of the starting of the gas turbine engine with a turbostarter is shown in Figure 8. The advantages of such a system are: a) comparatively low power consumption for starting the starter itself and consequently high autonomy of the system; b) high power output with small starter; c) absence of special working medium, since the starter uses the same fuel as the main engine. The starter systems of engines with turbocompressor starters are quite reliable. However, they complicate considerably the manufacture and operation of the engines, increase the overall starting time, since in addition to the time required for starting the main engines there is also the time required for starting the gas turbine starter itself.

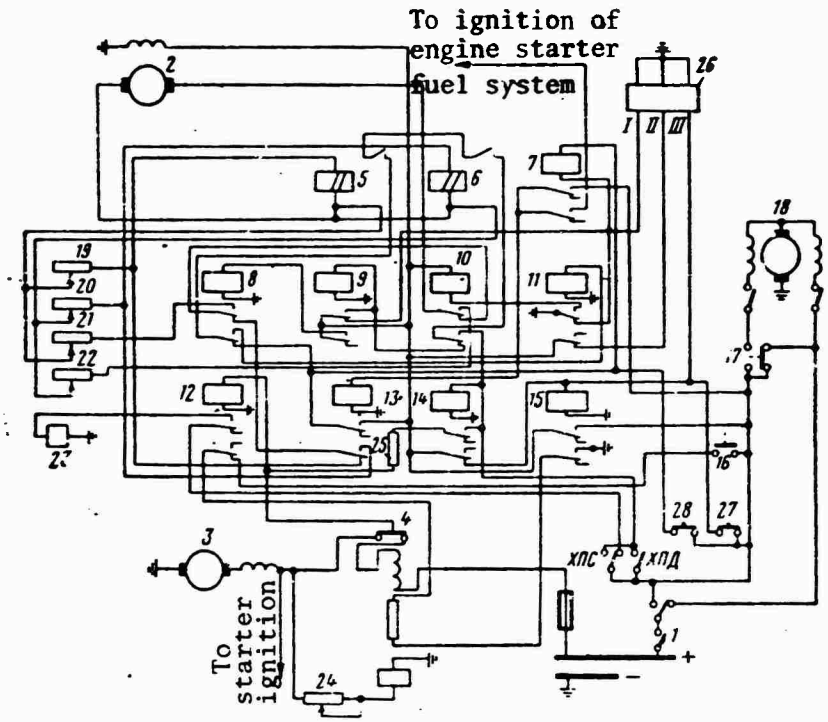

Figure 8. Schematic diagram of starting of AM-3 engine with turbostarter: 1 -- AZS [circuit breaker] of starter system power circuit; 2 -- DC velocity generator; 3 -- electric starter; 4 -- electric starter switch-on contactor; 5 and 6 -- signal relays; 7, 8, 9, 10, 11, 12, 13, 14 and 15 -- starter system relays; 16 and 17 -- terminal off switches of turbostarter exhaust damper opening mechanism; 18 -- exhaust damper opening mechanism; 19, 20, 21 and 22 -- resistances for adjusting actuation voltages of special relays; 23 -- electromagnetic fuel cock of starter; 24 -- resistances for adjusting contactor to turbostarter shut-off rpm; 25 -- resistance; 26 -- starter fuel distributor; 27 -- button for on the ground starting of engine; 28 -- in-air starting button; ХПС -- starter cold cranking switch; ХПД -- engine cold cranking switch.

§3. Starter Systems with Liquid-Fueled Turbostarter

A noncompressor turbostarter, the working medium of which is gas produced by the decomposition of single-component fuel, is also used for starting GTE. Isopropyl nitrate, which contains simultaneously both the fuel and the oxidizer, is most commonly used as such fuel. It does not require air (at high chamber pressure and temperature) for decomposition. The gases formed by the decomposition of isopropyl nitrate have a lower temperature than, for example, the combustion products of powder. Therefore liquid-fueled turbostarters can provide a rather long acceleration of the engine rotor.

The starter system operating on single-component liquid fuel includes, in addition to the starter itself, the following main components: fuel tank, electric motor with pump for fuel delivery, control and ignition systems (Figure 9).

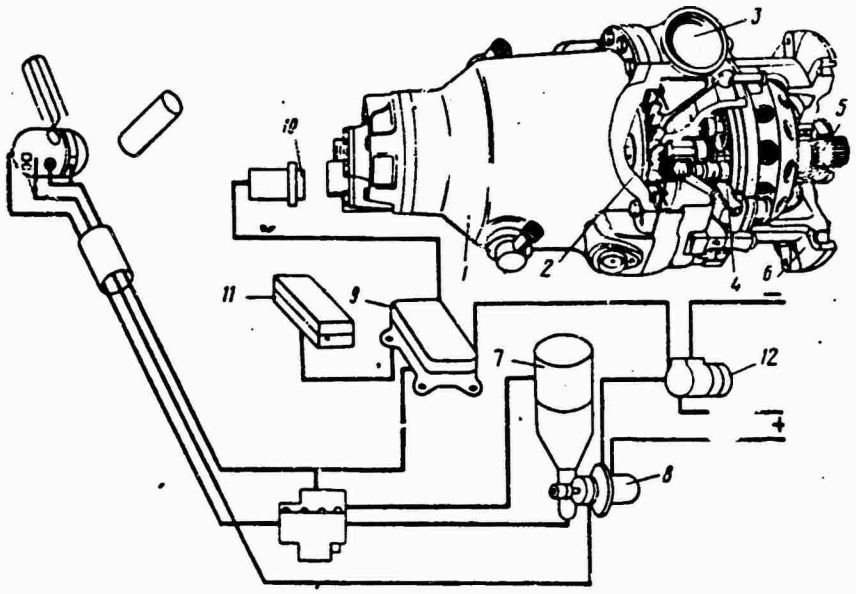

Figure 9. Starter system with single-component liquid-fueled turbostarter: 1 -- turbostarter; 2 -- turbine; 3 -- exhaust gases to atmosphere; 4 -- reducer; 5 -- shaft for engaging turbojet engine; 6 -- flange for fastening of starter to engine; 7 and 8 -- fuel system; 9 -- panel; 10, 11 and 12 -- ignition system.

The fuel tank and some of the apparatus can be housed in any part of the aircraft, and the rest of the components are installed on the engine.

The process of starting gas turbine engines with a liquid-fueled turbostarter proceeds in the following order. The electric motor of the air-fuel pump is turned on by pressing the starter button. The air forced by the pump into the combustion chamber of the turbostarter first purges it of residual combustion products.

After blowing of the combustion chamber fuel is admitted and the ignition system is turned on. The ignition and combustion of fuel is accompanied by an increase in pressure in the combustion chamber. The expanding gases create torque on the turbine of the starter, which is transmitted through the reducer to the shaft of the gas turbine engine being started. In the event of an unsuccessful attempt to ignite the fuel in the starter combustion chamber, a special automatic system shuts off the fuel supply.

After normal starting of the turbostarter the rotor of the GTE is

accelerated to rpm n_2. At this moment the starter automatically disengages and the engine goes independently to the low rpm state.

Starter systems with a single-component liquid-fueled turbostarter are small and light and offer rather high power output. Their specific power reaches 2.5-6.5 hp/kg of weight. Therefore a starter system with a liquid-fueled turbostarter can provide fast starting of GTE.

§4. Air Starter Systems

Starter systems that crank engines with the energy of compressed air are called air starter systems. Air can either be admitted directly to the engine turbine vanes or used for driving a special starter, which turns the engine.

Because of their low efficiency and high air flow rate when the air is admitted directly to the turbine vanes, this system is practically used only for starting small GTE. Such a starter system is suitable only for aircraft on which compressed air is supplied to an engine being started either from another operating engine or from a ground source.

The air starter can be designed as a rotary motor. Usually, however, the air starter system incorporates an axial or radial high rpm turbine, connected to the engine shaft through a reducer with a high gear ratio (i = 1/15 to 1/30). High rpm turbines can operate both on cold and preheated (hot) air.

When cold air is used as the energy supplier enormous quantities are required in order to start the engine. Moreover, the sudden drop of temperature of the air on expansion can lead to icing of the turbine. Therefore preheated compressed air is required in most cases.

The sources of compressed air can be: a) airfield or on-board cylinders; b) airfield compressors; c) auxiliary gas turbine units installed aboard the aircraft; d) compressor of one of the started engines of an aircraft with two or more engines.

A classification of air starter systems for gas turbine engines is shown in Figure 10.

The use of a special gas turbine unit of the airfield or on-board type as the source of compressed air required for the air starter system is of great importance.

The gas turbine power unit illustrated in Figure 11 consists of two basic components: gas turbine engine and two-stage compressor.

Figure 12 is a diagram of the starting of the turbojet engines of large aircraft with air turbostarters operating on low-pressure compressed air. The air is supplied by an auxiliary gas turbine engine installed

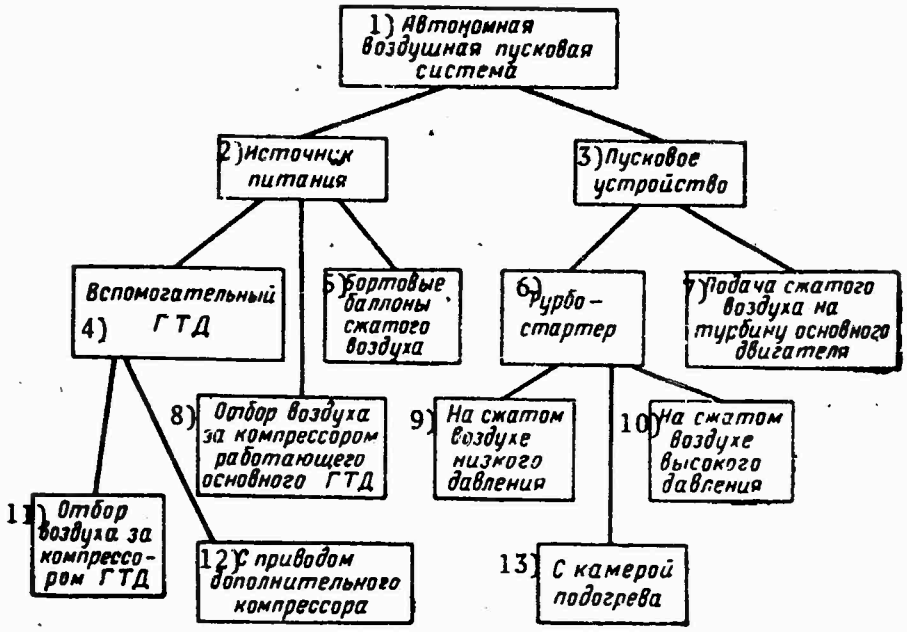

Figure 10. Classification of air starter systems.

KEY:
1. Independent air starter system
2. Power source
3. Starting equipment
4. Auxiliary GTE
5. On-board compressed air cylinders
6. Turbostarter
7. Delivery of compressed air to main engine turbine
8. Air from compressor of operating main GTE
9. On low-pressure compressed air
10. On high-pressure compressed air
11. Air from compressor of GTE
12. Driving auxiliary compressor
13. From preheater chamber

aboard the aircraft. This system consists of mobile gas turbine engine with turbine 1, combustion chamber 2 and compressor 3; direct action electric starter 4; air lines with shut-off valves 5 and air turbostarters installed on engines.

The auxiliary engine uses the same fuel as the main engines. The process of starting a turbojet engine with an air turbostarter proceeds as follows. Air, compressed in the compressor of the auxiliary gas turbine engine to a pressure of 3-4 atm, is admitted through lines 6 with shut-off valves 5 to the starter turbine vanes. The torque from the turbostarter is transmitted through the reducer to the shaft of the turbojet engine. After it is started the second engine is started in the same sequence after first closing valve 5 of the started engine.

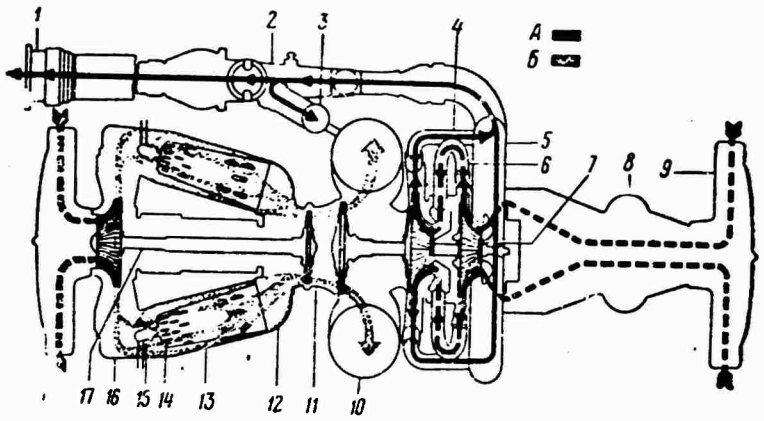

Figure 11. Boeing gas turbine power plant (compressed air turbogenerator): 1 -- compressed air exhaust; 2 -- air flow rate regulator; 3 -- air bypass line; 4 -- second stage compressor line; 5 -- air manifold; 6 -- first stage compressor line; 7 -- rotor assembly; 8 -- oil radiator; 9 -- intake noise suppressor; 10 -- exhaust manifold; 11 -- crossover with free turbine nozzle; 12 -- gas manifold; 13 -- combustion chamber; 14 -- sparkplug; 15 -- injector; 16 -- combustion chamber intake manifold; 17 -- rotor; A -- motion of air supplied to consumer (broken line -- low pressure, solid line -- high pressure); B -- motion of air in engine.

Air starter systems with air turbostarters are used on multiengine aircraft requiring starter system power exceeding 30-40 hp. The air pressure at the air turbostarter intake in low-pressure air systems is usually 2.5-5 atm and the air temperature varies from 150-200°C.

The air flow rate in the turbostarter varies from 0.35-0.4 kg/sec at a turbostarter power $N_{s.s}$ = 30-40 hp to 1.0-1.2 kg/sec at $N_{s.s}$ = 120-150 hp. For $N_{s.s}$ = 70 hp the air parameters at the air turbostarter intake should be: p_a = 3.1-3.3 atm, t_a = 160-180°C, G_a = 0.7-0.75 kg/sec.

The specific power of a low-pressure starting system using an on-board low-pressure power plant is 0.75-1.2 hp/kg of weight.

§5. Starter Systems with Powder-Fueled Turbostarter

A powder-fueled turbostarter is a compressorless gas turbine engine whose working medium is the gas produced by the combustion of solid fuel (powder) in cartridges. Such a starter consists of a gas turbine and gas generator.

The chief advantages of a starter system with a powder-fueled turbostarter are simplicity, relative ease of installation of the starter

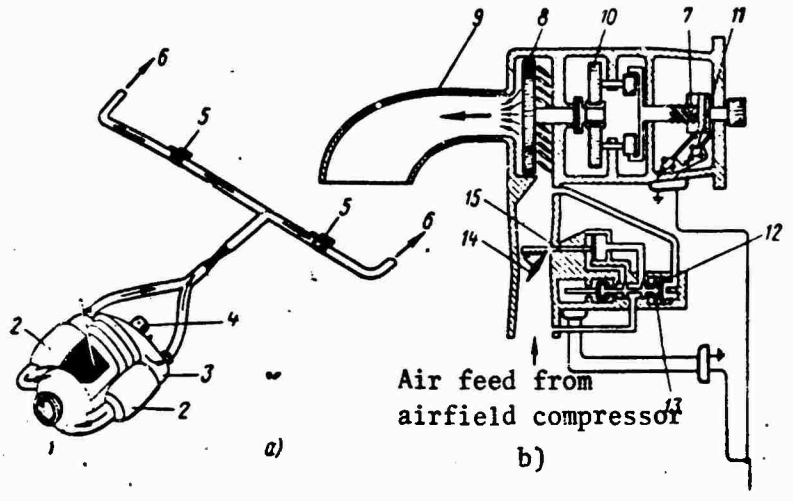

Figure 12. Starting of gas turbine engines by air turbostarters: a -- auxiliary power plant; b -- air turbostarter with regulating valve; 1 -- gas turbine; 2 -- combustion chamber; 3 -- compressor; 4 -- direct action electric starter; 5 -- shut-off valves; 6 -- lines to gas turbine engines; 7 -- clutch for engagement with engine; 8 -- turbine; 9 -- compressed air exhaust to atmosphere; 10 -- reducer; 11 -- centrifugal shut-offs; 12 -- membrane; 13 -- piston; 14 -- air damper; 15 -- piston with rack for opening and closing damper.

components on aircraft, reliability and light weight. This type of starter system is the lightest of all independent engine starting systems now in use. (specific power does not exceed 5-7 hp/kg).

A feature of a starter system with a powder-fueled starter is that once the combustion of the powder has started it cannot be terminated until completely burned up. Therefore if the rpm of the started engine reaches n_2 before the pressure of the powder gases in front of the turbostarter turbine drops to a safe level, then the turbine can over-rev to an intolerable rpm, leading to its destruction. To prevent this the access of the gas to the vanes should be terminated as soon as engine rpm reaches the value at which the starter is shut off. The great power of powder-fueled turbostarters enables them to be used for starting large engines (Figure 13).

The process of starting an engine with a powder turbostarter consists of the following operations. When switch 15 is turned on power flows from the on-board system to time relay 14, fuel pump 6 and starter system circuitry.

After 2 seconds the relay closes contacts A and the voltage on the electric primer of cartridge 11 drops. The powder in the cartridge ignites

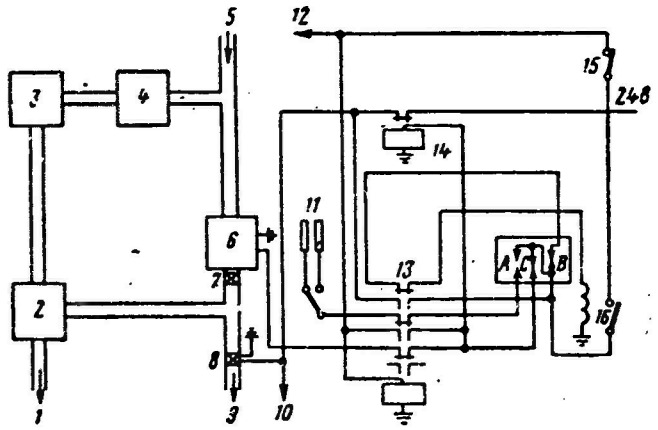

Figure 13. Possible diagram of starting system with solid-fueled turbostarters: 1 -- fuel supply to main injector; 2 -- fuel distributor; 3 -- fuel feed regulator; 4 -- main fuel pump; 5 -- fuel supply; 6 -- fuel pump; 7 and 8 -- valves; 9 -- fuel feed to starter injector; 10 -- fuel feed to starter igniters; 11 -- cartridges; 12 -- current to feathering pump; 13 -- relay; 14 -- time relay; 15 -- second engine starter switch; 16 -- powder turbostarter shut-off switch.

and the gases from its combustion turn the starter turbine, causing the engine shaft to turn.

CHAPTER 3. ENGINE ROTOR PREACCELERATOR UNITS

The development of jet engines led to decisive changes first of all of rotor preaccelerators. In order to prevent high gas temperatures in the engine duct, which can cause serious damage and reduce engine service life, the starters should participate in the starting process to speeds amounting to 25-60% of the nominal engine operating rpm.

In choosing the type of starter for engine start-up the following factors are taken into account: weight and dimensions of starters and power sources; autonomy of given type of starter; reliable starting of engines at lowest and highest ambient air temperatures; number of starts afforded by a starter system without charging or servicing power sources; possibility of using given type of starter for various aircraft; cost, features of production, shipping, storage and operation of products used for starter operation.

The starter should be powerful enough to rev a gas turbine engine to rpm n_2. It should also be simple to control and have an automatic system for engagement with and disengagement from the engine rotor.

Electric starters are less suitable for fast starting of engines, particularly with high thrust, than other types of preaccelerator units. The basic disadvantage of a starter system with an electric starter is the substantial increase of weight and dimensions of the power sources associated with increasing starter power. Therefore such a system cannot provide autonomous starting of powerful engines.

In recent years much effort has been devoted to the design of turbine starters for starting engines for the purpose of ensuring autonomous starting, improving reliability and reducing starting time. The turbines of these starters are turned to high rpm either with air (air turbostarters) or the products of combustion or decomposition of various substances. Turbine starters have considerable weight advantages over electric starters of equal power.

§6. Electric Starters

Only direct action electric motors (starters) powered by on-board or airfield power sources with direct current and low (24-30 V) and high (up to 112 V) voltage are used for starting gas turbine engines. An increase in power source voltage increases the efficiency of the power sources, improves their operating conditions, increases their power output, improves reliability and lengthens the battery service life. A direct action starter is an ordinary nonreversing motor with a short-term mode of operation. For starting gas turbine engines chiefly high-rpm direct action electric starters turning up to 10,000-13,000 rpm are employed. Direct action electric starters differ from electroinertial and combined starters in that they have no flywheels and are connected directly through the appropriate transmission to the engine rotor.

Direct action electric starters may be designed with excitation windings of the parallel and compound types. Parallel excitation (shunted) electric starters have less favorable starting properties by comparison with other electric motors. In order to reduce the effect of the decelerating moment of the magnetic field of the shunt winding in the starting regime at high rpm, starters with such an excitation winding operate jointly with a carbon current regulator.

Electric motors with compound and shunted excitation are most commonly used for starting GTE. During the starting process, after reaching a certain rpm, the shunt winding of such motors is turned off, since the magnetic field of this winding has a braking effect on the rpm of the motor as the rpm increases.

The use of compound excitation came about as the result of attempts to increase the torque, particularly at the beginning of acceleration, and also was stimulated by the fact that at the high rpm that must be imparted to the shaft of the gas turbine engine during start-up it is impossible to use reducers with a high gear ratio. Therefore the effort on a gas turbine starter reducer itself is not a load sufficient for protecting it from overspeeding. Compound excitation, in addition to incorporating a maximum rpm governor, protects a gas turbine engine electric starter from racing.

The direct action electric starter (Figure 14) consists of the following basic components: aluminum housing 1, steel housing 2 with poles 3 and excitation windings 4, armature 5 with winding and commutator 6, front 7 and back 8 plates.

Starter-generators are a further development of electric starters. Starter-generators are quite compact and are available in about the same sizes as ordinary direct action electric starters with a power output up to 30 hp in the starting regime.

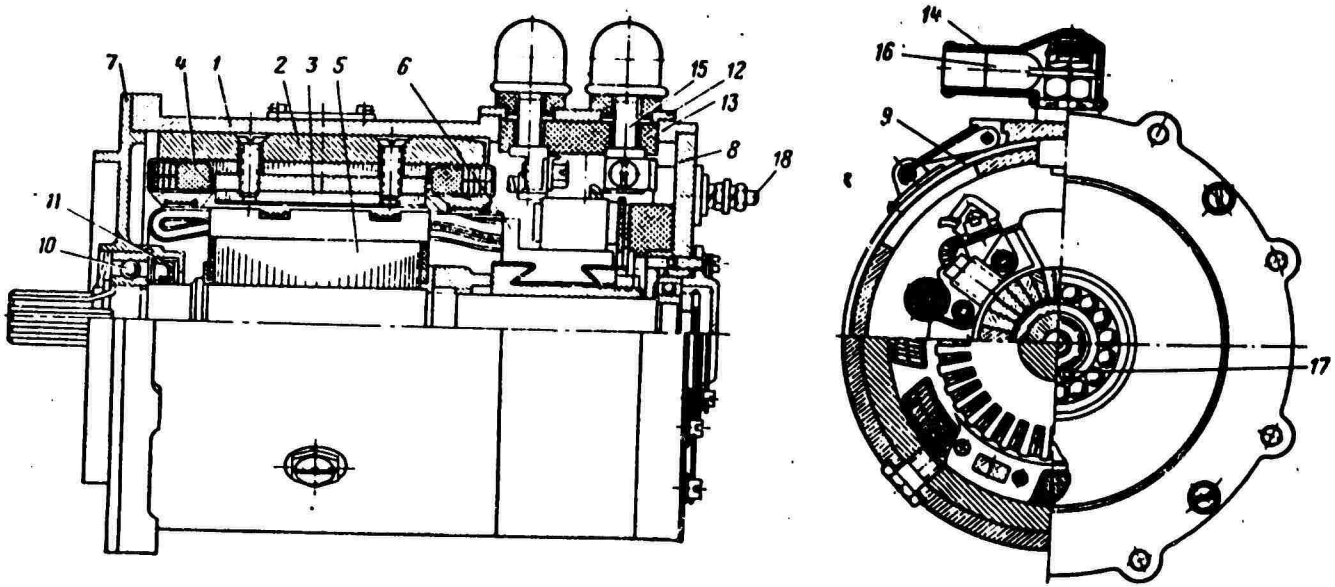

Figure 14. Longitudinal and cross sections of direct action electric starter: 1 -- aluminum housing; 2 -- steel housing; 3 -- pole; 4 -- winding; 5 -- armature; 6 -- commutator; 7 -- front plate; 8 -- back plate; 9 -- band; 10 -- ball bearing; 11 -- packing seal; 12 and 13 -- panel mountings; 14 -- rubber receptacle; 15 -- terminal; 16 -- cable receptacle; 17 -- locking ring; 18 -- terminal.

The chief advantage of the starter-generator is that instead of two units (starter and generator), only one unit is mounted on the engine, which functions during starting as the starter and during engine operation as the generator that powers the on-board electrical system of the aircraft with direct current.

Transmission of the torque from the starter-generator to the engine turbine shaft and its subsequent operation as the generator are achieved by connecting the unit by means of a splined shaft through a compact reducer, installed within the starter-generator itself or in the engine gear box.

The starter-generator is six-pole DC motor with three extra poles (Figure 15). Structurally the starter-generator is an electric motor of sealed design with external forced cooling (with outside air).

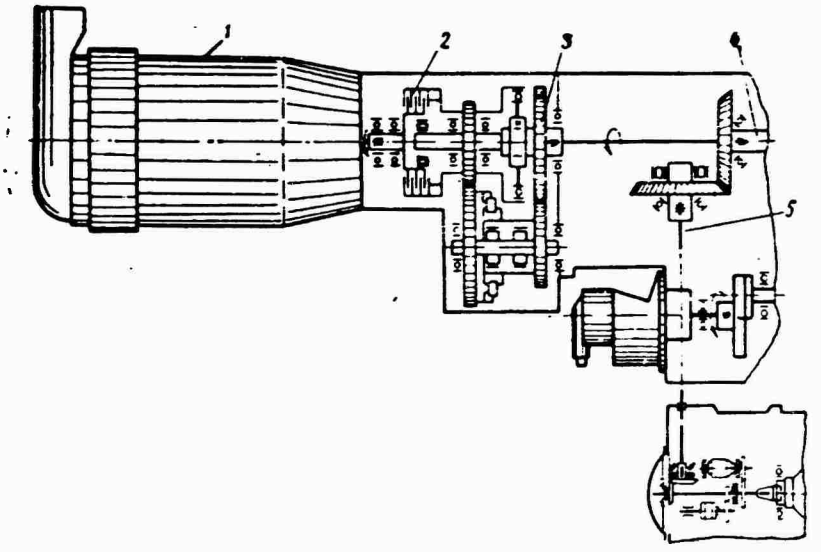

Figure 15. Starter-generator GSR-ST and its kinematic layout: 1 -- starter-generator; 2 -- friction clutch; 3 -- reducer; 4 -- shaft of turbojet engine; 5 -- accessory drive shaft.

Two free-running clutches -- ratchet and sprocket -- are used in the two-speed drive to ensure operation of the unit in the starter and generator modes.

The basic specifications of certain electric starters and starter-generators used for starting gas turbine engines are listed in Tables 1 and 2 and the performance characteristics of direct action starters are given in Figure 16.

Table 1. Basic Specifications of Direct Action Electric Starters

Parameters	Unit of measurement	Type	
		ST-2	ST-2-48
Nominal voltage	V	15	28
Nominal torque	kg·m	2.3	2.3
Rotating speed	rpm	2,850-2,900	3,000
Power	kW	6.75	7.1
Current used	a	700-690	340
Idling speed at nominal voltage	rpm	7,100	5,000
Weight	kg	16.7	16.7

Table 2. Basic Specifications of Starter-Generators

Parameters	Unit of measurement	Type		
		GSR-ST-I	GSR-ST-II	GSR-ST-III
Compound excitation:				
minimum rpm	rpm	1,400	1,500	1,300
moment	kg·m	1.8	2.5	2.5
current used	a	200	350	300
Series excitation:				
minimum rpm	rpm	2,400	2,500	1,800
moment	kg·m	1.8	2.5	2.5
current used	a	200	450	400

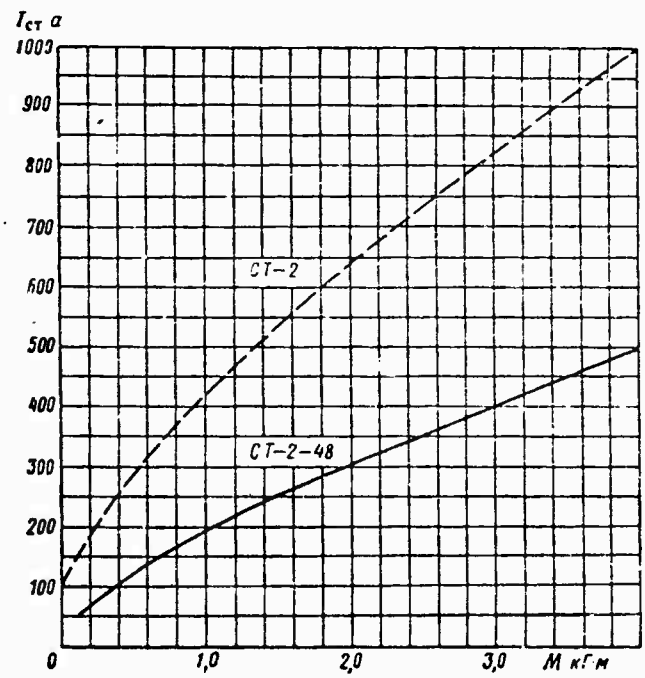

Figure 16. Performance characteristics of electric starters.

§7. Fuel-Air Turbostarters

The main engine fuel or some other fuel can be used to operate such a starter. The air required for fuel combustion is supplied either by the starter compressor or by special sources. In the former case the starter is a small-scale gas turbine engine with nearly all the systems and accessories required for operating a gas turbine starter, and in the latter case it is a rather simple and light apparatus.

The turbocompressor starter is a gas turbine engine whose surplus power is used for accelerating the rotor of the engine being started. The principal kinematic diagrams of such starters are shown in Figure 17.

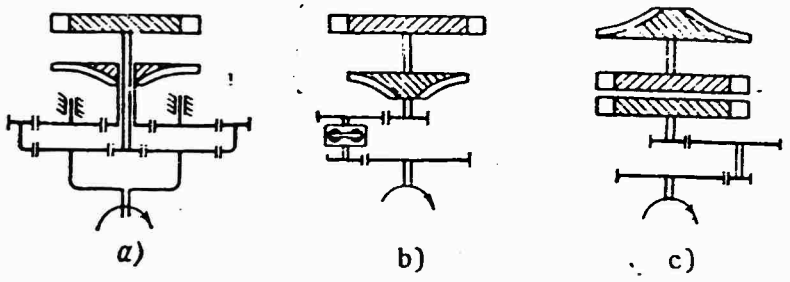

Figure 17. Kinematic diagrams of turbostarters: a -- with differential planetary reducer; b -- with fluid coupling; c -- with kinematically unconnected turbines.

The turbostarter consists of a centrifugal compressor with unilateral air intake, annular combustion chamber, gas turbine, exhaust nozzle, reducer with mechanism for engagement with engine rotor, starter engagement and disengagement systems. Turbostarters come in different sizes, have different characteristics, methods of control and transmission of power to the engine shaft. Two turbostarter control methods are used, one with constant fuel flow rate and one with constant rpm.

Control by constant rpm increases starter power at low ambient air temperatures and thereby substantially accelerates the engine starting process.

At high ambient air temperatures, however, starter pressure drops and the engine is sluggish in attaining the low rpm regime, since the power of the main engine's turbine also falls off under start-up conditions as the ambient air temperature increases. Power can be transmitted from the starter to the shaft of the engine being started either by different types of clutches (including the fluid type), or by means of gas coupling between two turbines, one of which is installed on the starter rotor and the other (starting) connected to the rotor of the engine being started.

In starters with two kinematically unconnected turbines the turbocompressor of the starter operates most of the time in a practically steady

state (not counting the acceleration time of the turbostarter at the initial moment), whereas the starting turbine operates at a steadily changing rpm, ensuring smooth acceleration of the engine during the starting process.

The flow rate of gas through the starting turbine remains constant, while the torque decreases as rpm increases. Such a character of change of torque provides maximum power at an rpm at which the engine's turbine power is still deficient.

Figure 18 illustrates a gas turbine starter with a single-stage turbine and its kinematic layout. The gas turbine starter installed on the RD-3M engine has the following parameters: working speed 31,000-33,000 rpm; maximum exhaust pipe temperature in working regime not greater than 750°C; time of continuous starter operation not exceeding 80 sec.

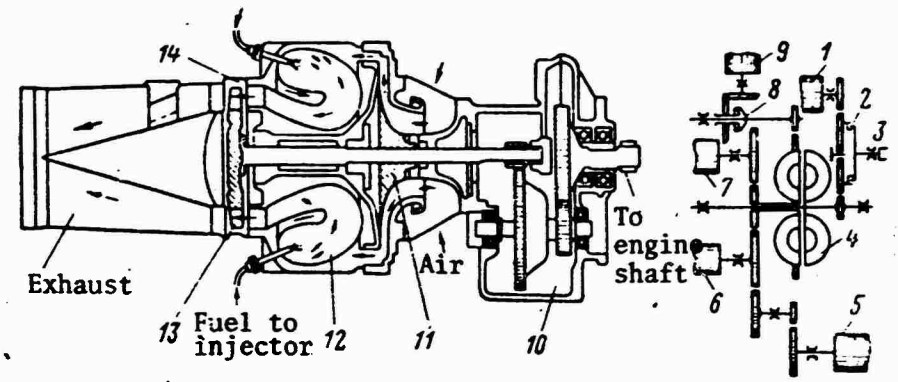

Figure 18. Diagram of gas turbine starter and its kinematics: 1 -- tachometer generator; 2 -- ratchet clutch; 3 -- drive shaft of turbojet engine; 4 -- fluid coupling; 5 -- tachometer; 6 -- fuel regulator pump; 7 -- oil pump; 8 -- free-running clutch; 9 -- direct action electric starter; 10 -- reducer with fluid coupling; 11 -- compressor; 12 -- combustion chamber; 13 -- turbine; 14 -- nozzle apparatus.

The specific power of a turbocompressor starter with the accessories that service it is 1.2-2 hp/kg, and at starter powers exceeding 100 hp may amount to 2.5-3.5 hp/kg.

In a fuel-air starter of the compressorless type compressed air for combustion of the fuel is supplied from cylinders, usually spherical, in which it is stored under a pressure of 200 kg/cm^2.

A fuel-air starter of the compressorless type (Figure 19) consists of combustion chamber 6, gas turbine 1, reducer and clutch 4. Fuel is fed to the combustion chamber from the aircraft fuel tank by a fuel pump. The supply of a certain quantity of air to the combustion chamber to ensure the required mixture composition is achieved with the aid of a calibrated orifice. The

dosing of air at the speed of sound ensures a constant air flow rate, regardless of back pressure in the combustion chamber.

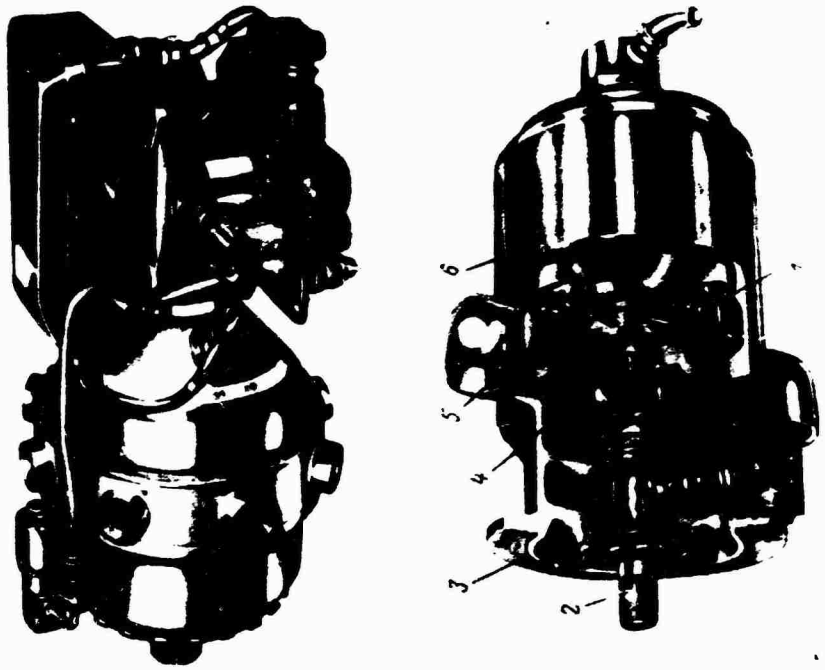

Figure 19. Fuel-air turbostarter: 1 -- turbine; 2 -- shaft for connection with turbojet engine; 3 -- flange for fastening starter to engine; 4 -- coupling; 5 -- exhaust gases to atmosphere; 6 -- combustion chamber; 7 -- compressed air feed.

When the starter turbine reaches maximum rpm the centrifugal switch, by means of a relay, shuts off the feed of fuel and air to the combustion chamber, combustion ceases and the starter stops.

The gas that drives the starter turbine in a fuel-air starter is formed by the combustion of a mixture of fuel and compressed air, admitted from the cylinders. The fuel burns with an air excess coefficient α = 1-2 and at a pressure of 15-20 kg/cm^2.

The gas reaches the working wheel of the turbine at high velocity, which ensures high turbine rpm and accordingly a smooth characteristic of change of starter torque as a function of rpm.

The moment produced by the fuel-air starter is determined by the following equation

$$M_{s.s} = M_0 - bn;$$

$$b = \frac{\pi}{30} \frac{1}{g} \frac{G_g R_{av}^2}{i^2}, \tag{3.1}$$

where G_g is the flow rate of gas through the starter turbine in kg/sec;

R_{av} is the average radius of working vanes in meters;

i is the ratio of the rpm of the engine rotor to the starter rpm.

Figure 20 shows a convenient nomogram for determination of the first, second and summary flow rates of compressed air, weights of starter and starter system, time of operation of the starter of an autonomous starter system with an air-fuel starter.

The required compressed air reserves in the cylinders is determined by the formula

$$G_{as} = \frac{q_a(\tau_{s.s} + 0,3)}{\beta_a i_{cy}} i_{st}, \tag{3.2}$$

where q_a is the required per second compressed air flow rate;

$\tau_{s.s}$ is the time of operation of the starter;

i_{st} is the required number of starts with a given power source without recharging;

i_{cy} is the number of cylinders;

β_a is the compressed air output coefficient of the power source (cylinder).

The amount of compressed air in the cylinder can be determined using the equation

$$G_{a.cy} = 0,341 \frac{p_{cy} V_{cy}}{T_{cy}}, \tag{3.3}$$

where p_{cy} is the compressed air pressure in the cylinder in kg/cm^2;

V_{cy} is cylinder volume in liters;

T_{cy} is air temperature in cylinder in °K.

Both metallic and lighter fiberglass cylinders, capable of withstanding compressed air pressures up to 200 kg/cm^2, can be used as the on-board air cylinders.

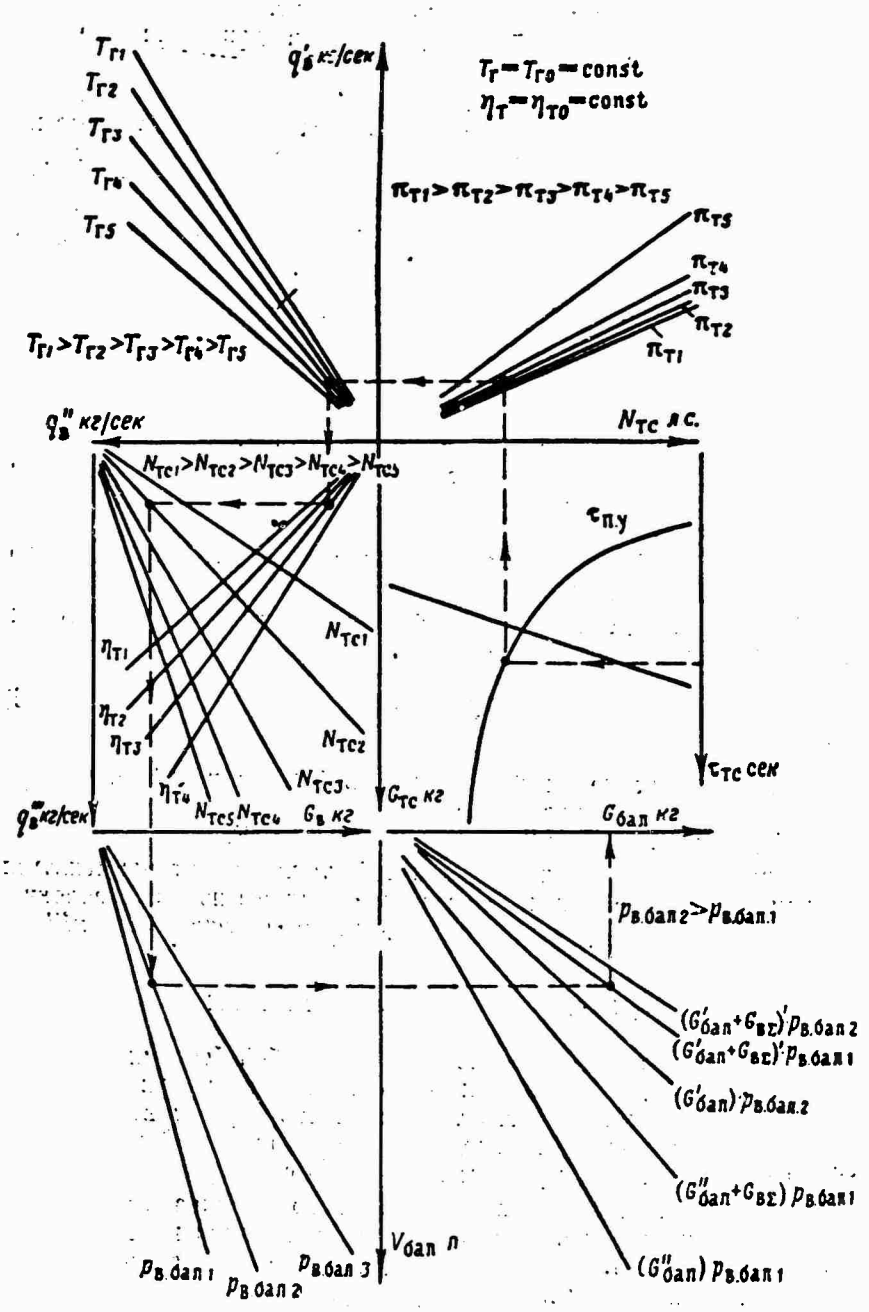

Figure 20. Nomogram for calculation of fuel-air starter. [Subscripts: Г = g; В = a; ТС = ts; П.у = s.s; В.бап = = a.cy; бап = cy].

§8. Liquid-Fueled Turbostarters

This type of turbostarter is a compressorless gas turbine engine in which the heat energy of the combustion products of single-component fuel is transformed into mechanical energy of rotation of the starter shaft. Its operation is similar to that of the powder-fueled starter.

The gases formed by the combustion of a single-component fuel have a lower temperature than the gases from powder, by virtue of which a liquid-fueled turbostarter can be used for longer acceleration processes.

Foreign turbostarters for gas turbine engines generally operate on unitary (single-component) fuel -- isopropyl nitrate. Hydrogen peroxide-fueled starters are also used (Figure 21).

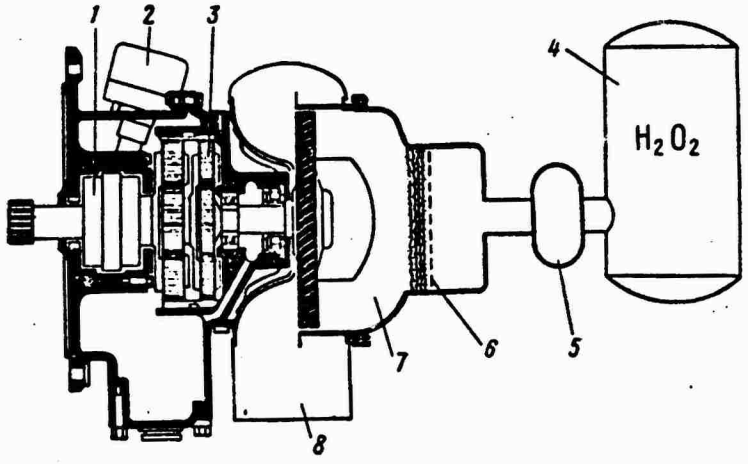

Figure 21. Liquid-fueled turbostarter using hydrogen peroxide as fuel: 1 -- clutch; 2 -- regulator; 3 -- reducer; 4 -- hydrogen peroxide tank; 5 -- pump; 6 -- catalytic combustion chamber; 7 -- steam and oxygen gas; 8 -- exhaust.

These turbostarters are light weight, are independent of external power sources and are capable of rapidly starting an engine to the mode of stable operation. The number of starts afforded by a given starter is limited only by the capacity of its fuel tanks. They do not require compressed air cylinders or the special equipment that are necessary for fuel-air starters. Liquid-fueled turbostarters have a smooth torque characteristic.

§9. Air Turbostarters

An air turbostarter is usually defined as a high-rpm air turbine of the axial or radial type (Figure 22), operating on cold or heated (hot) air. The air required for its operation can be obtained from a special gas turbine plant of the ground or on-board type, from a running engine or from special cylinders. The temperature of the air striking the starter turbine is usually 150-200°C, and its pressure does not exceed 3.5-4 kg/cm^2.

The maximum power of the turbostarter is 150 hp. Air turbostarters are most commonly used on multiengine aircraft.

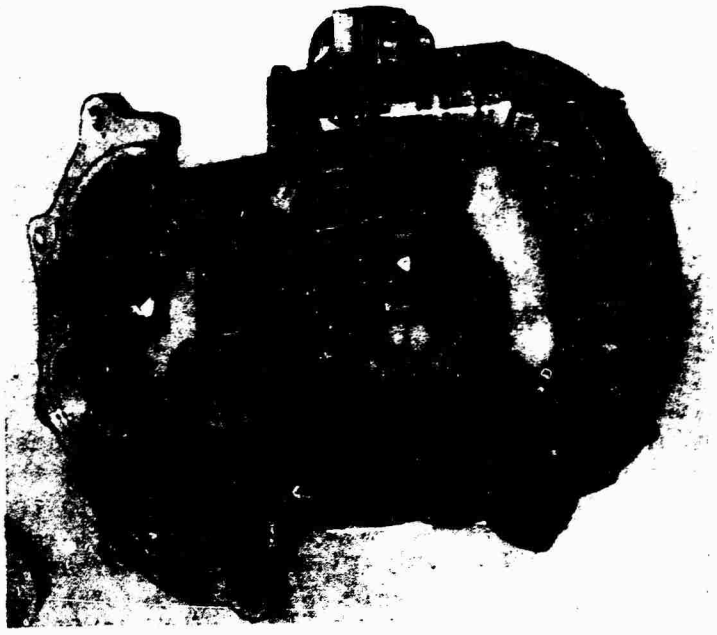

Figure 22. Air turbostarter.

Air turbostarters commonly have an axial single-stage active turbine, the shaft torque of which at constant draft can be determined by the equation

$$M_т = \frac{G_a R_{me} \eta_{red}}{g} (C_1 \cos\alpha_1 + \psi W_1 \cos\beta_2 - u), \qquad (3.4)$$

where α_1 is the exit angle of the nozzle vanes;

ψ is the coefficient of friction of the vanes;

G_a is per second air flow rate;

R_{me} is the mean turbine radius;

W_1 is relative velocity at vane intake;

β_2 is exit angle of turbine vanes;

u is circumferential velocity at mean radius;

η_{red} is reducer efficiency.

The torque on the shaft of the turbostarter is

$$M_{s.s} = M_t i \eta_{red}.$$

Air turbostarters operate at speeds up to 50,000-60,000 rpm and the specific power of turbostarters operating on low-pressure air is 7-10 hp/kg.

§10. Powder Turbostarters

Powder turbostarters consist of the following basic structural components: high-rpm turbine; reducer (usually of the planetary type); friction clutch, which absorbs impact loads while transmitting torque from the starter to the engine; regulator, which shuts the starter off after the engine or starter turbine reaches the appropriate rpm; powder generator (single-charge or multicharge gas generator-cartridge).

In order for the starter turbine to operate at maximum possible efficiency with minimum dimensions the turbine wheel must operate at speeds up to 45,000-50,000 rpm. Since the rpm of the gas turbine engine at which the starter must be shut off is much lower than that of the starter rotor, the starter is designed with a reducer whose gear ratio reaches up to 20.

There are several versions of pyroturbine starters, including single-charge with powder generator, double-charge and multicharge with special cartridges of the stationary and revolving types.

The single-charge pyroturbine starter (Figure 23) consists of turbostarter A and powder generator B, with safety valve 4 and vent 5. The powder combustion gases are admitted to turbine 7 of the starter through line 6. The starter is mounted on the engine by means of flange 11 and is coupled with a turbojet engine by means of shaft 12. The starter has reducer 9 and mechanism 10 for coupling starter shaft 12 with the shaft of the turbojet engine and for disengagement of the starter.

The gases produced by the combustion of the powder charge in generator B have a temperature up to 1,900°C; the pressure of the gas reaches 90 kg/cm^2. The temperature and pressure of the powder gases depend on the composition of the powder and its temperature. The powder gases flow through the gas line to nozzles, where they expand and then strike the starter turbine vanes and cause them to rotate.

Smokeless nitropowders with special additives -- retarders and combustion inhibitors -- are used for pyroturbine starters. The typical powder used in powder turbostarters contains 59% nitrocellulose, 20% nitroglycerin and 21% additives that control the rate of combustion. In recent years foreign pyroturbostarters have been fueled with a powder based on ammonium nitrate. The combustion of such a fuel produces gases at lower temperatures, by virtue of which starter operating time is increased to 15-20 sec. The gases of this powder have lowere aerosol and corrosive properties than the brand formerly used.

The important disadvantages of powder turbostarters are problems in the storage and transportation of the powder cartridges, considerable smoking and the toxicity of the combustion products, erosive and corrosive properties of the combustion products, resulting in reduced service life.

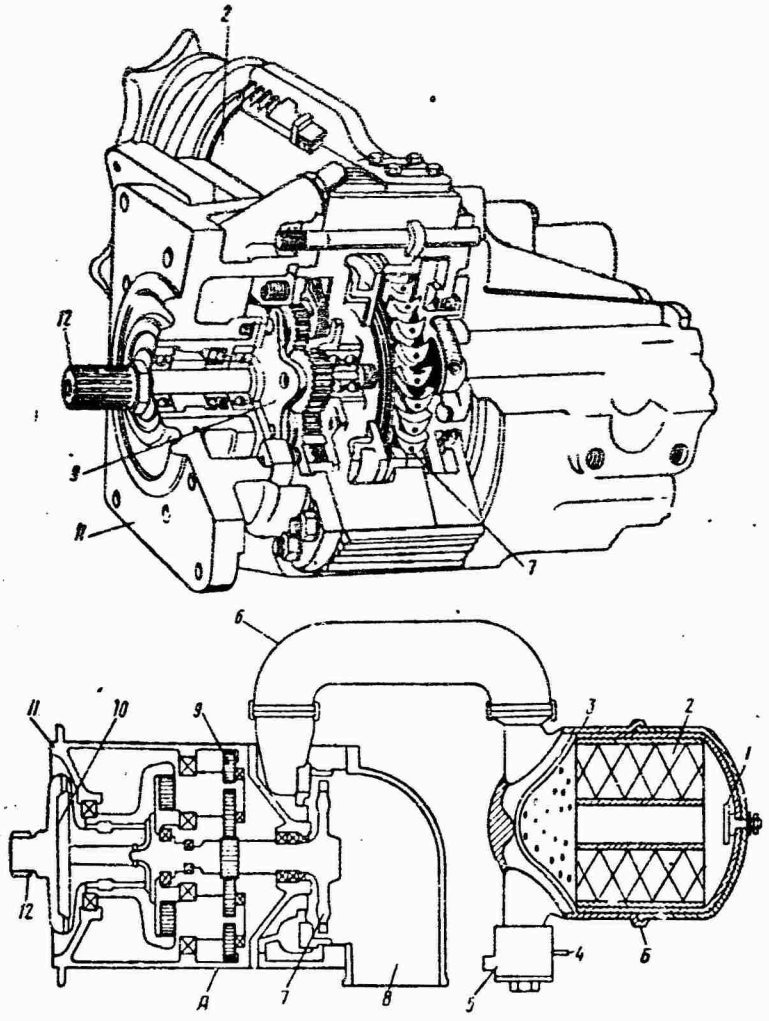

Figure 23. Pyroturbine starter with powder generator: A -- turbostarter; B -- powder generator; 1 -- electrical contact for ignition of powder charge; 2 -- powder charge in cartridge; 3 -- lattice; 4 -- safety valve; 5 -- exhaust vent for powder gases; 6 -- powder gas line to turbine; 7 -- starter turbine; 8 -- powder gas exhaust to atmosphere; 9 -- reducer; 10 -- clutch for engaging starter with engine; 11 -- starter mounting flange; 12 -- shaft to turbojet engine.

Pyroturbostarters are often equipped with an extra turbine, operating on compressed air, which serves as an aerodynamic brake, thereby increasing the reliability of the powder turbostarter.

A convenient nomogram for determining the weight of the powder charge and the weight of the powder turbostarter for various parameters of the working medium and starter is illustrated in Figure 24.

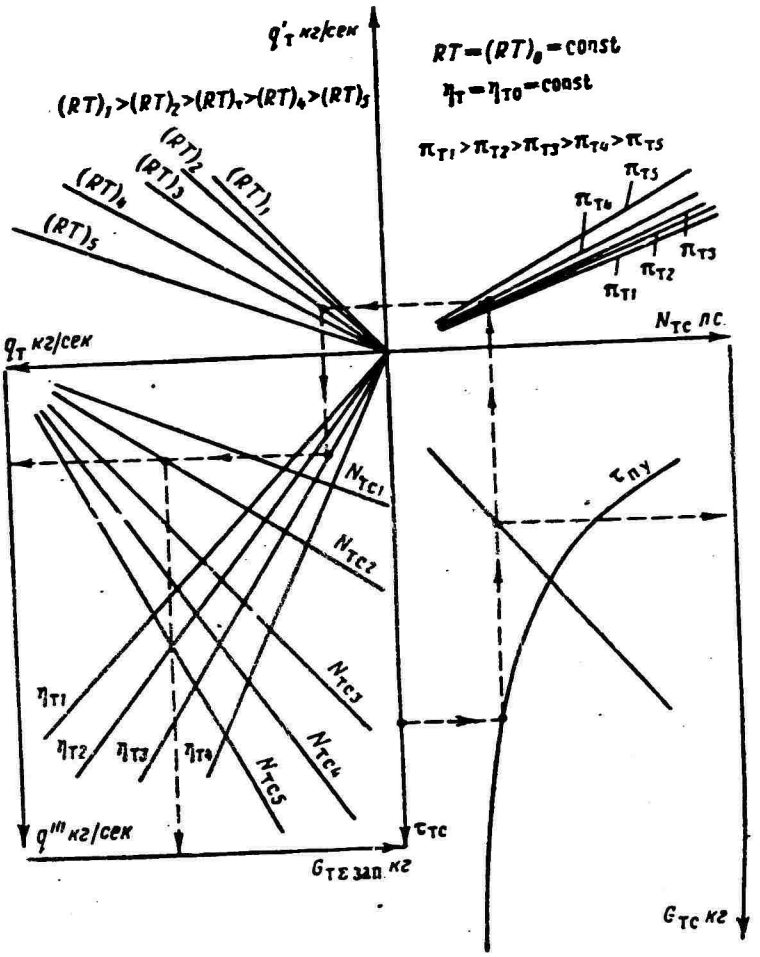

Figure 24. Nomogram for calculation of powder turbostarter. [Subscripts: TC = ts; зап = st; пу = ss].

CHAPTER 4. GAS TURBINE ENGINE STARTER CONTROL SYSTEM

Different types of equipment, mechanisms and parts, which perform certain auxiliary functions during start-up, are employed in the gas turbine engine starter control system.

The above-mentioned devices include starter panels, starter control apparatus, including a timer and different types of electromagnetic relays, equipment for controlling high-pressure and low-pressure starter fuel pumps and starter injector solenoids, solenoid valves, connective electric drives and different types of lines and manifolds.

If some type of starter other than electric (turbocompressor, air, powder, etc.) is used, then several independent electric circuits are provided, along with the corresponding apparatus that controls the starting of the starter itself.

§11. Starter Panels

The starter panel (Figure 25) provides for remote control of the sequence of actuation of all assemblies and components involved in engine start-up. During the starting process the starter panel is the central control organ. The control parameters of the panel are time, measured from the moment the starter button is pressed, and the rpm of the engine being started.

The starter panel combines all signal relays, contactors, starter resistances of the starter control system and serves as the junction between electric drive systems and power sources in the same sequence given by the timer during the starting process.

The starter panel and automatic timer control the following operations: on the ground engine start-up, cold cranking, mock starts, in-flight starting of engines. If necessary the panel provides for emergency termination of start and accelerates the completion of the cycle of the programmer.

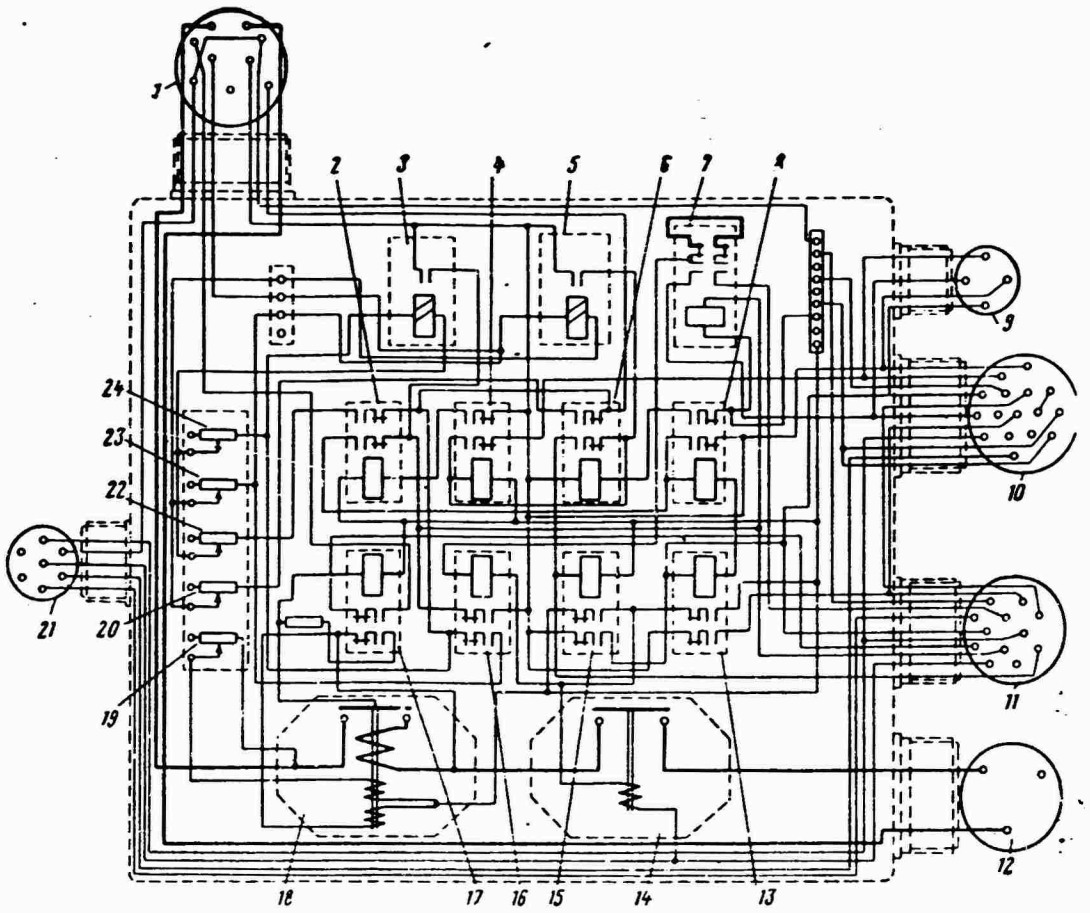

Figure 25. General view and schematic diagram of starter panel for starting AM-3 engine with gas turbine starter: 1, 9, 10, 11, 12 and 21 -- plug connections; 2, 4, 6, 8 and 16 -- intermediate relays; 3 and 5 -- signal relays (ignition on and off and opening of fuel regulator valves); 7 -- engine ignition relay; 13 -- automatic start relay; 14 -- contactor; 15 -- automatic equipment shut-off relay; 17 -- relay for shutting of electromagnetic fuel valve of gas turbine starter; 18 -- maximum rpm relay; 19, 20, 22, 23, 24 -- regulated resistances for adjusting automatic equipment.

§12. Automatic Timers

Automatic timers are used for automatic control of engine start-up. Individual types of timers differ from each other by the number of button switches and time intervals between switch activation.

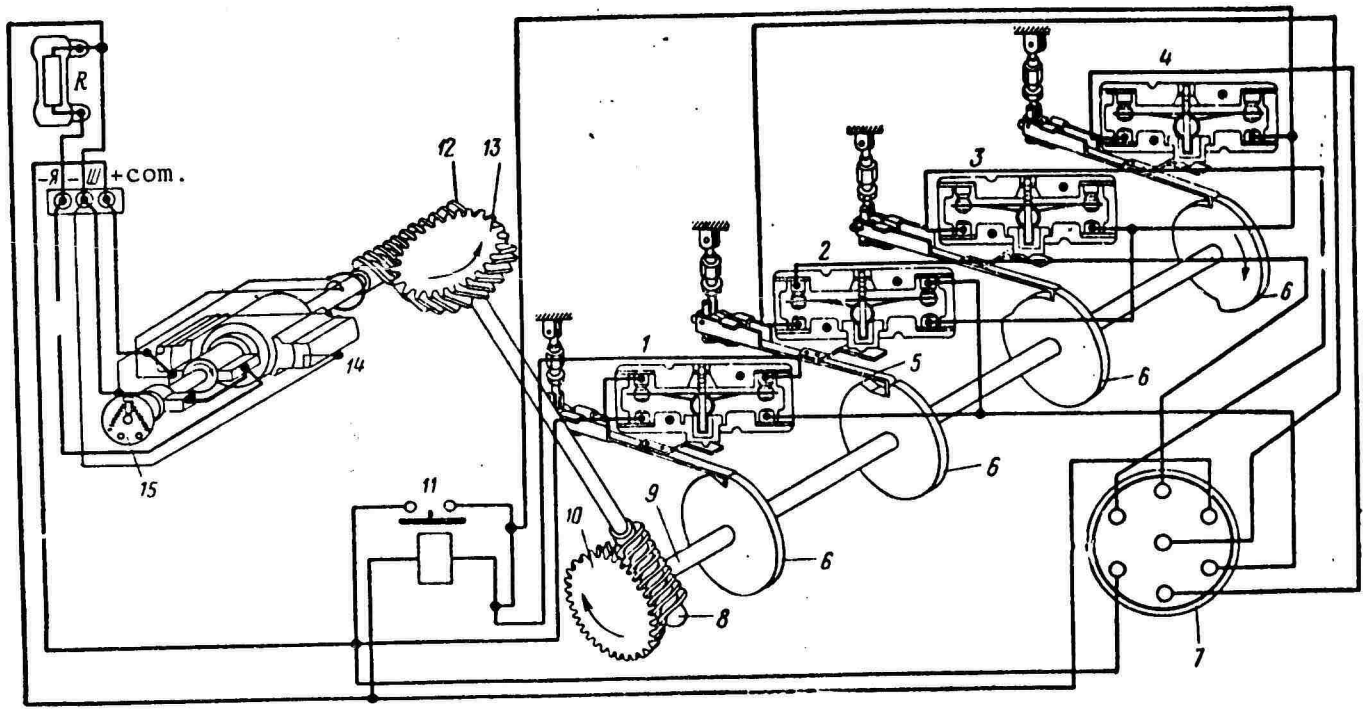

Figure 26. AVP-3A automatic timer: 1, 2, 3 and 4 -- microswitches; 5 -- lever; 6 -- cams; 7 -- plug connection; 8 and 12 -- worm gears; 9 -- shaft; 10 and 13 -- gears; 11 -- locking relay; 14 -- motor; 15 -- centrifugal rpm governor.

The timer (Figure 26) consists of electric motor 14 with electromagnetic brake; shaft 9, to which are attached profiled discs 6; microswitches 1, 2, 3 and 4; locking relay 11 and reducer with worm gear, which transmits rotation from the electric motor to the shaft. This transmission is designed so that the shaft makes only one revolution during the starting cycle. As the shaft rotates, the cams alternately close the microswitches of the relays and contactors that actuate the drive mechanisms.

The speed of the automatic timer motor should remain constant, regardless of voltage fluctuations and changes in ambient air temperature and load. For this purpose the motor is equipped with a special governor, which maintains constant rpm.

CHAPTER 5. ELECTRIC IGNITION SYSTEMS

An electric ignition system is essential for igniting a fuel-air mixture in the combustion chamber or in a starter igniter during engine start-up. Any ignition system used for gas turbine engines consists of the following components: ignition circuit, powered by a storage battery or generator, shielded conductors and spark plugs.

Low-voltage ignition systems have been used most widely in recent times. In addition to capacitance discharge systems with semiconductor plugs there are many low-voltage ignition systems with inductive discharge on the metal plated surface of the ceramic insulator of the spark plug. Low-voltage ignition systems have the following advantages over formerly used high-voltage ignition systems:

1) the system is almost insensitive to fouling of the spark plug electrodes and operates even when there are carbon deposits on the insulator;

2) the electrical and power characteristics are practically independent of pressure and temperature of the gas medium in which the plug discharge gap operates;

3) the absence of high voltage in the system increases operational reliability of the wires and ignition systems as a whole, especially under elevated conditions;

4) the energy and power of the discharge can be much greater than in an ordinary high-voltage ignition system.

The low-voltage ignition system (Figure 27) incorporates an electrical discharge on the surface of the spark plug semiconductor.

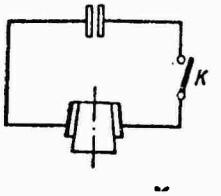

Figure 27. Schematic diagram of low-voltage ignition system.

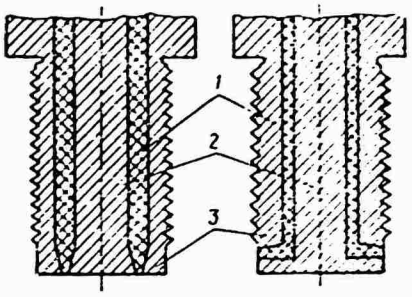

Figure 28. Possible forms of semiconducting material for low-voltage spark plugs: 1 -- semiconductor; 2 -- central electrode; 3 -- side electrode.

When switch K is closed the electrodes receive a potential difference equal to the potential difference between the plates of the precharged capacitor. At that moment a conducting "bridge" (path of least resistance) forms on the top surface of the semiconductor through the shortest distance between the electrodes.

The design of a surface discharge spark plug for a low-voltage ignition system is illustrated in Figure 28. Semiconductor 1 of special form is placed between the metallic electrodes of the spark plug. In contrast to metals, the overwhelming majority of semiconductors have a negative thermal resistance coefficient, so that conductance increases as the temperature rises.

A semiconductor is a ceramic mass containing the oxides of metals with a negative thermal coefficient. As current passes, the temperature rises, the resistance of the "bridge" decreases, there is intensive thermal ionization, with the result that the discharge voltage along a narrow path in the semiconductor drops sharply and between the electrodes forms an electrical arc which disappears when the energy reserve of the capacitor is used up.

The low-voltage discharge can be assumed to consist of two stages. During the first preparatory stage a conducting channel is formed and it is heated by the discharge current to the temperature at which the material begins to evaporate, with the result that the space between the electrodes is ionized. At the end of the first stage the electrical resistance of the channel between the electrodes drops sharply. Under these conditions the beginning of the second (spark) stage of discharge requires the presence of some voltage between the electrodes.

Energy is not stored in a capacitor in a low-voltage induction ignition system. The discharge between the electrodes of an electroerosion spark plug is inductive.

The first, preparatory stage of the low-voltage discharge takes place in the material of the semiconductor and is therefore practically independent of the parameters of the medium in which the discharge occurs.

Electroerosion spark plugs have silver (possibly made of nickel, of a palladium-silver alloy) central and side electrodes adjacent to a

sinoxal ceramic insulator. On the surface of ceramic insulator, which is the spark gap, is applied by the electroerosion method, the atomized material of the electrodes. The quality of these processes governs the efficiiency of erosion spark plugs. At the initial moment of starting the spark plug is subjected to ""conditioning" -- the ignition system is turned on prior to the delivery of fuel.

CHAPTER 6. ELECTRICAL POWER SOURCES

§13. Storage Batteries

Storage batteries are essential in any starting system both as the source of electricity for the starters and for other accessories and components of the starter control system.

Storage batteries convert the electricity supplied to them during charging into chemical energy and accumulate the latter to a certain limit. Then, during discharge, when the battery delivers current to the consumers, the chemical energy is converted back to electricity.

Storage batteries can be divided into the on-board and ground types, depending on purpose. Storage batteries used for starting engines should have good efficiency at high power levels.

The starting properties of storage batteries are determined by internal resistance, which should be very low (should not exceed hundredths of an ohm).

Basically lead-acid batteries were used in aviation until recently. The chief disadvantages of such batteries are short service life and relatively high specific weight.

Silver-zinc storage batteries began to be used recently for starting gas turbine engines. The positive electrode of these batteries is the oxide or dioxide of silver, and the negative electrode is a mixture of zinc and zinc oxide. Potassium hydroxide with a density of 1.33-1.54 g/cm^3 is used as the electrolyte.

The chemical reactions that occur in such a storage battery are expressed by the following equations:

during first charge

$$Ag+2KOH+H_2O+2Zn \rightarrow AgO+2KOH+2Zn+H_2;$$

during first discharge

$$AgO+2KOH+2Zn+H_2O \rightarrow Ag+K_2ZnO_2+Zn(OH)_2+H_2.$$

It is clear from these equations that the positive electrode is oxidized in the storage battery during the first charge, and potassium zincate which, as it dissolves in water, saturates the electrolyte with zinc, is formed during the first discharge.

The reversible reactions that occur during successive charges and discharges of the storage battery proceed by the equation

$$Ag+Zn(OH)_2 \rightleftarrows AgO+H_2O+Zn.$$

Here the left hand side expresses the condition of the storage battery in the discharge state and the right hand in the charge state.

When the storage battery is completely charged the positive electrode consists of silver oxide and the negative of metallic zinc. But when the storage battery is discharged oxygen is transported from the positive to the negative electrode and there oxidizes zinc to zinc oxide and zinc hydroxide.

Silver-zinc storage batteries are manufactured as individual cells, placed in individual plastic vessels (Figure 29). The cells are assembled into bundles of flat alternating positive 5 and negative 4 electrodes. Onto these electrodes is pressed a powdery active mass. Current-conducting leads run from the positive and negative electrodes individually to positive 1 and negative 2 terminals, respectively.

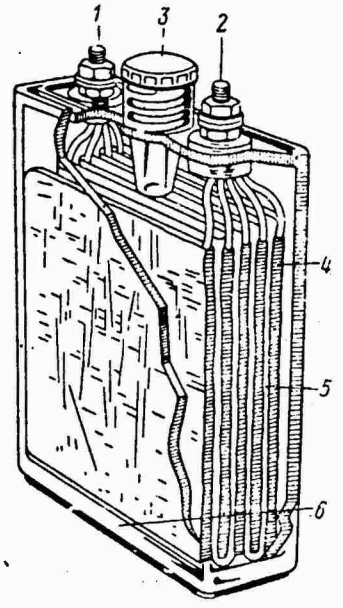

Figure 29. Cross section of silver-zinc storage battery cell: 1 -- positive terminal; 2 -- negative terminal; 3 -- fill and vent hole with cap; 4 -- negative electrode; 5 -- positive electrode; 6 -- casing.

The voltage discharge curves of the silver-zinc storage battery have a rather long level horizontal segment, on which the voltage level depends only on the discharge current. The comparative discharge characteristics at a current of 400 a (Figure 30) show that the silver-zinc storage batteries provide much higher voltages and discharge capacitances than lead-acid and cadmium-nickel batteries. After normal charging, silver-zinc storage batteries provide up to 90-95% capacitance and 80-90% power.

The installation of silver-zinc batteries on aircraft instead of lead-acid batteries yields substantial gains in weight, space and number of possible starts.

The chief disadvantages of silver-zinc storage batteries are: high cost, comparatively short service life, no possibility for fast charges at constant voltage, sensitivity to overcharging, etc.

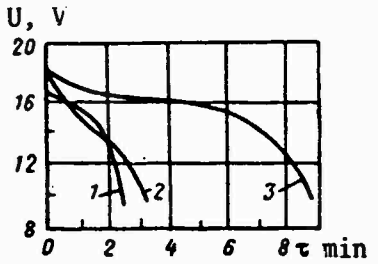

Figure 30. Discharge characteristics of storage batteries at 400 a current: 1 -- discharge curve of lead-acid storage battery; 2 -- discharge curve of cadmium-nickel storage battery; 3 -- discharge curve of silver-zinc storage battery.

§14. Electrical Power Units

Electricity can be obtained from generators powered by different types of engines. The generator and engine powering it form an electrical power unit. These units are usually installed on automotive chassis. On large aircraft the electrical power unit is an on-board system.

The electrical power unit installed on an automotive chassis consists of a gasoline engine, dc generator and storage battery. A schematic diagram of the electrical equipment of such a unit is illustrated in Figure 31.

The sources of current are generator 26 and storage battery 21. When knife switch 23 is switched to the right hand (on the diagram) terminals only current from the storage batteries can be "taken" from the right hand terminals, and from the other terminals, only generator current. For this reason, with the aid of a special device installed at the consumer, both parallel and series connection of the batteries and generator are possible. When knife switch 23 is switched to the left hand terminals current can be drawn either from the storage batteries (with the generator shut down) or from the storage batteries working with the generator. When knife switch 23 is placed in the middle position the storage battery is cut off both from the generator and from the right hand terminals.

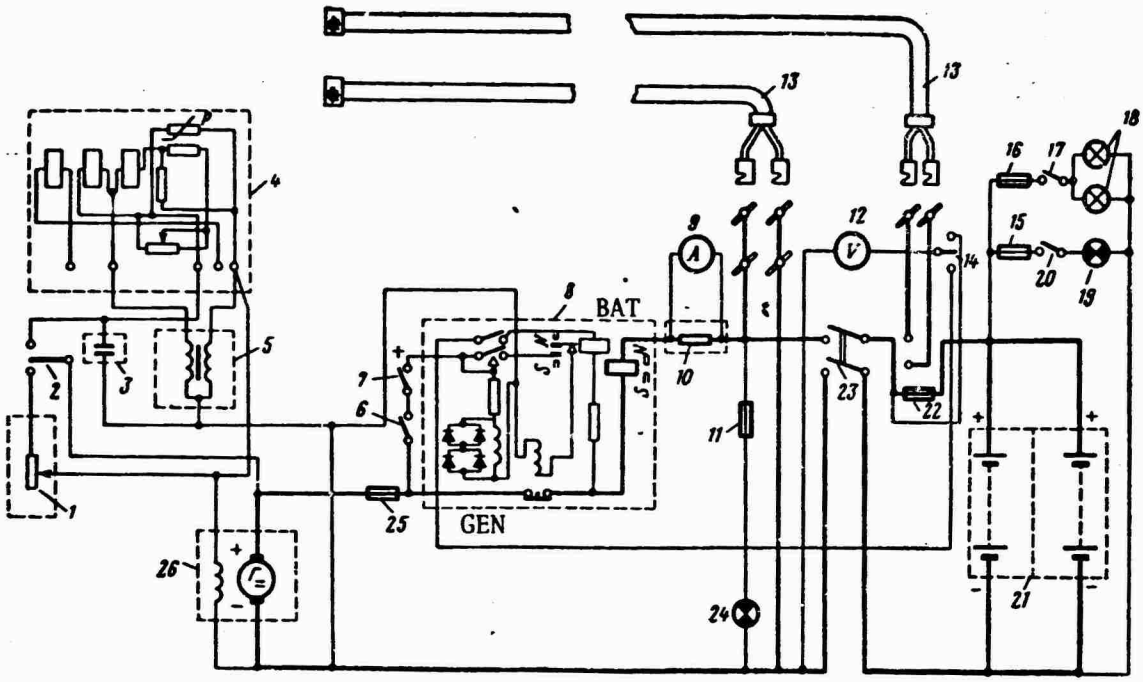

Figure 31. Schematic diagram of electrical equipment of APA-7 power unit: 1 -- rheostat for manual control of generator voltage; 2 -- switch for manual and automatic control of generator voltage; 3 -- capacitor; 4 -- automatic generator voltage regulator; 5 -- stabilizing transformer; 6 -- generator switch into circuit; 7 -- emergency generator switch from circuit; 8 -- differential minimal relay; 9 -- ammeter; 10 -- ammeter shunt; 11, 15, 16, 22 and 25 -- safety fuses; 12 -- voltmeter; 13 -- aircraft consumer power cable; 14 -- voltmeter switch; 17 and 20 -- off switches; 18 -- unit control panel illuminating lamp; 19 -- boundary light; 21 -- storage batteries; 23 -- dipole tumbler knife switch; 24 -- lamp signaling switching of generator into circuit; 26 -- generator.

The voltage on the generator terminals can be regulated automatically or manually. Manual voltage regulation is accomplished with the aid of slide rheostat 1 and is permissible only when the power unit is operating with a long-term constant load. Automatic generator voltage regulation is accomplished (for all cases of variable loading) with carbon regulator 4, operating along with stabilizing transformer 5 and capacitor 3.

CHAPTER 7. MECHANISMS FOR COUPLING THE STARTER WITH THE ENGINE ROTOR

For starting it is essential to connect the starter to the engine at the initial moment and to turn it off when the engine reaches the rpm that ensures independent running to the low rpm mode. Such operations are performed automatically by special coupling mechanisms installed between the starter and the engine rotor. Ratchet clutches, free running clutches and fluid couplings are commonly used as the coupling mechanisms on gas turbine engines.

The ratchet clutch (Figure 32) consists of two parts (internal and external), connected by ratchets. External part 5 of the clutch is connected to the starter and internal part 1 is connected through an intermediate shaft to the engine rotor.

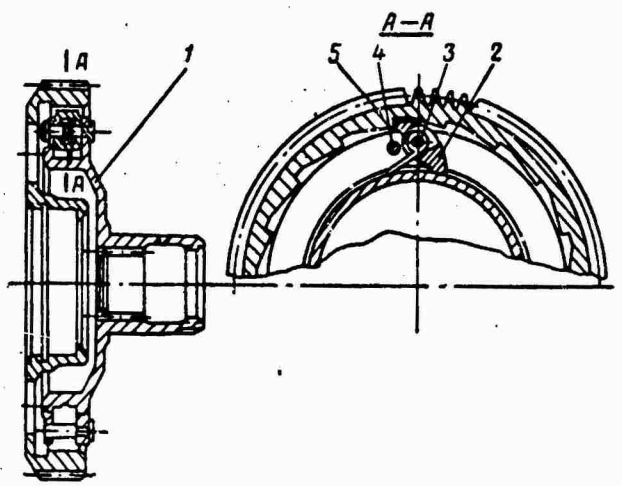

Figure 32. Ratchet clutch: 1 -- internal part; 2 -- ratchet; 3 -- spring; 4 -- detent; 5 -- external part of clutch.

At the initial starting period the ratchets, by the action of springs 3, engage the cogs of the external part of the clutch, thereby transmitting torque. At a certain engine rpm the centrifugal force of the ratchets

overcomes the tension of the springs and the friction between the ends of the ratchets and the cogs of the external part of the clutch. The ratchets are retracted into a groove in the internal part of the clutch and the starter is disengaged from the engine.

The free running clutch (Figure 33) provides smooth engagement of the starter with the engine rotor. It consists of carrier 1, separator 4, with rollers 2, limiting ring 3 and band 6. This clutch transmits torque only when the rollers are wedged between the chamfers of the carrier and band. The rollers become wedged at rpm's that are greater than the rpm of the carrier engaged with the engine rotor. When the engine rpm exceeds the rpm of the band the rollers are unwedged and the starter is disengaged from the engine.

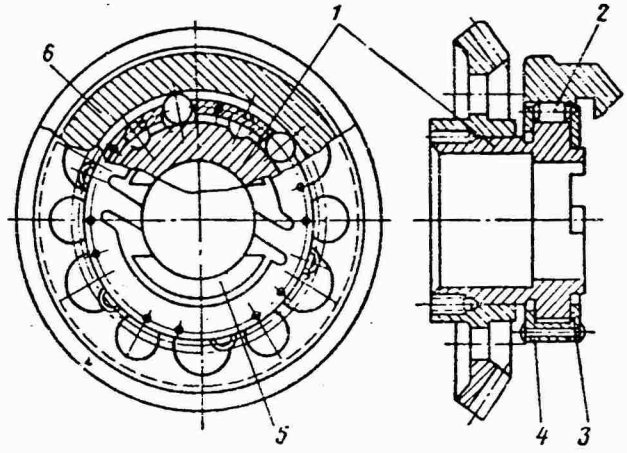

Figure 33. Free running clutch: 1 -- carrier; 2 -- roller; 3 -- ring; 4 -- separator; 5 -- carrier protrusions; 6 -- band.

The fluid coupling provides rapid turning of the turbostarter rotor and continued operation in the design mode at practically constant rpm, and also smooth engagement of the working starter with the engine. The working medium in fluid couplings is the oil on which the engine operates.

During the process of start-up and acceleration of the turbostarter oil is not admitted into the fluid coupling. When almost maximum rpm is attained the oil begins to enter the fluid coupling and the engine rotor begins to accelerate. During the engine starting process the flow of oil to the fluid coupling should be kept constant by means of a special regulator. Here the torque transmitted by the clutch is maintained constant and the power on the starter drive shaft increases in proportion to engine rotor rpm.

The fluid coupling (Figure 34) consists of a body, made of two halves: driving 4 and driven 6. The driving half of the coupling body rotates on a shaft on sliding bearing 1 and is connected through a system of gears to the starter shaft. The driven half is connected through a system of gears to the engine rotor.

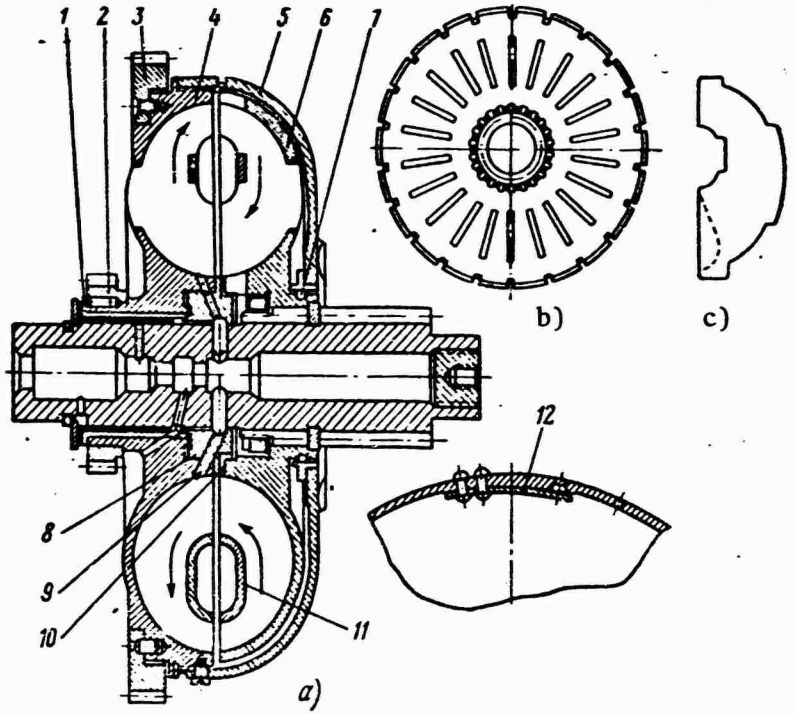

Figure 34. Fluid coupling: a -- cross section of coupling; b -- view of coupling body without vanes; c -- vane of fluid coupling; 1 -- sliding bearing; 2 -- pinion; 3 -- gear; 4 -- driving half of coupling body; 5 -- housing; 6 -- driven half of coupling body; 7 -- hub ring; 8 -- transition bushing; 9 -- retainer; 10 -- adjustment ring; 11 -- internal sesqui-ring; 12 -- plate valve.

Each half of the fluid coupling body is a sesqui-ring with radial vanes. When placed together with the open sides facing each other the halves of the fluid coupling form annular cavities in cross section. The coupling is enclosed by casing 5.

Oil is forced into the fluid coupling through a series of holes in bushing 8. There are four openings in casing 5. Three of the orifices, covered by plate valves 12, drain oil from the fluid coupling when it is disengaged. The plate valves are forced against the housing under the influence of centrifugal forces and close the orifices. When the starter is disengaged and its rpm decreases they are forced away from the housing and the oil drains from the fluid coupling. The fourth orifice is used for constant pumping of oil through the fluid coupling for the purpose of cooling it.

After the cavity of the fluid coupling is filled with oil, the driving half operates as a pump and the driven half as a turbine. As the driving

part of the fluid coupling (pump) rotates, the oil is put into motion in the radial direction under the influence of centrifugal forces. The extra motive force acquired by the oil at the exit from the pump is transmitted to the vanes of the driven part (turbine), forcing them to rotate. The oil extracted from the cavity of the driven part returns to the vanes of the driving part. Thus the oil circulates in the radial direction.

During circulation part of the energy acquired by the oil in the pump is lost to fluid friction, friction against the channel walls and friction of impact on the vanes. Because of these losses the driven part of the fluid coupling, i.e., the turbine, always has a smaller rpm than the driving pump part.

CHAPTER 8. FUEL APPARATUS OF GAS TURBINE ENGINE STARTER SYSTEM

Some gas turbine engines have an independent system for forcing starter fuel into the combustion chamber, which operates only during the starting process. After the engine reaches the prescribed rpm, or after a certain operating time, it shuts off automatically.

The starter fuel system consists of the following basic components: fuel tank, starter pump, filter, starter injectors, igniters, starter fuel manifold and automatic control equipment (starter fuel distributors, automatic start-up fuel system, fuel pump-regulator).

Starter fuel pumps are driven by an external power source (electric motors) and are of the rotary or gear type. The rotary type fuel pump (Figure 35) consists of three basic parts: fireproof series excitation motor, reducer and the pump itself.

The pump rotor, driven by the motor, has four working vanes 1, one end of which rests on central pin 2 and the other on the internal cylindrical surface of the pump housing. The pump housing is eccentric relative to the journals. As the motor turns the pump rotor, the vanes carry fuel from the suction side of the pump and force it into the discharge cavity of the pump, whence the fuel enters the fuel line leading to the injectors. The prescribed fuel pressure is maintained in the pump by bypassing excess fuel through reduction valve 3, which is under tension by spring 4; the tension on the spring is adjusted by means of a set screw.

The gear type starter fuel pump (Figure 36) consists of a fireproof DC series excitation electric motor, the pump itself and a terminal box.

The pump motor is connected in parallel to the starter winding blocks and operates simultaneously with the ignition system. The motor shaft is connected to the driving shaft of the pump by means of a coupling.

The pump consists of housing, cap, pumping assembly and reduction valve. The motor, through the coupling, imparts rotation to the pump drive shaft and driving gear. From there rotation is transmitted to the driven

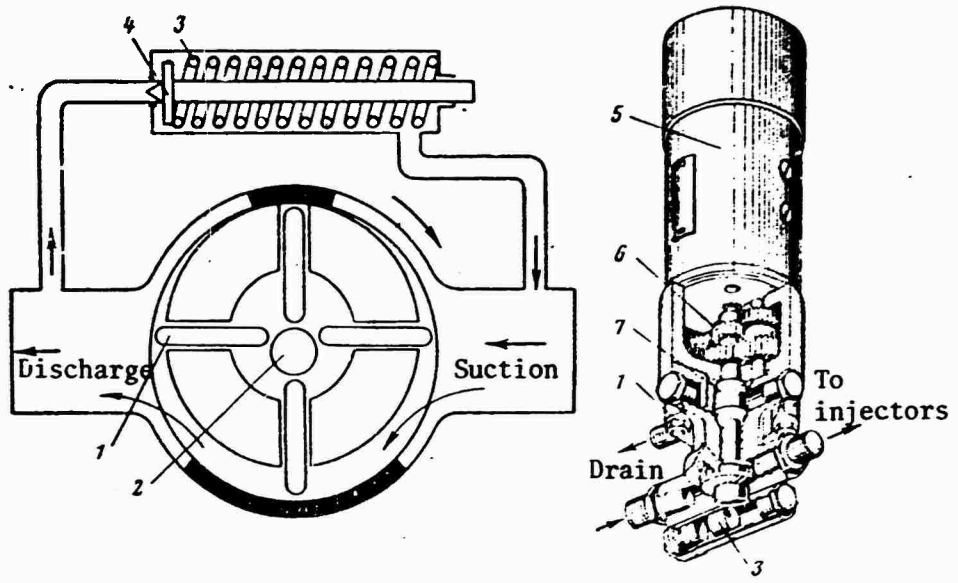

Figure 35. General view and diagram of operation of rotary type starter fuel pump: 1 -- vanes; 2 -- central pin; 3 -- reduction valve; 4 -- reduction valve spring; 5 -- motor; 6 -- reducer (i = 1/4); 7 -- eleastic coupling.

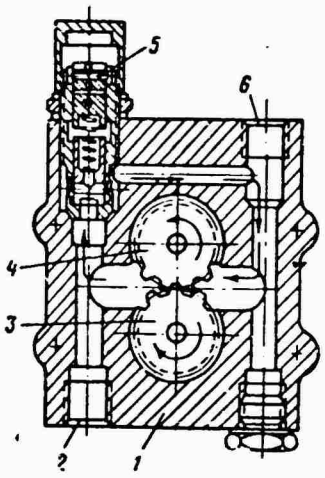

Figure 36. General view and diagram of operation of gear type starter fuel pump: 1 -- pump; 2 -- socket for fuel fitting to injectors; 3 -- driven gear; 4 -- driving gear; 5 -- reduction valve; 6 -- socket for fuel line fitting from starter tank.

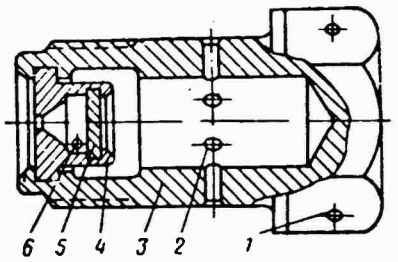

Figure 37. Starter injector of gas turbine engine: 1 -- mounting holes; 2 -- fuel intake orifice; 3 -- body; 4 -- atomizer; 5 -- floor of turbulence chamber; 6 -- nozzle orifice.

gear. The gear teeth on the suction side, as they leave engagement and expose the spaces between them, create a partial vacuum, under the influence of which the fuel enters the pump, fills the spaces between the teeth and is transported to the discharge side. Here the fuel is forced into the pressure line by the teeth going into mesh.

The starter injectors are used to obtain the required fuel-air mixture qualities. Most commonly used in starter systems are injectors with centrifugal atomization. These injectors provide a fine spray and short flame. The injector (Figure 37) consists of body 3 and atomizer 4. The stream of fuel, passing through tangentially arranged orifices, is twisted and forms a hollow flame at the exit from the central orifice.

Starter injectors are installed in starter igniters. The starter igniter (Figure 38) consists of a spark plug, starter injector, body and control mechanism -- solenoid valve. The walls of the spark cavity of the igniter, having several small orifices for air intake, protrude into the combustion chamber between the fire tube and the chamber walls.

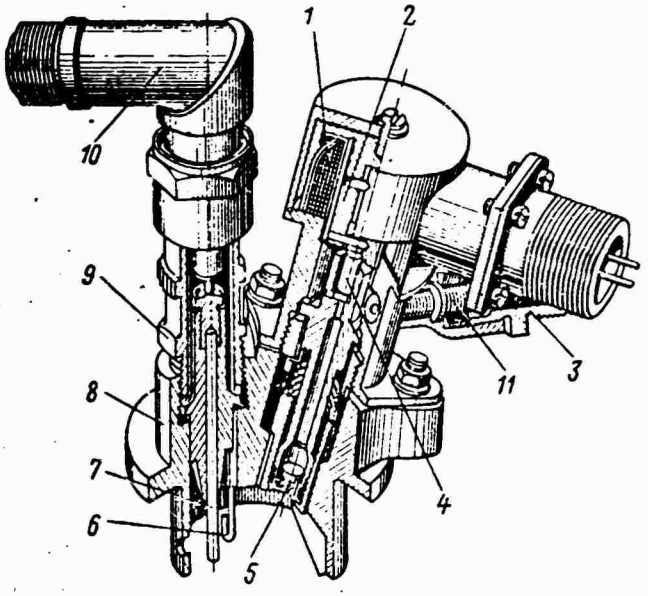

Figure 38. Start-up igniter: 1 -- solenoid winding; 2 -- core; 3 -- fitting for fuel line to injector; 4 -- solenoid needle valve; 5 -- starter injector swirler; 6 -- side electrode; 7 -- central electrode; 8 -- igniter body; 9 -- spark plug; 10 -- spark plug elbow; 11 -- filter.

During start-up of the engine the fuel passes through filter 11 and reaches needle valve 4 of the solenoid valve. When the solenoid circuit is closed the movable core lifts the needle and permits the fuel to enter injector swirler 5. The atomized spray is mixed with air entering the spark cavity and the resultant mixture is ignited by the spark plug. The flame that results is directed into the combustion chamber of the engine.

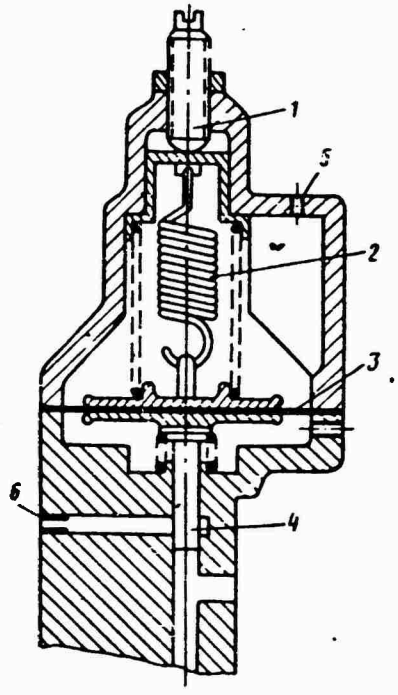

Figure 39. Automatic start-up fuel regulator (ASR): 1 -- adjustment screw; 2 -- spring; 3 -- membrane; 4 -- stem; 5 -- jet; 6 -- drain hole (jet).

The start-up fuel regulator (Figure 39) is designed to control the delivery of fuel during the automatic start-up process. The start-up fuel regulator, in terms of its operating principle, is a reduction valve of variable tension.

On shaft 4 of the start-up regulator, on whose position depends the amount of fuel bypassed, and consequently the pressure of the fuel in front of the engine injectors, act the fuel pressure, spring 2 and through membrane 3, air pressure behind the compressor.

The required fuel supply program is ensured during start-up by adjusting the start-up fuel regulator. The adjustment is made by changing the tension of spring 2 by means of set screw 1 and by changing the pressure in the air cavity of the start-up fuel regulator by releasing air through removable jet 5. At low rpm, when the pressure behind the compressor is low, the amount of fuel supplied is determined by the tension on spring 2, and at high rpm by the size of the orifice in the removable jet.

To limit the amount of fuel bypassed by the automatic regulator during in-flight start-up, jet 6 is installed in the drain fitting.

The purpose of the fuel pump (Figure 40) is to feed the required amount of fuel to the working injectors of the engine. The pump rotor is rotated through spring 1 by the engine rotor. The pump rotor has several plungers 4, one end of which rests on the bearing ring of an inclined washer, and the other on the spring.

When the slope of the washer changes, the capacity of the pump changes due to displacement of the piston of servo 6. The minimum and maximum capacities are limited by the corresponding stops.

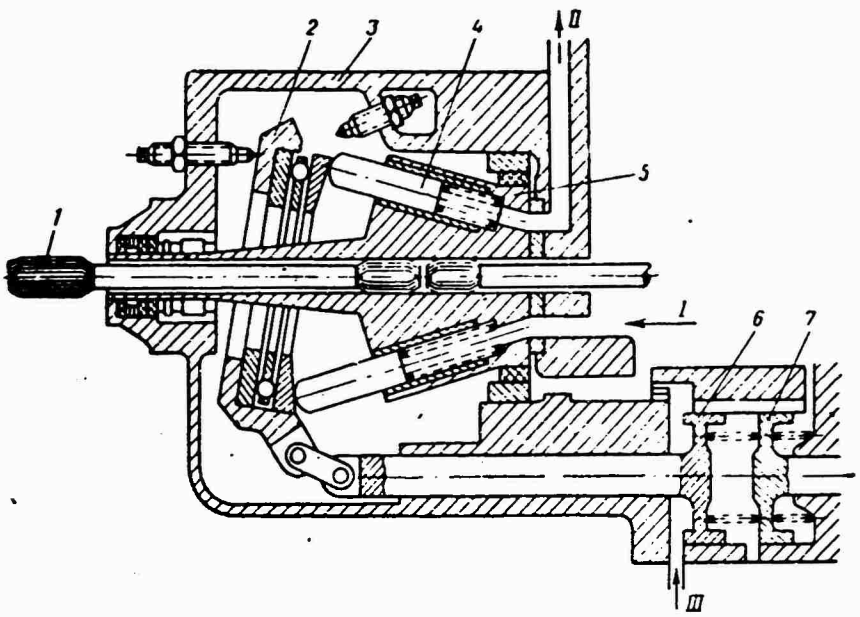

Figure 40. High-pressure plunger pump: 1 -- spring; 2 -- disc; 3 -- body; 4 -- plunger; 5 -- rotor; 6 -- inclined disc servo; 7 -- feedback servo piston; I -- fuel to pump; II -- fuel to throttle valve; III -- fuel from ASR.

PART TWO. ENGINE STARTING ON THE GROUND

CHAPTER 9. PROCESSES TAKING PLACE DURING ENGINE START-UP

The following are essential for engine start-up: the processes inherent to gas turbine engines must proceed stably in the combustion chambers; the fuel-air mixture must be ignited; all engine components must operate stably in unsteady modes during acceleration of the rotor to the low rpm mode.

We will examine the features of the above-stated processes during on the ground starting of an engine.

§15. Processes Taking Place during Preliminary Acceleration of Engine Rotor

The creation of combustion chamber conditions under which the processes inherent to the gas turbine engine can begin to proceed stably begins during cold motoring of the engine by the starter. The fuel cock is opened to the combustion chambers at the same time the starter button is pressed (and sometimes before and after the starter button is pressed). As the rpm of the engine rotor, and consequently of the fuel pump driven by the engine shaft increase, the fuel pressure increases on the discharge side of the pump, and all the fuel lines leading to the working injectors are gradually filled with fuel.

The fuel begins to enter the combustion chamber under pressure, which is sufficient for satisfactory atomization, as a rule, only by the end of the first start-up stage. The fuel-air mixture is formed as a result of mixing of air and atomized fuel. The character of mixing depends on the features of delivery of air and fuel to the combustion chamber.

The mixing process takes place in the primary zone of the combustion chamber, into which air is admitted through a special frontal device. The rest of the air entering the combustion chamber passes through openings on the side wall of the flame tube into the secondary mixing zone.

The frontal apparatus restricts the amount of air entering the primary zone and creates the required air pressure in it. Consequently a circulation zone with regions of back and forth air flows is formed in the

front part of the flame tube (Figure 41). The zone of back currents occurs in the middle of this circulation zone. Back flow is created in the flame tube of the combustion chamber by rarefaction caused by discharge of the basic mass of air admitted through the swirler of the frontal apparatus to the periphery. This back flow ensures flame stabilization in the flame tube after ignition of the fuel-air mixture.

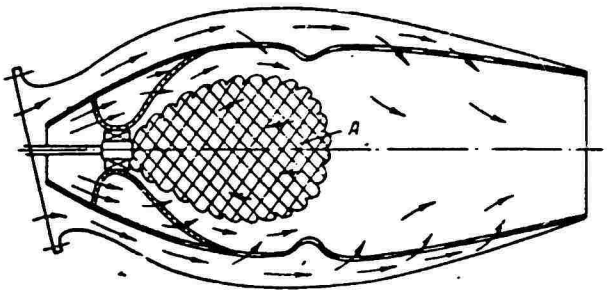

Figure 41. Diagram of air flow in individual combustion chamber: A -- circulation zone.

The pattern of air velocities in the flame tube of a combustion chamber with a swirler (in the absence of combustion) is depicted schematically in Figure 42. The flow character is qualitatively the same during fuel combustion. As conditions change, the general dimensions of the back flow zone (length, cross section) change only slightly.

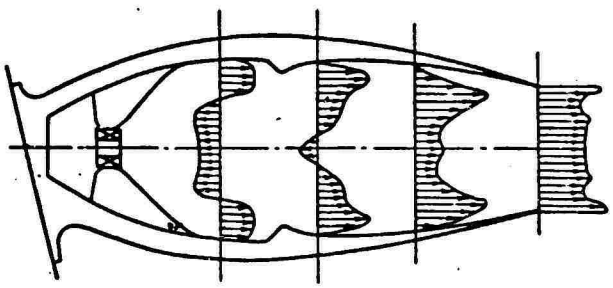

Figure 42. Schematic diagram of air velocities in various sections of individual combustion chamber.

The structure of the circulation zone in an annular combustion chamber differs substantially from that in an individual combustion chamber. The annular combustion chamber has an annular counterflow zone in contact at the top and bottom with annular forward flows. In an individual combustion chamber the counterflow zone fills the central part of the flame tube, outside of which is an annular straight flow. This difference in flow structure leads to different mixing processes in the annular and individual combustion chambers. The annular combustion chamber has certain advantages over the individual type in the starting modes.

The structure of the air flow and boundaries of the circulation zone in an annular combustion chamber, as in individual combustion chambers, do not depend on the air flow rate through the chamber, but are determined basically only by combustion chamber design, especially the design of the frontal apparatus.

The fuel distribution between the circulation zone and the straight flow is determined largely by the root angle of the fuel spray flame, fineness of atomization, fuel feed pressure and flow characteristics in the circulation zone. In the general case the larger the root angle of the flame, higher the fuel feed pressure and lower the quality of fuel atomization, the more fuel will enter the straight flow region.

Near the flame tube wall, as a rule, the fuel concentration is very low and the flame cannot propagate in such a mixture. The largest fuel droplets go into this zone; they have no bearing on the combustion process in the flame tube. The most favorable conditions for combustion of the mixture are created in the circulation zone: here the flow velocities are low and the fuel is well atomized.

The duration and character of mixing also depend on the process of atomization of the fuel forced by the injector into the engine combustion chambers into droplets. The characteristics of the working injector predetermine to a great extent the starting properties of the combustion chamber.

Centrifugal injectors of various designs (open, closed, single-channel, dual-channel, etc.) are generally used for the delivery of fuel into combustion chambers.

Because of the swirlers in centrifugal injectors the fuel acquires straight-line and rotary motion as it leaves the injector nozzle exit, with the result that the stream emerging from the injector nozzle acquires the form of a hollow cone. The thickness of this fuel cone diminishes by measure of distance from the nozzle, and then the cone breaks up into individual droplets. The droplets formed as a result of break-up of the fuel cone possess inertia: large droplets continue to travel for some time in a trajectory that depends on the direction and velocity which they had at the injector exit; fine droplets, however, are immediately captured by the air flow and mix with it.

When selecting the fuel injectors that are to be used, care is taken to ensure that most of the trajectory of the fuel in the fuel cone will fall within the counterflow zone. It is no less important to ensure good atomization of the fuel at the low fuel pressures that exist ahead of the working injectors, and which are characteristic of the starting conditions. The character and degree of atomization of the fuel in an engine depend also on the viscosity of the fuel and the conditions of the medium into which the fuel is sprayed. The quality of fuel atomization by the working injectors decreases as the viscosity of the fuel increases in cases where more viscous grades of fuel are used, or because of cooling of the fuel.

§16. Formation of Starting Flame

The fuel-air mixture that is formed in combustion chambers must be ignited before an engine can be started. Various sources of heat energy can be used for ignition of the mixture. The most commonly used, however, are electrical sources (spark plugs), which discharge thermal energy between electrodes.

The greater the radius of the initial flame source, the higher the temperature in it and the lower the thermal conductivity of the gas, the higher will be the igniting capacity of the spark between the spark plug electrodes. These parameters depend both on the ignition system and on the parameters of the air and fuel composition in the spark plug zone. Igniting capacity also depends on the heat energy released by the discharge and combustion of the mixture in the zone of the spark plug electrodes. It may be assumed in the first approximation that the ignitability of a mixture is determined by the average spark power at moderate electrical discharge energies.

The fuel-air mixture can be directly ignited in combustion chambers by a sufficiently powerful electrical discharge. This requires only the proper choice of location of the spark plug and exact determination of the spark power required for ignition.

In order to choose the location of the spark plug it is essential to know the laws of aerodynamic interaction of the fuel stream with the air passing through the combustion chamber. The precise laws of such interaction cannot be established, since not all the factors and conditions that influence this interaction are always known. It is clear, however, that there are always zones in a combustion chamber with a predominance of air, zones with a predominance of fuel and zones that are intermediate between them. Accordingly the composition of the mixture will be different at each point of each cross section of the combustion chamber. And it is always possible to find places in a combustion chamber where the conditions for ignition and combustion will be optimal throughout the entire chamber. When determining the location of the spark plug it is necessary to consider the temperature field in all modes of engine operation and the conditions of formation of carbon deposits, since they determine spark plug service life.

Considering the character of the fuel-air flow in combustion chambers it is possible to choose a zone with a low fuel mixture velocity and with sufficiently stable composition, in which should be placed the initial center of ignition (Figure 43). The chief advantage of such ignition is its design simplicity. Disadvantages are the limited choice of spark plug location and difficulty of cooling the spark plug in the basic operating modes, since under these conditions the spark plug is exposed to high-temperature gases.

The spark power required for igniting the mixture depends on many factors, chief among which are the composition of the mixture, pressure,

temperature, homogeneity, turbulence, etc. In the case of substantial deviation of these factors from the optimal values the spark energy required for ignition may increase several fold. Moreover, this power is affected by the orientation of the spark plug gap relative to the fuel flame. The mixture ignites faster when the discharge between the spark plug electrodes forms on the side exposed to the fuel flame.

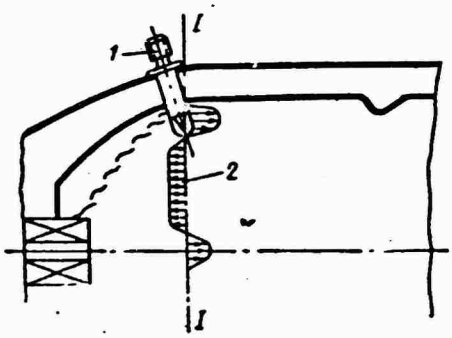

Figure 43. Location of spark plug in combustion chamber: 1 -- spark plug; 2 -- velocity field in section I-I.

Ignition systems with surface discharge spark plugs are used for immediate ignition of the mixture in the combustion chamber, since their energy depends little on the mixture parameters. However, a more commonly employed means of fuel-air mixture ignition in the combustion chamber is a flame created by starter igniters.

Starter igniters can be subdivided into three types, depending on the principle of organization of the working process: supplie' with air from the intertube channel of the combustion chamber; with an independent air source; operating on unitary fuel.

The chief disadvantage of the first type of igniters is the fact that changes in combustion chamber flow parameters influence the formation of the primary combustion center and flame.

Igniters of the second type provide a starting flame with any penetrating capacity, regardless of combustion chamber conditions.

The chief advantage of the third type of igniters (pyrocartridges for example) is that igniter operation does not depend on surrounding conditions.

A single-stage centrifugal injector and spark plug are installed on the igniter body. The inner cavity of the igniter has an ordinary system of screens and deflectors, which divert the flow into a certain direction. The main fuel is usually supplied to the igniters, but sometimes it is a special fuel (gasoline).

At a constant fuel flow rate through the injector of the igniter its start-up properties are determined basically by the fuel flow rate through it. The following relation can be used to calculate flame temperature at the igniter nozzle exit:

$$T_f = T_{\text{в}} + \Delta t_f,$$

$$\Delta t_f = \frac{H_u \xi_a}{\left(\frac{\alpha_a}{\Sigma} L_0 + 1\right) c_{pf}},$$

where α_a is the coefficient of excess air in the igniter;

Σ is the degree of fuel evaporation;

ξ_a is the coefficient of fuel combustion completeness in igniter;

c_{pf} is the average heat capacity of combustion products at igniter nozzle exit.

Igniter flame penetration into entraining flow is determined by the relative dynamic head

$$\bar{q} = \frac{q_f}{q} = \frac{\gamma_f W_f^2}{\gamma W^2},$$

where q_f is the dynamic head of the flame at igniter nozzle exit;

q is the dynamic head of the flow incident on the flame.

Flame penetrability for the given combustion chamber and igniter is determined basically by the temperature of the gas at the igniter nozzle exit. For a given fuel and constant rate of evaporation, and also constant combustion completeness, the gas temperature at the igniter exit will be a function only of the coefficient of excess air in the igniter. Since the fuel flow rate is usually maintained constant for igniters, the maximum gas temperature at the nozzle exit can only be achieved with a specific air flow rate (Figure 44). An increase or reduction of the air flow rate is accompanied by a reduction of this temperature.

Any starter igniter is characterized by a starter characteristic, usually defined as the range of flow velocities at the intake into the combustion chamber diffuser and range of excess air coefficient in the igniter, for which it operates stably (Figure 45). As in main combustion chambers, as the air pressure decreases, the working range of starter fuel feed pressures narrows and the limiting air velocity in the combustion chamber at which formation of a flame in the igniter is possible, drops simultaneously. At a certain pressure the range of stable operation is so narrow that this pressure is limiting for the given igniter.

Depending on the location of the igniter air intake, flow structure in it and mutual location of the injector and spark plug, the starting qualities of igniters may fluctuate within wide limits.

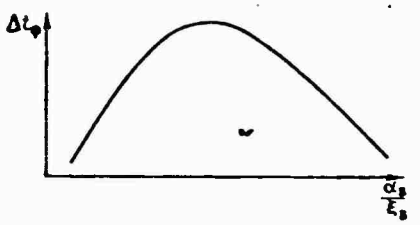

Figure 44. Flame temperature as function of mixture composition in starter igniter.

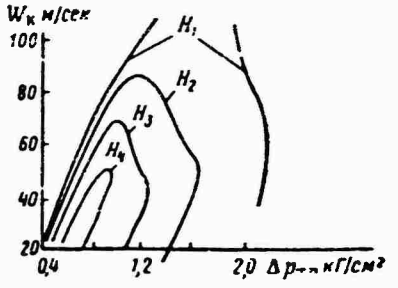

Figure 45. Starter characteristics of igniter: $H_1 < H_2 < H_3 < H_4$.

Igniter efficiency is determined by the temperature, depth of penetration of its flame into the fire tube and its location in the chamber. These factors depend on the composition of the mixture in the igniter and perfection of the working process in it. The air flow rate through the igniter depends substantially on the location of the manifold ports through the height of the channel and their location relative to the flow in the zone between the outer housing of the combustion chamber and the flame tube. The starter igniter is installed in such a way that its flame will reach into the zone where the velocities and thickness of the entraining flow layer, and also pulsation velocities are minimal and the fuel concentration sufficiently high.

It is known from experience in engine operation that igniters of the same series have different starting properties. The starting properties of igniters may differ from each other both in terms of the air excess coefficient and in terms of flow velocity by a factor of 1.5-2. The difference in characteristics is attributed to technological deviations tolerated in the production of the igniters, deviations in the characteristics of their injectors and other factors.

§17. Flame Propagation in Combustion Chambers

We will examine the conditions that are essential for the propagation of a flame from the flame source through the entire volume of the fuel-air mixture in combustion chambers.

In the initial spherical volume of the mixture, where the electrical discharge takes place, the amount of heat released is

$$Q_1 = \frac{4}{3}\pi r^3 q, \tag{9.1}$$

where r is the radius of the sphere;
q is the amount of heat liberated per unit volume of gas.

The heat liberated from this volume is

$$Q_2 = 4\pi r^2 \lambda \frac{\partial \theta}{\partial r} d\tau, \qquad (9.2)$$

where λ is the coefficient of thermal conductivity;
$\partial\theta/\partial r$ is the temperature gradient.

The larger the ratio Q_1/Q_2 the greater the possibility of flame propagation. As seen from equations (9.1) and (9.2), the greater the radius of the sphere the larger this ratio will be.

As a result of ignition and combustion of the fuel-air mixture the pressure increases in the starting igniters. The resulting pressure drop between the combustion chamber of the starter igniter and the combustion chamber of the engine causes hot gases to escape from the starter igniter into the hot part of the combustion chamber (in sectional and annular tube combustion chambers, through flame transfer pipes).

Successful flame propagation in combustion chambers depends on the ignitability of the departing flame (its kinetic energy and geometric dimensions) and characteristics of the mixture in the circulation zone of the cold flame tube and of the flow in the combustion chamber.

Flame kinetic energy is determined by the temperature in the flame tube, wherein the combustion process proceeds, and its temperature by the amount of air that mixes with the hot gases in the cold combustion chamber in the straight current zone. The geometric dimensions of an ignited flame with a constant pressure drop between flame tubes is affected only by the effective cross section of the flame transfer pipe. The effective cross sectional area of the pipe is selected so as to ensure satisfactory flame transfer in the required range of flight altitudes and velocities and cooling of the combustion chamber wall beyond the pipe.

The flame is capable of reliable ignition of the fuel-air mixture in the engine combustion chambers only if it penetrates into the zone of back currents of the circulation zone. A starter igniter flame that does not penetrate into the zone of counter currents and therefore remains entirely in the straight current zone, will ignite the fuel-air mixture on the periphery of the flame tube, but cannot create stable combustion of the mixture in the entire flame tube volume. This is attributed to the fact that the flame is constantly carried away by the flow, which travels at high velocity in the straight current zone.

The composition of the fuel mixture and quality of mixing determine the conditions for mixture ignition and flame propagation in the entire volume of the combustion chambers.

Fuel combustion is possible at certain fuel vapor-air ratios.

Complete combustion requires preliminary evaporation of the fuel, and then mixing of the fuel vapors with air in certain ratios. The time of preparation of the fuel-air mixture, which has the corresponding ignition limits, depends on the rate of evaporation, and on this time depends, at certain mixture velocities in the combustion chambers, the possibility of its combustion within the flame tube.

Unheated fuel droplets evaporate only from the surface. Therefore the time of evaporation of fuel admitted into the combustion chambers depends on the summary area of all droplets, and the smaller the droplets of atomized fuel formed, the less this time will be. During evaporation of fuel droplets without heating only the most volatile fractions evaporate.

If the flame reaches the countercurrent zone with relatively low velocities there will be intensive evaporation of the fuel droplets. During such evaporation all fractions of the fuel will be evaporated and the composition of the resulting vapors will correspond practically to the composition of the fuel in the evaporating droplets. The fuel-air mixture is ignited first in the countercurrent zone and then the ignition process spreads to the straight current zone. Combustion of the mixture in the straight current zone is perpetuated by the center of the flame in the countercurrent zone.

After creation of a stable process of fuel-air mixture combustion in the entire flame tube volume, the igniting flame from the starting igniter becomes unnecessary. At some moment of time, therefore, the igniters, at a certain engine rotor rpm, can be turned off.

The theoretical capabilities of a combustion chamber to ignite a fuel mixture are limited to its range of stable operation. These capabilities are never realized. The degree of their realization can be characterized by the relation

$$\Omega_{st} = F_{ig}/F_{stab},$$

where F_{ig} is the area of the ignition region;

F_{stab} is the area of the region of stable chamber operation.

If the starter characteristics of a combustion chamber (Figure 46) are represented in coordinates $W_k = f(p_k)$ or $W_k = f(t_k)$, then the degree of realization of the capabilities of a combustion chamber to ignite a fuel mixture can be determined by the ratio of the area between the abscissa and starting characteristics to the corresponding area bounded by the flame-out characteristics. The value of Ω_{st} is always less than one. At the limit, when the start-up characteristics coincide with the flame-out characteristics of the chamber, $\Omega_{st} = 1$. The absolute value of Ω_{st} indicates the extent to which a proposed ignition system can take advantage of the starting capabilities of the combustion chamber.

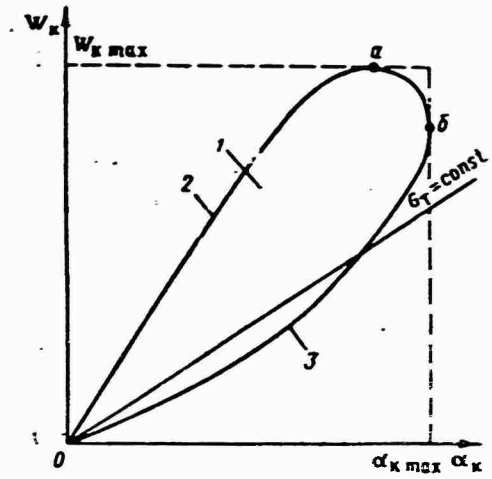

Figure 46. Starting characteristics of combustion chamber: 1 -- ignition zone; 2 -- upper boundary of ignition; 3 -- lower boundary of ignition; a -- maximum rate of stable combustion; b -- maximum coefficient α_k.

If parameters Ω_{st} are substantially less than one, then the starter characteristics of the chamber should be improved by using a better ignition system or by placing the starting igniter (spark plug) at a point more favorable for igniting the mixture. In cases when stabilization of the combustion process in the chamber is accomplished by the igniter itself, i.e., by the electrical discharge or high-temperature flame, the parameter Ω_{st} becomes meaningless.

The working mixture in the combustion chamber is heterogeneous in composition, and here the ratio between the vaporized and liquid fuel changes from one point to another.

If for a macrohomogeneous distribution of the vapor and liquid fuel $\alpha_u < \alpha_v < \alpha_l$ (where α_u and α_l are the excess air coefficients at the upper and lower concentration boundaries of flame propagation in a homogeneous mixture) and $\alpha_{li}/\alpha_v \gg 1$ (α_v and α_{li} are the fuel excess coefficients in the vapor and liquid phases), then ignition of such a mixture will be determined by the conditions of development of the initial combustion center in the gaseous medium. In cases when $\alpha_v \gg \alpha_{li}$ and $\alpha_{li}/\alpha_v < 1$, the development of the initial center will be governed primarily by the conditions of ignition of individual droplets and by the conditions of transfer of the flame from one droplet to another. Here the coarser the atomization of the fuel, the more the mechanism of ignition of a heterogeneous mixture will differ from that of ignition of a homogeneous mixture. Finally, there are also mixtures characterized by the summary coefficient of excess air $\alpha_\Sigma < \alpha_v$ and $\alpha_{li}/\alpha_v \approx 1$. In terms of both the mechanism of ignition and flame propagation, such mixtures occupy an intermediate position between the two extreme cases.

In principle the fuel-air mixture can possess any characteristics in the spark plug zone. In reality, however, in the starting regimes, when the fuel and air temperatures are low, a heterogeneous mixture will be similar to a mixture of the second class, i.e., $\alpha_v \gg \alpha_l$ and $\alpha_{li}/\alpha_l < 1$. Even if the air is saturated with fuel vapors, many grades of fuel at air and fuel temperatures corresponding to the starting regimes, cannot form homogeneous fuel mixtures. This does not mean that such mixtures cannot be ignited at low temperature.

Thus ignition of a working mixture in the combustion chamber amounts to the process of initial ignition, as a rule, of individual droplets and subsequent propagation of the flame through the entire fuel-air mixture. The combustibility of the mixture in the combustion chamber depends on the characteristics of the ignition source and characteristics of the mixture itself in the zone of the initial combustion center, almost like the ignition of a homogeneous mixture.

The flame propagates from the initial combustion center to the circulation zone, i.e., to the zone of stabilization if during the time of travel of the flame front through the primary zone it can pass from the point of ignition to the surface of the circulation zone. The condition of penetration of the flame into the circulation zone can be written in the following form:

$$\frac{w_{ci}}{U_g} \leqslant \frac{l_{ci} - x_c}{y_c - \frac{1}{2} d_{ci}},$$

where U_g is the turbulent velocity of flame propagation;

w_{ci} is the velocity of the air in the entraining flow;

y_c and x_c are the coordinates of the initial combustion center;

l_{ci} is the length of the circulation zone, measured, like x_c, from the injector nozzle;

d_{ci} is the diameter of the circulation zone.

In annular combustion chambers flame propagation through the entire volume of the flame tube depends on the characteristics of the mixture between the burners, determined by the distance (space) between the burners, length of the partitions between them and the flow rate of the air cooling them. In some engines additional jet injectors are installed to increase the flame propagation velocity.

§18. Acceleration of Engine Rotor to Low rpm Mode

After ignition and combustion of the fuel-air mixture in the combustion chambers the temperature of the gases increases in front of the turbine, affecting, as shown by equation (1.3), the power of the turbine. It can be shown that after the turbine goes into operation the magnitude of engine turbine acceleration depends on the excess fuel forced into the combustion chamber and on the power of the starter system.

On the one hand:

$$N_j = \Delta N_{t.n} + N_{s.s},$$

and on the other:

$$N_j=\left(\frac{\pi}{30}\right)^2\frac{1}{75}J_0 n\frac{dn}{dt}.$$

Then

$$\left(\frac{\pi}{30}\right)^2\frac{1}{75}J_0 n\frac{dn}{dt}=\Delta N_{t.n}+N_{s.s}.$$

Using heat supply equation

$$H_u\xi G_\tau=G_a c_{pg}(T_g^*-T_\kappa^*),$$

one can find

$$N_\tau=\frac{\left(H_u\xi\frac{G_\tau}{G_a}+c_{p\tau}T_\kappa\right)\left(1-\frac{1}{\pi_\tau^{*0.25}}\right)\eta_\tau^* G_g}{75A},$$

where A is the thermal equivalent of work.

Writing this equation for steady state and nonsteady state modes and assuming that in these modes at the same rpm the combustion completeness coefficient, air temperature behind the compressor, gas expansion ratio in the turbine and air (gas) flow rate through the engine remain the same, then

$$H_u\xi\Delta G_\tau=\frac{\Delta N_{t.n}}{75A\left(1-\frac{1}{\pi_\tau^{*0.25}}\right)\eta_\tau^*}=\frac{\left(\frac{\pi}{30}\right)^2\frac{1}{75}J_0 n\frac{dn}{d\tau}-N_{s.s}}{75A\left(1-\frac{1}{\pi_\tau^{*0.25}}\right)\eta_\tau^*}. \tag{9.3}$$

Engine rotor acceleration $dn/d\tau$ for $N_{s.s}$ = const will depend on the excess fuel supplied to the combustion chambers during acceleration compared to the fuel required for the steady state modes.

The temperature of the gases in front of the turbine depends on the ratio between the fuel and air in the combustion chambers and on the fuel combustion completeness in the flame tubes. These parameters of mixture composition and fuel combustion should ensure the maximum surplus gas turbine power in the starting regimes and stable compressor and combustion chamber operation during start-up.

By reducing fuel feed to the combustion chambers it is possible to create the conditions of stable engine operation at about 30-40% idling rpm after switching off the starter. If thereupon the temperature of the gas in front of the turbine is equal to the temperature in the steady modes of engine operation, then the turbine will drive the engine rotor without accelerating the rotor.

In order to ensure that the turbine takes part in the engine rotor acceleration in the starting regimes below the low rpm mode, it is necessary that the gas temperature in front of the turbine during start-up exceed by some magnitude the temperature of the gases during operation in the steady modes. This is the first condition for ensuring the required gas turbine efficiency under starting conditions.

The typical change of gas temperature in front of the turbine in the rpm range below the low power rpm in steady operating modes is depicted in Figure 47. As seen, at engine rotor rpm below the low rpm mode the gas temperature in front of the turbine, required for engine operation at steady state rpm, increases. Operation of individual engines at certain rpm's (at n'_c in Figure 47) in the steady state is possible only with the maximum tolerable (for the given engine) gas temperature in front of the turbine. And this means that the turbines of such engines cannot create the engine rotor acceleration required for starting below rpm n'_c unless the gas temperature in front of the turbine exceeds the maximum tolerable value. Surplus power for accelerating the engine rotor can be obtained from the turbine of such an engine only at rpm's exceeding n_c.

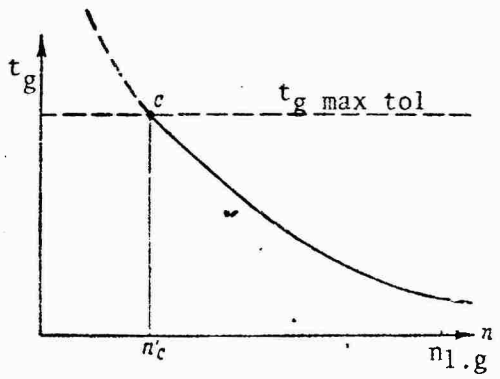

Figure 47. Typical change of gas temperature in front of turbine in steady modes: $t_{g\ max\ tol}$ -- maximum tolerable gas temperature during starting; n'_c -- minimum engine rpm in steady mode, determined by maximum tolerable gas temperature; $n_{l.p}$ -- low power rpm.

The second condition of required gas turbine efficiency under starting conditions consists in ensuring the proper flow of fuel to the engine during start-up so that the gas temperature in front of the turbine will be the maximum possible temperature from rpm n_c to almost the low power rpm. The limiting gas temperature in front of the turbine during start-up is determined either by the strength of the turbine vanes or by the possibilities of ensuring stable operation of individual engine components during start-up (primarily the compressor and combustion chamber). There are possible cases,

of course, when the maximum possible gas temperature in front of the turbine during start-up will be determined in one part of the range of start-up regimes from the point of view of ensuring reliable vane operation, and in another part, stable operation of individual components during start-up.

Figure 48 illustrates the change of temperature of gases in front of the turbine by rpm for the latter case of temperature limitation during start-up.

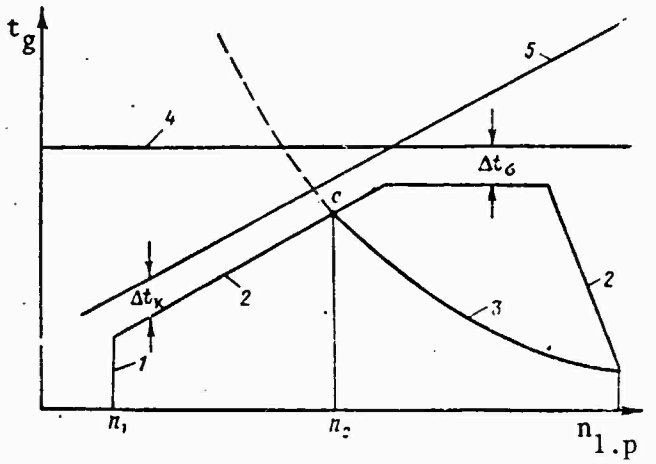

Figure 48. Change of gas temperature in front of turbine by rpm during start-up: 1 -- fuel ignition; 2 -- temperature of gases during engine start-up process (advisable law of change); 3 -- gas temperature under steady state starting conditions; 4 -- maximum tolerable gas temperature from the standpoint of strength; 5 -- gas temperature at limit of stable compressor operation; Δt_σ -- gas temperature margin, determined by the strength of turbine vanes; Δt_k -- gas temperature margin determined by stable compressor operation; n_c -- minimum rpm of stable engine operation in steady state modes, determined by stable compressor operation.

The fastest and most economical start is achieved by ensuring the maximum tolerable gas temperature in front of the turbine in the rpm range from n_1 to n_c (see Figure 48), since the engine turbine produces maximum power under these conditions. Because of the relative brevity of hot engine cranking in the above-stated rpm range and insignificance of the forces acting during this period on the turbine vanes, it is sometimes permissible, for the purpose of increasing turbine power, to have higher gas temperature in front of the turbine during starting than in the maximum engine operation

mode. Such a temperature increase is possible by ensuring stable operation of the compressor, combustion chambers and other engine components.

As a rule, however, the maximum possible gas temperature in front of the turbine during start-up is limited (especially at rpm's close to those at which the fuel-air mixture ignites in the combustion chambers) by the conditions of unstable operation of individual engine components, especially the compressor.

When the gas temperature in front of the turbine rises, the thermal resistance of the system, on which operates the compressor, increases due to the greater volume of gases passing through the nozzle and turbine stage. Therefore as the temperature of the gases in front of the turbine rises at the same engine rotor rpm the air flow rate through the compressor decreases. Also the compression ratio increases slightly in the compressor in the starting modes of engine operation. The reduced air flow rate through the compressor, naturally, also lowers the axial velocity of the air at the compressor intake.

As we know, when the axial velocity of the air in the compressor intake decreases at constant peripheral velocity of the compressor vanes, the angle of attack on the compressor vanes increases. If here the angle of attack increases to the value at which flow separation occurs the compressor will begin to operate unstably. Unstable operation is characterized by pulsations in the gas-air duct, which are audible (in some engines pulsations in the start-up modes are inaudible), reduced compressor efficiency (the air pressure behind the compressor drops sharply), and rapid increase of gas temperature behind the turbine. Because of pressure drop behind the compressor and consequently in front of the turbine, and also because of the high back pressure on the turbine due to fuel afterburning the magnitude of the pressure drop on the turbine decreases. Consequently the rate of increase of engine rpm during start-up decreases and sometimes the rpm hovers at some level.

Thus efficient engine acceleration during start-up can be achieved by supplying the quantity of fuel to the combustion chambers, which quantity is determined primarily by stable compressor operation in the starting modes and by its margin of stable operation.

Compressor stability is characterized by the stability criterion

$$K_s = \frac{\left(\frac{\pi_к^*}{G_a}\right)_{li}}{\left(\frac{\pi_к^*}{G_a}\right)_s},$$

where $G_{a.s}$; $\pi^*_{k.s}$ is air flow rate and degree of pressure increase in the compressor in steady operating modes;

$G_{a.li}$; $\pi^*_{k.li}$ are the same at the limit of stable compressor operation.

The fuel flow rate during engine start-up should ensure the following reserve of compressor stability:

$$K_{s.st}=\frac{\left(\frac{\pi_k^*}{G_a}\right)_{li}}{\left(\frac{\pi_k^*}{G_a}\right)_{st}},$$

where $G_{a.st}$; $\pi^*_{k.st}$ are the air flow rate and degree of pressure increase in the compressor corresponding to start-up conditions.

From the equation of the gas flow rate through the nozzle we obtain

$$\frac{T_{g.li}}{T_{g.s}}=\left(\frac{G_{a.s}}{G_{a.li}}\right)^2\left(\frac{\pi^*_{k.li}}{\pi^*_{k.s}}\right)^2\left[\frac{q(\lambda_{c.a})_{li}}{q(\lambda_{c.a})_s}\right]^2,$$

where $q(\lambda_{c.a})$ is the gas dynamic function of gas flow through the nozzle.

Assuming that in the starting modes at constant rpm

$$q(\lambda_{c.a})_{li}\approx q(\lambda_{c.a})_s,$$

we find from the preceding equation

$$K_s^2=\frac{T_{g.li}}{T_{g.s}} \text{ and } K_s=\sqrt{\frac{T_{g.li}}{T_{g.s}}}. \tag{9.4}$$

Analogously we obtain for the engine starting process

$$K^2_{s.st}=\frac{T_{g.li}}{T_{g.st}} \text{ and } K_{s.st}=\sqrt{\frac{T_{g.li}}{T_{g.st}}} \tag{9.5}$$

From equations (9.4) and (9.5) we have

$$T_{g.li}=K^2_s T_{g.s};\quad T_{g.li}=K^2_{s.st}T_{g.st}.$$

And then

$$T_{g.st}=\frac{K_s^2}{K^2_{s.st}}T_{g.s}.$$

The amount of heating of the air in the combustion chamber at which compressor operation becomes unstable can be found from the equation

$$\Delta T_{g.1i} = T_{g.1i} - T_{g.s} = T_{g.s}(K_s^2 - 1). \qquad (9.6)$$

Heating of the air in the combustion chamber corresponding to the actual starting process will be

$$\Delta T_{g.st} = T_{g.st} - T_{g.s} = T_{g.s}\left(\frac{K_s^2}{K_{s.st}^2} - 1\right). \qquad (9.7)$$

With K_s and $K_{s.st}$ known we can determine $T_{g.1i}$ and $T_{g.st}$ from equations (9.6) and (9.7). Very small compressor stability margins ($K_s < 1.1$) and, accordingly, small tolerable fuel flow rate surpluses necessitate seasonal adjustment of the fuel regulator and, in individual cases, manual adjustment of fuel delivery to the combustion chamber during the starting process.

Reliable automatic starting of engines with a single adjustment of the fuel system necessitates selection of a program of fuel feed to the combustion chambers and transfer of power from the starter system to the engine rotor that will ensure the required stability of compressor operation in the starting modes ($K_s > 1.1$).

We will evaluate the effect of the compressor stability margin in the starting modes on the required starter system power

$$N_{s.s} = N_j - \Delta N_t,$$

where N_j is the power spent on imparting kinetic energy to the engine rotor;

ΔN_t is surplus turbine power.

Surplus turbine power is

$$\Delta N_т = N_т - N_к = 1{,}57\, G_a T_g^* \left(1 - \frac{1}{\pi_т^{*0,25}}\right)\eta_т^* - N_к.$$

We will examine the case of acceleration of an engine with a given constant acceleration $j = dn/d\tau = \text{const}$, but with various gas temperatures T_g^* ahead of the turbine. Let the engine during the acceleration process achieve some rpm, to which corresponds the thrust curve on compressor characteristics illustrated in Figure 49. If at point c during acceleration with $j = \text{const}$ the gas temperature $T_{g\,c}$ is such that at this point the work of the turbine is equal to the work of the compressor, then $\Delta N_{t\,c} = 0$ and $N_{s.s} = N_j$.

As the gas temperature rises to $T_g' > T_{g\,c}$ the power $N_t > N_k$.

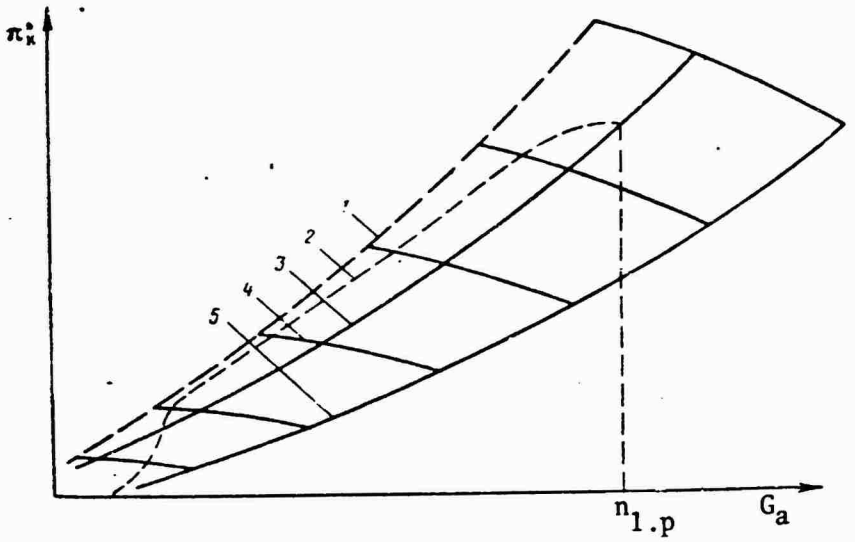

Figure 49. Compressor characteristics under starting conditions: 1 -- stable operation boundary; 2 -- line of joint operation of compressor and turbine in steady state modes; 4 -- thrust characteristics; 5 -- line of combined operation of compressor and turbine on cold air.

Assuming $\pi_к^* \approx \text{const}$, we obtain $G'_a\sqrt{T'_g} = G_{a\,c}\sqrt{T_{g\,c}}$.

Then

$$G'_a = G_{a\,c}\sqrt{\frac{T_{r\,c}}{T'_g}}$$

and

$$N'_т = aG'_aT'_g = aG_{a\,c}\sqrt{\frac{T_{g\,c}}{T'_g}}T'_g = aG_{a\,c}T_{g\,c}\sqrt{\frac{T'_g}{T_{g\,c}}},$$

where

$$a = 1{,}57\left(1 - \frac{1}{\pi_т^{*0.25}}\right)\eta_т^*.$$

Since

$$K_s = \sqrt{\frac{T_g}{T_{g\,c}}}\,li_н\;K_{s.st} = \sqrt{\frac{T_{g.}}{T'_g}}li,$$

then

$$N_т' = aG_{ac}T_g' \frac{K_s}{K_{s.st}}. \tag{9.8}$$

The required starter power for $T_g = T_g'$ will be

$$N_{s.s}' = N_j + N_к' - N_к \frac{K_s}{K_{s.st}}.$$

Assuming $N_k \approx N_k'$ for n = const, then

$$N_{s.s}' = N_j + N_к \left(1 - \frac{K_s}{K_{s.st}}\right).$$

Using this function we can determine the influence of the compressor stability margin on the required starter power. As K_s increases, this power decreases. With the given compressor stability margin K_s an increase in stability margin $K_{s.st}$ during the engine starting process (achieved through the corresponding reduction of fuel feed) leads to an increase in required starter power.

Stable engine starting requires the proper supply of fuel to the combustion chambers. The start-up fuel delivery law is determined by the characteristics of the compressor and combustion chambers under start-up conditions. In view of the complexity of the relationships between the gas dynamic parameters of engines and our inability to calculate the characteristics of the compressor and combustion chambers, the optimal start-up fuel delivery law is generally determined experimentally. Here we must take into account the effect of the ambient air temperature and engine arrangement on the aircraft on the law of fuel delivery to the combustion chambers.

Compressor characteristics, as we know, can be plotted for any engine (in the coordinates: air flow rate -- air compression ratios in the compressor), even in the starting modes. On these characteristics are superposed the lines of combined operation of the compressor, combustion chamber and turbine and the boundary of stable compressor operation. The approximate form of such compressor characteristics in the starting modes is illustrated in Figure 50.

To avoid unstable engine operation during start-up due to deficient fuel feed to the combustion chambers, there should be enough surplus fuel so that the line of combined operation of the turbocompressor not extend into the unstable operation zone. If the boundary of stable combustion in the combustion chamber passes below the boundary of the tolerable gas

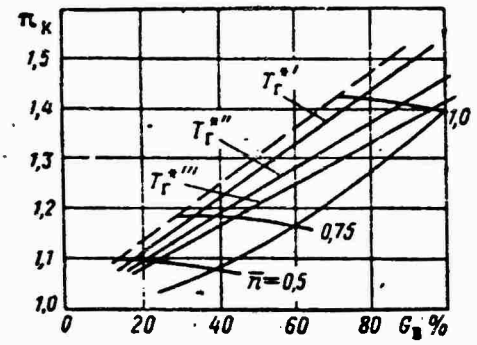

Figure 50. Air flow rate through compressor as function of change of gas temperature in front of turbine: $T_g^{*'} > T_g^{*''} > T_g^{*'''}$.

temperature in front of the turbine, then this also limits the feed of extra fuel into the combustion chamber.

Fuel is forced into the main working injectors by the fuel pump. Plunger type fuel pumps are generally used at this time. The main component of these pumps is the pumping assembly. The pumping assembly consists of a rotor and plungers installed in it at some angle to its axis, the ends of which rest on a disc. Pump capacity depends on the angle of inclination of the disc.

At the initial moment of start-up the inclined disc is in the position that ensures maximum pump capacity. This continues until the differential valve, which maintains a constant pressure drop on the throttle valve, is activated. When the throttle valve remains at a constant position in the "idle" setting the capacity of the fuel pump will be constant. At this moment the inclination of the disc decreases so that a constant pressure drop is maintained on the throttle valve. Figure 51 shows the available characteristics of the plunger type fuel pump in the starting modes.

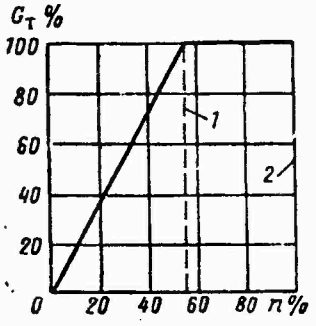

Figure 51. Characteristics of fuel pump in starting modes (pump capacity changes as a function of engine rotor rpm): 1 -- actuation of differential valve; 2 -- low rpm mode.

Fuel feed to the combustion chambers during starting can be limited manually or by means of special accessories -- automatic starter fuel regulator (SFR) or starter fuel distributors (SFD). Automatic starter fuel regulators are most commonly used, since they provide smooth changing of fuel feed to the combustion chambers during starting. Starter fuel distributors offer step-by-step change of fuel feed to the combustion chambers by rpm, since the SFD slide valves open sequentially as a function of the rpm.

The air pressure behind the compressor is used as the controlling parameter in SFR, since this pressure

is a function of engine rpm and can approximately characterize the air flow rate through the engine.

Automatic starters bypass fuel to the fuel pump intake according to the law of change of air pressure behind the compressor and according to the characteristics of the spring. As the air pressure behind the compressor increases, the amount of fuel bypassed decreases, and when the engine reaches the low rpm mode the bypassing of fuel is terminated.

The required law of fuel flow rate in the automatic starter fuel regulator during start-up is achieved by:

1) changing the diameter of the air jet on the air cavity of the regulator;

2) changing the tension of the spring that controls the position of the needle valve.

Each of these controlling elements has a different effect on the character of change of fuel feed to the combustion chambers during start-up.

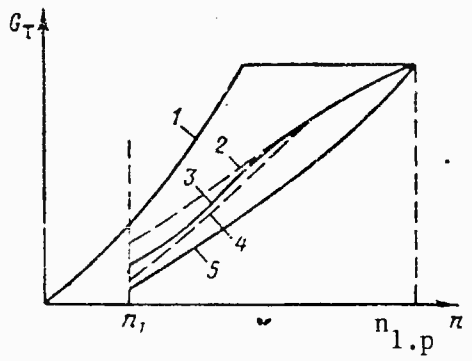

Figure 52. Amount of fuel admitted to combustion chambers during start as function of position of automatic fuel regulator spring and engine rotor rpm: 1 -- pump capacity; 2 -- fuel feed with set screw tightened; 3 -- initial characteristic; 4 -- fuel feed with set screw loosened; 5 -- fuel flow rate in steady states; n_1 -- rpm at which fuel delivery begins; $n_{1.g}$ -- engine rpm in low rpm regime.

Change in the amount of fuel admitted to the working injectors is illustrated in Figure 52 as a function of the position of the set screw of the automatic starter fuel regulator. As seen, adjustment of the amount of fuel fed to the working injectors by means of the set screw of the automatic fuel regulator spring is more effective during the initial moments of start-up and less effective at rpm close to the low rpm regime.

By changing the diameter of the air release jet of the automatic fuel regulator it is possible to regulate fuel feed to the combustion chambers in a different way. Changing the jet diameter obviously has a greater effect on fuel feed to the combustion chambers at revolutions close to the low power rpm. With all these adjustments fuel pump capacity remains constant; only the amount of fuel bypassed to the drain by the automatic starter fuel regulator is changed.

The automatic starter fuel regulator offers the following law of

change of fuel pressure on the working injectors (p_f) according to the pressure of the air from the compressor (p_k), which is a function of engine rpm:

$$p_f = p_{f0} + B(K'p_к - p_н) = p_{т0} + BP_э(K'\pi_к - 1),$$

where p_{f0} is the fuel pressure at the initial moment of fuel feed to the combustion chambers, determined by the tension of the SFR spring.

By substituting p_f into the equation for the fuel flow rate through the injectors

$$G_f = A\sqrt{p_f - p_k},$$

we obtain, after simple conversions,

$$\frac{G_f^2}{p_н} = A^2\left[\frac{p_{т0}}{p_н} + B(K'\pi_к - 1) - \pi_к\right], \qquad (9.9)$$

where A, B and K are constant coefficients.

By multiplying the numerator and the denominator of the left hand side of the last equation by $p_n T_n$ we obtain, finally, for π_k = const

$$G_{f.re}^2 p_n T_n = A^2\left[\frac{p_{т0}}{p_н} + B(K'\pi_к - 1) - \pi_к\right]. \qquad (9.10)$$

The fuel delivery provided by the automatic starter fuel regulator for constant π_k (i.e., at the same rpm n_{re}) depends on the temperature and pressure of the ambient air. It follows from equation (9.10) that at negative ambient air temperatures the automatic starter fuel regulator supplies a larger quantity of fuel than at positive temperatures, and the working starter line comes closer to the boundary of stable compressor operation. This necessitates changing the adjustment of the automatic starter fuel regulator as a function of the ambient air temperature.

Thus, by ensuring during the starting process the corresponding fuel feed to the combustion chambers it is possible to ensure participation of the turbine in acceleration of the engine up to low power rpm. With this the starting process is concluded and the entire starter fuel regulator system is automatically returned to the position required for the next engine start-up.

CHAPTER 10. BALANCE OF POWERS (MOMENTS) DURING ENGINE START-UP

§19. Start-up Periods

The process of starting an aviation gas turbine engine can be broken down conditionally into three periods (phases).

In the first phase, which begins at the moment of engagement of the starter with the engine rotor and concludes at the moment of ignition of the fuel-air mixture in the combustion chambers, only the starter system participates in engine rotor acceleration. It can be assumed that the engine turbine starts active operation at the beginning of ignition of the fuel-air mixture in the combustion chambers.

The starter system is automatically coupled to the engine rotor by special starter panels after depression of the starter button. During the first start-up phase pure air flows through the entire gas-air duct of the engine, and its quantity and pressure on the compressor increase as the engine rotor rpm increases. The maximum rpm to which the starter system can accelerate the engine rotor (cranking rpm) is selected so that conditions will be created in the combustion chambers for stable ignition and combustion of the fuel-air mixture under all operating conditions at this rpm (and even at somewhat lower rpm).

In the second starting phase, which begins with the ignition of the fuel-air mixture in the combustion chambers and ends with the disengagement of the starter from the engine rotor, acceleration is performed simultaneously by the starter and the engine turbine. The starter automatically disengages from the engine rotor as soon as the engine reaches a certain rpm, at which time the turbine has a sufficient power reserve to turn the engine rotor to the low power rpm. In individual cases the starter is turned off after a certain time of operation of the starter panel. When this method of starter disengagement is used there may be cases when the turbine does not achieve sufficient rpm to place the engine in the low power mode before the conclusion of the starter panel operation cycle. Consequently engine start-up may take a long time or will not take place at all.

In the third starting phase, which starts with the shutting off of the starter and ends when the engine attains the low rpm mode, the engine rotor is accelerated by the turbine alone.

The examined starting phases characterize the process by which most modern gas turbine engines are brought up to the low rpm mode. In the case of fast acceleration of the rotors of individual types of engines to the low rpm state the third phase is sometimes omitted. Such engines are brought up to the low power rpm by the combined actions of the starter and turbine.

§20. Starter Torque

The moment generated by the starter changes as a function of rpm in accordance with its characteristics and can decrease by measure of engine rotor acceleration, remain constant or increase. Experience shows that the starter moment is a nearly linear function of rpm (Figure 53). For the starters most commonly used at this time (electric starters, air turbostarters, turbocompressor starters with kinematically unconnected turbines, etc.) this function can be represented in the form

$$M_{s.s} = M_0 \pm bn, \tag{19.1}$$

where M_0 is the initial starter moment;

n is engine rotor rpm;

b is a constant coefficient depending on the angle of inclination of the starter characteristic to the abscissa axis.

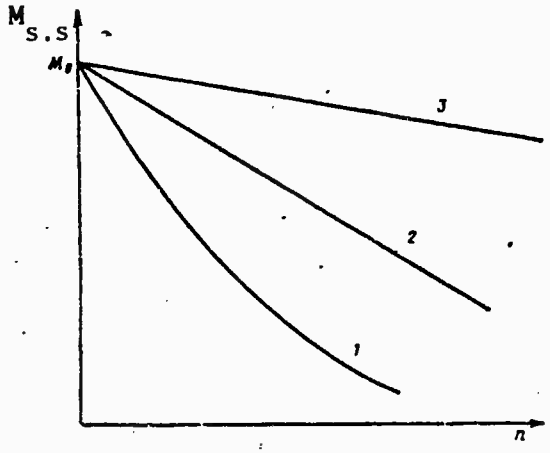

Figure 53. Typical character of change of torque of various types of starters: 1 -- electric starter; 2 -- air turbostarter; 3 -- fuel-air turbostarter.

Starters that incorporate various devices (fluid couplings, differential reducers) transmit to the engine rotor a practically constant

moment to revolutions close to the rpm at which the starter disengages from the engine.

For the law of change of the starter moment by rpm $M_{s.s} = M_0 - bn$ the engine rpm at which the starter power is maximum is given by the equation

$$n_m = M_0/2b.$$

The proper choice of initial starter moment and coefficient b ensures that the starter for a given engine will develop maximum power in the range of change of revolutions from n_1 to n_c, i.e., from the instant of ignition of the fuel-air mixture in the combustion chambers to the development of positive surplus turbine power.

The minimal starter power is that required for accelerating the engine rotor to the rpm at which the turbine goes into operation. To ensure reliable starting under different operating conditions, however, the starter power at the specified rpm is increased 2.5-3 fold.

Sometimes the moment produced by the starter cannot be completely transmitted to the engine rotor by the coupling mechanism. This occurs, in particular, when this mechanism is a fluid coupling. The fluid coupling consists of two working wheels: the pump and turbine. Torque is transmitted in the fluid coupling not mechanically, but hydraulically through the working fluid. The torque, applied to the pump wheel from the starter causes the wheels of the fluid coupling to slip, and this slippage increases as the resistance moment of the engine increases and as the rpm of the pump wheel decreases.

The moment transmitted through the fluid coupling is related to the rpm n_p of the pump and active diameter D of the coupling by the equation

$$M_{re} = A7.162 \cdot 10^{-4} n_p^2 D^5,$$

where A is the power coefficient.

The power coefficient for a given fluid coupling depends on slippage S of the wheels:

$$S = \frac{\omega_p - \omega_t}{\omega_p} = 1 - \frac{\omega_t}{\omega_p},$$

where ω_p is the angular velocity of the pump wheel;

ω_t is the angular velocity of the turbine.

This relation can also be expressed in the form

$$A = A_d[1 + \alpha(S - S_d) - \beta(S - S_d)^2 - \gamma(S - S_d)^3],$$

where A_d, S_d are the design coefficients of power and slippage of the fluid coupling;

α, β, γ are constant coefficients for a given type of fluid coupling.

§21. Engine Resistance Moment

Most of the power during engine start-up is used for overcoming the forces of resistance of air to compression in the compressor. The power used for driving the components of gas turbine engines, for overcoming the forces of friction in the bearings and other work, amounts to 3-5% of the power required for turning the compressor. The relations of power used by the oil systems of the AI-20 engine are shown in Figure 54 for different oil temperatures.

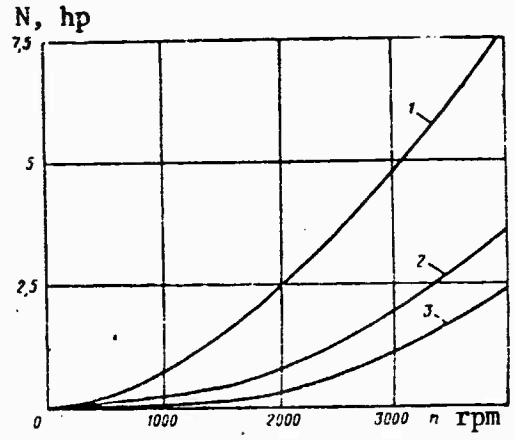

Figure 54. Power used by oil systems of AI-20 engine as function of rpm: 1 -- t_o = 15°C; 2 -- t_o = 30°C; 3 -- t_o = 80°C.

Experiments confirm that the moment used for accelerating the compressor during start-up will be

$$M_k = cn^x, \qquad (10.2)$$

where c and x are coefficients.

The values of coefficient c and exponent x are, in the general case, variable and depend on the efficiency of the given compressor in the starting regime. Exponent x will be close to two in the starting regime. The value of c can be found from the following considerations.

The moment used for turning the compressor will be

$$M_к = \frac{30 L_{ад.к} G_в}{\pi n \eta_к}. \quad *$$

We will find $L_{ad.k}$ and G_a in the starting regimes, using their values in the low rpm regime.

In the starting regimes the air flow rate changes in proportion to rpm (Figure 55), and the value of $L_{ad.k}/\eta_k$ changes in proportion to the square of rpm. Then

$$\frac{G_в}{G_{в.м.г}} = \frac{n}{n_{м.г}}; \quad \frac{L_{ад.к}/\eta_к}{(L_{ад.к}/\eta_к)_{м.г}} = \left(\frac{n}{n_{м.г}}\right)^2,$$

where the subscript "1.p" denotes the corresponding parameter in the low power regime;

$$\frac{L_{ад.к} G_в}{\eta_к} = \frac{L_{ад.к} n^2 G_{в.м.г} n}{\eta_{к.м.г} n^3_{м.г}} = \frac{(L_{ад.к} G_в)_{м.г}}{(\eta_к n^3)_{м.г}} n^3,$$

therefore

$$M_к = \frac{30 (L_{ад.к} G_в)_{м.г}}{\pi (\eta_к n^3)_{м.г}} n^2; \quad c = \frac{30 (L_{ад.к} G_в)_{м.г}}{\pi (\eta_к n^3)_{м.г}}.$$

The dependence of the resistance moment on the rpm in the starting regimes that we have found concurs satisfactorily with experimental data (Figure 56).

The coefficient c is easily determined for each engine, since the values η_k, G_a, n and $L_{ad.k}$ are always known in the low power mode.

§22. Gas Turbine Torque

The moment developed by the gas turbine can be calculated through the equation

$$M_т = \frac{G}{g} (C_{1u} - C_{2u}) r = \frac{Gg}{g} \Delta C_u r,$$

where G_g is the air (gas) flow rate through the turbine;

C_{1u} and C_{2u} are the average peripheral components of absolute velocities of the air at turbine intake and exhaust;

r is the equivalent radius of the working vanes of the turbine.

*[Subscripts: ад.к = ad.k; в = a; м.г = 1.p]

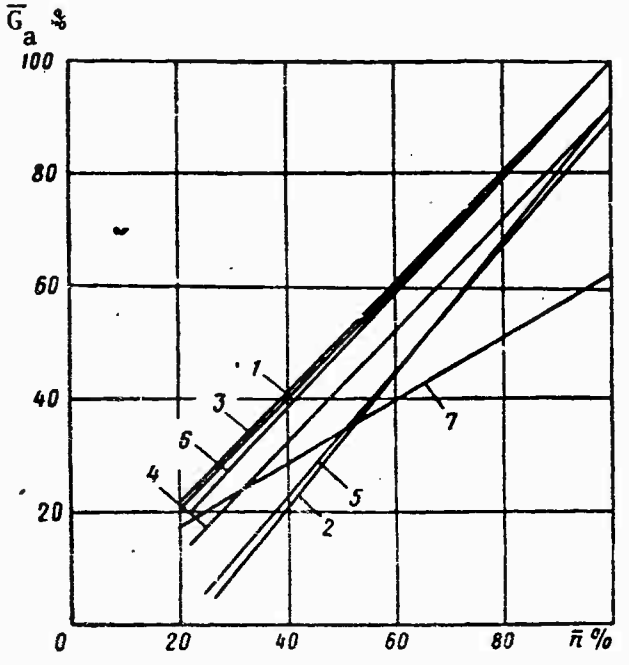

Figure 55. Air flow rate through engine as function of rpm: for turboprop engine: 1 -- in steady state modes; 2 -- at limit of stable operation; 6 -- during engine run-down with bypass open; 7 -- during engine run-down with bypass closed; for turbojet engines: 3 -- in steady state modes; 4 -- during starting; 5 -- at boundary of stable operation.

The turbine can produce a positive moment only when ΔC_u is positive. The angular velocity of the turbine at which a positive ΔC_u is possible is determined by the air (gas) flow rate through the turbine and by its profile.

In the initial starting phase (during cold cranking) a gas turbine, as a rule, creates almost no positive moment. This is particularly characteristic of the multistage turbine. The engine turbine is usually a brake in the initial starting phase. The reason for this is that during cold cranking the angles at which the air strikes the vanes of the turbine differ greatly from the angles at which the vanes are set, and the air flow on leaving the vanes is deflected strongly in the direction of rotation of the turbine. Through the entire height of a vane the air strikes the working turbine vane profile at substantially negative angles of attack. All of this causes large pressure losses in the working turbine without creating a torque on the turbine.

At certain engine rotor revolutions, when ignition of the fuel-air mixture in the combustion chambers is ensured, the absolute velocity of the gases at turbine intake increases and turbine efficiency improves.

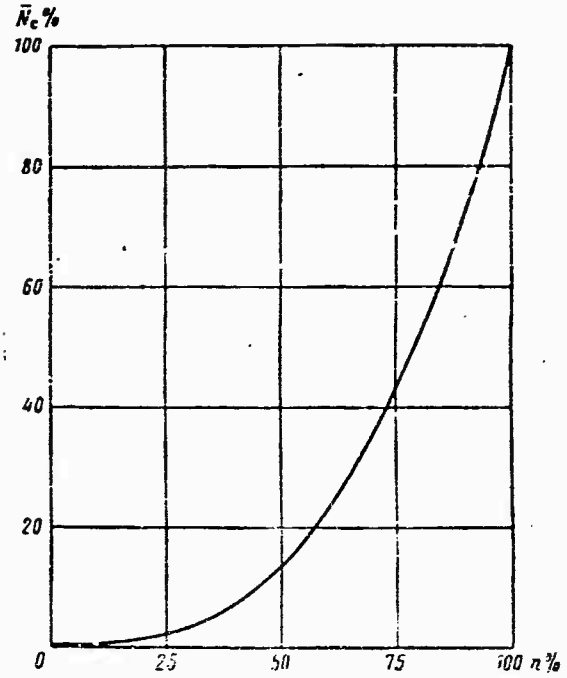

Figure 56. Change of relative resistance moment as function of rpm of gas turbine engine.

After the gas turbine enters operation its power increases rapidly with rpm, and after some time it takes on the main work of turning the engine rotor. When a turbojet engine reaches about 25-30% of its rpm, and a turboprop engine about 40-50% of its rpm in the low rpm regime the power of the gas turbine is comparable to the power spent on overcoming engine resistance.

In order to reduce the required starter power it is essential that the turbine begin to develop a positive moment at the lowest possible rpm. This rpm depends on many factors, determined by the characteristics of the compressor, turbine and combustion chamber.

Since $n_{t.n} = n_{t.s}$ when $T_{g.n}/T_{g.s} \leq 1.4$, then for smooth compressor characteristics when $n_{re} = \text{const}$

$$M_{т.н} \approx M_{т.у} \sqrt{\frac{T^*_{г.н}}{T^*_{г.у}}}. \quad *$$

When $n < n_{l.p}$

*[Subscripts: T.H = t.n; t.y = t.s; Г.H = g.n; Г.y = g.s; M.Г = l.p].

$$M_{т.у}=(M_{т.у})_{м.г}\left(\frac{n}{n_{м.г}}\right)^2$$

and then

$$M_{т.н}=(M_{т.у})_{м.г}\bar{n}^2\sqrt{\bar{T}^*_{г.н}}.$$

We will determine the amount of surplus turbine moment (in unsteady modes of operation during engine start-up) required for accelerating the engine rotor. This surplus is found as the difference between the moment $M_{t.n}$ developed by the turbine and the moment $M_{k.n}$ required for rotating the compressor during engine start-up:

$$\Delta M_{т.п}=M_{т.п}-M_{к.п}.$$

We will divide the right and left sides of the above equation by the turbine moment $M_{t.s}$ required for engine operation at steady rpm below the low rpm:

$$\frac{\Delta M_{т.н}}{M_{т.у}}=\frac{M_{т.н}}{M_{т.у}}-\frac{M_{к.н}}{M_{т.у}}.$$

In the steady state regimes $M_{t.s} = M_{k.s}$, and then

$$\frac{\Delta M_{т.н}}{M_{т.у}}=\frac{M_{т.н}}{M_{т.у}}-\frac{M_{к.н}}{M_{к.у}}.$$

By substituting into the above equation the moments entered in it, expressed through engine parameters, we obtain

$$\frac{\Delta M_{т.н}}{M_{т.у}}=\frac{G_{г.н}c_{p\,г}T^*_{г.н}\left(1-\frac{1}{\pi^{*0.25}_{т.н}}\right)\eta_{т.н}}{G_{г.у}c_{p\,г}T^*_{г.у}\left(1-\frac{1}{\pi^{*0.25}_{т.у}}\right)\eta_{т.у}}-\frac{G_{вн}c_{p\,в}T_1\left(\pi^{*0,286}_{к.н}-1\right)\eta_{к.у}}{G_{в.у}c_{p\,в}T_1\left(\pi^{*0.286}_{к.у}-1\right)\eta_{к.н}},$$

where $G_{g.n}(G_{g.s})$ is the gas flow rate through the turbine;

$G_{a.n}(G_{a.s})$ is the air flow rate through the compressor;

T_1 is the air temperature in the compressor intake;

$T^*_{g.n}(T^*_{g.s})$ is the gas temperature in the stagnant flow in front of the turbine;

$\pi^*_{k.n}(\pi^*_{k.s})$ is the air compression ratio in the compressor;

*[Subscripts: B.H. = a.n; k.y = k.s; k.H = k.n; B.y = a.s].

$\pi^*_{t.n}(\pi^*_{t.s})$ is the gas expansion ratio in the turbine;

$\eta_{k.n}(\eta_{k.s})$ is compressor efficiency;

$\eta_{t.n}$, $\eta_{t.s}$ is turbine efficiency.

Comment. The parameters in the nonsteady state are denoted through the subscript "n" and in the steady state by the subscript "s."

The air compression ratios in the compressor for n = const in the unsteady and steady modes of engine operation below the low rpm are practically equal.

For constant air compression ratios in the compressor the gas expansion ratios in the turbine are also the same. Moreover, during actual start-up the current ratios of peripheral turbine vane velocity to the absolute gas velocity at the intake into the working vanes, on which depends turbine efficiency, differ little from the value of this ratio at the same rpm of the steady state, i.e., $\eta_{t.n} = \eta_{t.s}$. Therefore after simplification we obtain

$$\frac{\Delta M_{т.н}}{M_{т.у}} = \frac{G_{г.н}T^*_{г.н}}{G_{г.у}T^*_{г.у}} - \frac{G_{в.н}\eta_{к.у}}{G_{в.у}\eta_{к.н}},$$

or

$$\frac{\Delta M_{т.н}}{M_{т.у}} = \frac{G_{г.н}T^*_{г.н}}{G_{г.у}T^*_{г.у}} - \frac{G_{г.н}\eta_{к.у}}{G_{г.у}\eta_{к.н}},$$

since in the gas turbine engine $G_g = G_a + G_f$, where G_f is the fuel flow rate through the combustion chambers (G_f is 2-3% of G_a, and therefore it need not be taken into account in the calculations).

If in the latter equation we express $G_{g.n}$ and $G_{g.s}$ through the pressure and temperature of the gases in front of the turbine we obtain

$$\frac{\Delta M_{т.н}}{M_{т.у}} = \frac{p^*_{г.н}}{p^*_{г.у}}\sqrt{\frac{T^*_{г.н}}{T^*_{г.у}}} - \frac{p^*_{г.н}}{p^*_{г.у}}\frac{\eta_{к.у}}{\eta_{к.н}}\sqrt{\frac{T^*_{г.у}}{T^*_{г.н}}}.$$

§23. Dynamic Equilibrium of Engine Rotor

The duration of each phase of the starting process may vary, but the second phase is generally the longest. The duration of the phases is determined by the relation (balance) of moments acting on the engine rotor during the starting process.

During start-up various moments act on engine parts. The engine

parts, under the influence of these moments, go into a state of dynamic equilibrium, in which the actions of the starter and turbine are balanced by the moments from the forces of inertia and resistance.

We will analyze the balance of moments equations during the starting process, assuming all moments acting on the engine to be reduced to the engine rotor axis. In this case the mass of revolving parts remains constant in relation to the engine axis. Consequently the moment of inertial forces will depend only on the angular acceleration of the rotor.

If between the output shaft of the starter and the engine shaft is installed a redueer with the gear ratio i_r, then in the absence of losses in the reducer the torque of the starter will be reduced to the engine shaft according to the equation

$$M_{s.s} = i_r M_{a.a}.$$

The following torque equations can be written for the three phases of on the ground starting:

for phase one

$$M_{s.sI} = M_{cI} + M_{jI};$$

for phase two

$$M_{n.yII} + M_{TII} = M_{cII} + M_{jII};$$

for phase three

$$M_{TIII} = M_{cIII} + M_{jIII},$$

where $M_{s.sI}$, $M_{s.sII}$ are starter torques in the corresponding phases;

M_{cI}, M_{cII}, M_{cIII} are engine resistance torques in the corresponding phases;

M_{tII}, M_{tIII} are turbine torques in the corresponding phases;

M_{jI}, M_{jII}, M_{jIII} are the torques of inertial forces during engine rotor acceleration in the corresponding starting phases.

Considering that the torque

$$M_j = \frac{\pi}{30} J_0 \frac{dn}{d\tau},$$

and the surplus turbine torque $\Delta M_t = M_t - M_c$, then for the three starting

phases we may write the equations of engine rotor motion:

$$\frac{\pi}{30} J_0 \left(\frac{dn}{d\tau}\right)_I = M_{s.sI} - M_{cI};$$

$$\frac{\pi}{30} J_0 \left(\frac{dn}{d\tau}\right)_{II} = M_{s.sII} + \Delta M_{tII};$$

$$\frac{\pi}{30} J_0 \left(\frac{dn}{d\tau}\right)_{III} = \Delta M_{tIII}.$$

With these equations we can solve a number of problems related both to the choice of starter for an engine and to evaluation of the starting properties of a proposed engine with its starter. If, for example, the moment characteristics of the compressor, turbine and also the breakdown of the overall starting time by phases are known, the required starter moment characteristics can be determined in order to ensure that the engine achieves the low rpm regime within the established time. And, conversely, if the moment developed by the starter is known the time within which the engine can be placed in the low rpm regime can be determined with sufficient accuracy.

The change of surplus turbine torque in the second starting phase can be expressed approximately through the linear function

$$\Delta M_{tII} = K_t (n - n_c) \tag{10.3}$$

The engine rotor motion equations for the first and second starting phases, with consideration of laws (10.1), (10.2) and (10.3), acquire the following form:

$$\frac{\pi}{30} J_0 \left(\frac{dn}{d\tau}\right)_I = M_0 \pm bn - cn^2;$$

$$\frac{\pi}{30} J_0 \left(\frac{dn}{d\tau}\right)_{II} = M_0 \pm bn + K_t (n - n_c).$$

The duration of the first phase is

$$\tau_I = \frac{\pi}{30} J_0 \int_0^{n_1} \frac{dn}{M_0 \pm bn - cn^2}.$$

The solution of the stated integral yields:

for $M_{s.s} = M_0 - bn$

$$\tau_I = \frac{\pi}{30} J_0 \left[\frac{1}{\sqrt{4cM_0 + b^2}} \ln \frac{2cn + b + \sqrt{4cM_0 + b^2}}{2cn + b - \sqrt{4cM_0 + b^2}} \right]_0^{n_1} =$$

$$= \frac{\pi}{30} J_0 \frac{1}{\sqrt{4cM_0 + b^2}} \ln \frac{(b - \sqrt{4cM_0 + b^2})\, n_1 - 2M_0}{(b + \sqrt{4cM_0 + b^2})\, n_1 - 2M_0};$$

for $M_{s.s} = M_0 + bn$

$$\tau_I = \frac{\pi}{30} J_0 \left[\frac{1}{\sqrt{4cM_0 + b^2}} \ln \frac{-2cn + b - \sqrt{4cM_0 + b^2}}{-2cn + b + \sqrt{4cM_0 + b^2}} \right]_0^{n_1} =$$

$$= \frac{\pi}{30} J_0 \frac{1}{\sqrt{4cM_0 + b^2}} \ln \frac{(b + \sqrt{4cM_0 + b^2})\, n_1 + 2M_0}{(b - \sqrt{4cM_0 + b^2})\, n_1 + 2M_0}.$$

When the starter supplies constant torque $M_{s.s} = M_0 = \text{const}$ to the engine rotor the duration of the first phase is

$$\tau_I = \frac{\pi}{60} \frac{J_0}{\sqrt{cM_0}} \ln \frac{\sqrt{\frac{M_0}{c}} + n_1}{\sqrt{\frac{M_0}{c}} - n_1}.$$

The duration of the second phase is

$$\tau_{II} = \frac{\pi}{30} J_0 \int_{n_1}^{n_2} \frac{dn}{M_0 \pm bn + K_T (n - n_c)}.$$

The solution of the stated integral yields:

for the law $M_{s.s} = M_0 - bn$

$$\tau_{II} = \frac{\pi}{30} \frac{J_0}{K_T - b} \ln \left[(K_T - b)\, n + (M_0 - K_T n_c) \right]_{n_1}^{n_2} =$$

$$= \frac{\pi}{30} \frac{J_0}{K_T - b} \ln \frac{(K_T - b)\, n_2 + (M_0 - K_T n_c)}{(K_T - b)\, n_1 + (M_0 - K_T n_c)};$$

for the law $M_{s.s} = M_0 + bn$

$$\tau_{II} = \frac{\pi}{30} \frac{J_0}{K_T + b} \ln \frac{(K_T + b)\, n_2 + (M_0 - K_T n_c)}{(K_T + b)\, n_1 + (M_0 - K_T n_c)};$$

for the law $M_{s.s} = M_0 = \text{const}$

$$\tau_{II} = \frac{\pi}{30} \frac{J_0}{K_T} \ln \frac{M_0 + K_T (n_2 - n_c)}{M_0 - K_T (n_c - n_1)}.$$

The summary duration of starter operation will be

$$\tau_{s.s} = \tau_I + \tau_{II}.$$

The duration of the third phase is

$$\tau_{III}=\frac{\pi}{30} J_0 \int_{n_2}^{n_1} \frac{dn}{\Delta M_{tIII}}.$$

Time τ_{III} can be determined either by calculation, solving the integral for the analytical function $\Delta M_t = f(n)$, or by the graphic integration method.

The above equations make it possible to calculate the effect of various factors on starter operation time and time required for engine to reach the low rpm regime.

The cranking time (first starting phase) can also be determined if final number of revolutions n_f of the engine rotor in the cranking regime is used instead of the coefficient c. At this engine rotor revolution the torque of the forces of resistance will be

$$M_{c.k} = cn_f^2,$$

and the coefficient will be

$$b=\pm\frac{M_0 \pm M_{c.k}}{n_f}.$$

Then the starter torque will be

$$M_{s.s}=\left(1-\frac{n}{n_f}\right)M_0+cn_f n,$$

and the duration of the first phase is

$$\tau_1=\frac{\pi}{30}\frac{J_0 n_f}{M_0+cn_f^2}\ln\frac{1+\frac{cn_f}{M_0}n_1}{1-\frac{n_1}{n_f}}. \qquad (10.4)$$

With a linear law of change of starter torque and known final cranking rpm the change of the starter torque can be characterized by the parameter $\bar{m} = M_0/M_{c.k}$.

Then $M_0 = \bar{m}cn_k^2$; $\bar{m} = 1$ when $M_{s.s} = M_0 = \text{const}$; $\bar{m} = 2$ for the case when the starter produces maximum power when $n_m = n_f$.

We will denote the ratio of the final cranking rpm n_f to the fuel feed

rpm n_1 through the coefficient a (for modern gas turbine engines a = 1.1-1.15 for engine starting time τ_{st} = 40-90 sec).

Then equation (10.3) will acquire the form

$$\tau_1 = \frac{\pi}{30} \frac{J_0}{c n_f (\bar{m}+1)} \ln \frac{a + \frac{1}{\bar{m}}}{a-1}.$$

After conversions this expression becomes

$$\frac{\tau_1 c}{J_0} n_f = \frac{\pi}{30} \frac{1}{\bar{m}+1} \ln \frac{a + \frac{1}{\bar{m}}}{a-1}. \qquad (10.5)$$

As seen, for the given law of change of starter torque ($\bar{m}$ = const) with the selected ratio n_f/n_1 = a = const, the right hand side of expression (10.5) is constant. Then

$$\frac{\tau_1 c}{J_0} n_f = \theta = \text{const}.$$

This dimensionless parameter determines all dynamic parameters characterizing the process of engine rotor acceleration by the starter. Therefore the parameter θ can be called the generalized dynamic cranking parameter.

The generalized dynamic characteristic, by means of which several problems are readily solved, is shown in Figure 57. Thus, for the given power characteristics of the starter and given engine characteristics we can: determine the time of acceleration; determine the law of change of the required starter torque as a function of the given acceleration time or change of torque of resistance forces.

Acceleration time is usually determined with the aid of the generalized dynamic cranking parameter as a function of the starter torque which, in particular, is essential for the choice of type and optimal parameters of the starter and starter system for newly designed and improved gas turbine engines.

The theoretical curves $\tau_I = f(M_0)$, determined by means of the generalized characteristics for a turbojet engine with J_0 = 0.7 kg·m·sec^2, are illustrated by way of example in Figure 58. Comparison of the experimental data with the theoretical indicates that the difference in the determination of acceleration time τ_I does not exceed 5%.

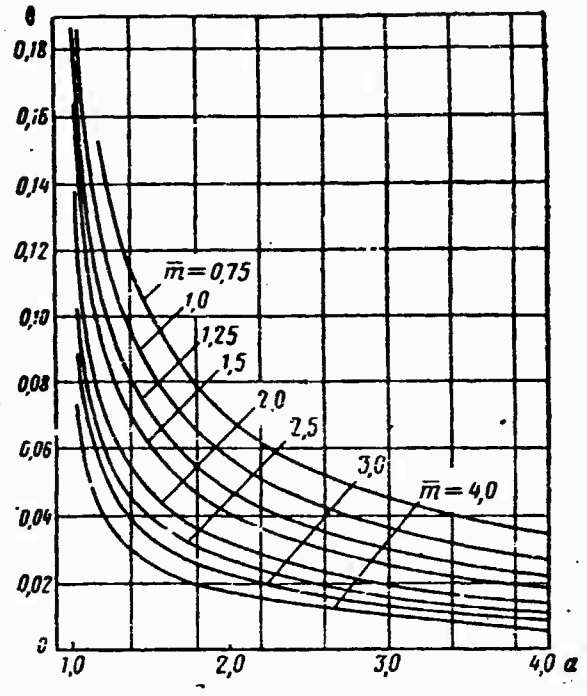

Figure 57. Generalized dynamic cranking parameter as function of coefficient a for various $\bar{m}$.

The curve A-A, corresponding to the law $\bar{m} = 1$ of change of starter torque ($M_{s.s} = M_0 = \text{const}$) is shown in Figure 58. To the right of this curve is the range of change of torque corresponding to the law $\bar{m} > 1$ ($M_{s.s} = M_0 - bn$; $M_0 > M_{c.k}$), and to the left is the range of change of torque corresponding to the law $\bar{m} < 1$ ($M_{s.s} = M_0 + bn$; $M_0 < M_{c.k}$).

The theoretical and experimental curves $\tau_I = f(M_{s.s})$ are shown by way of example in Figure 59 for a turbojet engine for $c = 3.9 \cdot 10^{-6}$ kg·m/(rpm)^2; $J_0 = 0.7$ kg·m·sec^2.

Analysis of the curves shows that during accelerated starts of the engine or when it is necessary to reduce acceleration time (to reduce the flow of energy from the power sources) the most convenient law of change of starter torque will be $\bar{m} = 1$. In these cases the use of the law $\bar{m} > 1$ is not advisable, since an increase in starter torque with a practically small reduction of acceleration time necessitates increasing the weight and dimensions of the starter and leads to undesirable dynamic overloading of the drives.

The second engine starting phase is characterized by the following equation of rotor motion:

$$\frac{\pi}{30} J_0 \frac{dn}{d\tau} = M_{s.s} + \Delta M_t,$$

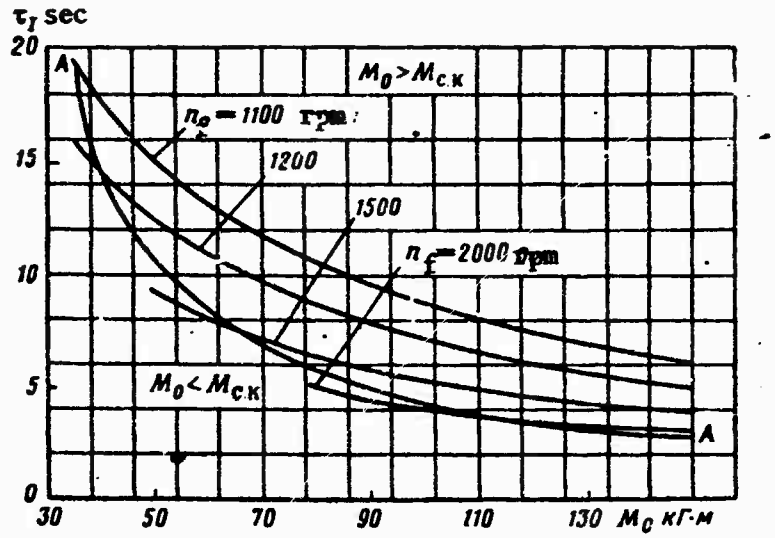

Figure 58. Theoretical dependences of cranking time of turbojet engine on parameters of linear law of change of starter torque.

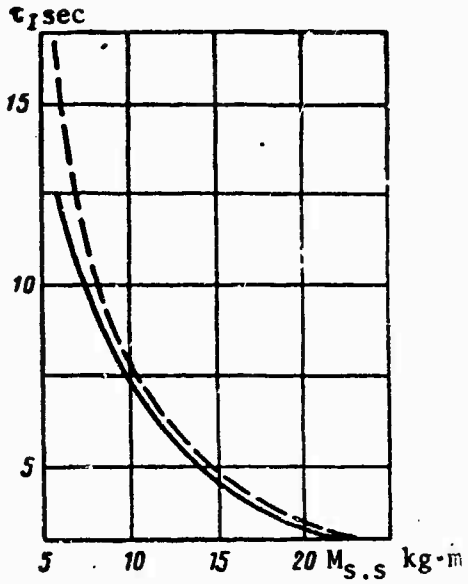

Figure 59. Theoretical (broken curve) and experimental (continuous curve) dependences of turbojet engine cranking time on starter torque.

where $\Delta M_t = M_t - M_c$ is the surplus turbine torque.

The starter characteristics of the engine in this starting phase govern the required fuel feed law and law of change of required starter power and also maximum starter power.

The required starter power in the second phase will be

$$N_{s.s} = N_j - \Delta N_t,$$

where N_j is the power consumed in overcoming inertial forces;
ΔN_t is surplus turbine power.

The engine rpm corresponding to the maximum required starter power (n_m) is determined by the following equation for $n = n_m$:

$$\frac{dN_{s.s}}{dn} = \frac{d(N_j)}{dn} - \frac{d(\Delta N_t)}{dn} = 0,$$

or

$$\frac{d(\Delta M_{т})_{м}}{dn} n_{м} + \Delta M_{т.м} = \frac{dM_{j_{м}}}{dn} n_{м} + M_{j_{м}}.$$

The required starter power should be evaluated from the standpoint of ensuring uniform acceleration of the engine rotor by the starter.

Uniform acceleration makes it possible to reduce the weight and dimensions of the starter by reducing the required starter torque in the first engine starting phase and required starter power in the second phase for the prescribed starting time (τ_{st} = const).

In the case of fast engine starting, when the torque of inertial forces substantially exceeds the torque of the forces of resistance, uniform acceleration is also optimal.

The choice of uniform acceleration simplifies the procedure for evaluating the required starter power. By using the principle of uniform acceleration we can represent the equation for determination of rpm n_m in the form

$$\frac{d(\Delta M_{т})_{м}}{dn} n_{м} + \Delta M_{т.м} = M_{j\,\mathrm{av}}$$

where

$$M_{j\mathrm{av}} = \frac{\pi}{30} J_0 j_{\mathrm{avII}};$$

j_{avII} is the average rate of acceleration (average rate of picking up rpm) in the second starting phase.

It is usually assumed in calculations that

$$j_{avII} \approx j_{av} = n_{1.p}/\tau_{st}.$$

For most modern gas turbine engines the change of surplus turbine torque in the second starting phase can be expressed approximately through the linear function

$$\Delta M_{тII} = K_{т}(n - n_c),$$

where n_c is the rpm at which $M_t = M_c$.

Then, assuming $\Delta M_{tII} = K_t(n - n_c)$, from the above equation we determine the rpm for uniform acceleration:

$$n_M = \frac{M_{Jcp} + K_T n_c}{2K_T}.$$

The maximum required starter power is

$$N_{s.s.m} = \frac{M_{s.y} n_M}{716,2} = \frac{(M_{Jcp\,II} - \Delta M_{t\,II})_K n_M}{716,2},$$

or for $\Delta M_{tII} = K_t(n - n_c)$

$$N_{s.s.m} = \frac{[M_{Jcp\,II} - K_T (n_M - n_c)]\, n_M}{716,2}.$$

Reduction of surplus turbine torque and displacement of rpm n_c toward higher rpm lead to a substantial increase in rpm n_m and correspondingly to an increase in maximum required starter power.

In order to reduce the maximum required starter power it is desirable that after fuel feed for $n = n_1$ the required starter power be reduced, i.e., for $n \geq n_1$

$$\frac{dN_{ss}}{dn} \leqslant 0.$$

Converting to torques, with consideration of uniform acceleration, this condition will be expressed as follows:

$$\frac{d(\Delta M_T)_1}{dn} n_1 + \Delta M_{T1} > M_{Jav}.$$

In the given case, with the assumed linear law of change of surplus turbine torque, the following conditions must be satisfied:

$$n_c \leqslant \frac{M_{Jav} - 2\Delta M_{T1}}{M_{Jav} - \Delta M_{T1}}$$

(for $n = n_1$ because $M_c > M_t$ $\Delta M_t < 0$);

$$K_T \geqslant \frac{M_{Jav}}{2n_1 - n_c}.$$

For the linear law of change of starter torque $M_{s.s} = M_0 - bn$ the maximum available starter power (for $n = n_m$) is given by the equation

$$N_{s.s.m} = \frac{M_0^2}{716.2 \cdot 4b} = 3{,}5 \cdot 10^{-4} \frac{M_0^2}{b}$$

and takes place at engine rotor rpm

$$n_m = M_0/2b.$$

Expressing n_m through the final cranking rpm n_f, we obtain

$$n_м = \frac{M_0}{M_0 - M_{c.к}} \frac{n_f}{2}.$$

Then $M_{ss.m} = M_0/2$;

$$N_{s.s.m} = 3{,}5 \cdot 10^{-4} \frac{M_0^2 n_f}{M_0 - M_{c.к}}.$$

For constant available starter torque on the engine rotor shaft $M_{s.s} = M_0 = \text{const}$ the maximum starter power will occur at the time of its disengagement, when $n_m = n_2$. Then

$$N_{s.s.m} = M_0 n_2/716.2.$$

We will determine the final rpm of engine rotor cranking by the starter, proceeding from the above-derived equations for determination of $N_{s.s.m}$ and n_m.

From the condition of linearity of starter torque we find

$$M_0 = 2M_{s.s.m} = 2(M_{j\ av} + \Delta M_{tII})_m.$$

Substituting the expression obtained for M_0 into the equation

$$n_м = \frac{M_0}{M_0 - M_{c.к}} \frac{n_f}{2},$$

we obtain

$$M_{c.k} = 2M_{s.s.m} - \frac{n_f}{n_m} M_{s.s.m}.$$

The values n_f and $M_{c.k}$ are determined graphically on the basis of the experimental function $M_c = f(n)$. If the moment of the forces of resistance can be expressed through parabolic function $M_c = cn^2$, then

$$n_{\kappa}=\frac{\sqrt{\left(\frac{M_{\text{в.у.м}}}{n_{\text{м}}}\right)^2+8cM_{\text{в.у.м}}}-\frac{M_{\text{в.у.м}}}{n_{\text{м}}}}{2c}. \qquad (10.6)$$

If we know the maximum required starter power $N_{s.s.m}$ and rpm n_m at which this maximum power occurs, then we can evaluate the parameters of the linear law of change of starter torque, specifically:

$$M_0 = 2M_{s.s.m}=2\cdot 716{,}2\frac{N_{s.s.m}}{n_{\text{м}}}.$$

The available starter power on the engine rotor shaft will change according to the equation

$$N_{s.s}=\frac{n}{n_{\text{м}}}\left(2-\frac{n}{n_{\text{м}}}\right)N_{s.s.m}.$$

Finding according to equation (10.5) the final cranking rpm n_f, using the generalized characteristics $\theta = f(\bar{m}, a)$ we can determine the duration of the first starting phase τ_I. Here the following condition must be satisfied:

$$\tau_I \leq \tau_{m.t},$$

where $\tau_{m.t}$ is the maximum tolerable acceleration time, which can be determined on the basis of the prescribed time of starting τ_{st} and uniform acceleration $\tau_I = \tau_{st}\frac{n_1}{n_{1.p}}$. When $\tau_I > \tau_{m.t1}$ the parameters M_0 and n_f must be changed, whereupon for the purposes of improving engine starting reliability it is better to increase n_f, almost without changing M_0.

The duration of the second engine starting phase τ_{II} should also not exceed the maximum tolerable value:

$$\tau_{II}\leqslant\tau_{m.tII};$$
$$\tau_{m.tII}=\tau_{st}\frac{(n_2-n_1)}{n_{1.p}}.$$

The duration of the second starting phase is

$$\tau_{II}=\frac{\pi}{30}J_0\int_{n_1}^{n_2}\frac{dn}{M_{\text{п.у}}+\Delta M_{\text{т}}}.$$

For the assumed linear law of change of excess turbine torque $\Delta M_t = K_t(n - n_c)$, assuming a linear law of change of starter torque $M_{s.s} = M_0 - bn$, the duration of the second engine starting phase will be

$$\tau_{II} = \frac{\pi}{30} \frac{J_0}{K_T - b} \ln \frac{(K_T - b) n_2 + (M_0 - K_T n_c)}{(K_T - b) n_1 + (M_0 - K_T n_c)};$$

for b = 0

$$\tau_{II} = \frac{\pi}{30} \frac{J_0}{K_T} \ln \frac{M_0 + K_T (n_2 - n_c)}{M_0 - K_T (n_c - n_1)}.$$

The choice of rpm of starter shutdown is very important in the choice of starter parameters. This rpm must not be less than the required rpm $n_{2\,0}$ determined from the condition $M_{s.s} = 0$. Early disengagement of the starter results in prolongation of engine starting time, increase in the gas temperature and, accordingly, reduction of engine starting reliability. Consequently the starter should accompany the engine rotor to at least the rpm $n_{2\,0}$.

Therefore the rpm of starter disengagement n_2 can be determined from the condition

$$\Delta M_T \geqslant M_{jII}.$$

If we assume

$$\Delta M_T = K_T (n - n_c) \quad \text{and} \quad M_j = M_{j\text{av}} = \frac{\pi}{30} J_0 \frac{nf}{\tau_{st}},$$

then

$$n_2 \geqslant \frac{M_{j\text{av}} + K_T n_c}{K_T}.$$

The design turbostarter turbine power corresponds to the nominal rpm of its rotor. From considerations of strength the maximum tolerable turbostarter turbine rpm should not exceed its rpm in the nominal mode by P fold:

$$n_{t\ max} \leq P n_{t.nom}.$$

For turbocompressor starters with two kinematically disjoint turbines

the coefficient P = 1.5-1.7. For air turbostarters operating on air at a temperature of 150-220°C P = 1.8-2.0.

Thus for turbostarters the condition

$$n_2/n_m \leq P$$

must be satisfied or the maximum available starter power should be developed when $n_m \geq n_2/P$.

If rpm n'_m corresponding to the maximum available turbostarter power is greater than rpm n_m corresponding to maximum required starter power then it will be necessary to increase the available turbostarter power in order to meet the acceleration deadline (in particular $\tau_I \leq \tau_{m.tI}$).

The available turbostarter power can, of course, be reduced to the required value, but this involves substantial sophistication of the automatic equipment and is not advisable since higher turbostarter power facilitates an increase in engine starting reliability.

§24. Power Consumed by Starter to Start Engine

Acceleration of the engine rotor and overcoming of the forces of resistance in the first and partially in the second starting phases are performed by the power that is transmitted to the rotor from the starter. This power can be determined from the following equation:

$$L_{s.s} = 75\int_0^{n_2} N_{s.s}\,d\tau = 75\left[\int_0^{n_1} N_{s.s}\,d\tau + \int_{n_1}^{n_2} N_{s.s}\,d\tau\right] = L_{s.sI} + L_{s.sII}.$$

From the equation of motion for the first starting phase we have

$$d\tau = \frac{\pi}{30} J_0 \frac{dn}{M_{n.y1} - M_{c1}}.$$

Considering that $M_c = cn^2$, and for most modern starters $M_{s.s} = M_0 \pm bn$, we obtain

$$L_{s.sI} = 75\int_0^{n_1} N_{s.s}\,d\tau = \left(\frac{\pi}{30}\right)^2 J_0 \int_0^{n_1} \frac{(M_0 \pm bn)\,ndn}{(M_0 \pm bn) - cn^2},$$

and after integration we find:

for the case $M_{s.s} = M_0 + bn$

$$L_{s.sI} = \left(\frac{\pi}{30}\right)^2 \frac{J_0}{2c^2}\left[\frac{b^3+3bcM_0}{\sqrt{4cM_0+b^2}}\ln\frac{(b-\sqrt{4cM_0+b^2})n_1+2M_0}{(b+\sqrt{4cM_0+b^2})n_1+2M_0} - \right.$$
$$\left. -(cM_0+b^2)\ln\frac{M_0+bn_1-cn_1^2}{M_0} - 2bcn_1\right]; \tag{10.7}$$

for the case $M_{s.s} = M_0 - bn$

$$L_{s.sI} = \left(\frac{\pi}{30}\right)^2 \frac{J_0}{2c^2}\left[\frac{b^3+3bcM_0}{\sqrt{4cM_0+b^2}}\ln\frac{(b+\sqrt{4cM_0+b^2})n_1-2M_0}{(b-\sqrt{4cM_0+b^2})n_1-2M_0} - \right.$$
$$\left. -(cM_0+b^2)\ln\frac{M_0-bn_1-cn_1^2}{M_0} + 2bcn_1\right]; \tag{10.8}$$

for the case $M_{s.s} = M_0 = \text{const}$

$$L_{s.sI} = \left(\frac{\pi}{30}\right)^2 \frac{J_0}{2c} M_0 \ln\frac{M_0}{M_0-cn_1^2}. \tag{10.9}$$

By introducing dimensionless coefficients $\bar{m} = M_0/M_{c.k}$ and $a = n_f/n_1$ we can reduce equations (10.7)-(10.9) to the following form:

for the case $M_{s.s} = M_0 \pm bn$

$$L_{s.sI} = \left(\frac{\pi}{30}\right)^2 \frac{J_0}{2} n_f^2\left\{\frac{\bar{m}^3-1}{\bar{m}+1}\ln\frac{1-\frac{1}{a}}{1+\frac{1}{\bar{m}a}} - \right.$$
$$\left. -(\bar{m}^2-m+1)\ln\left[\left(1-\frac{1}{a}\right)\left(1+\frac{1}{\bar{m}a}\right)\right]+\frac{2}{a}(\bar{m}-1)\right\}; \tag{10.10}$$

for the case $M_{s.s} = M_0 = \text{const}$

$$L_{s.sI} = \left(\frac{\pi}{30}\right)^2 \frac{J_0}{2} n_f^2 \ln\frac{1}{1-\frac{1}{a^2}}, \tag{10.11}$$

It follows from equations (10.10) and (10.11) that when $\bar{m} = \text{const}$ and $a = \text{const}$

$$\frac{L_{s.sI}}{J_0 n_f^2} = \Omega_1 = \text{const}.$$

Thus, using the coefficient Ω we can determine the work of the starter in the cranking regime. This coefficient can be called the energy parameter of the starter in the cranking regime.

Figure 60, where the functions $\Omega_I = \Omega(a)$ are given for various values

of the parameter $\bar{m}$, shows that when a > 1.5-2 (during fast engine starts) the dimensionless energy characteristics of the cranking regime change very little in a rather wide range of change of the starter torque parameter ($\bar{m}$ = = 1-4).

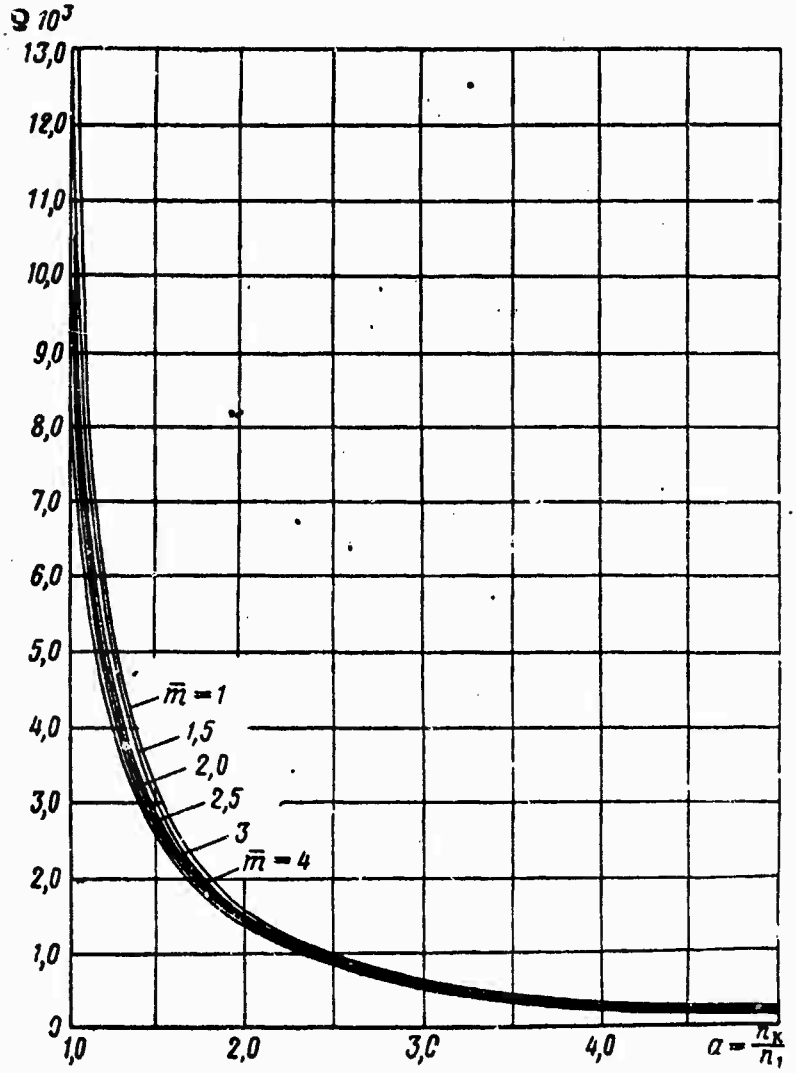

Figure 60. Dimensionless energy characteristics of starter for various $\bar{m}$.

With equations (10.10) and (10.11) it is easy to solve a number of practical problems. Thus, if for two types of engines the coefficients $\bar{m}$ and a are identical, then

$$\frac{L''_{s.sI}}{L'_{s.sI}} = \frac{J''_0}{J'_0}\left(\frac{n''_f}{n'_f}\right)^2.$$

For a given type of engine (J_0 = const) and starter ($\bar{m}$ = const) a change in atmospheric conditions is accompanied by a change in the torque of resistance forces, and the power of the starter in the cranking regime remains constant for a = const:

$$n_f' = n_f \frac{n_1'}{n_1}.$$

By way of example we will evaluate the effect of starter torque on $L_{s.sI}$ for two types of engines: turbojet engine (J_0 = 4.0 kg·m·sec^2; c = $= 30 \cdot 10^{-6}$ kg·m/(rpm)^2; n_1 = 1,000 rpm) and turboprop engine (J_0 = 0.82 kg·m·sec^2; c = 2.0 10^{-6} kg·m/(rpm^2); n_1 = 1,800 rpm).

The functions $L_{s.sI} = f(M_0, n_f)$ for the cranking regimes of the stated turbojet and turboprop engines are shown in Figures 61 and 62. For the cranking regimes of these engines we will use the law of change of starter torque $\bar{m}$ = 1 ($M_{s.s} = M_0$ = const).

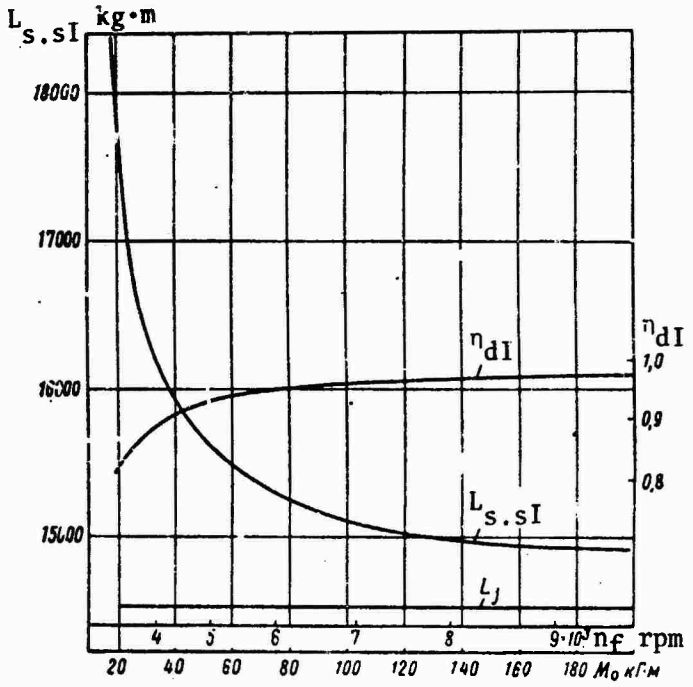

Figure 61. Effort of starter and dynamic efficiency as functions of starter torque during cranking of turboprop engine.

We see that as the available starter torque increases its effort in the cranking regime drops, and as $M_{s.s}$ increases, $L_{s.sI}$ drops notably.

Since $L_{s.sI} = L_{cI} + L_{jI}$ and the kinetic energy $L_{s.sI}$ for the given type of engine (J_0 = const) for n_1 = const does not depend on the law of change of starter torque, then the decrease of $L_{s.s}$ as $M_{s.s}$ increases is attributed to the reduction of power spent on overcoming the forces of friction.

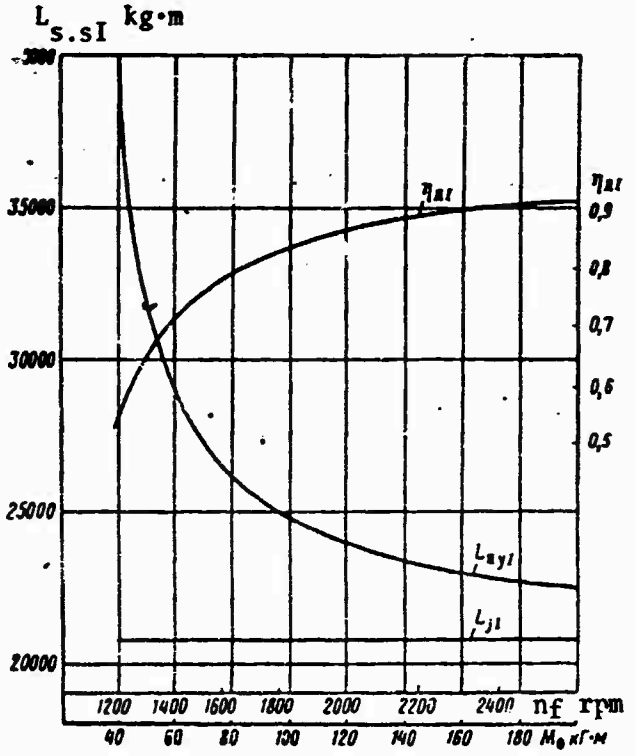

Figure 62. Effort of starter and dynamic efficiency as functions of starter torque during cranking of turbojet engine.

In the limiting case

$$\lim L_{s.sI} = L_{jI} \text{ for } \lim L_{cI} = 0$$
$$M_{s.s} \to \infty.$$

The reduction of power expended on overcoming the forces of friction is attributed to the notable reduction of cranking time as the starter torque (power) is increased.

Both analysis of the functions $\tau_I = \tau(M_0, n_f)$ and analysis of the energy functions $L_{s.sI} = L(M_0, n_f)$ show that as starter torque is increased the advantage of using the law of change of torque $\overline{m} > 1$ ($M_{s.s} = M_0 - bn$)

diminishes. The law $\bar{m} = 1$ ($M_{s.s} = M_0 = \text{const}$) is more advantageous for fast acceleration of the engine rotor in the first starting phase.

The less inertia (the smaller the values J_0, c) an engine possesses the more advantageous it is to convert to the law $M_{s.s} = M_0 = \text{const}$. An increase in starter torque during the initial phase of engine rotor acceleration $M_0 > M_{c.k}$ ($\bar{m} > 1$) results in unnecessary increases in weight and dimensions of the starter and transmission, and also reduction of the efficiency of the starter due to increased losses in the circuit and in the starter.

The effectiveness of utilizing the mechanical power of the starter in the cranking regime can be determined with the aid of the dynamic efficiency:

$$\eta_{dI} = L_{jI}/L_{s.sI}.$$

Since for $M_{s.s} = M_0 = \text{const}$ the power is

$$L_{s.sI} = \left(\frac{\pi}{30}\right)^2 \frac{J_0}{2c} M_0 \ln \frac{M_0}{M_0 - cn_1^2},$$

then

$$\eta_{dI} = \frac{cn_1^2}{M_0 \ln \frac{M_0}{M_0 - cn_1^2}}.$$

The dynamic efficiency in the cranking regime is shown in Figures 61 and 62 as a function of starter torque for turbojet and turboprop engines. From the point of view of efficient utilization of the starter in the cranking regime, each type of engine has its own range of reasonable increase of torque. A further increase in torque involves undesirable increases in the weight and dimensions of the starter.

Since the previously determined dimensionless energy parameter Ω characterizes the power of the starter in the cranking regime we may determine the relation between η_{dI} and Ω.

For this purpose we will substitute in the expression of the parameter $\Omega = L_{s.sI}/J_0 n_f^2$ the value $n_f = an_1$; multiplying the numerator and denominator by $2\left(\frac{\pi}{30}\right)^2$ we obtain

$$\Omega = \frac{\left(\frac{\pi}{30}\right)^2 L_{s.sI}}{2a^2 \left(\frac{\pi}{30}\right)^2 \frac{J_0}{2} n_1^2}.$$

But since

$$L_{j1}=\left(\frac{\pi}{30}\right)^2 J_0 \frac{n_1^2}{2},$$

then

$$\Omega=\frac{\left(\frac{\pi}{30}\right)^2}{2a^2}\frac{L_{s.sI}}{L_{jI}}.$$

Since

$$\eta_{dI} = L_{jI}/L_{s.sI},$$

then

$$\Omega=\frac{\left(\frac{\pi}{30}\right)^2}{2a^2}\frac{1}{\eta_{dI}}.$$

Hence

$$\eta_{dI}=\frac{5.48\cdot10^{-3}}{a^2}\frac{1}{\Omega}.$$

Consequently, knowing the generalized characteristics $\Omega = \Omega(\bar{m}, a)$ we can determine the dynamic efficiency η_{dI} for the given or determined laws of change of torque $(\bar{m})$ and coefficient a. This especially simplifies the calculation for $\bar{m} \neq 1$.

The curves $\eta_{dI} = f(\Omega)$ are shown in Figure 63 for different values of the coefficient a.

From the equation of motion for the second starting phase we obtain

$$d\tau=\frac{\pi}{30}\,I_0\frac{dn}{M_{n.yII}+\Delta M_{\tau II}}.$$

Then

$$L_{s.sII}=75\int_{n_1}^{n_2} N_{s.s}\,d\tau=\left(\frac{\pi}{30}\right)^2 J_0\int_{n_1}^{n_2}\frac{M_{s.sII}^{ndn}}{M_{s.sII}+\Delta M_{tII}}$$

or

$$L_{s.sII}=\left(\frac{\pi}{30}\right)^2 J_0 \int_{n_1}^{n_2} \frac{n\,dn}{1+\frac{\Delta M_{TII}}{M_{s.sII}}}.$$

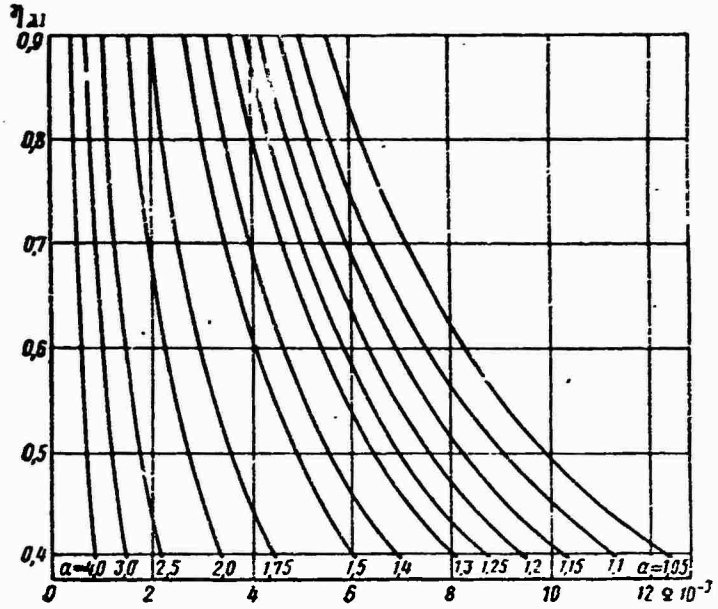

Figure 63. Dynamic efficiency as function of energy parameter of gas turbine engine cranking regime.

We will estimate the effect of starter torque and surplus turbine torque on starter operation in the second starting phase under the following assumptions:

a) a constant torque is supplied by the starter to the engine rotor;

b) the surplus turbine torque is proportional tc engine rotor rpm:

$$\Delta M_{TII}=K_T(n-n_c).$$

Obviously

$$\frac{\Delta M_{tII}}{M_{s.sII}}=\frac{K_T}{M_0}(n-n_c)$$

and then

$$L_{s.sII} = \left(\frac{\pi}{30}\right)^2 J_0 \int_{n_1}^{n_2} \frac{n\,dn}{1 + \frac{K_T}{M_0}(n - n_c)}.$$

After integration we obtain

$$L_{s.sII} = \left(\frac{\pi}{30}\right)^2 J_0 \left[\frac{n_2 - n_1}{\frac{K_T}{M_0}} - \frac{1 - \frac{K_T}{M_0} n_c}{\left(\frac{K_T}{M_0}\right)^2} \ln \frac{1 + \frac{K_T}{M_0}(n_2 - n_c)}{1 - \frac{K_T}{M_0}(n_c - n_1)} \right].$$

The dependence of starter operation in the second starting phase of a turbojet engine is shown in Figure 64.

We will determine the fraction of useful work of the starter and turbine in the kinetic energy imparted to the rotor in the second engine starting phase.

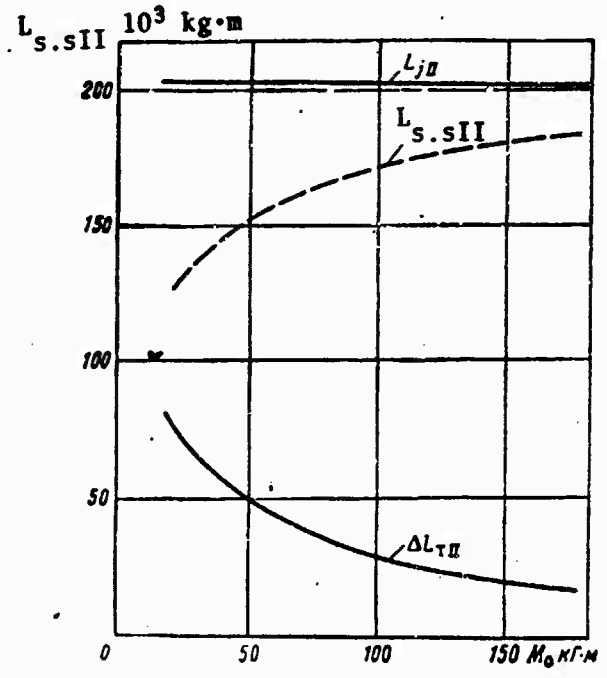

Figure 64. Power of starter in second starting phase as function of starter torque (J_0 = 4 kg·m·sec^2; $\overline{n_2} = n_2/n_{max} = 0.4$; $\overline{m} = 1$).

As starter torque increases, the share of the starter work increases and the share of the turbine work decreases (Figure 64). As the surplus turbine moment increases, the share of the turbine work increases and that of the starter decreases.

When $M_{s.s} = M_0 - bn$ and $\Delta M_t = K_t(n - n_c)$ the power of the starter in the second phase of the engine starting process will be given by the expression

$$L_{s.sII} = \left(\frac{\pi}{30}\right)^2 J_0 \left[\frac{n_2 - n_1}{B^2}(M_0 B - Ab) - \frac{b}{B}\frac{n_2^2 - n_1^2}{2} - \frac{1}{B^3}(M_0 AB + A^2 b)\ln\frac{A + Bn_2}{A + Bn_1}\right],$$

where

$$A = M_0 - K_t n_c;$$

$$B = K_t - b.$$

We may assume approximately for many types of gas turbine engines that acceleration of the engine rotor in the second starting phase will be close to uniform (j_{II} = const).

When $M_{s.s} = M_0 - bn$ and $\Delta M_t = K_t(n - n_c)$ this condition will correspond to equality of the torque coefficients of the starter and turbine, i.e., when j_{II} = const, $b = K_t$.

In this case

$$L_{s.sII} = \left(\frac{\pi}{30}\right)^2 J_0 \left[\frac{M_0}{M_0 - K_T n_c}\frac{n_2^2 - n_1^2}{2} - \frac{K_T}{M_0 - K_T n_c}\frac{n_2^3 - n_1^3}{3}\right],$$

or

$$L_{s.sII} = \left(\frac{\pi}{30}\right)^2 J_0 \left[\frac{1}{1 - \frac{K_T}{M_0} n_c}\frac{n_2^2 - n_1^2}{2} - \frac{1}{\frac{M_0}{K_T} - n_c}\frac{n_2^3 - n_1^3}{3}\right]. \qquad (10.12)$$

Since for $j = \text{const}$ $\frac{M_0}{K_T} = \frac{M_0}{b} = n_{20}$,

where n_{20} is the design rpm of the engine rotor for $M_{s.s} = 0$, then

$$L_{s.sII} = \left(\frac{\pi}{30}\right)^2 J_0 \left[\frac{1}{1 - \frac{n_c}{n_{20}}}\frac{n_2^2 - n_1^2}{2} - \frac{1}{n_{20} - n_c}\frac{n_2^3 - n_1^3}{3}\right]. \qquad (10.13)$$

Transforming this expression we obtain

$$\frac{L_{s.sII}}{J_0 n_1^2}=\left(\frac{\pi}{30}\right)^2\left[\frac{1}{1-\frac{\bar{n}_c}{\bar{n}_{20}}}\frac{\bar{n}_2^2-1}{2}-\frac{\bar{n}_2^3-1}{3(\bar{n}_{20}-\bar{n}_c)}\right],$$

or

$$\frac{L_{s.sII}}{J_0 n_1^2}=\left(\frac{\pi}{30}\right)^2\frac{1}{\bar{n}_{20}-\bar{n}_c}\left[\frac{\bar{n}_{20}(\bar{n}_2^2-1)}{2}-\frac{\bar{n}_2^3-1}{3}\right], \qquad (10.14)$$

where

$$\bar{n}_{20}=\frac{n_{20}}{n_1};\ \bar{n}_c=\frac{n_c}{n_1};\ \bar{n}_2=\frac{n_2}{n_1}.$$

If after shutting off the starter its torque is equal to zero ($n_2 = n_{2\,0}$), then equation (10.14) will become

$$\frac{L_{s.sII}}{J_0 n_1^2}=\left(\frac{\pi}{30}\right)^2\frac{1}{\bar{n}_{20}-\bar{n}_c}\left[\frac{\bar{n}_{20}(\bar{n}_{20}-1)}{2}-\frac{\bar{n}_{20}^3-1}{3}\right]. \qquad (10.15)$$

We will denote the dimensionless value in the left hand side of equation (10.15) through

$$\Omega=\frac{L_{s.sII}}{J_0 n_1^2} \qquad (10.16)$$

We will use this dimensionless value as the energy parameter of the starter in the second starting phase during uniform acceleration of its rotor.

If we know the energy parameter during uniform acceleration we can find by means of expression (10.16) the power of the starter in the second engine starting phase and can therefore determine the power consumed by the starter.

CHAPTER 11. RELIABLE STARTING ON THE GROUND

§25. Some Basic Causes of Unreliable Engine Starting on the Ground

During the starting process an aviation gas turbine engine operates in a rather complex unsteady state. Starting reliability depends on the reliability and stability of various processes taking place in the engine and starter system components.

Reliable start-up under all conditions requires that there be a certain program by which the power of the starter is transmitted to the rotor and heat supplied to the combustion chamber. Modern aviation engines are equipped for these purposes with special starter, fuel and electrical automatic control systems. Engine starting reliability depends on the reliability and proper functioning of these systems.

The problem of reliable engine start-up can become complicated by a narrow range of stable compressor operation, insufficient starter power, improper fuel feed to the combustion chamber during the starting process.

We will examine the basic causes of unreliable engine starting by starting phases.

In the first phase starting reliability may be reduced basically as the result of inadequate starter power, the consequence either of malfunctioning of individual components of the starter system (improper adjustment, deterioration of starter characteristics, power leaks between the power source and starter) or of deterioration of power source characteristics.

The amount of available starter power can be characterized by the final rpm n_f during acceleration of the engine without fuel feed into the combustion chamber. This engine speed must exceed rpm n_1 at which fuel feed begins by a factor of 1.1-1.15, i.e., $n_f \geq (1.1\text{-}1.15)n_1$. At lower speeds n_f starting time increases and extra power must be drawn from the power sources during the starting process. When $n_f < n_1$ reliable engine

starting is altogether impossible, since rpm n_1 is established from the standpoint of reliable ignition and combustion of the fuel in the combustion chambers, stable operation of the engine and its components and positive turbine power.

When $n = n_f$ the power developed by the starter is equal to engine resistance:

$$N_{s.s.f} = N_{c.k} = a_N n_f^3,$$

where $a_N = c/716.2$.

It follows from this equation that when starter power drops 3% the final cranking speed drops 1%.

The law of change of the moment of most starters can be expressed with sufficient accuracy by a linear function of the form

$$M_{s.s} = M_0 - bn.$$

This means that rpm n_f can be judged indirectly on the basis of the torque (and power) of the starter. It should be borne in mind, however, that in order to evaluate starter power according to n_f it is necessary to know the character of change of the forces of resistance under various climatic conditions.

During the engine starting process the starter power can also be determined indirectly on the basis of the duration of the first starting phase (time of rotor acceleration to the beginning of fuel feed to the combustion chambers).

It follows from the equation for the time of the first starting phase

$$\tau_1 = \frac{\pi}{30} J_0 \int_0^{n_1} \frac{dn}{M_{s.s} - M_c}$$

that for a given engine (J_0 = const, M_c = const) $\tau = f(M_{s.s})$ and the time of the first phase increases as starter torque decreases.

The second starting phase is the most important and, in most cases, determines the reliability with which the engine goes into the low power regime. Here unsuccessful attempts to start an engine are generally the result of deviations in the programs of fuel supply and starter power transmission.

Because of the narrow range of compressor stability in the second starting phase the supply of greater quantities of fuel results in unstable compressor operation. Stall oscillations spread through the entire compressor, causing pulsations in the air-gas duct of the engine, reduction of compressor thrust and rise of the gas temperature behind the turbine.

In most cases automatic engine start-up cannot be achieved when there are pulsations because the engine "hovers" at intermediate rpm. Hovering is a result of reduced turbine power output as a consequence of reduced air pressure behind the compressor and reduced air flow rate through the engine associated with compressor stalling, and also pre-ignition of fuel in the turbine duct.

Unstable engine operation may also be the result of fuel ignition delay in the combustion chambers because, for example, of poor atomization of the fuel by the injectors or improper operation of ignition system components. Fuel ignition delay in engines with powerful starters and relatively short starting time is difficult to detect by readings of thermocouples with high inertia.

The required engine rotor acceleration is governed by the selected programs by which starter power is transmitted to it, fuel is supplied to the combustion chamber and main engine components are regulated.

The following equation of engine rotor rotation is valid for the second starting phase:

$$\frac{\pi}{30} J_0 \frac{dn}{d\tau} = M_{s.s} + \Delta M_t,$$

where ΔM_t is surplus turbine torque expended on engine rotor acceleration.

Surplus turbine torque depends on very many parameters, especially maximum achievable gas temperature ahead of the turbine during the second starting phase. The maximum achievable gas temperature in front of the turbine during the starting process is determined by the compressor stability range (tolerable margin of stable compressor operation), fuel combustion completeness in the combustion chambers and heat resistance of heated engine parts.

The surplus turbine torque in the second starting phase is described approximately for most modern gas turbine engines by the linear function

$$\Delta M_t = K_t(n - n_c),$$

where n_c is engine rotor rpm at which $M_t = M_c$ [$n_c = (0.1\text{-}0.15)n_p$ for turbojet engines and $n_c = (0.3\text{-}0.4)n_p$ for turboprop engines, where $n_p = n_{max}$].

Limitation of the gas temperature, deterioration of compressor, combustion chamber and turbine performance influence the surplus torque of the turbine and consequently the increase of rpm n_c. An increase in n_c leads to a decrease of the rate of acceleration.

The character of engine rotor acceleration during starting can be controlled up until starter shut-off by the duration of the second starting phase

$$\tau_{II} = \frac{\pi}{30} J_0 \int_{n_1}^{n_2} \frac{dn}{M_{s.s} + \Delta M_t},$$

The minimum tolerable rate of acceleration is usually determined on the basis of the average acceleration during engine starting:

$$j_{av} = n_{1.p}/\tau_{st};$$

then

$$\tau_{II} = \frac{n_2 - n_1}{n_{1.p}} \tau_{st}. \qquad (11.1)$$

Unstable compressor operation during the second phase in the left (stall) region of the characteristic can be the cause of unsuccessful starting attempts.

The rpm of starter shut-off is selected such that the engine will proceed after starter shut-off to the low power regime with at least the average acceleration and without a rise in gas temperature in front of the turbine above the tolerable value. Therefore

$$j_{III} \geq n_{1.p}/\tau_{st}$$

or

$$\tau_{III} = \frac{n_{1.p} - n_2}{n_{1.p}} \tau_{st}. \qquad (11.2)$$

Early shutdown of the starter results in prolongation of the starting process, rise of temperature in the engine duct and consequently less engine starting reliability.

§26. Effect of Gear Ratio on Starting Reliability

The gear ratio of the drive from the starter to the engine shaft has a great effect on the required starter moments in the engine starting process.

The gear ratio of the reducer is the parameter that determines the matching of the starter torque characteristic with the engine characteristic.

The reducer gear ratio is determined by the ratio of the number of starter rotor revolutions to engine rotor revolutions. It changes the relationship between the moment and rpm after the starter reducer, the power of which here naturally remains constant. As the gear ratio is increased the moment on the reducer output increases and the rpm decreases. Conversely, as the gear ratio decreases, the moment on the output decreases and rpm increases.

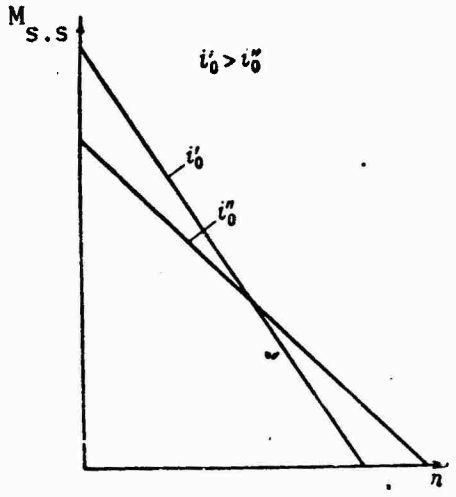

Figure 65. Moment characteristics on output shaft of starter for different reducer gear ratios.

The slope of the moment characteristic of the starter changes as a function of the reducer gear ratio (Figure 65). As seen in the figure, when the gear ratio is increased the slope of the moment characteristic to the abscissa increases.

The gear ratio from the starter to the engine has an effect on the moment transmitted to the engine. There is an optimal gear ratio that guarantees the most efficient utilization of the starter power characteristic.

In the general case

$$M_{s.s} = M_{s.s.p} i_o = M_{s.s.p} i_{red} i_g,$$

where $M_{s.s.p}$ is the torque on the starter rotor shaft;

i_o is the common gear ratio between the starter rotor and engine rotor;

i_{red} is the gear ratio of the reducer built into the starter;

i_g is the gear ratio of the reducer built into the engine.

If the starter torque on the engine rotor shaft is expressed by the relation

$$M_{s.s} = M_0 - bn,$$

and the torque of the starter on its rotor shaft is

$$M_{s.s.p} = M_{0p} - b_p n_p,$$

then

$$M_{s.y}=M_{s.y.p}i;\quad M_0=M_{0p}i;\quad b=b_p i_o^2;\quad n=\frac{n_p}{i_o}.$$

When the law of change of the torque of resistance forces is parabolic ($M_c = cn_f^2$) the final rpm of engine rotor cranking by the starter will be determined as a function of the gear ratio by the expression

$$n_f=\frac{\sqrt{b_p^2 i_o^4+4cM_{0p}i}-b_1 i_o^2}{2c}. \qquad (11.3)$$

The gear ratio corresponding to maximum cranking rpm ($n_{f.m}$) is given by the equation

$$i_{o.m}=\sqrt[3]{\frac{cM_{0p}}{2b_p^2}}.$$

With this gear ratio the maximum cranking rpm will be

$$n_{f.m}=\sqrt[3]{\frac{M_{0p}^2}{4cb_p}}. \qquad (11.4)$$

Considering that when the law of change of starter torque is linear ($M_{s.s} = M_0 - bn$) the maximum engine rotor cranking rpm takes place when maximum starter power is reached for $n_{f.m} = n_m$; then for $M_0 = 2M_{c.k}$

$$n_{f.m}=\frac{M_0}{2b}=\sqrt{\frac{M_{c.k}}{c}}=\sqrt{\frac{M_0}{2c}}$$

or

$$n_{f.m}=\sqrt{\frac{M_{0p}i_{o.m}}{2c}}.$$

These dependences can be used not only for calculating the common gear ratio i_o, but also for determining the gear ratio i_g of the engine drive with known i_{red}.

The curves of the dependence of the final rotor cranking rpm of a turbojet engine ($c = 30\cdot10^{-6}$ kg·m/(rpm)^2; $J_0 = 3.8$ kg·m·sec^2) by a turbocompressor starter ($M_{0p} = 3.44$ kg·m; $b_p = 50.2\cdot10^{-6}$ kg·m/rpm) are shown in Figure 66.

The maximum rpm $n_{f.m}$ of engine rotor acceleration by the turbostarter is 1,259 rpm and takes place when $i_{red.m} = 27.2$.

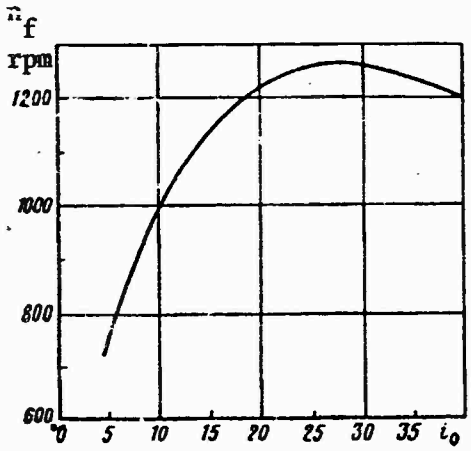

Figure 66. Final cranking rpm of turbojet engine rotor by turbocompressor starter as function of common reducer gear ratio.

Shown in Figure 67 is the curve of rotor cranking time of the examined type of engine by a turbostarter for different reducer gear ratios.

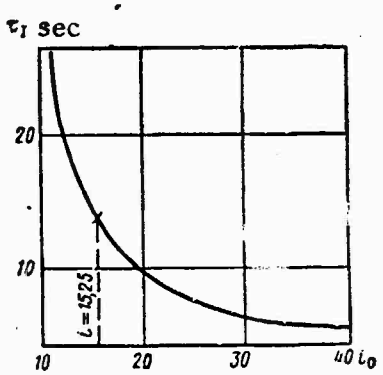

Figure 67. Engine rotor cranking time by turbostarter as function of common reducer gear ratio.

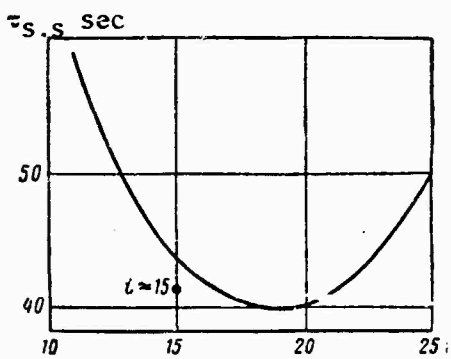

Figure 68. Summary engine rotor cranking time by turbostarter as function of common gear ratio.

In the second engine starting phase, during combined rotor acceleration by the starter and turbine and with a linear law of change of surplus turbine torque [$\Delta M_t = K_t(n - n_c)$], the acceleration is

$$j_{II} = \frac{9.55}{J_0}\left[M_{0p}i_0 - b_p i_0^2 n + K_T(n - n_c)\right].$$

The duration of the second engine starting phase with linear laws of change of starter torque and surplus turbine torque will be

$$\tau_{II} = \frac{\pi}{30} J_0 \left[\frac{2.31}{K_\tau - b_p i_0^2} \lg \frac{(K_\tau - b_p i_0^2) n_2 + (M_{0p} i_0 - K_\tau n_c)}{(K_\tau - b_p i_0^2) n_1 + (M_{0p} i_0 - K_\tau n_c)} \right]. \qquad (11.5)$$

Figure 68 illustrates the curve of the summary rotor acceleration time of an engine ($c = 30 \cdot 10^{-6}$ kg·m/(rpm)^2; $J_0 = 3.8$ kg·m·sec^2, for which $n_1 = 1{,}000$ rpm, $K_t = 0.0416$ kg·m/rpm) by a turbostarter.

For the purpose of improving the starting reliability of certain types of engines (for instance turboprop engines) the gear ratio is selected such that the engine is accompanied by the starter to high rpm $n = (50\text{-}60\%)n_{1.p}$.

§27. Effect of Engine Design Features on Starting Reliability

In the starting regimes surplus turbine torque depends on the air pressure developed by the compressor and on the tolerable heating of air in the combustion chambers. The tolerable heating of air in the combustion chambers is determined from the standpoint of ensuring stable compressor operation in the entire range of starting regimes.

As a rule axial compressors with a high compression ratio, reaching values of 10-12 at maximum rpm, are used for modern turbojet engines. The need to reduce compressor weight prompted the development of compressors with supersonic stages.

A compressor is chosen for an engine from the point of view of achieving the best indices in the design regime. Compressor losses are minimized in this regime by arranging the rotating and fixed vanes so that conditions of unbroken flow around them are created.

In lower (compared to the design) operating regimes the axial velocities of the air through the compressor stages differ from those in the design regime. Thus the axial velocities by stages are different. The air velocity at compressor intake changes only as a result of changing the air flow rate through the engine (the density of air in the intake cross section remains constant). In all subsequent (and especially in the last) compressor stages this velocity changes not only as a result of change of the flow rate but also of the density of air. For continuous flow in compressor intake and exhaust sections the following expression can be derived for the ratio of axial velocities in the stated sections:

$$\frac{C_{2a}}{C_{1a}} = \frac{f_1}{f_2} \frac{1}{\pi_x^n}, \qquad (11.6)$$

where f_1 and C_{1a} are the cross sectional area and velocity of air in the compressor intake;

f_2 and C_{2a} are the same at compressor exhaust;

π_k is the compression ratio in the compressor;

n is the index of the polytropic curve of compression.

In the case of constant (for a planned engine) cross sectional areas f_1 and f_2 the ratio of axial velocities depends only on the compression ratio. As rpm decreases, the compression ratio in the compressor decreases and accordingly the ratio of axial velocities at compressor exhaust and intake increases, i.e., the axial velocity drops more rapidly in the compressor intake as rpm decreases than at compressor exhaust. It follows from equation (11.6) that the higher the air compression ratio in the compressor in the design mode the greater the difference between the air velocities at the compressor intake and exhaust during engine operation in modes below the design mode. Consequently individual stages of the compressor and the entire compressor may operate unstably in nondesign modes. Thus a higher air compression ratio in the compressor causes a great rearrangement of operation of compressor stages in nondesign regimes.

Axial compressors cannot operate stably in the entire engine rpm range. The higher the air compression ratio in the compressor in the maximum regime, the narrower its range of stable operation. The placement of the first high-pressure supersonic stage in a multistage compressor has the same effect.

The result of a great reduction of the axial velocity of the air flow in the compressor intake in regimes less than the design regime is that the angle at which the flow strikes the vane profiles in the intake increases as the engine operating mode is decreased. The flow breaks away from the profiles when the critical angle is reached and the compressor ceases to operate stably.

Under such conditions it is impossible to bring an engine with a high-compression axial compressor into the low power regime without regulating the compressor.

The compressor is regulated by special devices whereby it is possible to change the geometry of individual sections of the flow part of the compressor and to disrupt air flow continuity in the duct. The required air parameters can thus be maintained in nondesign regimes with high compressor efficiency.

Specific problems of regulating the compressor of each engine are many and varied and depend on the type, purpose and design parameters of each engine. All these problems, however, can be solved by a comparatively few control methods.

Compressor operation in nondesign regimes is controlled basically by bypassing air from the intermediate compressor stages and by rotating guide vanes.

Air is bypassed through special ports in the compressor housing. These ports are closed automatically by special shrouding strips or valves on transition of the compressor to stable operating modes and in the absence of air bypass from the compressor.

Due to the escape of air through the bypass ports the air flow rate through the stages in front of the bypass ports is increased at the same compressor rotor rpm compared to the flow rate without the air bypass. This results in increased axial velocity of the air in the compressor intake, reduced angle of incidence of the air on the compressor vane profiles and more stable compressor operation.

The change of the basic engine parameters by rpm in the steady state modes of operation below the low power rpm with closed and open bypass shroud is depicted in Figure 69. The air and fuel flow rates and the gas temperature behind the turbine (and consequently in front of the turbine) have higher values at identical rpm with the bypass strip open. The fuel flow rate and heating of air in the combustion chambers with the bypass strip open are increased in connection with the increased air flow rate through the compressor between the intake and the bypass cross section. Consequently high turbine power is needed for turning the compressor rotor to the speeds at which the bypass strip is closed.

Using the heat balance equation for the combustion chamber during engine operation at certain steady state rpm with open and closed bypass strip we can determine the change in air flow rate through the combustion chamber when air is bypassed from the compressor. We may assume that fuel combustion completeness in the combustion chamber remains constant at the same rpm during engine operation with open and closed bypass strip. Then, after simple conversions of the thermal balance equations, we obtain

$$G_{a.op} = G_{a.cl} \frac{G_{f.op}}{G_{f.cl}} \frac{(c_{pg}T^*_g - c_{pa}T^*_k)_{cl}}{(c_{pg}T^*_g - c_{pa}T^*_k)_{op}}, \qquad (11.7)$$

Calculation of $G_{a.op}$ using this equation with respect to the data in Figure 69 shows that the air flow rate through the combustion chamber in the start-up regimes remains practically the same as without air bypassage.

The adiabatic pressure head developed by the compressor is greater with the bypassing of air from the compressor than without (Figure 70a). Using the obvious equation

$$\frac{\overline{H}_{ad.op}}{\overline{H}_{ad.cl}} = \frac{\pi^{*0.286}_{k.op} - 1}{\pi^{*0.286}_{k.cl} - 1},$$

it can be shown that the curve of combined compressor and turbine operation in the steady state starting regimes with open and closed bypass does not change (see Table 3 and Figure 70b). When air is bypassed, however, the

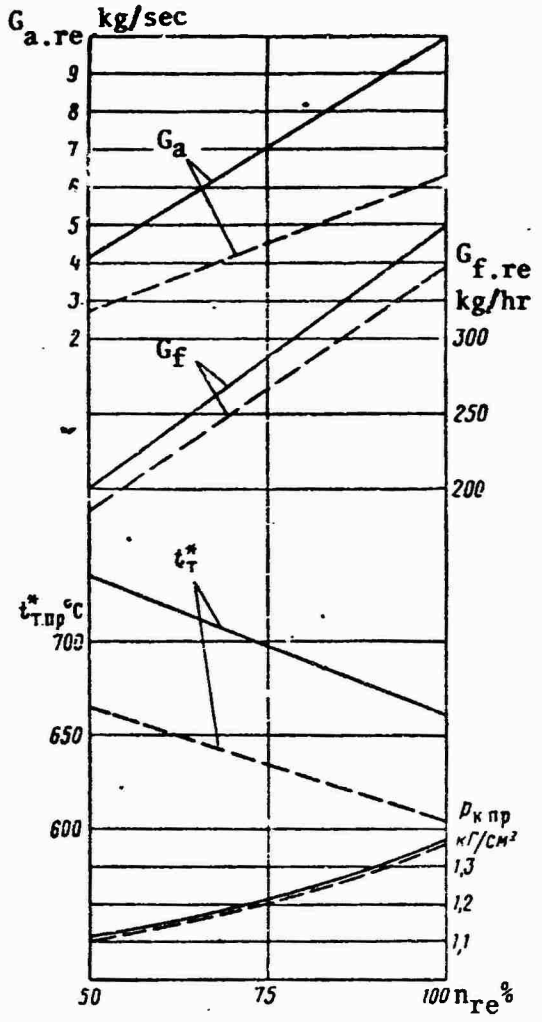

Figure 69. Change of basic engine parameters by rpm during starting with open (continuous curve) and closed (broken) bypass strip: G_a -- air flow rate; G_f -- fuel flow rate; t_t -- gas temperature behind turbine; p_k -- air pressure behind compressor.

combined operation curve is displaced toward larger compressor stability margins.

Since the bypassing of air increases the air flow rate through the first compressor stages the available compressor stability margin is accordingly also increased. Therefore engine starting properties are improved. The change of rpm and gas temperature behind the turbine during starting of the same type of engine with open and closed air bypass from the compressor of the same starter is shown in Figure 71.

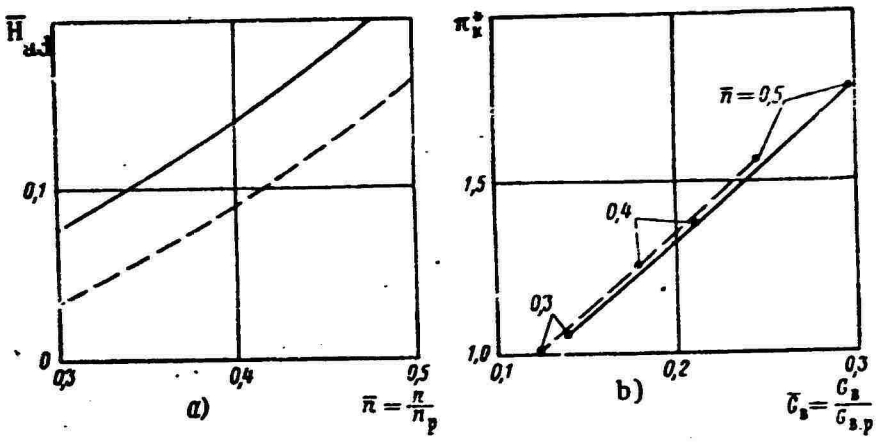

Figure 70. Change in relative adiabatic pressure by rpm (a) and change in compression ratio in compressor by relative air flow rate (b) in steady state regimes: continuous curve -- bypass open, broken curve -- bypass closed.

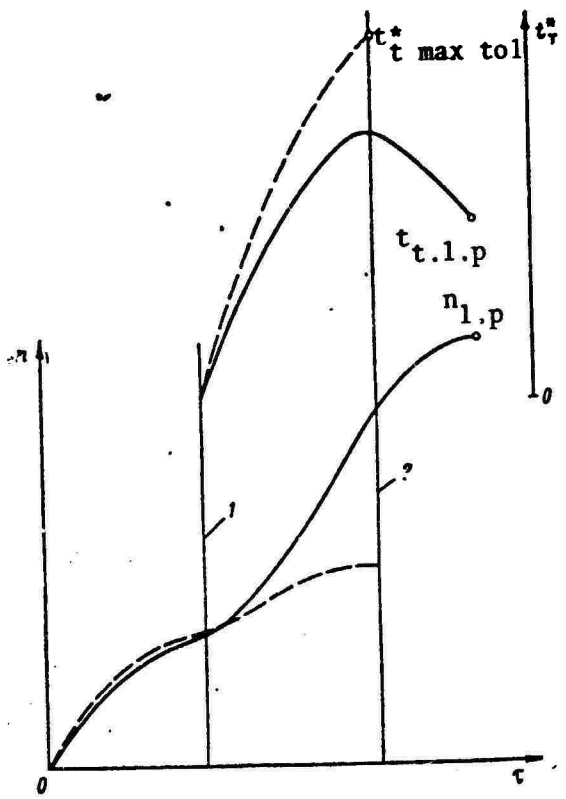

Figure 71. Change in engine rotor rpm and gas temperature behind turbine during starting with open (continuous curve) and closed (broken curve) bypass strips: 1 -- fuel begins to burn; 2 -- end of starting.

Table 3. Adiabatic Pressure, Compression Ratio in Compressor and Relative Air Flow Rate at Various rpm

$\bar{n}$	0.3	0.4	0.5
$\bar{H}_{ad.op}$	0.095	0.15	0.22
$\bar{H}_{ad.cl}$	0.05	0.1	0.17
$\pi_{k.op}$	1.05	1.35	1.7
$\pi_{k.cl}$	1.025	1.23	1.52
$\bar{G}_{a.op}$	0.14	0.21	0.30
$\bar{G}_{a.cl}$	0.12	0.18	0.245

In engines with a compressor compression ratio up to seven to one it is nearly always possible to ensure stable compressor operation by means of air bypass in one middle section, both in the starting regimes and regimes above the low power. For higher compression ratios more sophisticated compressor control is required; rotation of the guide vanes of the first compressor stages is required along with the bypassing of air in more than one section. Rotation of the guide vanes of the first stages in the direction of rotation of the working wheel (negative angle) reduces the area of the passage section and increases the air velocity through the guide apparatus. This, furthermore, reduces the angle of incidence of the flow on the working vanes of the compressor. Rotation of the guide vanes in the intake and in front of the first subsonic stage of the compressor is most effective.

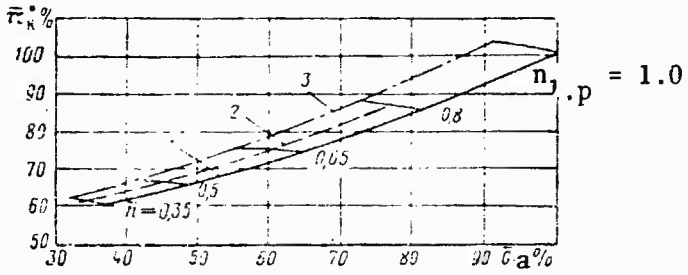

Figure 72. Compressor characteristics in starting regimes with intake guide vanes in different positions: 1 -- in steady state regime; 2 -- at boundary of stable operation with small rotation of guide vane; 3 -- at boundary of stable operation with large rotation of vanes.

When the guide vanes of one compressor stage are rotated, the curve of combined compressor and turbine operation in steady regimes does not change, but the boundary of stable compressor operation is displaced toward larger stability margins (Figure 72).

§28. Effect of Ambient Air Temperature on Starting Reliability

Turbojet engines can operate in aircraft in a wide range of ambient air temperatures from +50 to -50°C and more in the 780-500 mm Hg pressure range (the pressures at high-mountain airfields).

We will discuss the effect of ambient air temperature on the starting properties of engines with constant starter power.

The engine must be revved up to the steady state rpm of the low power regime within the required time and with gas temperatures in front of or behind the turbine not exceeding the maximum tolerable value of a given engine, regardless of the ambient air temperature.

At constant starter power the character of rotor acceleration with changing ambient air temperature during on the ground starting will depend chiefly on the magnitude by which turbine power exceeds engine resistance. The amount of surplus power is determined basically by how much the gas temperature in front of the turbine during start-up exceeds the gas temperature in front of the turbine in the steady state regimes. To start engines at various ambient air temperatures within a given period of time it can be assumed that the gas temperature in front of the turbine in unsteady regimes must exceed by an equal magnitude the gas temperature in front of the turbine in the steady regimes.

The air flow rate through the engine changes at the same engine rpm as the ambient air temperature changes, whereas the fuel flow rate through the combustion chambers remains practically constant. In this connection the temperature of the gases in front of the turbine also changes in the steady state operating modes below the low power rpm: under these conditions the gas temperature rises as the ambient air temperature both rises and falls.

In the case of constant regulation of the fuel system the gas temperature in front of or behind the turbine is higher when the engine is started at high ambient air temperature. At some ambient air temperature the gas temperature in front of or behind the turbine can reach the maximum tolerable level in certain types of engines (Figure 73). In these cases an engine can be brought into the low power regime at higher ambient air temperatures only by decreasing the fuel flow rate into the combustion chambers, and consequently by decreasing the gas temperature in front of or behind the turbine during the starting process. Here the time required for revving the engine up to the low power regime increases.

As the ambient air temperature changes the positions of the curve of combined turbine and compressor operation in the steady state regimes and the compressor stability boundary on its characteristics change (Figure 74). As seen in Figure 74 the range of change of air flow rate between the steady state and the compressor stability boundary narrows at the same measured rpm as the ambient air temperature rises. Since the magnitude of change of the air flow rate in the specified range determines

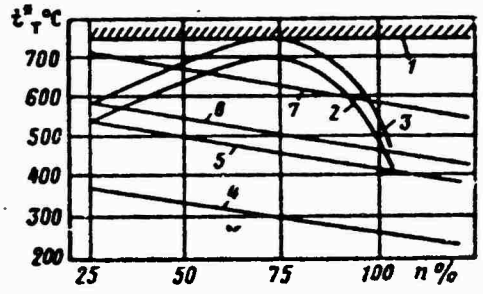

Figure 73. Change of gas temperature behind turbine by rpm at various ambient air temperatures: 1 -- maximum tolerable gas temperature behind turbine during starting; 2 -- gas temperature behind turbine during starting at ambient air temperature of 0°C; 3 -- likewise at ambient air temperature +15°C; 4 -- gas temperature behind turbine in steady state regimes at ambient air temperature of -50°C; 5 -- likewise at 0°C; 6 -- likewise at +15°C; 7 -- likewise at +50°C.

the maximum amount of fuel that can be injected into the combustion chambers, then as the ambient air temperature rises the compressor will begin to operate unstably with smaller surpluses of fuel injected into the combustion chambers. Consequently less fuel must be supplied to the engine to achieve stable compressor operation at a high ambient air temperature.

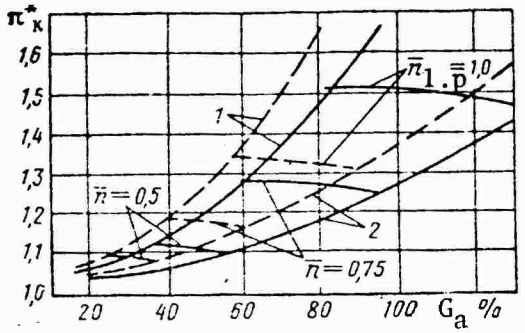

Figure 74. Engine compressor characteristics at ambient air temperature -50°C (continuous curve) and +50°C (broken curve): 1 -- at compressor stability boundary; 2 -- in steady regimes.

With constant control of the engine fuel system (i.e., with constant fuel feed to the combustion chambers during starting) and low ambient air temperature (especially negative values) engine rotor speed drops to the rpm at which it is turned by the starter in connection with the increased resistance of the engine (Figure 75).

We will examine how surplus engine power will change in the assumption that resistance is governed basically by the power consumed by the compressor for the compression of air.

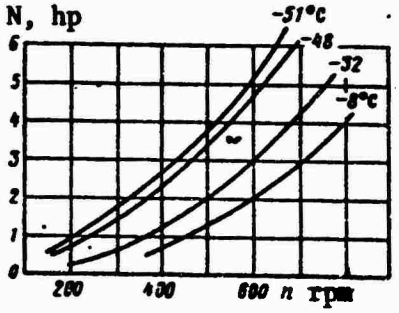

Figure 75. Powers of resistance of jet turbine engines (with centrifugal compressor) at various ambient air temperatures.

The power expended to overcome the friction of sliding turbojet engine parts is only an insignificant fraction of the total engine resistance. As the ambient air temperature drops, the resistance increases due to increasing oil viscosity. The effect of oil viscosity with falling ambient air temperature on starting is strongly manifested in turboprop engines, since oil with higher viscosity than the oil for turbojet engines must be used to ensure reliable operation of propellor reducer gears.

It can be assumed that the moment at which the engine turbine goes into stable operation after start-up is determined by the mass flow rate of air through the engine. It is clear from Figure 76 and Table 4 that the turbine begins to operate at lower rpm at negative ambient air temperatures during rotor acceleration by the starter.

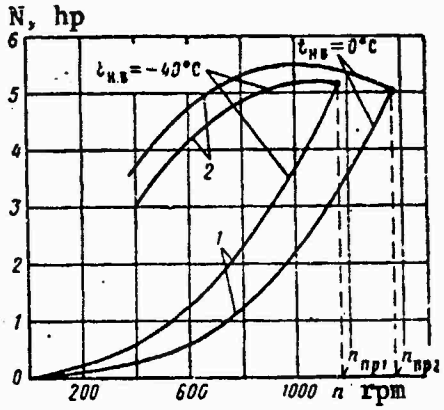

Figure 76. Change of starter power and resistance of engine with centrifugal compressor as function of engine rotor rpm (at various ambient air temperatures): 1 -- resistance; 2 -- starter power.

Table 4. Change of rpm at Which Engine Turbine with Centrifugal Compressor Begins to Operate at Various Ambient Air Temperatures

Ambient air temperature, °C	rpm--engine turbine begins to operate	
	rpm	%
+20	860	100
—20	760	88,5
—30	730	85

Because of the earlier operation of the turbine at negative temperatures the surplus power of the engine increases and the turbine therefore makes a bigger contribution to acceleration of the engine rotor. The result is that at negative ambient air temperatures the surplus engine power increases and the starter is capable of starting the engine.

The starting properties of an engine are also adversely affected by negative ambient air temperatures because the power produced by the starter drops and the quality of preparation of the fuel-air mixture for ignition in the starting igniters and main combustion chambers is lowered.

If an electric starter is used the temperature of the electrolyte of the storage batteries has an effect on its power. A lowering of electrolyte temperature reduces the supply of power from the batteries due to an increase in their internal resistance and therefore leads to sluggish acceleration of the engine by the starter to lower rpm.

In engines using turbostarters with a fluid coupling unsatisfactory filling of the fluid coupling with oil may result from negative ambient air temperatures below a certain temperature. This can be caused by different factors, chief among which is an increase in hydraulic losses in the suction lines. If the fluid coupling is not completely filled with the working medium its torque transmitting efficiency decreases, leading to sluggish engine rotor acceleration to lower rpm.

At negative ambient air temperatures the viscosity of fuel increases and its evaporability decreases. Increased viscosity reduces the fineness of fuel atomization and its low evaporability at negative temperatures adversely affects the ignition activity of the fuel-air mixtures.

As the fuel viscosity increases, the root angle of the flame decreases and the distribution of fuel in the combustion chamber changes. The higher the viscosity of the fuel and the greater the temperature derivative of viscosity, the greater will be the effect of fuel temperature on atomization.

Experience shows that the root angle of the fuel spray and droplet dimension after atomization of the fuel, the viscosity of which does not exceed 0.02 poise, differ little from the spray and droplets when an ideal liquid is atomized. In this case the chief factor is fuel evaporability.

At a given summary excess air coefficient of readily evaporating fuel heterogeneous mixtures with a low α_v/α_{li} are formed, and this has a favorable effect on ignition, since α_v is usually greater than one during start-up. Furthermore, when a readily evaporating fuel is used the initial center needs less energy to form a combustible mixture in the layers of the heterogeneous mixture adjacent to it.

The stated factors also determine the substantial displacement of the starting characteristics of the chamber to the region of richer fuel

mixtures after changing from readily evaporating B-70 fuel to a fuel with less evaporability. Increased fuel volatility, as a rule, leads to displacement of the lower and upper boundaries of the ignition zone toward higher summary excess air coefficients.

The igniting capacity of the starting flame decreases in connection with poor atomization and lower fuel evaporability. It is readily blown away by the air flow and the fuel-air mixture in the combustion chambers does not ignite.

Thus, clearly, both high positive and low negative ambient air temperatures on the ground considerably worsen engine starting reliability. And if the appropriate adjustment of the fuel system sometimes suffices for starting an engine at high temperatures, starting at low ambient air temperatures requires that even more additional measures be taken.

§29. Effect of Aircraft Air Intake on Starting Reliability

Aircraft are equipped with air intake and exhaust apparatus to ensure normal air supply to the engine compressor and discharge of gases. The air intakes of modern aircraft are especially complex, since they must provide for normal engine operation in a wide range of flight altitudes and velocities.

Supersonic intake diffusers, in which stagnation of the incident flow is accomplished successively in several oblique shock waves created by the cone stages, are used for supersonic aircraft.

The intake diffuser must be controlled in order to ensure favorable characteristics in a wide range of Mach numbers. Diffusers that are controlled by moving the central body and changing the throat area give satisfactory results. The basic problem of such control is to match the compressor and diffuser capacities in various flight regimes without lowering the pressure recovery coefficient.

Extra openings are made for delivery of air to the engine to improve intake characteristics during takeoff and at low flight speeds.

The resulting irregularity of pressures and velocities, both in terms of radius and circumference, substantially reduce the range of stable compressor operation. The irregularity can be caused by flow breakaway in the intake or by flow turbulization due to excessive diffusion, sharp edges and other design and mechanical features.

The intake ducts of modern aircraft are long, generally with a curved median line, with special devices for controlling the air flow rate through the intake under changing flight conditions. During installation of an engine in an aircraft it is sometimes necessary to increase the length of the exhaust system. The intake and exhaust systems of aircraft change compressor and turbine operating conditions.

Any intake duct creates resistance to the movement of air with the result that total pressure is decreased and the velocity field at compressor intake is altered, and the air flow rate through the engine is also reduced. The effect of the intake duct on the starting qualities of an engine is manifested in a change of the curve of combined compressor and turbine operation in the steady state starting regimes, and also in a change of the compressor stability boundary.

The air flow rate through an engine with an intake system is lowered in accordance with pressure losses in the intake duct. The air compression ratio in the compressor remains practically the same. Thus the line of combined compressor and turbine operation in the steady starting regimes is displaced to the left under the influence of the intake system, and consequently the compressor stability range in the starting regimes is reduced.

As seen in Figure 77, when total pressure losses in the compressor intake are increased by the intake system, the line of combined compressor and turbine operation approaches the compressor stability boundary. With an aircraft air intake system, furthermore, the greater the irregularity of the velocity field (pressure field) created by the intake system, the farther to the right the curve of stable compressor and turbine operation in the starting regimes is displaced. Such a displacement of the boundary of stable compressor operation further reduces the range of compressor stability in the starting regimes.

If during actual engine start-up, in the absence of total pressure losses and in the presence of a uniform velocity field in the compressor intake, the air flow rate and compression ratio change as indicated in Figure 77 by the continuous curve, then, obviously, it is impossible to start an engine with an air intake system without changing the adjustment of the fuel system. This is explained by the fact that the curve of combined compressor and turbine operation extends beyond the stability boundary. In this case starting is possible only by reducing the fuel flow rate in the starting regimes to the value at which the curve of combined compressor and turbine operation is located during starting to the right of the stability boundary of a compressor of an aircraft engine with an air intake system (see the broken curve in Figure 77).

A reduction of fuel flow rate in the starting regimes increases the time for running the engine up to low power (with the same starter). In individual cases this time may exceed the permissible time for starting an engine with the installed starter.

As the length of the exhaust duct increases, the pressure losses in the exhaust system increase and consequently the pressure drop on the turbine, and by the same token available turbine power, decrease. This also adversely affects engine starting properties.

Acoustical vibrations of the gas column that sometimes form in the exhaust system also adversely affect the starting qualities of an engine with a long exhaust system. These vibrations occur at a certain exhaust

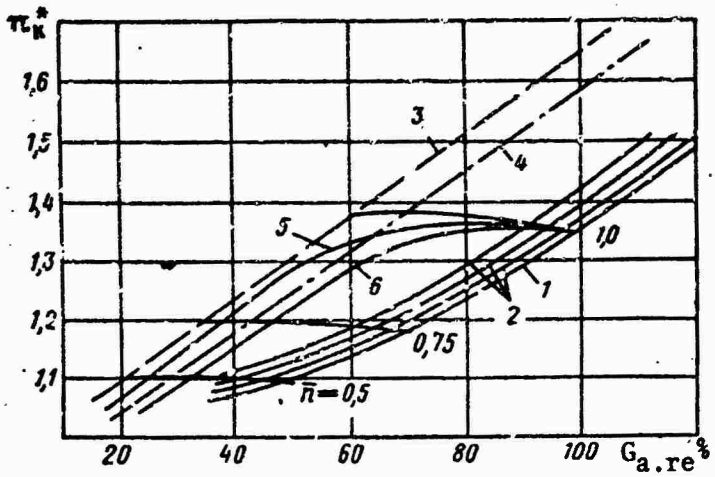

Figure 77. Compressor characteristics of engine in starting regimes for various full pressure losses in intake system: 1 -- curve of combined compressor and turbine operation in steady state regimes with air intake without losses; 2 -- curve of combined compressor and turbine operation in steady state regimes with various full pressure losses; 3 -- compressor operation stability boundary with air intake without losses; 4 -- likewise with losses; 5 -- starting curve with air intake without losses; 6 -- likewise with losses.

system length, completely defined for each type of engine. The acoustical vibrations can be eliminated, as a rule, by changing the length of the exhaust system, making it either longer or shorter than this critical length.

§30. Effect of Exhaust Nozzle Area on Starting Reliability

The exhaust nozzle area of engines with an afterburner behind the turbine can be changed within the same limits as the accepted degree of increased engine performance. It sometimes becomes necessary to evaluate the starting properties of such an engine with different exhaust nozzle areas.

The pressure and temperature of the gases in front of the nozzle should be changed as the nozzle area is changed, and consequently all engine duct parameters should be changed. The extent of change of these parameters depends on the relative change of area of the nozzle and compressor starting characteristics. Since the relative change of nozzle area is known or can be determined, compressor characteristics will have the greatest effect on the engine duct parameters.

The change to be made in engine duct parameters is determined by the slope of the dynamic characteristics of the compressor after changing the resistance of the system on which the compressor operates. In the starting regimes the air pressure behind the compressor generally remains constant

(the pressure branches of compressor characteristics are horizontal) in the starting regimes after a change in the resistance of the system. In this connection a change in the resistance of the system results basically in a change in the air flow rate through the compressor.

Since the air pressure behind the compressor is not changed by changing the system's resistance the fuel flow rate through the engine remains practically the same during starts with constant regulation of the automatic fuel control system. The extent of change of engine parameters in the steady state starting regimes therefore affect the starting qualities of the engine when the nozzle cross section is altered.

The gas flow rate through the engine, as is known, is determined by the equation

$$G_g = \frac{p_c^* F_c}{\sqrt{T_c^*}} \lambda_c \left(1 - \frac{k_g - 1}{k_g + 1} \lambda_c^2\right)^{\frac{1}{k_g - 1}} \left[\frac{2k_g}{R(k_g + 1)}\right]^{\frac{1}{2}}.$$

Writing this expression for two different nozzle areas and taking the gas flow rate quotient, we obtain

$$\frac{G_g'}{G_g^*} = \frac{F_c'}{F_c^*} \sqrt{\frac{T_\tau^{*\prime}}{T_\tau^{*\prime\prime}}} \frac{\lambda_c'}{\lambda_c^*} \left[\frac{1 - \frac{k_g - 1}{k_g + 1} \lambda_c'^2}{1 - \frac{k_g - 1}{k_g + 1} \lambda_c''^2}\right]^{\frac{1}{k_g - 1}}. \tag{11.8}$$

The following equation is valid for identical rpm:

$$\frac{G_g' \sqrt{T_g^{*\prime}}}{p_g^{*\prime}} = \frac{G_g^* \sqrt{T_g^{*\prime\prime}}}{p_g^{*\prime\prime}} \text{ or } \frac{G_g'}{G_g^*} = \sqrt{\frac{T_g^{*\prime\prime}}{T_g^{*\prime}}}. \tag{11.9}$$

It may be assumed in the first approximation from comparison of equations (11.8) and (11.9) that

$$\frac{F_c'}{F_c^*} \approx \frac{\lambda_c' \left[1 - \frac{k_g - 1}{k_g + 1} \lambda_c'^2\right]^{\frac{1}{k_g - 1}}}{\lambda_c^* \left[1 - \frac{k_g - 1}{k_g + 1} \lambda_c''^2\right]^{\frac{1}{k_g - 1}}}.$$

Thus, knowing the change of nozzle area we can determine the velocity coefficient in the exhaust nozzle and gas pressure behind the turbine, since

$$\lambda_c^2 = \left[1 - \left(\frac{p_H}{p_\tau^*}\right)^{\frac{k_g - 1}{k_g}}\right] \frac{k_g + 1}{k_g - 1}.$$

When the dynamic characteristics are not horizontal, the air pressure behind the compressor after changing the exhaust nozzle area can be found from the condition of constant drop in the starting regimes, developed on the turbine at the same rpm:

$$\frac{p_g^{*'}}{p_t^{*'}} = \frac{p_g^{*''}}{p_t^{*''}} = A,$$

and then

$$p_g^{*''} = Ap_t^{*''} = p_k^{*''}.$$

Taking the quotient of the fuel balance equations for the combustion chamber for the two different nozzle areas we obtain, after simple conversions

$$\frac{c_{p_g}T_g^{*''} - c_{p_a}T_k^{*''}}{c_{p_g}T_g^{*} - c_{p_a}T_k^{*''}} = \frac{G_f'}{G_f}\frac{G_a^{*}}{G_a'}.$$

The air temperature behind the compressor in the starting regimes will, for all practical purposes, not depend on the resistance of the system on which the compressor operates, and the fuel flow rate ratio for the two nozzle areas will remain constant in the entire starting range:

$$\frac{c_{p_g}}{c_{p_a}T_k^{*}}T_g^{*''} - 1 = \frac{G_f'}{G_f}\frac{G_a^{*}}{G_a'}\left(\frac{c_{p_g}}{c_{p_a}T_k^{*}}T_g^{*} - 1\right). \qquad (11.10)$$

Since all values entering into equation (11.10) are known, $T_g^{*''}$ can be determined. In the second approximation it is necessary to take into account in equation (11.8) the known temperature ratio $T_g^{*'}:T_g^{*''}$ when determining engine parameters with a different exhaust nozzle area.

All parameters on which compressor and turbine powers depend, and then ΔN_t for the new exhaust nozzle area, can be determined in the stated order.

The basic parameters are illustrated in Figure 78 as functions of rpm in the steady state regimes for two different exhaust nozzle areas.

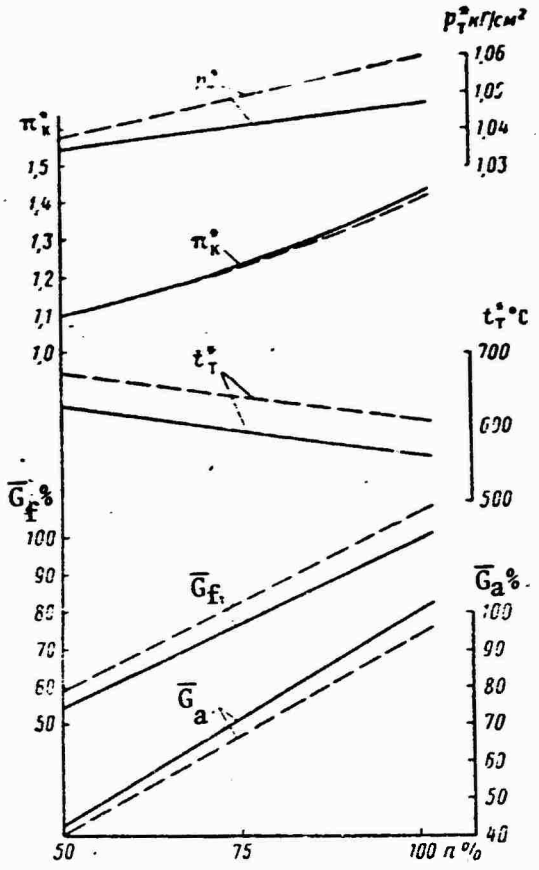

Figure 78. Engine parameters in steady state starting regimes for different exhaust nozzle areas (broken curves give parameters for $F_{c.in}$ and solid curves for $1.25F_{c.in}$).

CHAPTER 12. EFFICIENCY OF STARTING SYSTEMS

§31. Electric Starter

The power delivered by the power source is expended on mechanical work performed by the starter, losses in the starter and losses in the system:

$$L_{p.s} = L_{s.s} + \Delta L_{s.s} + \Delta L_{sy} = L_e + \Delta L_{sy}, \qquad (12.1)$$

where L_e is the electricity consumed by the starter (electric starter or starter-generator).

The power losses in the system can be determined by the equation

$$\Delta L_{sy} = \int_0^{\tau_s} \Delta N_{sy}\, d\tau;$$

$$\Delta N_{sy} = \frac{I_a^2 R_c}{1000}\text{kW} \quad \text{or} \quad \Delta N_{sy} = \frac{I_a^2 R_c}{736}\text{hp},$$

where I_a is power circuit current in ampere;

R_c is power circuit resistance in ohm.

The power losses in an electric starter consist of electrical losses $\Delta L_{s.s.e}$, comprising most of the losses, and also mechanical and other losses $\Delta L'_{s.s}$

$$\Delta L_{s.s.e} = \int_0^{\tau_s} \Delta N_{s.s.e}\, d\tau;$$

$$\Delta N_{s.s.e} = \frac{I_{ar}^2 R_{ar}}{1{,}000}\text{kW} \quad \text{or} \quad \Delta N_{s.s.e} = \frac{I_{ar}^2 R_{ar}}{736}\text{hp},$$

where I_{ar} and R_{ar} are armature current and armature winding resistance, respectively.

Assuming $I_a \approx I_{ar}$ for electric starters with series, parallel or combined excitation windings we obtain the summary power expenditure of the power source per start

$$L_{p.s} = L_{s.s} + 0.102(R_{ar} + R_c)\int_0^{\tau_s} I_a^2 d\tau + \Delta L'_{s.s} \text{ kg·m.} \qquad (12.2)$$

The power circuit current has a considerable effect on the efficient use of electric power sources, reliability and service life. A growth of I_a, increasing starter power, decreases $L_{s.s}$ during the starting process, and on the other hand is accompanied by a sharp increase in summary losses in the starter and in the system. Consequently the energy expended by the power source also increases. Therefore starter power in such systems should be increased by increasing source voltage and by improving starter and power source characteristics.

Each type of electric starter system has an optimal power circuit current, for which the power source discharges minimal energy per start.

By way of example we will determine the optimal current for accelerating a gas turbine engine with a constant torque from an electric starter (starter system type I = const). In this case

$$L_{s.sI} = \left(\frac{\pi}{30}\right)^2 \frac{J_0}{2c} M_0 \ln \frac{M_0}{M_c - cn_1^2}.$$

The torque on the engine shaft is

$$M_0 = M_e i_{o.e},$$

where M_e and $i_{o.e}$ are the torque on the armature shaft and gear ratio between the starter armature shaft and engine.

For electric starters with combined or parallel excitation the torque on the starter armature shaft is proportional to the current:

$$M_e = c'_e I_a.$$

Then for the cranking regime

$$L_{p.sI} = A I_a \ln \frac{1}{1 - \frac{B}{I_a}} + 0{,}102 (R_{ar} + R_c) I_a^2 \tau_I + \Delta L'_{s.s},$$

where

$$A=\left(\frac{\pi}{30}\right)^2 \frac{J_0}{2c} i_{o.e} c'_e;$$

$$B=\frac{cn_1^2}{i_{o.e} c'_e}.$$

$$\tau_1=\frac{\pi}{30}\frac{J_0}{\sqrt{cM_0}}\ln\frac{\sqrt{\frac{M_0}{c}}+n_1}{\sqrt{\frac{M_0}{c}}-n_1} \text{ (for } M_{s.s}=\text{const)}. \qquad (12.3)$$

For electric starters with combined excitation $M_e = c''_e I_a^2$ and then

$$L_{pssI}=AI_a^2\ln\frac{1}{1-\frac{B}{I_a^2}}+0{,}102\,(R_{ar}+R_c)I_a^2\tau_I+\Delta L'_{s.s}.$$

Depending on the type of excitation

$$M_0 = i_{o.e} c'_e I_a$$

or

$$M_0 = i_{o.e} c''_e I_a^2.$$

Equating the first derivative of the function $L_{p.sI}$ with respect to power circuit current to zero, we obtain:

for combined excitation electric starters

$$A\ln\frac{I_a}{I_a-B}-\frac{AB}{I_a^2-B}+0{,}204\,(R_{ar}+R_c)\tau_I I_a=0; \qquad (12.4)$$

for series excitation electric starters

$$2A\ln\frac{I_a^2}{I_a^2-B}-\frac{2AB}{I_a^2-B}+0{,}204\,(R_{ar}+R_c)\tau_I I_a=0. \qquad (12.5)$$

Solving these equations we can determine for the given electric starting system the power circuit current I_a at which power consumption in the cranking regime will be minimal. Let us determine for example the optimal current I_a during cranking of the VK-1A engine ($J_0 \approx 0.73$ kg·m·sec^2;

$c \approx 5$ kg·m/(rpm)^2; $i_{o.e} = 2.8$) with ST-2-48 ($R_{ST} = 0.0095$ ohm) and ST-2 ($R_{ST} = 0.0023$ ohm) electric starters. The torques of the starters are:

$$M_{e.ST-2} = 4 \cdot 10^{-6} I_a^2 \text{ kg·m};$$

$$M_{e.ST-2-48} = 16 \cdot 10^{-6} I_a^2 \text{ kg·m}.$$

Calculations show that minimum power consumption for cranking the VK-1A engine with $M_{s.s} = \text{const}$ (resistance of the air frame part of the starter system $R_{af} \approx 0.007$ ohm) corresponds to the current $I_a \approx 300$ amp for the ST-2 starter and $I_a \approx 600$ amp for the ST-2-48 starter, which has better characteristics.

The higher power voltage and better characteristics of the starter make it possible to reduce losses in the circuit and the starter itself with identical available power, and thereby to reduce the expended power and available energy of the power source. The power distribution curves and data on power consumption and losses during starting of the VK-1A engine with the ST-2 electric starter, operating on 24 volts, and with the ST-2-48 starter, operating on a 24/48-volt power circuit, are presented in Figure 79. Starting of the VK-1A engine with the ST-2-48 starter with a 24/48-volt power circuit requires only about half the battery power as the 24-volt ST-2 starter (14,850 and 27,350 kg·m, respectively).

Higher power source voltage and the associated reduction of currents in the power circuit reduces the summary losses in the starter and in the circuit (approximately 2.4-fold) and the power expenditure of the storage batteries (approximately 2.6-fold). The ratio of the mechanical power developed by the starter to the power produced by the power source (electrical efficiency of starter system) for the starter system with the ST-2 starter is 0.32, and for the starter system with the ST-2-48 starter, 0.48. Thus an electric starting system with higher power voltage and with a starter possessing improved performance characteristics improves the efficiency of the power source in converting its energy into mechanical work during the engine starting process.

§32. Turbostarter System

The summary flow rate of the working medium (gas) for starting an engine is determined for turbostarter systems by the expression

$$G_{t\Sigma} = q_g \tau_{II}, \tag{12.6}$$

where q_g is the gas flow rate in kg/sec.

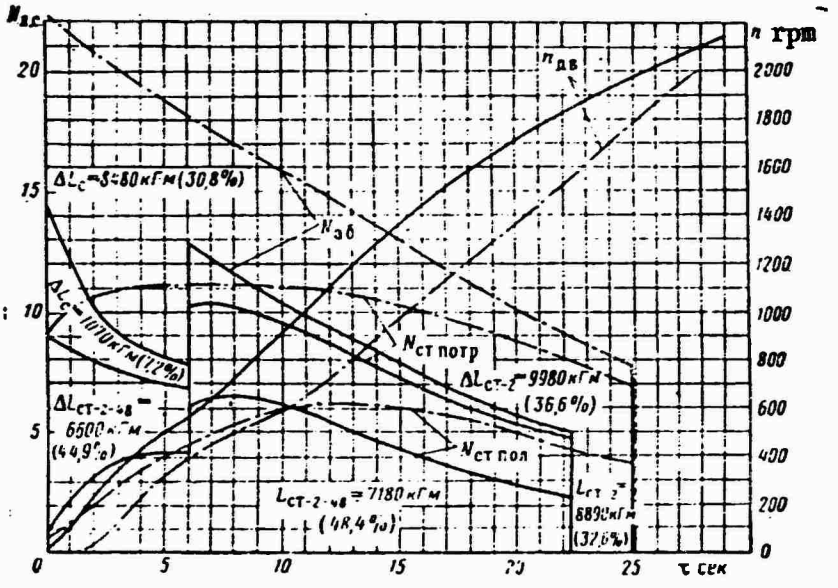

Figure 79. Power characteristics of electric starters when starting engine (continuous curve shows characteristics of ST-2-48 electric starter; broken curve -- characteristics of ST-2 starter): $N_{s.b}$ -- power delivered by storage batteries; $N_{co.st}$ -- electricity consumbed by starter; $N_{st.pol}$ is mechanical power of starter; ΔL_c -- power losses in circuit; ΔL_{st} -- power losses in starter; $L_{ST-2-48}$ and L_{ST-2} -- useful work of ST-2-48 and ST-2 starters.

The flow rate for turbostarters is

$$q_g = \frac{75N_{ts}}{L_{ад.т}\eta_т^*\eta_{red}} = \frac{75N_{ts}}{\frac{k_g}{k_g-1}R_gT_g^*\left[1-\frac{1}{\pi_т^{*\frac{k_г-1}{k_г}}}\right]\eta_т^*\eta_{red}}, \qquad (12.7)$$

and with a constant temperature drop on the turbostarter turbine

$$q_g = a_N N_{ts}.$$

For large temperature drops in the turbine the turbostarter turbine torque changes smoothly as engine rpm increases (the turbine torque decreases only 15-20% by the end of turbostarter operation) and therefore it may be assumed approximately that

$$M_{s.s} = M_0 = \text{const} \quad (\bar{m} = 1).$$

Then the maximum power developed by the turbostarter will be

$$N_{ts} = M_0 n_2/716.2,$$

and the required gas flow rate will be

$$q_g = a_m M_0.$$

For the first starting phase

$$G_{g\Sigma I} = q_g \tau_I = a_м M_0 \tau_I = \frac{\pi}{30} \frac{a_м J_0}{2} \sqrt{\frac{M_0}{c}} \ln \frac{\sqrt{\frac{M_0}{c}} + n_1}{\sqrt{\frac{M_0}{c}} - n_1} \tag{12.8}$$

and for the second

$$G_{g\Sigma II} = a_m M_0 \tau_{II}.$$

Assuming the law of change of surplus turbine torque in the second starting phase to be linear

$$\Delta M_{\tau II} = K_\tau (n - n_c),$$

we obtain

$$G_{g\Sigma II} = \frac{\pi}{30} \frac{a_м M_0 J_0}{K_\tau} \ln \frac{M_0 + K_\tau (n_2 - n_c)}{M_0 - K_\tau (n_c - n_1)} \tag{12.9}$$

Then

$$G_{g\Sigma} = G_{gI} + G_{gII} = \frac{\pi}{30} a_м J_0 \left[\frac{1}{2} \sqrt{\frac{M_0}{c}} \ln \frac{\sqrt{\frac{M_0}{c}} + n_1}{\sqrt{\frac{M_0}{c}} - n_1} + \right.$$
$$\left. + \frac{M_0}{K_\tau} \ln \frac{M_0 + K_\tau (n_2 - n_c)}{M_0 - K_\tau (n_c - n_1)} \right] \tag{12.10}$$

Analysis of this equation shows that the summary gas flow rate decreases as the available starter torque increases and as the starting characteristics of the engine improve (as the coefficient of surplus turbine torque K_t increases and rpm's n_c and n_2 decrease).

When using solid (powder) or liquid single-component fuel

$$q_g = q_t;$$

for fuel-air or vapor-gas (for example fuel-oxygen) turbostarters

$$q_g = q_t(1 + \alpha L_0),$$

where α is the coefficient of excess air (oxidant);
L_0 is the theoretical quantity of air (oxygen) required for combustion of 1 kg of fuel.

As turbostarter power increases, the gas flow rate increases and, on the other hand, the time of turbostarter operation decreases. Consequently, from the point of view of achieving the minimal gas (working medium) flow rate there is an optimal turbostarter power.

As starter torque (power) increases the summary gas flow rate drops sharply at first, and then, in the region of high torque, a substantial increase of $M_{s.s}$ does not lead to a substantial reduction of the summary gas flow rate (Figure 80).

An increase in the gas flow rate is accompanied by an increase in the summary gas flow rate and displacement of the optimal torque according to the summary gas flow rate toward high values.

When selecting the type of self-contained turbostarter system, powered by a source with a limited fuel reserve, it is essential that the selected turbostarter parameters correspond to those that provide the lowest possible summary gas flow rate. This is achieved, on the one hand, by increasing starter power. However, due to restrictions on the weight and dimensions of the starter and the small gain achieved by reducing starting time it is advisable to increase starter power above the optimal value. On the other hand the summary gas flow rate can be reduced by lowering the per second gas flow rate, governed by the parameters of the given turbine for given power and geometry of the turbostarter and also by the gas constants.

In determining the parameters of independent starting systems operating on two component mixtures (fuel-air or fuel-oxygen) it is essential to determine the summary flow rate of the component per second (basically the oxidizer), the reserve of which aboard the aircraft is limited and which determines the weight and dimensions of the system.

The per second oxidizer (compressed air, oxygen, etc.) flow rate is

$$q_{ox} = \frac{q_g}{1 + \frac{1}{q_{ox} L_{0\,ox}}},$$

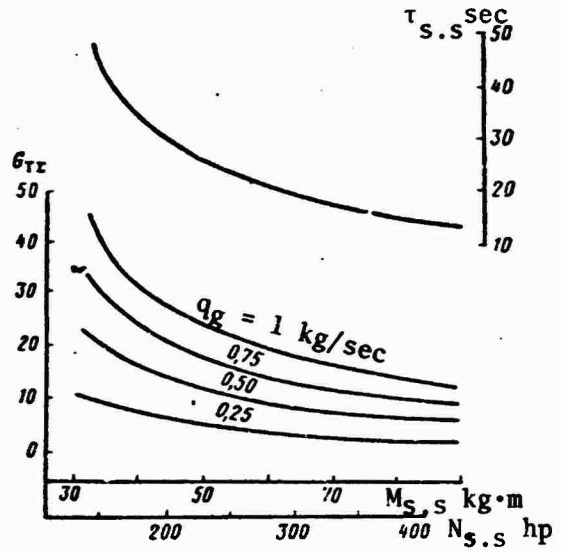

Figure 80. Summary gas flow rate and starter operating time as functions of available starter torque and power during start-up of turbojet engine with J_0 = 4.0 kg·m·sec^2.

where α_{ox} is the coefficient of excess oxidizer;

L_{0ox} is the amount of oxidizer theoretically required for the combustion of 1 kg of fuel.

The use of oxygen instead of compressed air as the oxidizer in a vapor-gas starter system greatly reduces the required quantity of the working medium.

Pressure drop π^*_{t0} (the compression ratio of the gas) in the starter turbine has a great effect on the per second and summary flow rate of the working medium. This influence can be evaluated with the aid of the influence coefficient.

Taking the logarithm of equation (12.7), we obtain

$$\ln q_g = \ln 75 + \ln N_{ts} - \ln\left(\frac{k_g}{k_g - 1} R_g\right) - \ln T^*_g - \ln\left(1 - \frac{1}{\pi^{*\frac{k_g - 1}{k_g}}_\tau}\right) -$$

$$- \ln \eta^*_\tau - \ln \eta_{red}.$$

Differentiating the equation obtained and considering that

$$d(\ln x) = \frac{dx}{x}; \quad \frac{k_g}{k_g - 1} R_\tau = \text{const}; \quad \eta_{red} = \text{const};$$

$$N_{ts}=\text{const};\ \frac{dq_g}{q_g}=\delta q_g,$$

we obtain an equation in small deviations (for N_{ts} = const)

$$\delta q_g=-\delta T_g^*-\frac{\frac{k_g-1}{k_g}}{1-\pi_T^{\frac{k_g-1}{k_g}}}\delta\pi_T^*-\delta\eta_T^*. \qquad (12.11)$$

The coefficient for $\delta\pi_t^*$ in the right hand side of the equation is the coefficient of the influence of π_t on q_g:

$$A_{\pi_t}=\frac{\frac{k_g-1}{k_g}}{\pi_T^{*\frac{k_g-1}{k_g}}-1}.$$

A 1% increase in the gas temperature T_g or turbostarter turbine efficiency, assuming other conditions to be constant, leads to a 1% reduction of the per second gas flow rate. A 1% increase of the pressure drop in the turbine, however, decreases the gas flow rate $A\pi_t$%, i.e., a reduction of the per second gas flow rate depends on the absolute value of π_t.

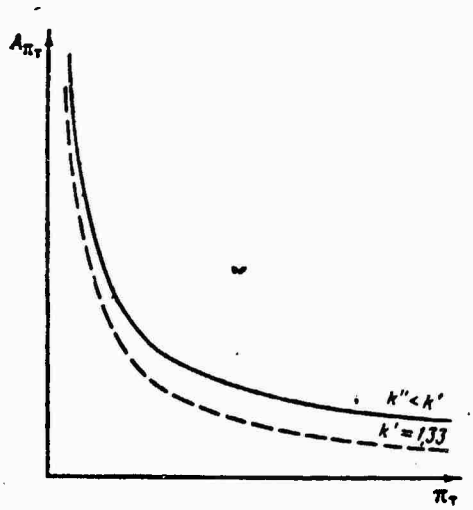

Figure 81. Coefficient A_{π_t} as function of pressure drop in turbostarter turbine.

The curve of the influence coefficient as a function of the pressure drop in the turbostarter turbine (Figure 81) for gas (k_g = 1.33) shows the lessening influence of π_t on the per second gas flow rate as the absolute value of π_t increases. The change of π_t has the greatest effect on the per second gas flow rate in the region of π_t up to 20. In the region of higher values of π_t (at which powder starters operate) this influence diminishes.

The curves of the compressed air flow rate as a function of expansion in the turbine of an air turbostarter during operation of an independent high-pressure air starter system (Figure 82) are presented for various air flow powers in the starter intake:

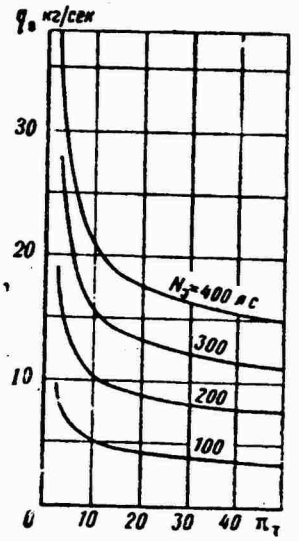

Figure 82. Compressed air flow rate as function of expansion in air turbostarter turbine.

$$q_a = \frac{75N_e}{102{,}5T_{in}\left[1-\frac{1}{\pi_т^{\frac{k-1}{k}}}\right]},$$

where

$$N_e = N_{ts}/\eta_t.$$

For independent air starter systems operating on high-pressure compressed air the optimal value of π_t, from the point of view of the advisable reduction of the per second compressed air flow rate, is, as we see, 30-35. At these values of π_t the summary compressed air flow rate is close to minimal. A further reduction of π_t, both for the purposes of reducing $G_{a\Sigma}$ and as a result of a marked reduction of turbostarter turbine efficiency by decreasing the parameter u/C_{ad}, is unadvisable.

Evaluation of the effectiveness of self-contained starter systems with turbostarters, for which there is a limited reserve of fuel aboard the aircraft, should be done in terms of the specific per second flow rate of the working medium:

$$C_{G_f} = \frac{q_t}{N_{ts}}.$$

For fuel-air turbostarters operating on a mixture of the main fuel (kerosene) with high-pressure compressed air (the gas pressure in the combustion chamber is 14-20 kg/cm^2, the excess air coefficient of the mixture is α = 1.5-2.0), for example, the specific per second compressed air flow rate reaches 1.3-1.9 g/hp sec.

The curves of change of the summary working medium flow rate (compressed air, oxygen and solid fuel) as a function of turbostarter power are shown in Figure 83.

The relatively low summary fuel rate of oxygen and solid fuel (powder) in the corresponding types of independent starter systems makes these systems preferable from the standpoint of power to, for example, systems with a fuel-air turbostarter, with a turbostarter operating on liquid single-component fuel, and especially to a system with a turbostarter operating on compressed air.

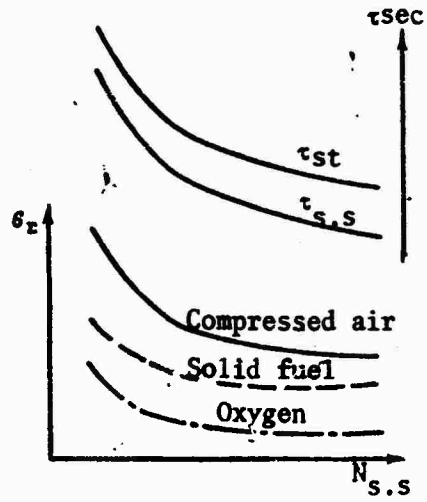

Figure 83. Change of summary gas flow rate, starter operating time and starting time as functions of turbostarter power.

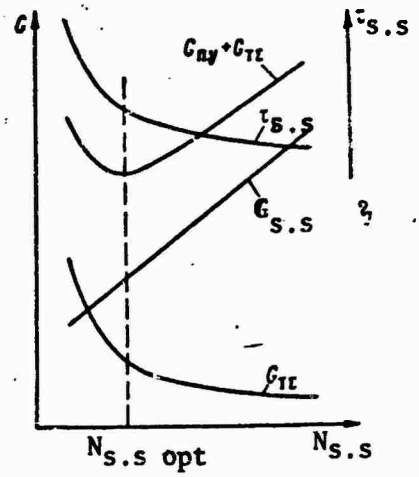

Figure 84. Summary weight of starter and working medium as functions of starter power.

As the power of the starter increases, its weight increases and the summary gas flow rate $G_{t\Sigma}$ decreases (Figure 84). Hence the optimal starter power corresponding to the minimum $G_{s.s} + G_{t\Sigma}$ can be determined by equating the first derivative of this value to zero. The optimal moment (power) corresponds to the minimum weight of the starter and working medium.

§33. Air Starter System

The question of the efficiency of power sources for an air starter system is just as important as for a self-contained electric starter system.

By increasing the air turbostarter efficiency and decreasing the losses in the system (in the air lines) the available turbostarter power on the engine rotor shaft can be increased. An increase of starter system efficiency for a given starter power by reducing losses in the starter system and in the network cuts the weight of the starter system and substantially improves power source reliability. In this case power source reliability is improved by decreasing the compressed air flow rate, and consequently, when a compressed air turbogenerator is used, by lowering the gas temperature (Figure 85) and sometimes by further reducing the turbocompressor rotor rpm.

Thus air pressure losses in the starter system air lines, on the one hand, determine the starter power on the engine rotor shaft and, on the other hand, the flow rate and pressure of the air taken from the compressed air source and, consequently, the mode of operation of the compressed air turbogenerator or operating engine.

The parameters that govern air turbostarter power are found from the conditions of combined operation of the turbostarter and compressed air source with allowance for network losses (resistance of air lines).

The characteristic of the compressed air source is expressed by the function $p^*_{a.f} = f(G_{a.f})$ at constant rotor rpm of the power unit. The air turbostarter turbine characteristic is expressed through the parameter that determines the reduced air flow rate:

$$\frac{G_a\sqrt{T^*_a}}{p^*_a} = A_{ts}. \qquad (12.12)$$

Considering that a supercritical pressure drop occurs in modern air turbostarter turbines A_{ts} = const for a given type of turbine and the air flow rate is proportional to the pressure in the starter turbine intake.

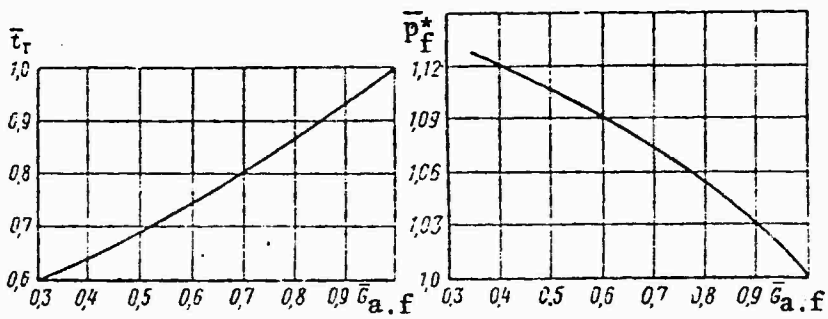

Figure 85. Characteristics of power unit (compressed air turbogenerator) for n_{des}: $\bar{G}_{a.f}$ -- relative air flow rate ($\bar{G}_{a.f} = G_{a.f}:G_{a.f}$ for t_{max}); $\bar{p}_{a.f}$ -- relative air pressure ($\bar{p}_{a.f} = p_{a.f}:p_{a.f}$ for t_{max}); $\bar{t}_g$ -- relative gas temperature behind power unit turbine during admission of air.

The characteristics of combined operation of a compressed air turbogenerator (CATG) and air starter turbine are depicted schematically in Figure 86. Point A of the intersection of the characteristics of both units represents the mode of combined operation of the CATG and turbostarter turbine without allowance for network losses. In the presence of pressure losses in the network the point of combined operation is displaced with respect to the TS turbine characteristic in the direction of lower values of p^*_a and G_a (point B).

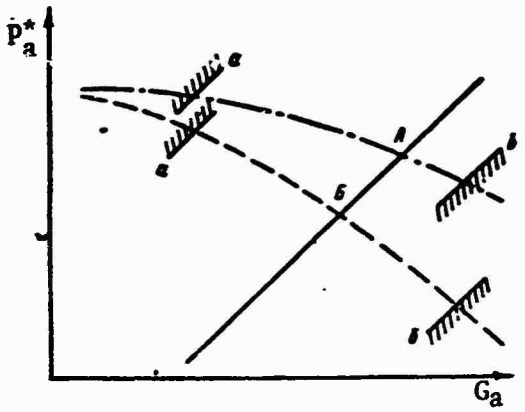

Figure 86. Characteristics of combined operation of compressed air turbogenerator and air turbostarter turbine without losses and with allowance for network pressure losses (continuous line represents characteristic of turbostarter turbine for T_a^* = = const, dot-dash curve represents characteristic of isolated CATG and broken curve -- characteristic of CATG in the presence of network pressure losses): a -- boundary of stable operation of CATG compressor; b -- boundary of maximum tolerable gas temperature.

Due to a change of the air flow rate through the turbostarter turbine the magnitude of network losses will change as the turbine characteristic shifts from point A to point B.

To find the point of combined operation of the compressed air source (CATG) and air turbostarter in the presence of network pressure losses it is necessary to solve a system of three equations that determine the characteristics of the compressed air source, turbostarter and network.

The power of the air turbostarter turbine is determined by the equation

$$N_{ts} = \frac{k}{75(k-1)} G_a R_a T_a^* \left[1 - \left(\frac{p_n}{p_a^*} \right)^{\frac{k-1}{k}} \right] \eta_t^* \qquad (12.13)$$

From equation (12.12) the air flow rate through the turbine will be

$$G_a = \frac{A_{ts} p_a^*}{\sqrt{T_a^*}} . \qquad (12.14)$$

The air pressure in the turbostarter turbine intake differs from the pressure of the air from the power source by the magnitude of network losses, i.e.,

$$p_a^* = p_{a.f}^* - \Delta p. \tag{12.15}$$

For a given network it may be assumed approximately that the pressure losses in it are proportional to the square of the air flow rate (air leaks in the network can be disregarded, i.e., $G_a \approx G_{a.f}$; these losses usually do not exceed 2-3% of the air flow rate from the power source in executed systems). Then

$$\Delta p = aG_a^2, \tag{12.16}$$

where a is the coefficient of resistance of the lines.

Coefficient a can be found from the known equation of network hydraulic resistance:

$$\Delta p = \xi_\Sigma \frac{\gamma_a W_a^2}{2g} 10^{-4} \text{ kg/cm}^2,$$

where ξ_Σ is the summary coefficient of resistance of the system;

γ_a is the density of air in kg/m^3;

W_a is the velocity of air in m/sec.

Hence

$$a = 2{,}42\left(\lambda \frac{l}{d} + \xi_m\right)\frac{10^{-8}}{d^4}\frac{T_{a.f}^*}{p_{a.f}^*}, \tag{12.17}$$

where λ is the coefficient of friction of a unit of relative length of the line;

ξ_m is the coefficient of local resistances;

l is the length of the line in meters;

d is the inside diameter of the line in meters;

$T_{a.f}^*$ is the temperature of the air from the power source in °K;

$p_{a.f}^*$ is the air pressure of the power source in kg/cm^2.

Comment. Since the air density in the air lines decreases due to the reduction of the air temperature and pressure because of losses, then equation (12.16) can be corrected with respect to the average air density, i.e.,

$$\Delta p = a' \frac{T_a^* + T_{a.f}}{p_a + p_{a.f}} G_a^2,$$

where

$$a' = 2{,}42\left(\lambda \frac{l}{d} + \xi_{in}\right) \frac{10^{-8}}{d^4}.$$

In approximate calculations, however, equation (12.16) can be employed.

In connection with the use of heat insulated air lines in air starter systems an air temperature drop Δt_a ~ 8-10° for every 5-7 meters of length of the air lines can be tolerated.

Equation (12.16), after substitution in it of the air flow rate from expression (12.14), acquires the form

$$\Delta p = a \frac{A_{ts}^2 p_a^{*2}}{T_a^*}. \tag{12.18}$$

Solving equations (12.15) and (12.18) in terms of p_a^* we obtain

$$p_a^* = \frac{\sqrt{1 + \frac{4aA_{ts}^2 p_{a.f}^*}{T_a^*}} - 1}{\frac{2aA_{ts}^2}{T_a^*}}. \tag{12.19}$$

The expression that determines turbostarter turbine power (12.13), after substitution in it of the values of (12.14) and (12.19), can be converted to the form

$$N_{ts} = \frac{k}{75(k-1)} R_a \sqrt{T_a^*} A_{ts} \frac{\sqrt{1 + \frac{4aA_{ts}^2 p_{a.f}^*}{T_a^*}} - 1}{\frac{2aA_{ts}^2}{T_a^*}} \times$$

$$\times \left[1 - \left(\frac{p_n \frac{2aA_{ts}^2}{T_a^*}}{\sqrt{1 + \frac{4aA_{ts}^2 p_{a.f}^*}{T_a^*}} - 1}\right)^{\frac{k-1}{k}}\right] \eta_T^* \tag{12.20}$$

The nomograms furnished by engineer A. R. Ivanov (Figure 87) can be used for preliminary assessment of the mutual influence of parameters in choosing the optimal conditions of joint operation of the compressed air source and air turbine with allowance for network pressure losses.

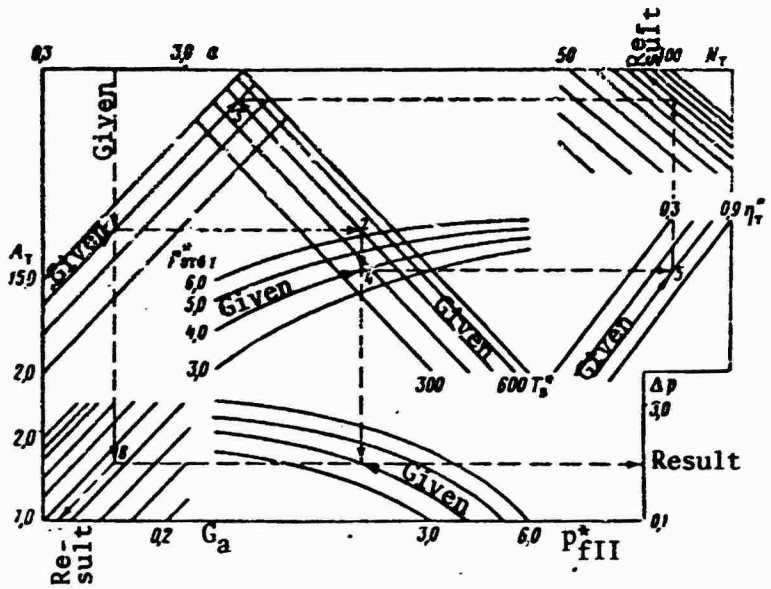

Figure 87. Nomogram for choice of optimal conditions of joint operation of compressed air source and air turbine of turbostarter: p^*_{fI} -- compressed air pressure field for determination of turbine power; p^*_{fII} -- compressed air pressure field for determination of network pressure losses and air flow rate through turbostarter turbine.

The following conventional symbols, replacing combinations of certain parameters, are introduced for plotting nomograms:

$$a A_{ts}^2 = X_1; \quad p_a^* \left[1 - \left(\frac{p_n}{p_a^*}\right)^{\frac{k-1}{k}}\right] = X_3;$$

$$\frac{X_1}{T_a^*} = X_2; \quad A_{ts}\sqrt{T_a^*} = X_4;$$

$$\frac{\sqrt{1 + 4X_2 p^*_{a.f}} - 1}{2X_2} = p_a^*; \quad \frac{k}{75(k-1)} R_a \eta_T^* X_3 = X_5.$$

Then turbine power can be represented in the form $N_{ts} = X_4 X_5$, network pressure losses

$$\Delta p = (p^{*2}_{a.f} - 2p^*_{a.f}\Delta p + \Delta p^2)X_2,$$

and air flow rate

$$G_a = \sqrt{\Delta p / a}.$$

An increase in the turbine efficiency of the air turbostarter has a considerable effect on the effectiveness of utilization of the energy of compressed air from the power source.

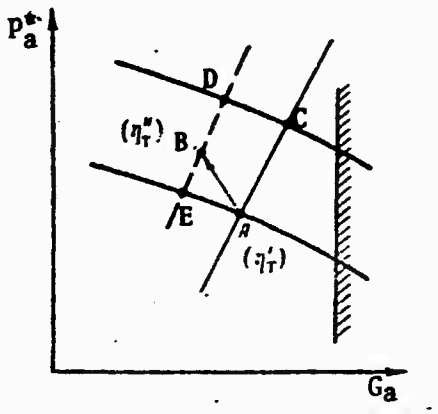

Figure 88. Effect of turbine efficiency of air turbostarter on effective utilization of the energy from compressed air: $\eta_t'' > \eta_t'$.

Higher turbine efficiency increases the air turbostarter power on the engine shaft ($N_B > N_A$) while simultaneously lowering the compressed air flow rate from the power source (Figure 88). And reduction of the air flow rate $G_{a.f}$ in turn leads to a reduction of pressure losses in the air lines and reduction of the temperature of the gases from the power source (CATG), i.e., facilitates an increase in its reliability and service life.

Higher turbine efficiency of the air turbostarter increases its power ($N_E > N_A$) despite a lower compressed air flow rate from the power source, even with the same network losses.

Thus, for instance, an increase of turbine efficiency of the air turbostarter from $\eta_t = 0.5$ to $\eta_t = 0.7$ made it possible to increase turbine power 30% with about an 11% decrease in the air flow rate.

By increasing starter efficiency 40% for $p_a^* \approx 2.9$ atm it was possible to increase the power approximately 23% with about a 16% reduction of the compressed air flow rate from the power source with the same network losses.

Reduction of the compressed air flow rate from the power source and corresponding reduction of network losses at higher starter turbine efficiency results in more effective utilization of the energy of the compressed air.

An increase in starter efficiency as a result of lowering the compressed air flow rate with constant air turbostarter power on the engine shaft leads to a decrease of the equivalent power source power ($N_{a.eq} = G_a L_{ad}/75$ is the power of the compressed air stream) and, accordingly, to an increase in the power efficiency of the starter system ($\eta_N = N_{ts}/N_{eq}$).

Thus, for instance, during starting of the AI-20 turboprop engine with two types of turbostarters (one with $\eta_t' \approx 0.5$ and the other with

η_t'' ≈ 0.7) with the same starter air pressure (p_a^* ≈ 3.1 atm) from a CATG, a 40% increase in starter efficiency resulted in an increase in power efficiency of the air starter system from η_N' = 0.47 to η_N'' = 0.58, i.e., approximately 23%.

Thus in order to use the energy of the compressed air in the air starter systems more effectively, increase the available turbostarter power on the engine shaft, improve the power source reliability and increase its service life it is essential in the design of such starter systems and choice of working parameters to strive for turbostarters with the highest efficiencies and minimal losses in the network (lines).

Axial single-stage turbines with efficiencies η_t ≈ 0.75-0.8 or centripetal (radial) turbines with η_t ≈ 0.8-0.85 can be used in air turbostarters.

CHAPTER 13. STARTING FEATURES OF TWO-ROTOR TURBOJET ENGINES

Two-rotor turbojet engines (Figure 89) are now used extensively in addition to single-rotor turbojet engines. The engine has two mechanically independent rotors, called the low-pressure rotor and high-pressure rotor. Accordingly the compressor stages and turbine stages have the same names.

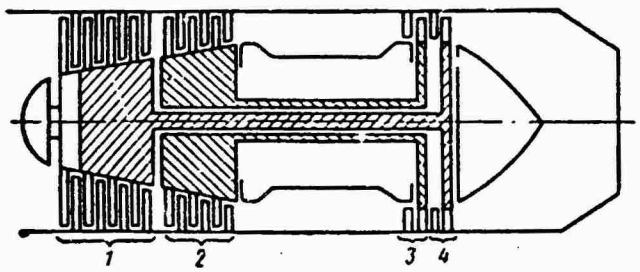

Figure 89. Schematic diagram of two-rotor turbojet engine: 1 -- low-pressure compressor; 2 -- high-pressure compressor; 3 -- high-pressure turbine; 4 -- low-pressure turbine.

The characteristic feature of two-rotor engines is that in the starting and all other modes of operation the rotors turn at different rpm (slip). The difference in the speeds of the rotors depends on the assumed distribution of work between the compressor stages and, accordingly, on the distribution of the total drop produced on the turbines (between the turbine stages). The rotor slippage of a given engine depends on the mode of operation, jet nozzle area and atmospheric conditions. During engine start-up the starter system, which imparts higher rpm to the rotor to which it is connected, has a considerable effect on rotor slip.

Faster rotation of one rotor in relation to the other increases the air flow rate through the slower rotor, and this increases the stability of the compressor operating at lower rpm. Since unstable compressor operation during start-up is attributed principally to the character of operation of the first stages it is essential, naturally, that the first stages rotate at lower rpm than the subsequent in order to ensure stable compressor operation.

During start-up, therefore, the high-pressure rotor must always rotate faster than the low-pressure rotor. In one limiting case, in the absence of rotor slip, a two-rotor engine becomes a single-rotor engine. It is advisable to change the characteristics of the two-rotor engine in the starting modes, and also its starting properties, beginning with this limiting case. The dependences of change of rotor rpm at various rates of slip are usually close to linear (Figure 90).

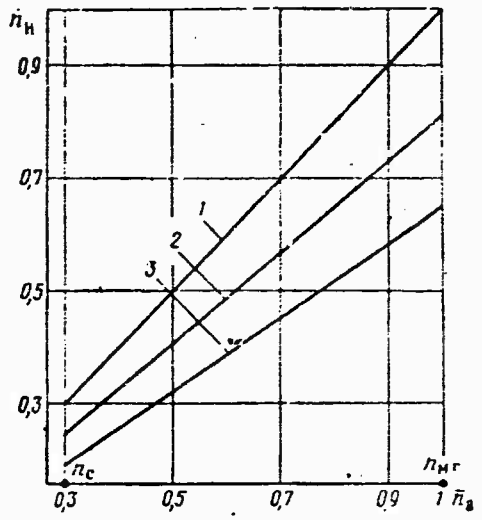

Figure 20. Dependence of rpm of engine rotor at various slip rates in steady starting regimes: 1 -- single-rotor engine; 2 and 3 -- two-rotor engine.

A change of rotor slip has an effect on the characteristics of both compressor stages. Therefore, in contrast to the compressor characteristics of a single-rotor engine, the compressor characteristics of a two-rotor engine must be plotted for different rotor slips (Figure 91).

When the rpm of the low-pressure compressor (LPC) changes, the air parameters in the intake of the high-pressure compressor (HPC) (chiefly the pressure and air flow rate) also change. Increased rotor slip due to reduction of low-pressure rotor (LPR) rpm at constant high-pressure rotor (HPR) rpm leads to a reduction of the air flow rate through the engine, and consequently to convergence on the boundary of stable HPC operation. The high-pressure compressor can be made to operate unstably in all starting modes by increasing rotor slip.

Increased rotor slip at constant LPR rpm increases the air flow rate through the LPC, by virtue of which, as we know, its stability margin is increased. Compressor operation converges on the stability boundary when rotor slip is reduced.

When starting a two-rotor engine it is essential that each rotor be brought from the state of rest to idling speed at different rpm. There are three methods of starting a two-rotor engine:

1) the starter turns the high-pressure rotor and the rpm of the low-pressure rotor increases as a result of the gas coupling between the rotors;

2) the starter turns the low-pressure rotor and the high-pressure rotor turns because of the gas coupling between the rotors;

3) the starter turns both rotors.

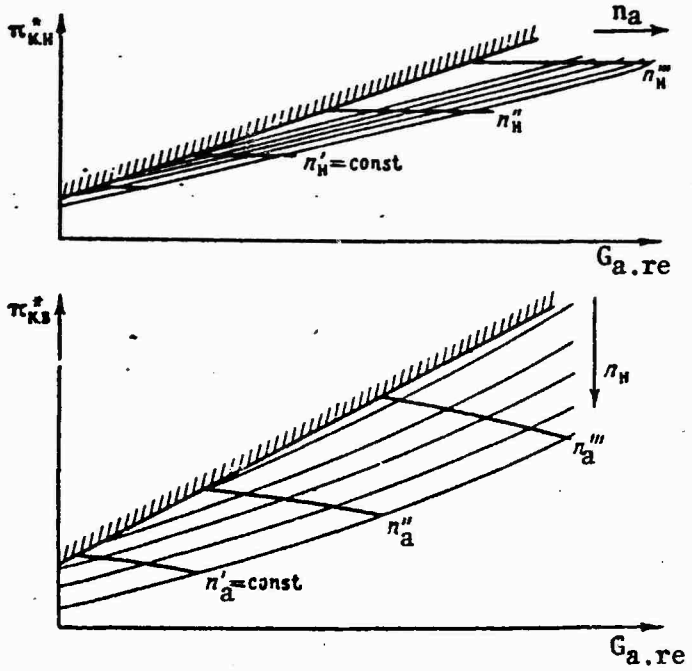

Figure 91. Characteristics of low-pressure and high-pressure compressors of two-rotor engine (the cross hatched curve is the boundary of stable operation of the low- and high-pressure compressors).

In any case the starters drive the rotors so that the speed imparted to them ensures independent running of the engine up to idle speed.

If the starter turns one rotor then the second rotor will autorotate until the turbine is placed into active operation. During autorotation the air pressure does not rise after passing through the rotor, but to the contrary falls.

When the starter turns both rotors, neither of them operates in the autorotation regime, and therefore the pressure behind the high-pressure rotor rises faster than the pressure behind the compressor when only one of the rotors is accelerated. In the former case the turbine begins to operate sooner and produces a lot of power during the starting process. Therefore engine starting is improved.

The turning of both rotors by the starters, however, is a difficult design problem. Moreover such a design increases the weight of the starter system. Therefore the starter turns only one of the rotors during starting of a two-rotor engine.

The starting of a two-rotor engine by turning the low-pressure rotor is not practiced in modern engines as a rule for the following reasons:

1. The inertia of the low-pressure rotor is usually greater than that of the high-pressure rotor, and therefore a more powerful starter is required to drive it. Furthermore the design is executed so that a smaller pressure drop is developed on the turbine connected to the low-pressure stage than on the turbine connected to the high-pressure stage. This means that at the initial moment of start-up, prior to operation of the high-pressure turbine, the low-pressure rotor is turned basically by the starter, which has to be sufficiently powerful for this purpose.

2. When starting an engine by turning the low-pressure rotor the rpm of this rotor exceeds that of the low-pressure rotor. Therefore the range of stable compressor operation in the starting regime is narrowed, necessitating a reduction of fuel feed to the combustion chambers. Consequently the turbine operates less efficiently in the starting regimes.

Thus two-rotor engines are started by turning the high-pressure rotor with starter. Operation of the low-pressure rotor during the initial starting period in the autorotation mode reduces the stable operation reserve of the high-pressure compressor, necessitating cranking of the engine rotor by the starter to relatively higher rpm compared to single-rotor engines.

The range of compressor stability may be narrowed considerably in certain types of two-rotor engines in connection with the above-examined features of the operation of their stages during the initial starting period. Precise control of the amount of fuel delivered to the combustion chambers during this period is required in order to ensure reliable starting of such engines. The best results are obtained by initial acceleration of an engine without fuel feed to certain rpm (to point A, Figure 92).

After the turbine of the low-pressure rotor goes into operation the efficiency of the low-pressure stage and of the entire compressor increases. Consequently the pressure in front of the turbines and their surplus power increase. The engine rotors increase rpm rapidly and reach idling speed. This concludes on the ground starting of the two-rotor engine.

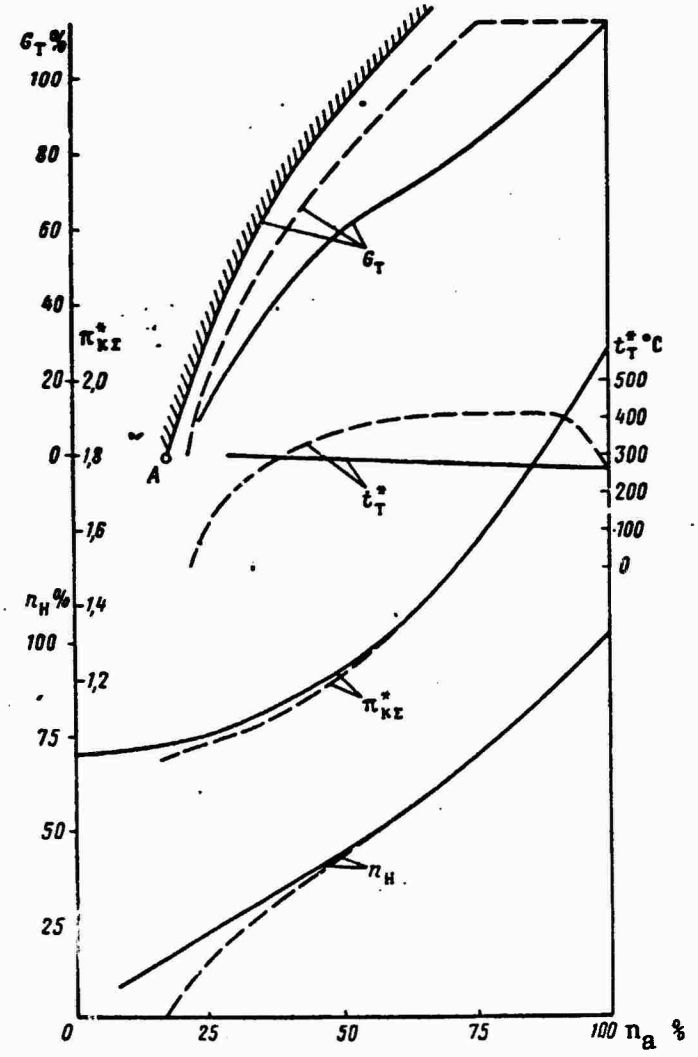

Figure 92. Parameters of two-rotor engine during start-up (continuous curves represent parameters in steady states; the broken curves represent parameters during starting; the cross hatched curve -- on the stability boundary).

reliable engine idling is achieved, can be obtained by changing flight speed. Otherwise the process of in-flight engine starting is in principle the same as the process of on the ground engine starting. Some of the same units, systems and equipment participate in in-flight starting as in on the ground starting.

Thus for in-flight starting of an engine (with the starter igniters) the following conditions are essential:

a) formation of reliable flame in starter igniter;

b) ignition, propagation of flame through flame tube and stable combustion of main fuel in combustion chamber;

c) stable engine operation in the starting regime and continuous acceleration of the rotor to idling speed.

Under these conditions in-flight engine starting proceeds as follows.

Within the range of flight velocities and speeds that ensure reliable engine starting the units that create the initial flame are switched on and main fuel is delivered to the combustion chamber almost simultaneously (either manually or automatically) in the quantity required for normal acceleration of the engine rotor to idling rpm. After the idling regime is reached the main fuel ignition system is shut off (manually or automatically). The engine is then changed to the required mode of operation.

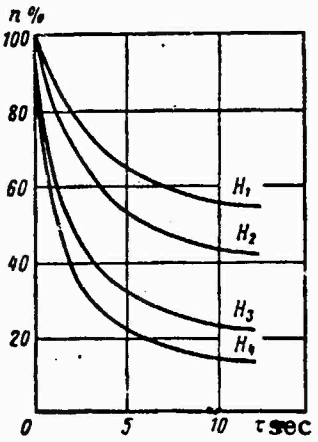

Figure 93. Change of engine rpm after flame-out at different altitudes: $H_1 > H_2 > H_3 > H_4$.

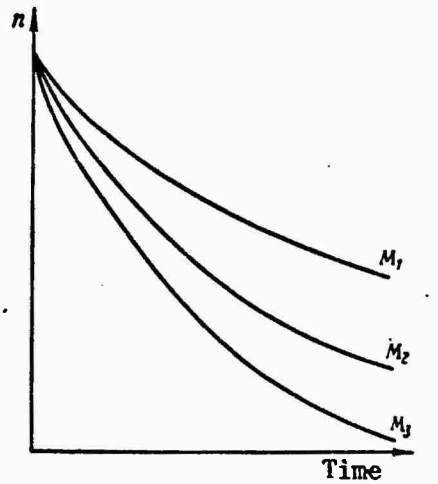

Figure 94. Change of engine rotor rpm after flame-out at different flight speeds: $M_1 > M_2 > M_3$.

§36. Starting Phases

The in-flight engine starting process can be broken down into two phases:

1. Spontaneous insertion of engine into stable autorotation regime.

2. Combined acceleration of rotor by incident flow and engine turbine after ignition of the main fuel in the combustion chamber.

After cessation of fuel combustion in the combustion chamber in flight, as on the ground, rpm falls and after some interval of time becomes equal to the rpm of the steady autorotation mode. The rate of decrease of rpm depends on flight altitude and speed at the moment of flame-out and on the characteristics of individual engine components. The character of change of rotor rpm after flame-out at different altitudes and at the same flight speed is shown in Figure 93, and at the same altitude but at different speeds in Figure 94.

CHAPTER 15. ENGINE CHARACTERISTICS AND PARAMETERS IN AUTOROTATION REGIME

§37. Physical Essence of Autorotation Regime

We will first examine what causes the rotor to rotate and how rotor rpm and the air parameters change in the duct of an autorotating engine as flight altitude and speed change.

The air passing through the engine interacts with the vanes of the compressor and turbine, causing the rotor to rotate.

As during on the ground engine starting, the turbine begins to operate actively only in the presence of a certain pressure in front of it and certain air flow rate through it. Until then the turbine acts as a brake and not only does not accelerate the engine rotor, but conversely consumes energy for rotation. Consequently the compressor must rotate the rotor for a certain time.

A compressor, as we know, is in principle a brake and it can rotate only when energy is supplied to it. The compressor rotates in the autorotation mode at the expense of part of the pressure (and consequently the energy) created in the compressor intake by dynamic pressure. The reduction of pressure in the compressor in the autorotation mode at different flight speeds prior to active turbine operation is illustrated in Figure 95. In the stated range of flight velocities the compressor obviously operates like a turbine, for which reason the air pressure is lower at compressor exhaust than at compressor intake.

At the instant the turbine goes into active operation it begins to accelerate the engine. The compressor, receiving energy from the turbine, gradually acquires its inherent character of operation and thereby provides the required air pressure increase.

Rotor rpm and the air parameters through the duct change in the autorotation mode as functions of flight velocity and altitude so that their reduced values remain constant for the same Mach numbers. The typical curves of the reduced rpm, compression ratio of the compressor, air flow rate through

the engine, velocities and pressures of the air in the combustion chamber intake are shown in Figure 96 as functions of the Mach number for a turbojet engine with an axial nine-stage compressor.

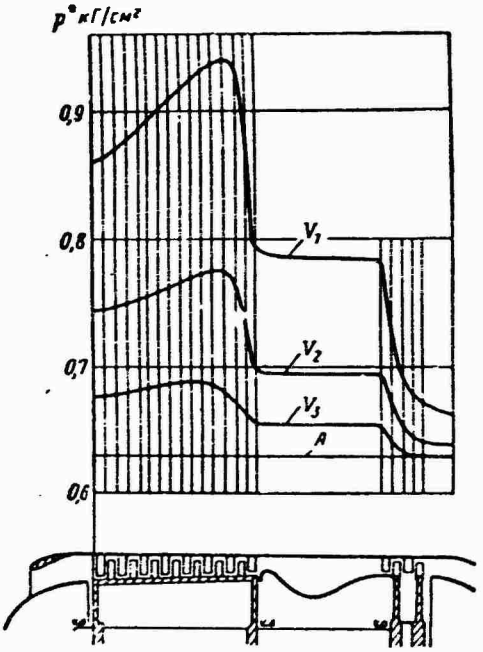

Figure 95. Change of air pressure in engine duct in autorotation mode at different flight velocities: $V_1 > V_2 > V_3$; A -- ambient air pressure line.

An increase in the Mach number leads to an increase in the reduced engine rotor rpm in the autorotation mode. The rate of change of engine parameters increases starting at some Mach number (M > 0.85 in Figure 96), determined for each engine.

As seen in Figure 96 the autorotation mode is characterized by a unique change of air parameters through the duct. The compression ratio in the compressor decreases up until Mach 0.85, and then begins to increase as the Mach number increases. The reduced air pressure behind the compressor changes similarly with the Mach number.

The air velocity behind the compressor (in the combustion chamber intake) increases in the autorotation mode as the Mach number increases until the Mach number corresponding to the critical discharge through the nozzle of the first turbine stage. From this Mach number the air velocity in the combustion chamber intake increases in proportion to the square root of the air stagnation temperature in the incident flow. The attainment of the critical air discharge velocity from the turbine nozzle in the autorotation mode at low Mach numbers is characteristic of engines with a high compression ratio.

At the onset of the critical air discharge mode in the turbine nozzle the air flow rate also decreases with increasing Mach number.

The air flow rate through the engine in the autoration mode, as seen in Figure 96, is substantially greater than the air flow rate through the engine in the steady modes of on the ground engine operation.

Using the equations of reduction we can determine the change of the various true engine parameters in the autorotation mode with flight altitude at constant air speeds. The higher the flight speed with the engine shut down the more the true engine rotor rpm will increase in the autorotation mode at constant air speed as flight altitude increases (Figure 97).

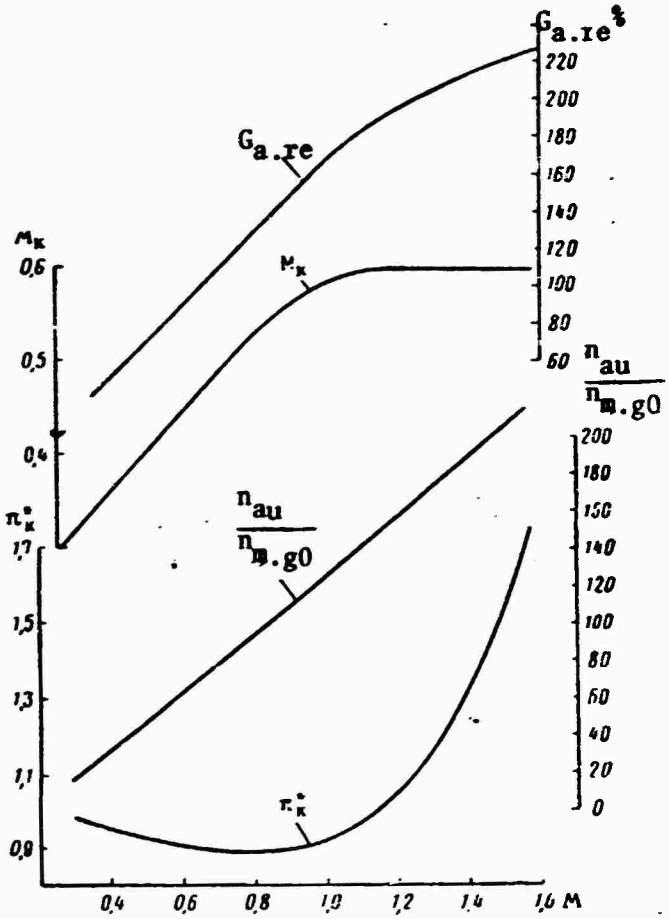

Figure 96. Reduced engine rotor rpm in autorotation mode, compression ratio in compressor in autorotation mode, air velocity at compressor exhaust in autorotation mode and air flow rate through engine in autorotation mode as functions of the Mach number.

As altitude increases, the air flow rate through the engine decreases at all flight speeds. The air pressure behind the compressor drops as the altitude increases to a certain value, but then this pressure can increase (Figure 98) as a result of an increase in Mach number.

The air velocity at the combustion chamber intake increases with increasing altitude to the velocity at which the critical air discharge through the nozzle of the first turbine stage is achieved (Figure 99).

§38. Methods of Calculating Autorotation Mode

Determination of Mode of Combined Compressor and Turbine Operation

Calculation of the autorotation modes poses certain difficulties. Due to the complexity of the flow forms in the compressor and turbine, development

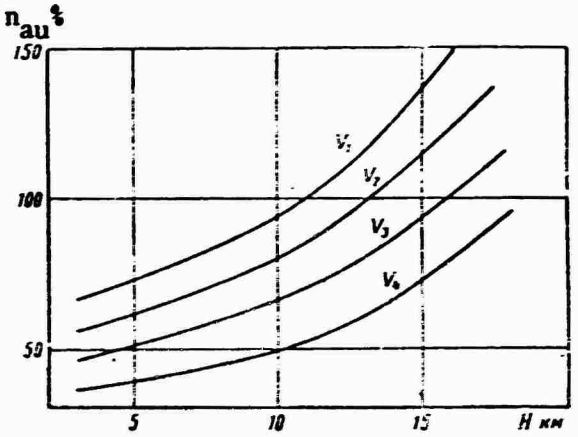

Figure 97. Measured engine rotor rpm in autorotation mode as function of flight altitude (the autorotation rpm is given in percent of the idling rpm on the ground) $V_1 > V_2 > V_3 > V_4$.

of secondary flows, flow separation zones, etc.) in the autorotation modes and the presence of subcritical flows through the entire engine duct (at low Mach numbers) the equations that describe the processes in the main engine components and the interaction among them cannot be solved purely analytically. Therefore various approximate grapho-analytical calculation methods are used with experimental characteristics of the components.

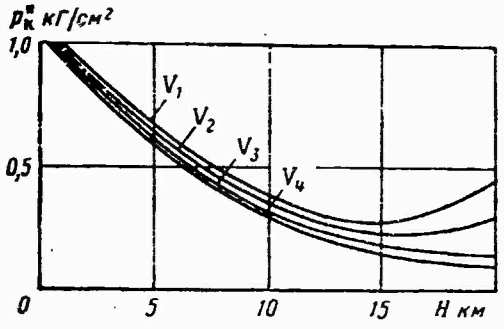

Figure 98. Measured air pressures behind compressor in autorotation mode as function of flight altitude.

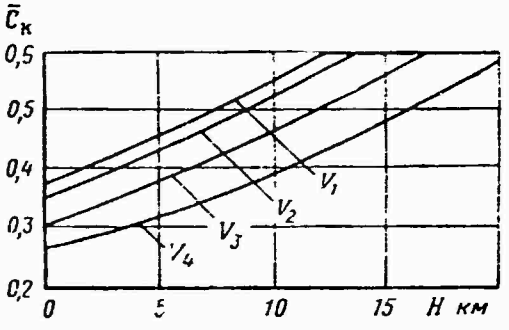

Figure 99. Air velocity at compressor exhaust in autorotation mode as function of flight altitude.

A method based on the solution of an equation system, each equation of which determines the characteristics of an individual engine component, by successive approximation can be used as one of the methods of calculating the autorotation modes of a turbojet engine with an afterburner (TJEA) in the self-modeling region with respect to the Reynolds number.

The characteristics of the components of ordinary TJEA can be represented by the following graphical functions:

Air intake

$$\sigma_a = f_1\left[M;\ \frac{G\sqrt{T_a^*}}{p_a^*}\right]. \tag{15.1}$$

Compressor

$$\pi_k^* = f_2\left[\frac{n_k}{\sqrt{T_a^*}};\ \frac{G\sqrt{T_a^*}}{p_a^*}\right]; \tag{15.2}$$

$$\tau_k^* = f_3\left[\frac{n_k}{\sqrt{T_a^*}};\ \frac{G\sqrt{T_a^*}}{p_a^*}\right]; \tag{15.3}$$

$$\frac{G\sqrt{T_k^*}}{p_k^*} = f_4\left[\frac{n_k}{\sqrt{T_a^*}};\ \frac{G\sqrt{T_a^*}}{p_a^*}\right]. \tag{15.4}$$

Combustion chamber

$$\sigma_g = f_5\left[\frac{G\sqrt{T_k^*}}{p_k^*}\right]. \tag{15.5}$$

Turbine

$$\pi_T^* = f_6\left[\frac{n_T}{\sqrt{T_g^*}};\ \frac{G\sqrt{T_g^*}}{p_g^*}\right]; \tag{15.6}$$

$$\tau_T^* = f_7\left[\frac{n_T}{\sqrt{T_g^*}};\ \frac{G\sqrt{T_g^*}}{p_g^*}\right]; \tag{15.7}$$

$$\frac{G\sqrt{T_T^*}}{p_T^*} = f_8\left[\frac{n_T}{\sqrt{T_g^*}};\ \frac{G\sqrt{T_g^*}}{p_g^*}\right]. \tag{15.8}$$

Jet nozzle

$$\sigma_c = f_9\left[\frac{G\sqrt{T_T^*}}{p_T^*};\ F_c\right]. \tag{15.9}$$

Used, in addition to the above-stated characteristics of the components, are the relations among them, dictated by engine design. The following coupling equations are characteristic of the autorotation modes.

Equation of rpm of compressor and turbine

$$\frac{n_к}{\sqrt{T_a^*}} = \frac{n_т}{\sqrt{T_g^*}} \sqrt{\tau_к^*}. \tag{15.10}$$

Equation of air flow rate in compressor and turbine intakes

$$\frac{G\sqrt{T_a^*}}{p_a^*} = \frac{G\sqrt{T_g^*}}{p_g^*} \frac{\pi_к^* \sigma_g}{\sqrt{\tau_к^*}}. \tag{15.11}$$

Equation of air temperature drop in compressor and turbine

$$\tau_k^* = \tau_t^*. \tag{15.12}$$

Equation of pressure and expansion ratios in engine

$$\pi_V^* \sigma_a \sigma_g \sigma_c \pi_k^* = \pi_t^* \pi_c^*. \tag{15.13}$$

The above 13 equations contain 14 variables, not counting the controlled geometric parameters, known during determination of the autorotation mode. These 14 parameters, characterizing the autorotation mode, include the Mach number as an independent argument. By assigning the Mach number it is possible to solve uniquely the stated equation system.

Equation (15.12) in the autorotation mode is identical to the equation of the equality of compressor and turbine work, usually used for calculating engine operating modes. It is better to use the temperature drop values for calculating the autorotation modes, since this obviates consideration of compressor and turbine efficiencies. The latter either play a minor role or, for example for the compressor at low Mach number (when several stages operate in the "turbine" mode) are altogether meaningless.

Equation system (15.1)-(15.13) should be solved in the following order:

1) we are given a series of values of π_k^* on the pressure branch of the compressor $n_k/\sqrt{T_a^*}$;

2) we find according to compressor characteristics π_k^* and $\frac{G\sqrt{T_a^*}}{p_a^*}$ for the given values π_k^* and $n_k/\sqrt{T_a^*}$;

3) we determine the reduced turbine rpm

$$\frac{n_т}{\sqrt{T_g^*}} = \frac{n_к}{\sqrt{T_a^*}} \frac{1}{\sqrt{\tau_к^*}}$$

and the reduced gas flow rate through the turbine nozzle

$$\frac{G\sqrt{T_g^*}}{p_g^*}=\frac{G\sqrt{T_a^*}}{p_a^*}\frac{\sqrt{\tau_*^*}}{\pi_*^*\sigma_p};$$

4) we find on turbine characteristics τ_t^* and τ_t^* according to known $\frac{n_t}{\sqrt{T^*}}$ and $\frac{G\sqrt{T_g^*}}{p_g^*}$;

5) we determine the mode of combined turbine and compressor operation.

The compressor-turbine mode, as we know, is determined by two similitude parameters. One of them, $n_k/\sqrt{T_a^*}$, is known. As the second similitude parameter for the compressor we may use one of the following:

$$\pi_k^*,\ \frac{G\sqrt{T_a^*}}{p_a^*};\ \tau_k^*.$$

It is better to use the parameter τ_k^*, since then the problem of determining the mode of combined turbine and compressor operation consists in solving equation (15.12) by successive approximations or graphically.

After determining the mode of combined compressor and turbine operation we still have to find the flight mode (Mach number) corresponding to the given turbocompressor mode. The calculation is done in the following order.

We find the reduced flow rate at the turbine exhaust

$$\frac{C\sqrt{T_\tau^*}}{p_\tau^*}=\frac{G\sqrt{T_g^*}}{p_g^*}\frac{\pi_\tau^*}{\sqrt{\tau_\tau^*}}$$

and then, according to the characteristic of the jet nozzle for the known exhaust area F_c we determine the expansion ratio π_c^*.

We determine the Mach number on the basis of the equality of the compression and expansion ratios in engine components:

$$\pi_V^*\sigma_a=\frac{\pi_k^*\sigma_r\sigma_c}{\pi_\tau^*\pi_c^*}=\sigma_a\left[1+\frac{k-1}{2}M^2\right]^{k/k-1}.$$

The Mach number is found by successive approximations or graphically in those cases when

$$\alpha_a = f\left[M;\ \frac{G\sqrt{T_a^*}}{p_a^*}\right] \neq \text{const.}$$

As already pointed out, of the reduced parameters entering into equation system (15.1)-(15.13), determining the autorotation mode of TJEA, only the Mach number is an independent parameter. This fact means that the engine parameters in the autorotation mode (reduced parameters) can be expressed uniquely through the Mach number in the self-modeling region with respect to the Reynolds number.

Dependence of Autorotation Mode of TJEA on Mach Number

Results of calculation of autorotation modes of one TJEA by the procedure described above are presented in Figures 100 and 101. It follows from Figure 101 that the compressor in all autorotation modes is a consumer of power developed by the turbine by the action of dynamic pressure.

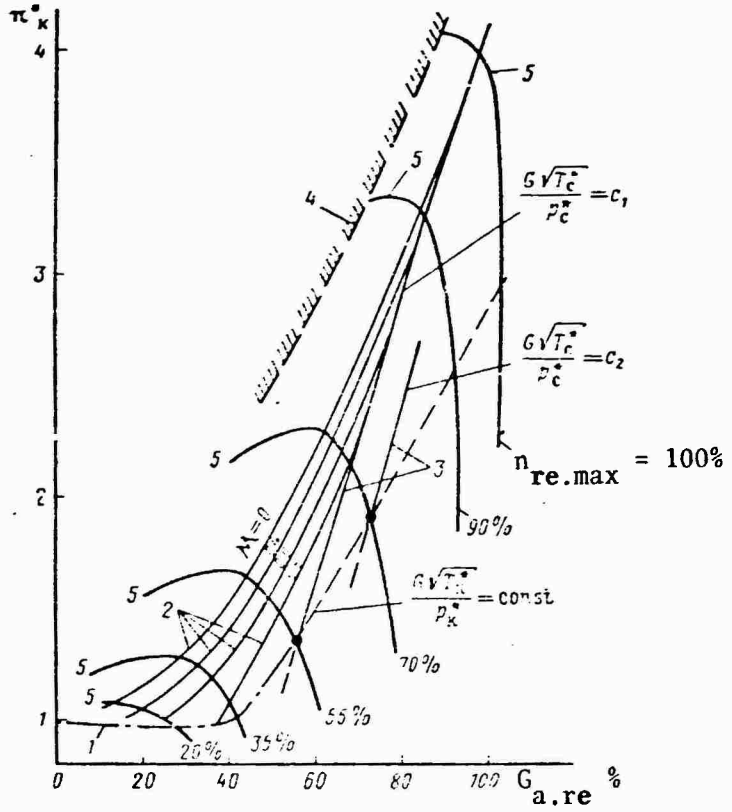

Figure 100. Distribution of curves of autorotation modes on TJEA compressor characteristics: 1 -- curve of autorotation modes; 2 -- curves of operating modes at various Mach numbers; 3 -- curves of critical modes for various jet nozzle cross section areas; 4 -- compressor stability boundary; 5 -- compressor pressure branches at various rpm n_{re}.

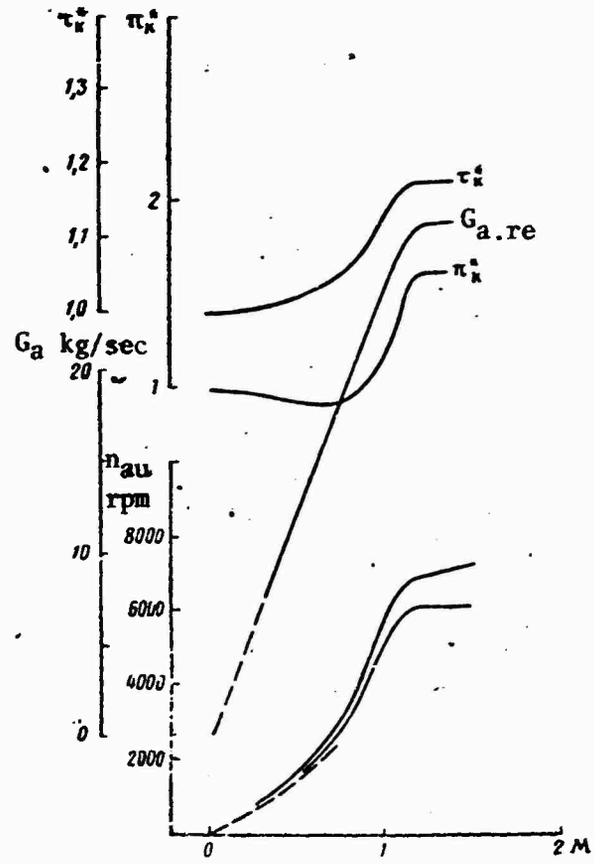

Figure 101. TJEA parameters as functions of Mach number in autorotation mode (top curve -- $n_{phys.au}$, bottom -- $n_{re.au}$).

At low Mach numbers, as we know, the last stages of an autorotating compressor operate in the region of "turbine" modes and can perform some work. However, due to the low efficiency of the compressor stages operating in the turbine mode the work of compression in the first compressor stages and losses to friction predominate in the overall balance.

At M < 0.8 the pressure ratio is less than one as a result of exhaustion of part of the pressure drop in the last compressor stages operating in the turbine mode. The lowest π_k^* correspond to M = 0.6-0.7. As M increases to 0.7 and beyond the values of π_k^* increase in connection with the approach of the "choking" mode of the first turbine stage nozzle. The critical flow mode in the nozzle usually occurs at Mach numbers greater than 0.8-0.9. For the case at hand the engine rpm in this mode is about 35% maximum. After "choking" of the turbine nozzle the pressure ratio π_k^* increases with increasing M on the curve of the joint turbocompressor modes, given by the equation

$$\frac{G\sqrt{T_a^*}}{p_a^*}=\frac{G\sqrt{T_g^*}}{p_g^*}\frac{\pi_{\kappa g}^*}{\sqrt{\tau_\kappa^*}}=\text{const}\cdot\frac{\pi_\kappa^*}{\sqrt{\tau_\kappa^*}}. \tag{15.14}$$

The presence of the critical discharge in the turbine nozzle simplifies determination of the autorotation mode, since in this case the assignment of $n_k/\sqrt{T_a^*}$ immediately determines the mode of joint turbine and compressor operation. The other parameters and the relation between the Mach number and turbocompressor mode ($n_k/\sqrt{T_a^*}$) are determined by the above-described procedure.

On reaching velocities corresponding to M = 1.2-1.7 (for the example depicted in Figure 101 for M = 1.3), the jet nozzle goes into the "choking" mode, or perhaps the expansion limit of the turbine is reached. Consequently the reduced turbine power is fixed and remains constant with a further increase of the Mach number (at constant jet nozzle area).

The determined constant reduced autorotation rpm ($n_{re.au}$) is established in connection with the leveling off of turbine power. Here the curve of the autorotation modes degenerates to a point on the engine component characteristics (in reduced coordinates). On the compressor characteristics this point is the intersection of the mode curve described by equation (15.14) and the curve of critical (operating) modes

$$\frac{G\sqrt{T_a^*}}{p_a^*}=\left(\frac{G\sqrt{T_c^*}}{p_c^*}\frac{a_{cg}\sqrt{\tau_\tau^*-1}}{\pi_\tau^*}\right)\frac{\pi_\kappa^*}{\sqrt{\tau_\kappa^*-1}}=\text{const}\cdot\frac{\pi_\kappa^*}{\sqrt{\tau_\kappa^*-1}}. \tag{15.15}$$

In the example depicted in Figure 100 the maximum reduced rpm in the autorotation mode is 55% $n_{re\ max}$.

Determination of Maximum Reduced Autorotation rpm of TJE and TJEA

Since the mode of maximum autorotation rpm is located on the critical curve of turbocompressor modes ($G\sqrt{T_c^*}/p_c^*$ = const, Figure 100), we may derive a rather simple analytical dependence of the maximum reduced autorotation rpm on TJE parameters in the design mode. We will examine the case when control (mechanization) of the compressor is not employed and the operating modes are located on a single critical curve passing through the point of the design mode and point of maximum autorotation rpm.

As pointed out above, the mode of maximum reduced autorotation rpm is characterized by the point of intersection of the curve of "choking" modes of the turbine nozzle of a "cold" engine and the curve of critical turbocompressor modes. Therefore it is necessary in the general case, in order to find the maximum autorotation rpm, to plot on the compressor characteristic the stated curves according to the equations

$$\frac{G\sqrt{T_a^*}}{p_a^*}=\text{const}\cdot\frac{\pi_\kappa^*}{\sqrt{\tau_\kappa^*}}\quad\text{and}\quad\frac{G\sqrt{T_a^*}}{p_a^*}=\text{const}\cdot\frac{\pi_\kappa^*}{\sqrt{\tau_\kappa^*-1}}.$$

Assuming that compressor operation is proportional to the square of the rpm on the curve of critical modes and ignoring the change of heat capacity of the working medium as its temperature changes, then the maximum reduced autorotation rpm can be determined from the equality of the reduced turbine rpm in the autorotation mode and in the maximum (design) mode on the ground, i.e.,

$$\frac{n_{re.au\ max}}{\sqrt{T^*_{k.re}}} = \frac{n_0}{\sqrt{T^*_{g0}}}. \qquad (15.16)$$

The assumption $L_k = L_t = An^2$ for engines with axial compressors leads to somewhat understated maximum reduced autorotation rpm. For many problems, however, the accuracy of determination of these maximum rpm's can be disregarded and then it becomes convenient to resort to purely theoretical determination of engine parameters in the autorotation modes. Furthermore the compressor and turbine characteristics can be dispensed with when calculating autorotation modes by the above-described method.

It follows from condition (15.16) that

$$n_{re.au\ max} = n_0 \sqrt{\frac{T^*_{kre}}{T^*_{g0}}} = n_0 \sqrt{\tau^*_{k.au} \frac{T^*_{a0}}{T^*_{g0}}};$$

or

$$\bar{n}_{re.au\ max} = \frac{n_{re.au\ max}}{n_0} = \sqrt{\tau^*_{k.au} \frac{T^*_{a0}}{T^*_{g0}}}. \qquad (15.17)$$

The value $\tau^*_{k.au}$ in the mode of maximum reduced autorotation rpm is equal to τ^*_{t0} in the design mode. This can be proved with the aid of the power balance equations or air flow rate equation. Thus

$$\tau^*_{k.au} = \tau^*_{t0} = \left[1 - \frac{T^*_{a0}}{T^*_{g0}} \frac{\pi^{*\frac{k-1}{k}}_{k0} - 1}{\eta^*_{k0}\eta^*_{t0}}\right]^{-\left[\frac{n-1}{n}\frac{k}{k-1}\right]}. \qquad (15.18)$$

We will substitute the value of $\tau^*_{k.au}$ into equation (15.17), disregarding the difference between the indices of polytropy and adiabatic expansion in the turbine. Then, finally, the equation for approximate determination of the maximum autorotation rpm of TJE will be

$$\bar{n}_{re.au\ max} = \left[\frac{T^*_{g0}}{T^*_{a0}} - \frac{\pi^{*\frac{k-1}{k}}_{k0} - 1}{\eta^*_{k0}\eta^*_{t0}} \right]^{-0,5}. \qquad (15.19)$$

The change of maximum autorotation rpm, calculated according to equation (15.19), is shown in Figure 102 as a function of TJE parameters in the design mode. The highest autorotation rpm, all other conditions being equal, correspond to low-temperature and high-pressure engines. The maximum reduced autorotation rpm for TJE with the most common parameters today is 50-70% of the design rpm.

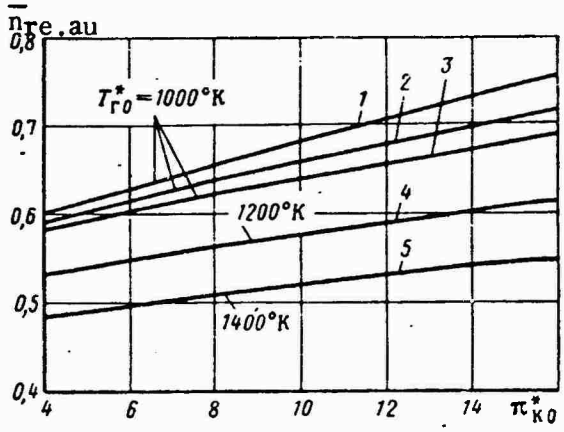

Figure 102. Maximum autorotation rpm as function of TJE parameters in design mode: 1 -- $\eta^*_{k0}\eta^*_{t0} = 0.7$; 2, 4 and 5 -- $\eta^*_{k0}\eta^*_{t0} = 0.8$; 3 -- $\eta^*_{k0}\eta^*_{t0} = 0.9$.

After in-flight flame-out of a TJEA operating in the afterburner mode the nozzle flaps may remain for some period of time in the position corresponding to the afterburner mode. Since the curve of critical turbocompressor modes is displaced toward higher flow rates as the jet nozzle area is increased (see Figure 100), then the maximum reduced autorotation rpm increases continuously until "choking" of the working wheel of the last turbine stage takes place. To each TJEA jet nozzle area corresponds a certain maximum reduced autorotation rpm, assuming that the position of the other controlled geometric engine parameters remains constant.

We will consider the case when engine performance is such that when the afterburner chamber is shut off and the nozzle flaps are open the curve of critical turbocompressor modes is determined by "choking" of the jet nozzle, and the maximum temperature drop in the turbine is determined in accordance with this condition.

Then

$$\bar{n}_{b.au\ max}=\sqrt{\frac{T^*_{a0}}{T^*_{g0}}\tau^*_{\tau 0}\frac{\tau^*_{tb}-1}{\tau^*_{\tau 0}-1}}. \qquad (15.20)$$

As in the case of TJE we will assume that $L_k = An^2$ and consequently all equilibrium modes on the turbine characteristic are located on a single parabola

$$\frac{L_\tau}{T^*_g}=\text{const}\cdot\left(\frac{n}{\sqrt{T^*_g}}\right)^2.$$

As before, we will disregard the change of the physical constants of the working medium with temperature.

From the equations of equality of gas flow rates through the intake and exhaust sections and equation of polytropy of gas expansion we derive the following expression for the temperature drop on the turbine during critical discharge in the turbine nozzle:

$$\tau^*_\tau=\left[\frac{F_\tau}{F_{ca}}q(\lambda_\tau)\right]^{\frac{2(n-1)}{n+1}}.$$

Using this expression we will determine the maximum temperature drop on the turbine for the given jet nozzle area:

$$\tau^*_{t.b}=\tau^*_{\tau 0}\left[\frac{q(\lambda_\tau)_b}{q(\lambda_\tau)_0}\right]^{\frac{2(n-1)}{n+1}}.$$

If we assume that afterburning does not lead to additional "constriction" of the main contour, then the following relations should be satisfied:

$$\frac{q(\lambda_\tau)_b}{q(\lambda_\tau)_0}=\frac{F_{c.b}}{F_{c0}}=\sqrt{\frac{T^*_{b0}}{T^*_{\tau 0}}}=\frac{R_b}{R_0}=1+\delta R_b,$$

where R_0 and R_b are the thrusts in the nonafterburner and afterburner modes.

Then we may write

$$\tau^*_{t.b}=\tau^*_{\tau 0}\left(\frac{F_{c.b}}{F_{c0}}\right)^{\frac{2(n-1)}{n+1}}=\tau^*_{\tau 0}(1+\delta R_b)^{\frac{2(n-1)}{n+1}}. \qquad (15.21)$$

Substituting $\tau^*_{t.b}$ into equation (15.20) we obtain the following equation, which determines the maximum reduced autorotation rpm of TJEA (with jet nozzle flaps in the "afterburner" position) as a function of engine parameters in the design mode and relative change of jet nozzle area (Figure 103):

$$\bar{n}_{b.au\ max} = \bar{n}_{au\ max} \sqrt{\frac{\left[\frac{F_{c.b}}{F_{c0}}\right]^{\frac{2(n-1)}{n+1}} - 1}{\frac{T^*_{a0}}{T^*_{g0}} \frac{\pi^{*\frac{k-1}{k}}_{k0} - 1}{\eta^*_{k0}\eta^*_{T0}}} + 1}. \qquad (15.22)$$

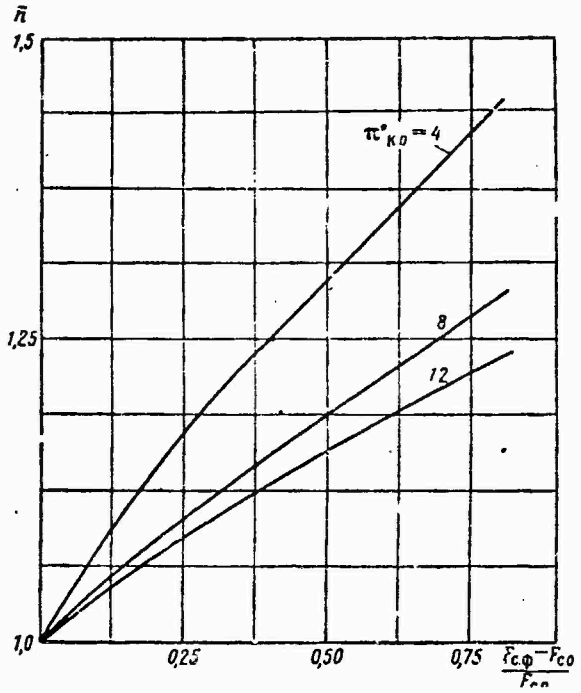

Figure 103. Maximum autorotation rpm as function of jet nozzle area for T^*_{g0} = 1,200°K ($\bar{n}$ = $= \bar{n}_{b.au\ max}/\bar{n}_{au\ max}$).

Change in the jet nozzle area has the greates effect on the autorotation rpm of engines with low π^*_{k0}. Reduction of the jet nozzle area causes faster change of autorotation rpm than an increase in nozzle area, which is explained by the character of change of turbine power as $q(\lambda_t)$ changes.

The reduced autorotation rpm can increase substantially when the jet nozzle area is increased. Thus, when the nozzle area is increased 50%

for $\pi^*_{k0} = 8$ and $T^*_{g0} = 1{,}200°K$ the maximum reduced autorotation rpm is 20% higher than with the design nozzle area.

The Mach number at which "choking" of the nozzle takes place (we will denote it through M_a) and the maximum reduced autorotation rpm is established can be determined from the condition of equality of the compression and expansion ratios in the engine: $\pi^*_V\sigma_a = (\pi^*_1\pi^*_c)/(\pi^*_{ka}\sigma_g\sigma_c)$.

For this purpose we will substitute into it $\pi^*_c = \pi^*_{c.cr} = 1.895$ and $\pi^*_t = \pi^*_{t\ max}$ for the given jet nozzle area (or given λ_t corresponding to $\lambda_c = 1$). We may assume with some approximation that

$$\pi^*_\tau = \pi^*_{\tau 0} = \left[1 - \frac{T^*_{a0}}{T^*_{g0}} \frac{\left(\pi^{*\frac{k-1}{k}}_{k0} - 1\right)}{\eta^*_{k0}\eta^*_{t0}}\right]^{k'/1-k'}.$$

The value of π^*_{ka} corresponding to the maximum reduced autorotation rpm is found from the condition of proportionality of compressor operation to the square of the rpm:

$$L_{k.au} = L_{k0}\bar{n}^2_{au},$$

hence

$$\pi^*_{ka} = \left[\left(\pi^{*\frac{k-1}{k}}_{k0} - 1\right)\frac{\eta^*_k}{\eta^*_{k0}}\bar{n}^2_{au} + 1\right]^{k/k-1}.$$

The final expression for determination of M_a will acquire the form

$$\pi^*_V\sigma_a = \frac{\pi^*_{c.cr}}{\left[\left(\pi^{*\frac{k-1}{k}}_{k0} - 1\right)\frac{\eta^*_k}{\eta^*_{k0}}\bar{n}^2_{au} + 1\right]^{\frac{k}{k-1}}\sigma_c\sigma_g\left[1 - \frac{T^*_{a0}}{T^*_{g0}}\left(\frac{\pi^{*\frac{k-1}{k}}_{k0} - 1}{\eta^*_{k0}\eta^*_{t0}}\right)\right]^{\frac{k'}{k'-1}}}.$$

M_a is shown in Figure 104 as a function of engine parameters in the design mode and compressor efficiency η^*_k for $n_{re.au\ max}$. Analysis of compressor characteristics reveals that $\eta^*_k \approx 0.6\text{-}0.7$ in the region of $n_{re.au\ max}$. Furthermore, as follows from Figure 104, an error of the order of about 15% in η^*_k yields an error of approximately 4-6% in determination of M_a. Therefore the approximate assignment of $\eta^*_k = 0.6\text{-}0.7$ in the mode $n_{re.au\ max}$ is quite acceptable for most problems.

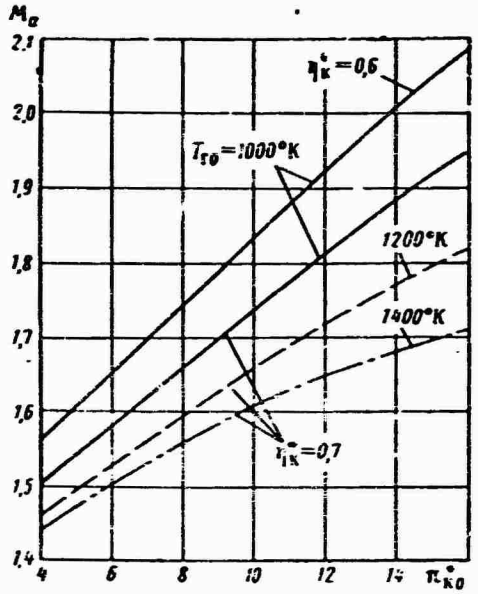

Figure 104. M_a at which maximum reduced autorotation rpm is established as function of TJE parameters in design mode for $\eta^*_{k0} = 0.85$; $\eta^*_{t0} = 0.94$; $\sigma_g = 0.8$; $\sigma_c = 0.9$.

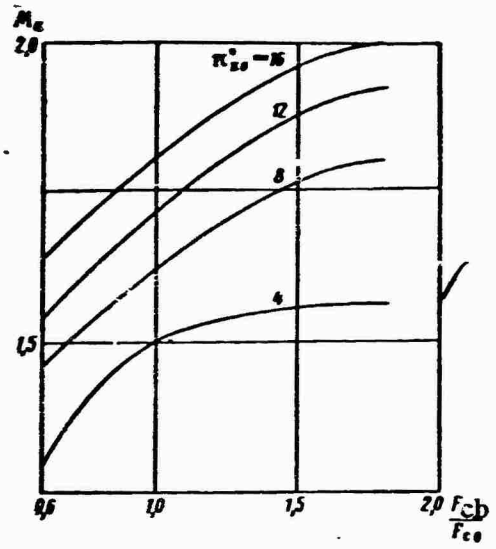

Figure 105. M_a as function of change of jet nozzle area for $T_{g0} = 1,200°K$; $\eta^*_{k0} = \eta^*_{g0} = 0.8$; $\eta^*_k = 0.7$.

The maximum autorotation rpm is established at higher M_a in engines with high compression ratios and low gas temperatures in front of the turbine than in high-temperature and low-pressure engines.

For TJEA the dependence of M_a on engine parameters in the design mode is obtained by substituting in the initial equation the value $\pi^*_{t.b}$ and the corresponding jet nozzle area $F_{c.b}$ instead of $\pi^*_t = \pi^*_{t0}$:

$$\pi^*_{t.b} = (\tau^*_{t.b})^{n/n-1} = \tau^{*\,n/n-1}_{\tau 0}\left[\frac{F_{c.\phi}}{F_{c0}}\right]^{\frac{2n}{\tau+1}}.$$

Then we obtain the following expression for M_a for $F_{c.b} \neq F_{c0}$:

$$\pi^*_V\sigma_a = \frac{\pi^*_{c.np}\left[F_{c.\phi}/F_{c0}\right]^{2n/n+1}}{\left[\pi^*_{k0}\left(\frac{k-1}{k}-1\right)\frac{\eta^*_k}{\eta^*_{k0}}\pi^{-2}_{b.au}+1\right]^{\frac{k}{k-1}}\sigma_c\sigma_g\left[1-\frac{\tau^*_{a0}}{T^*_{g0}}\left(\frac{\pi^{*\,\frac{k-1}{k}}_{k0}-1}{\eta^*_{k0}\eta^*_{\tau 0}}\right)\right]^{\frac{k'}{k'-1}}}.$$

As seen in Figure 105, an increase in jet nozzle area has practically no effect on M_a. Thus, when $\pi^*_{k0} = 8$ an 80% change in nozzle area changes M_a by only 0.2. This is explained by the nearly identical change in the compression ratio in the chamber due to an increase of $\bar{n}_{b.au}$ and expansion ratio in the turbine due to an increase of $q(\lambda_t)$ as $F_{c.b}$ changes.

At numbers $M > M_a$ the reduced autorotation rpm of TJE and TJEA, like all other reduced turbocompressor parameters, remain constant. Therefore at $M > M_a$ all engine operating modes are located on the same critical mode curve corresponding to the given jet nozzle area. In this sense M_a is a unique criterion of the validity of assuming the critical mode curve as the turbocompressor operating mode curve for some given Mach number. In other words, if the number $M > M_a$, then all turbocompressor operating modes are located on the compressor characteristic on the same "critical" curve.

Internal Resistance of Autorotating Engine

Resistance during autorotation can be determined in the general case by the procedure explained above. For $M > M_a$ the resistance of an autorotating engine is readily found analytically, using the TJE design parameters.

To determine the internal resistance of an autorotating engine we will use the force pulse equation. Since the static pressure at the jet nozzle exit is equal to atmospheric pressure when $M = M_a$ the force pulse equation will be

$$X = \frac{G_a}{g}(C_c - V).$$

Substituting the expression for the air flow rate and velocity at the nozzle exit through the gas dynamic functions and converting, we obtain an equation for determining the internal resistance of an autorotating engine at maximum reduced autorotation mode for $M = M_a$:

$$X_a = F_c p_H \left(k - k \sqrt{\frac{k+1}{2}} \frac{M_a}{\sqrt{1 + \frac{k-1}{2} M_a^2}} \right).$$

In the range of numbers $M = 0\text{-}M_a$ the internal resistance of an autorotating engine can be interpolated with sufficient accuracy with a straight line passing through the origin of the coordinate system and the resistance $M = M_a$ ($X = X_a$), because of the nearly linear dependence of the air flow rate in the autorotation mode on M (see Figure 101).

At $M > M_a$ the engine is completely "cut off" at the exhaust, with the result that the operating modes of its components do not change. Therefore the exhaust pulse is determined entirely by the change of pressure drop π_c^* in the jet nozzle, which is proportional, in turn, only to dynamic pressure:

$$\pi_{c}^{*}=\pi_{ca}^{*}\frac{\pi_{V}^{*}\sigma_{a}}{(\pi_{V}^{*}\sigma_{a})_{a}}.$$

In the case of incomplete expansion of the gas in the jet nozzle the internal resistance of an autorotating engine at $M > M_a$ will be determined by the equation

$$X=F_{c}p_{a}\left\{\frac{\pi_{V}^{*}\sigma_{a}}{(\pi_{V}^{*}\sigma_{a})_{a}}\left[k-k\sqrt{\frac{k+1}{2}}\frac{M}{\sqrt{1+\frac{k-1}{k}M^{2}}}+1\right]-1\right\}.$$

In the case of complete expansion of the gas in the nozzle at $M > M_a$, disregarding losses in the supersonic part of the nozzle, the equation for determining the internal resistance will become

$$X=F_{c}p_{a}\left\{\frac{\pi_{V}^{*}\sigma_{a}}{(\pi_{V}^{*}\sigma_{a})_{a}}\left[k\sqrt{\frac{k+1}{k-1}\left(1-\frac{1}{\left(\frac{2}{k+1}\right)\left(\frac{\pi_{V}^{*}\sigma_{a}}{(\pi_{V}^{*}\sigma_{a})_{a}}\right)^{\frac{k-1}{k}}}\right)}-k\sqrt{\frac{k+1}{2}}\frac{M}{\sqrt{1+\frac{k-1}{k}M^{2}}}\right]\right\}.$$

To establish the general principles of change of internal resistance of an engine on the Mach number we will relate this resistance to the test stand thrust in the design mode:

$$R_{0}=F_{c}p_{0}\left\{(k+1)\left(\frac{2}{k+1}\right)^{k/k-1}\sigma_{g}\sigma_{c}\sigma_{a}\pi_{k0}^{*}\times\right.$$
$$\left.\times\left[1-\frac{c_{p}}{c_{p}'}\frac{T_{a0}^{*}}{T_{g0}^{*}}\left(\frac{\pi_{k0}^{*\frac{k-1}{k}}-1}{\eta_{k0}^{*}\eta_{T0}^{*}}\right)\right]^{k'/k'-1}-1\right\}.$$

The relative internal resistance ($\overline{X}_a$) in the mode corresponding to $M = M_a$ and $H = 0$ is represented in Figure 106 as a function of TJE parameters in the design mode.

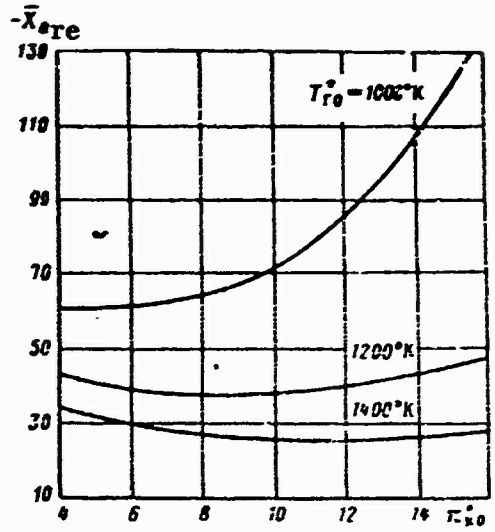

Figure 106. Internal resistance during autorotation at M = M_a as function of design parameters of engine.

The resistance in the mode of maximum reduced autorotation rpm is high for engines with high compression ratios in the compressor and low gas temperatures in the design mode. For engines with design gas temperatures of 1,200-1,400°K and π_k^* in the range from 4 to 16 the internal resistance depends little on π_k^* and amounts to approximately 25-48% (for M = M_a; H = 0) of the design thrust of the engine.

The change of relative internal resistance of an autorotating engine is shown in Figure 107 as a function of the Mach number for H = 0. As seen, when M increases, the resistance increases sharply due to the increased intake pulse, and at Mach numbers of the order of three can exceed 2-3-fold the design thrust of the engine (with incomplete expansion of the gas in the nozzle and pressure losses in the intake diffuser corresponding to the optimal shock wave system).

The resistance of an autorotating engine is much lower with complete gas expansion in the jet nozzle than with incomplete expansion. In the region of M ≈ 3 the resistance with complete expansion is approximately 50% less. In many cases this circumstance should be taken into account when selecting the program of control of supersonic nozzle components.

As flight altitude increases at constant Mach number the resistance of an autorotating engine decreases in proportion to pressure p_n.

If necessary the internal resistance of an autorotating engine can be decreased by reducing the air flow rate through the engine by means of the corresponding change of F_c or reduction of σ_a by regulating the area

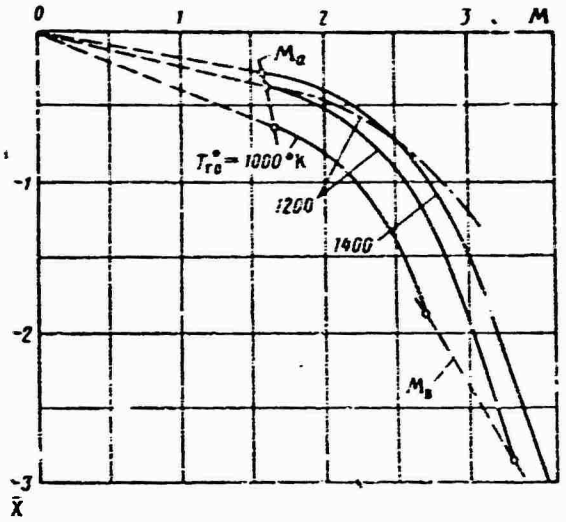

Figure 107. Internal resistance of autorotating engine as function of Mach number for $\pi_{k0}^* = 8$; solid curve shows resistance with incomplete gas expansion in jet nozzle; broken line -- with complete expansion.

of the air bypass ports, position of the air intake cone, etc. In determining the effectiveness of each of these measures it is necessary to take into account the change of external drag. Thus, for instance, covering the jet nozzle flaps decreases internal resistance, but at the same time increases the drag of the engine nacelle.

Flow Parameters in Combustion Chamber Intake, Determining Its Starting Properties

In order to evaluate the starting properties of the combustion chamber and main fuel ignition system it may become necessary to know the following flow parameters at the combustion chamber intake: pressure p_k^*, temperature T_k^* and velocity C_k.

Because the compressor operating mode remains at the same point of the characteristic at Mach numbers $M > M_a$ it is not very difficult to determine the stated air parameters in the combustion chamber intake. Thus, the pressure and temperature will be

$$p_k^* = p_n \pi_V^* \sigma_a \pi_{k\ a}^*;$$

$$T_k^* = T_n \tau_V^* \tau_{k\ a}^*.$$

The air velocity in the combustion chamber intake is found from the condition of "rubbing" of the first turbine nozzle:

$$C_{\text{в}}=\frac{\text{const}\cdot\tau(\lambda_{\text{в}\,a})\,q_{r\,a}R}{F_{\text{в}}\Pi(\lambda_{\text{в}\,a})}\sqrt{T_{\text{в}}\tau_V^*\tau_{\text{в}\,a}^*},$$

where

$$\text{const}=\frac{G\sqrt{T_g^*}}{P_g^*}.$$

We will relate the velocity in the autorotation mode to the velocity at the combustion chamber intake in the design mode:

$$C_{\text{в}0}=\frac{\text{const}\cdot\tau(\lambda_{\text{в}0})\,q_{r0}R}{F_{\text{в}}\Pi(\lambda_{\text{в}0})}\sqrt{T_{a0}^*}\sqrt{\frac{T_{a0}^*}{T_{g0}^*}\left[\left(\frac{\pi_{\text{в}0}^{*\frac{k-1}{k}}-1}{\eta_{\text{в}0}^*}\right)+1\right]};$$

then

$$\bar{C}_{\text{в}}=\frac{C_{\text{в}}}{C_{\text{в}0}}=\sqrt{\frac{T_{\text{в}}}{T_{a0}^*}}\,\frac{\sqrt{\tau_V^*\tau_{\text{в}\,a}^*}}{\sqrt{\frac{T_{a0}^*}{T_{g0}^*}\left(\frac{\pi_{\text{в}0}^{*\frac{k-1}{k}}-1}{\eta_{\text{в}0}^*}\right)}}.$$

The chief difficulties of starting in the autorotation mode in the region of supersonic flight velocities are related to ignition processes, flame propagation and stable combustion of the fuel-air mixture at high flow velocities in the engine combustion chamber. Thus, for instance, when M = 3 the velocity in the combustion chamber intake is 50-90% higher in the autorotation mode than in the design mode. In the range of Mach numbers M = 2-3 difficulties caused by high air velocities in the combustion chamber intake are compounded at high altitudes in connection with the low air pressures in the combustion chamber

Assessing the Possibility of Starting TJEA

At Mach numbers $M > M_a$ the reduced autorotation rpm remains constant, assuming that increased pressure losses in the intake diffuser with increasing Mach number do not cause subcritical flow in the jet nozzle. The physical rpm of an engine increases continuously with increasing M in proportion to the square root of the air temperature in the engine intake. Here the relation between the physical and reduced autorotation rpm is determined by the ordinary equation of similitude theory:

$$n_{au}=n_{re.au}\sqrt{\frac{T_a^*}{T_{a0}^*}}=n_{re.au}\sqrt{\frac{T_{\text{в}}}{T_{a0}^*}\left(1+\frac{k-1}{2}M^2\right)}. \qquad (15.23)$$

At some number $M = M_d$ the physical autorotation rpm can reach the maximum engine rpm n_{max}. This number M_d can be found from equation (15.23), assuming $n_{phy.au} = n_{max}$:

$$M_d = \sqrt{\frac{2}{k-1}\left[\frac{T^*_{a0}}{T_н \cdot n^2_{au.max}} - 1\right]} \qquad (15.24)$$

When $M = M_d$ the reduced engine rpm is equal to the maximum reduced autorotation rpm and the physical autorotation rpm is equal to the maximum physical engine rpm, respectively. It is easy to show that for TJE operating in the maximum mode M_d corresponds to its "degeneration" as an engine. It follows both from examination of the thermodynamic cycle of the engine and from analysis of the proposed dependence of the number M_d on the design parameters of TJE (Figure 108) that "degeneration" occurs earlier for high-pressure and low-temperature TJE.

For TJEA the number M_d at which the physical autorotation rpm reaches maximum can be determined by the equation

$$M_{ab} = M_{a0}\sqrt{\frac{1 - n^2_{max}(n_b\, n_{max})^2}{(1 - n^2_{max})(n_b\, n_{max})^2}}, \qquad (15.25)$$

in which the ratio n_b/n_{max} corresponds to the given value of $F_{c.b}/F_{c0}$.

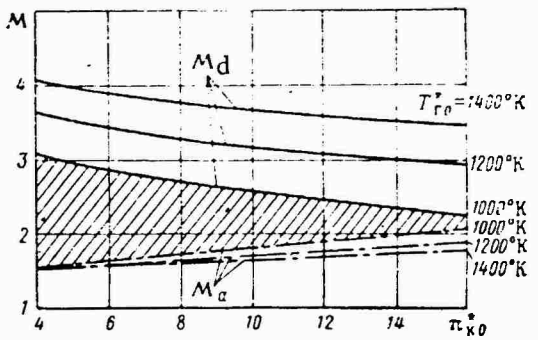

Figure 108. Theoretical dependence of M_d on design parameters of TJE for $\eta^*_{k0} = 0.85$; $\eta^*_{t0} = 0.94$; $\eta^*_k = 0.7$.

A change in the jet nozzle area has a slight effect on M_a (see Figure 108) and a notable effect on M_d. For example, an 80% increase in

nozzle area changes M_a by only 0.2, but M_d from 3.3 to 2.24. As a result of reduction of M_{db} when the jet nozzle is opened it is possible to accelerate the engine in the autorotation mode in the range of working numbers $M_a \leq M \leq M_d$ after in-flight engine flame-out if there is no way of preventing it automatically.

It follows from Figure 109 that an engine with $M_d = 3.3$ and jet nozzle area $F_{c.b} = 1.6F_{c0}$ will have maximum rpm in the autorotation mode at Mach number M ~ 2.35. Therefore when M > 2.35 the engine rotor may be accelerated to beyond the limit that is tolerable from the standpoint of strength of engine components. Several measures can be instituted to prevent such acceleration: the reactive nozzle area can be reduced, the bypass ports of the air intake can be opened, etc. In any case the problem of determining the required functioning time of the regulating apparatus must be solved.

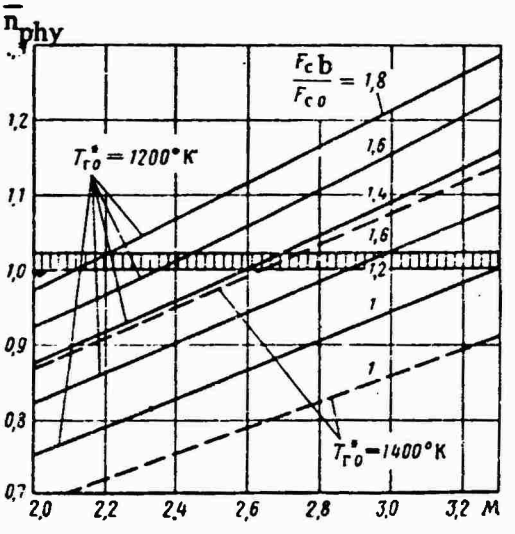

Figure 109. Change of autorotation rpm as function of Mach number and jet nozzle area for $T_H = 288°K$, $\pi^*_{k0} = 8$; $\eta^*_{t0}\eta^*_{k0} = 0.8$ (theoretical dependence).

The required operating speed of the regulating apparatus can be determined by solving the equation of engine rotor motion during acceleration from autorotation rpm n_a, corresponding to area F_{c0} in the maximum regime to rpm n_b corresponding to $F_{c.b}$.

The character of transition to the autorotation mode may be accompanied, in the general case, both by a reduction and increase of rpm, depending on the initial engine operating mode (mode A' or A'' in Figure 110).

This corresponds in Figure 110 to transitions A"-b"-b and A'-b'-b. Transitions A'-b' and A"-b", caused by flame-out, proceed at the speed of sound and take incomparably less time than acceleration or deceleration of the engine rotor. Therefore all ensuing discussions will pertain to transitions b'-b and b"-b.

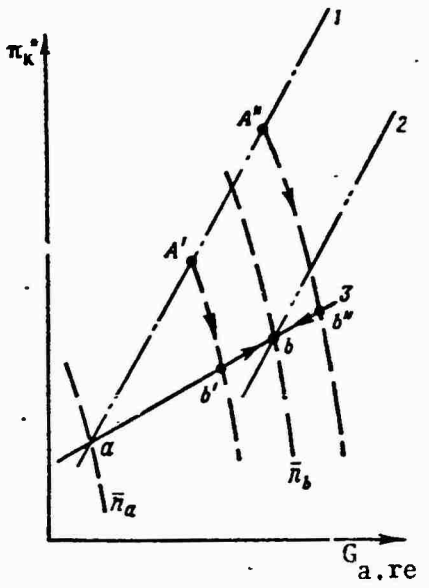

Figure 110. Diagram of establishment of autorotation: 1 -- line of operating modes corresponding to F_{c0}; 2 -- line of operating modes corresponding to $F_c = F_{c.b}$; 3 -- line of autorotation mode.

The rotor motion equation has the form

$$J\frac{d\omega}{dt}=\Delta M$$

or

$$\frac{\pi}{30}\frac{Jn^2_{max}}{716{,}2}\frac{\bar{n}d\bar{n}}{d\tau}=N_j.$$

Surplus power N_j that creates acceleration can be found as follows:

$$N_j=N_т-N_к=\frac{G_a T^*_a}{75}\times$$

$$\times\frac{L_{к0}}{T^*_{a0}}(\bar{n}^2_b-\bar{n}^2),$$

where $\bar{n}_b$ is relative final rpm (after reaching the steady state autorotation mode).

It is assumed here that in view of the "choking" of the jet nozzle turbine power will be constant during the entire acceleration process and equal to the final power in the steady state autorotation mode for $\bar{n} = \bar{n}_b$ (see Figure 108).

Substituting this value of N_j into the motion equation and assuming that the change of the air flow rate in the autorotation mode is proportional to the change of rpm the current air flow rate, consequently, can be expressed with some approximation through the air flow rate in the maximum mode:

$$G_a = G_{a0}\bar{n}\sqrt{\frac{T^*_{a0}}{T^*_a}\frac{p^*_a}{p^*_{a0}}}.$$

Introducing the concept of the reduced rotor inertia

$$J_{re} = J \frac{p^*_{a0}}{p_a} \sqrt{\frac{T^*_a}{T^*_{a0}}}$$ and denoting the complex

$$\frac{G_{a0} L_{k0} 716.2 \cdot 30}{J \cdot n^2_{max} 75\pi} = B$$

we obtain, finally, after several conversions, the following differential equation of rotor motion

$$\frac{d\bar{n}}{d\tau} + B\bar{n}^2 - B\bar{n}_b^2 = 0. \qquad (15.26)$$

The above equation is a special case of the Riccati equation, by which the general solution can be found by separation of variables.

We will separate the variables in the equation

$$\frac{d\bar{n}}{\bar{n}_b^2 - \bar{n}^2} = B d\tau.$$

Expanding the left hand side of the equation into simple fractions and applying the method of indeterminate coefficients we obtain

$$\frac{d\bar{n}}{\bar{n}_b^2 - \bar{n}^2} = \left(\frac{A}{\bar{n}_b - \bar{n}} + \frac{D}{\bar{n}_b + \bar{n}}\right) d\bar{n} = \frac{d\bar{n}}{2(\bar{n}_b - \bar{n})} + \frac{d\bar{n}}{2(\bar{n}_b + \bar{n})} = B d\tau.$$

We integrate the expression obtained by parts:

$$-\ln(\bar{n}_b - \bar{n}) + \ln(\bar{n}_b + \bar{n}) = \ln \sigma + 2B\tau.$$

Raising to the higher power we find the general solution of the differential equation of rotor motion in implicit form

$$\frac{\bar{n}_b + \bar{n}}{\bar{n}_b - \bar{n}} = \sigma e^{2B\tau}.$$

We determine the integration constant σ from the initial condition $\bar{n} = \bar{n}_a$ for $\tau = 0$:

$$\sigma = \frac{\bar{n}_b + \bar{n}_a}{\bar{n}_b - \bar{n}_a}.$$

Substituting the integration constant and solving the equation in terms of $\bar{n}$ we obtain

$$\bar{n} = \bar{n}_b \frac{\frac{\bar{n}_b + \bar{n}_a}{\bar{n}_b - \bar{n}_a} e^{2B\tau} - 1}{\frac{\bar{n}_b + \bar{n}_a}{\bar{n}_b - \bar{n}_a} e^{2B\tau} + 1}. \qquad (15.27)$$

The equation describes acceleration from autorotation rpm $\bar{n}_a$ to $\bar{n}_b$.

The character of change of autorotation rpm described by this equation is illustrated in Figure 111 for the special case when perturbation is caused by instantaneous opening of the jet nozzle flaps.

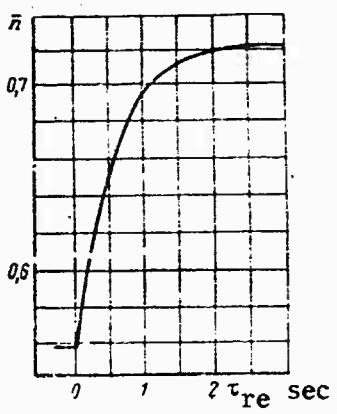

Figure 111. Character of acceleration of engine from $\bar{n}_a$ to $\bar{n}_b$ for $\pi^*_{k0} = 8$; $T^*_{g0} = 1{,}200°K$; $M_a = 1.6$; $F_{c.b}/F_{c0} = 1.8$.

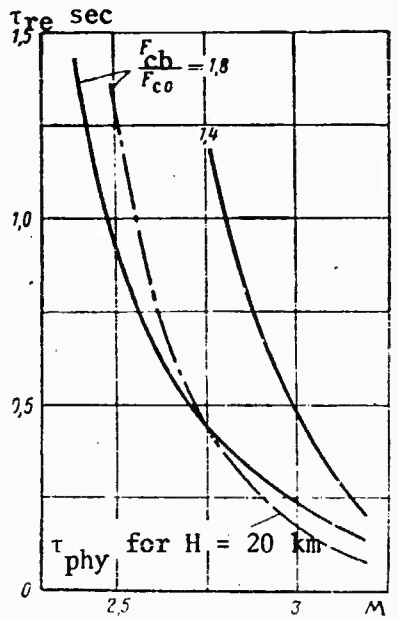

Figure 112. Theoretical dependence of reduced engine acceleration time on Mach number and $F_{c.b}/F_{c0}$ for B = 1; $T^*_{g0} = 1{,}200°K$; $\pi^*_{k0} = 8$; $\eta_{k0}\eta_{t0} = 0.8$; $\Delta n_{max} = 2\%$.

The time required for reaching engine rpm that is maximum tolerable in terms of strength is determined from the same rotor motion equation.

Through $\Delta n_{max} = (n_{max\ tol} - n_{max})/n_{max}$ we will denote the maximum tolerable relative excess of design rpm. This value is usually 2-4%.

Then

$$n_{\max\ tol} - n_{\max} = \bar{n}_{\max} n \sqrt{\frac{T_a^*}{T_{au}^*}} - n_{max} = n_{max}\left(\bar{n}\sqrt{\frac{T_a^*}{T_{a0}^*}} - 1\right)$$

or

$$\bar{n}_{max} = (1 + \Delta\bar{n}_{max})\sqrt{\frac{T_a^*}{T_{a0}^*}}.$$

Substituting the values $\bar{n}_{max}$ into the motion equation and solving it in terms of time, we obtain

$$\tau_{re} = \frac{\lg \dfrac{(1 + \Delta\bar{n}_{max})\sqrt{T_{a0}^*/T_a^*} + \bar{n}_b}{\left[\bar{n}_b - (1 + \Delta\bar{n}_{max})\sqrt{T_{a0}^*/T_a^*}\right]\bar{n}_b + \bar{n}_a/\bar{n}_b - \bar{n}_a}}{2B \lg e}. \qquad (15.28)$$

The reduced acceleration time from the initial to maximum tolerable engine rpm is shown in Figure 112. Also shown there is the change of the physical acceleration time for one of the cases ($F_{c.b} = F_{c0} = 1.8$; H = 20 km). The acceleration time, as seen, is extremely short, even at comparatively high altitude (H = 20 km).

For small acceleration (tolerable above maximum design rpm), consequently, high-speed automation and servomechanisms, designed to prevent excessive acceleration, are required.

CHAPTER 16. CONDITIONS IN THE LOW RPM REGIME

An engine is placed in minimum stable operation when the engine control lever (ECL) is moved to the idling position. This is the last step of the in-flight starting process. During in-flight starting of a turbojet engine its parameters change from the values characterizing the autorotation regime to those in idling regime.

We will determine the importance of turbojet engine parameters in the in-flight idling regime. For this purpose it is essential to know the character of change of rotor rpm at in-flight idling. If we know the in-flight idling rpm we can determine all other gas dynamic parameters in this regime.

Engine rpm at idle is determined basically by the character of change of the fuel flow rate as the altitude and speed are changed with the ECL always in the idle position.

The fuel regulating apparatus of modern turbojet engines automatically executes a certain program of fuel feed to the engine with the ECL in the idle position (Figure 113). At altitudes from 0 to H_1 the differential valve maintains constant fuel pressure drop on the fuel pump throttle valve with the result that the fuel flow rate through the engine at these altitudes is practically constant.

Starting at altitude H_1 the fuel flow rate decreases and becomes equal to the capacity of the fuel pump in the minimum delivery setting (at altitude H_2'), or equal to the fuel delivery through the low-pressure valve (at altitude H_2''). In engines without the low-pressure valve (i.e., with minimum capacity setting) the fuel flow rate at altitudes greater than H_2'' will increase with altitude.

With this program of change of the actual fuel flow rate with the ECL in the idle position the characteristic of change of idle rpm with altitude and speed can be calculated for each engine. This characteristic

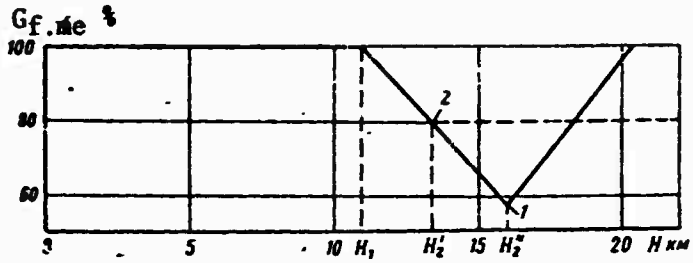

Figure 113. Typical character of change of fuel flow rate through engine at idle with changing flight altitude: 1 -- actual capacity of pumps at lowest capacity setting; 2 -- actual fuel feed to engine provided by minimal pressure valve.

can be determined from the consideration that the reduced (to standard conditions on the earth) actual fuel flow rate should fall on the same curve as a function of the reduced idling rpm in flight. This curve is the dependence of the reduced fuel flow rate on the reduced rpm [$G_{f.re} = f(n_{re})$], which can be found on the basis of on the ground engine test results.

The dependence of the parameters reduced according to the similitude equations to surface standard conditions with respect to temperature and pressure of a completely stagnant ambient air flow on the reduced rpm at M = const differs for various Mach numbers. Therefore the direct use of the characteristic taken for the same Mach number for determination of the reduced engine parameters for a different Mach number is impossible.

The dependence of the relative reduced parameters on the relative reduced rpm for M = const (relative reduced characteristic) is identical with an accuracy of ±3% for different Mach numbers.

The ratio of the reduced engine rpm (to T = 288°K with respect to T_n^*) to the maximum rpm (prescribed by the technical specifications) is called the relative reduced rpm.

The ratio of the reduced value of this parameter at a given Mach number to the reduced value of this parameter at maximum (prescribed by the technical specifications) engine rpm at the same Mach number is called the relative reduced arbitrary parameter.

The relative reduced characteristics of many engines, built on the basis of ground (test stand or on the aircraft) engine tests in the operating rpm range also fall within the limits of ±3% of the deviations that occur in the relative reduced characteristics of each engine at different Mach numbers. Therefore the relative reduced characteristic of a given engine can be used with an accuracy sufficient for practical purposes, for reducing the basic in-flight engine parameters to MSA [Mezhdunarodnaya standartnaya atmosfera; International Standard Atmosphere].

The engine parameters reduced to MSA for n_{me} = const; p_H = const; M = var are determined by the equations

$$\left.\begin{aligned} p_{iH\,re} &= p_{iH\,me}\,\frac{p_{H\,ct}}{p_H}\,\frac{\bar{p}^{*}_{iH}(n^{*}_{ct})}{\bar{p}^{*}_{iH}(n^{*}_{H})}\,\frac{\varkappa'_2(M_{ct})}{\varkappa'_2(M)};\\ T_{iH\,re} &= T_{iH\,me}\,\frac{T_{H\,ct}}{T_H}\,\frac{\bar{T}^{*}_{iH}(n^{*}_{H\,ct})}{\bar{T}^{*}_{iH}(n^{*}_{H})}\,\frac{\varkappa'_3(M_{ct})}{\varkappa'_3(M)};\\ G_{\tau H\,re} &= G_{\tau H\,me}\,\frac{p_{H\,ct}}{p_H}\sqrt{\frac{T_{H\,ct}}{T_H}}\,\frac{\bar{G}^{*}_{\tau H}(n^{*}_{H\,ct})}{\bar{G}^{*}_{\tau H}(n^{*}_{H})}\,\frac{\varkappa'_1(M_{ct})}{\varkappa'_1(M)}, \end{aligned}\right\} \qquad (16.1)$$

where $p^{*}_{iH}(n^{*}_{H\,ct})$, etc. are determined with the aid of nomograms, and the corrections for fluctuations in the Mach number are introduced through the functions κ'_1, κ'_2, κ'_3;

p_{iH}, T_{iH} are the pressure and temperature in an arbitrary cross section of the engine duct, and the values $p^{*}_{iH}(n^{*}_{Hct})$, $p^{*}_{iH}(n^{*}_{H})$, $T^{*}_{iH}(n_{Hct})$, $T^{*}_{iH}(n^{*}_{H})$, $G^{*}_{fH}(n^{*}_{Hct})$ and $G^{*}_{fH}(n^{*}_{H})$ are determined according to the known relative reduced characteristic with the aid of the nomogram;

n^{*}_{H} is engine rpm reduced to T = 288°K with respect to T^{*}_{H};

n^{*}_{Hct} is engine rpm reduced to T = 288°K with respect to T^{*}_{Hct};

G_{fH} is measured fuel flow rate per hour.

We will determine analytically the engine rpm in the in-flight idling regime on the following segments (Figure 114):

segment I -- before automatic operation;

segment II - from automatic operation rpm to the rpm at which minimum fuel feed to engine is achieved;

segment III - from the rpm at which minimum fuel feed to engine is achieved to maximum rpm.

The curves $G_{f.re} = f(n_{re})$ for modern gas turbine engines show that the actual dependence of the reduced fuel flow rate on the reduced rpm can be replaced on the specified segments by a straight line.

By replacing curve AB on the segment from on the ground idling rpm to the rpm of automatic operation of the governor (segment I) with a straight line we may write, on the basis of the similarity of triangles n'B"B' and n'AA', the following equation:

$$\frac{G_{f.re.Hl}}{G_{f.re0}} = \frac{n_{reHl} - n'}{n_{re0} - n'}, \qquad (16.2)$$

where $G_{f.reHl}$ and n_{reHl} are the reduced (to standard atmospheric conditions on the earth) measured fuel flow rate and engine rpm in the in-flight idling regime;

$G_{f.re0}$ and n_{re0} are the reduced fuel flow rate and rpm in the on the ground idling regime;

n' is the rpm intersected on the abscissa axis by straight line AB" of the function $G_{f.re} = f(n_{re})$.

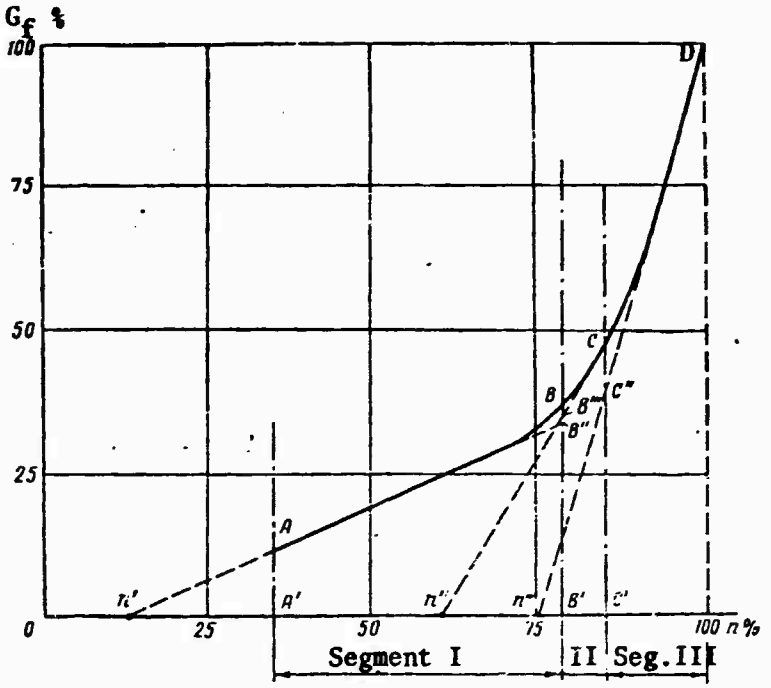

Figure 114. Typical dependence of reduced fuel flow rate on reduced rpm.

Fuel flow rate and in-flight rpm reduced to standard conditions on the ground are determined by the following equations of reduction:

$$G_{f.re\ H} = G_{f.me\ H}\frac{760}{p_H^*}\sqrt{\frac{288}{T_H^*}} \text{ and } n_{reH} = n_{me\ H}\sqrt{\frac{288}{T_H^*}}.$$

By substituting the reduced fuel flow rate and rpm into equation (16.2) we obtain

$$\frac{G_{fme\ H}\frac{760}{p_H^*}\sqrt{\frac{288}{T_H^*}}}{G_{fme\ 0}\frac{760}{p_0}\sqrt{\frac{288}{T_0}}} = \frac{n_{me\ H}\sqrt{\frac{288}{T_H^*}} - n'}{n_{me0}\sqrt{\frac{288}{T_0}} - n'}. \qquad (16.3)$$

Recalling that on the examined altitude segment the measured on the ground and in-flight fuel flow rates remain constant with the ECL in the idling position, after simplification and simple conversions of equation (16.3) we obtain

$$n_{me\ H} = \frac{p_0}{p_H^*}\left(n_{me0} - n'\sqrt{\frac{T_0}{288}}\right) + n'\sqrt{\frac{T_H^*}{288}}, \qquad (16.4)$$

where $n_{me\ H}$ is the measured engine rotor rpm in the in-flight idling regime on segment I;

n_{me0} is the measured rpm in the on the ground idling regime;

p_H^* and T_H^* are the pressure and absolute temperature of the air in flight in stagnant flow;

p_0 and T_0 are the pressure and absolute temperature of the air on the ground.

Using equation (16.4) we can determine the in-flight idling rpm as a function of altitude and flight speed for a specific engine with known on the ground idling rpm (n_{me0}) and known rpm at which the tangent to the function $G_{f.re} = f(n_{re})$ intersects the abscissa axis on segment I.

Using equation (16.4) we can also find the altitude at which the rpm of automatic governor operation is reached at different flight speeds.

Now we will find the maximum altitude at which the fuel pump capacity will drop to the value limited by the low-pressure valve or low-feed setting. For this purpose we will replace curve BC of the function $G_{f.re} = f(n_{re})$ on segment II with the straight line B'''C. Then, from the similarity of triangles n"B'''B' and n"CC' we can write the equation

$$\frac{G_{f.re\ H1}}{G_{f.re\ H2}} = \frac{n_{re\ H1} - n''}{n_{re\ H2} - n''}, \qquad (16.5)$$

where $G_{f.re\ H1}$ and $n_{re\ H1}$ are the reduced measured fuel flow rate and rpm at flight altitudes and speeds at which the rpm of automatic operation is reached with the ECL in the idling position;

$G_{f.re\ H2}$ and $n_{re\ H2}$ are the current values of the reduced fuel flow rate and rpm on segment II;

n" is the rpm cut on the abscissa axis by straight line CB''' of the function $G_{f.re} = f(n_{re})$.

After substituting the measured parameters into equation (16.5) instead of the reduced we obtain

$$\frac{G_{fme\ H1}\frac{760}{p^*_{H1}}\sqrt{\frac{288}{T^*_{H1}}}}{G_{f.me\ H2}\frac{760}{p^*_{H2}}\sqrt{\frac{288}{T_{H2}}}}=\frac{n_{me\ JIAP}\sqrt{\frac{288}{T^*_{H1}}}-n''}{n_{me\ JIAP}\sqrt{\frac{288}{T^*_{H2}}}-n''}. \tag{16.6}$$

From equation (16.6) we can determine according to air pressure the altitude at which the minimum fuel flow feed to the engine is reached, determined either by the minimum capacity or by adjustment of the low-pressure valve:

$$p_{H2}=\frac{p^*_{H_1}\left(n_{me\ JIAP}\sqrt{\frac{288}{T^*_{H1}}}-n''\right)}{(1+0{,}2M^2_{H2})^{3,5}\left(n_{me\ JIAP}\frac{G_{f.me_{H1}}}{G_{fme\ H2}}\sqrt{\frac{288}{T^*_{H1}}}-n''\frac{G_{f.me_{H1}}}{G_{fme\ H2}}\sqrt{\frac{T^*_{H2}}{T^*_{H1}}}\right)}. \tag{16.7}$$

The values p^*_{H1} and T^*_{H1} entering into equation (16.7) are determined by equation (16.4) with the condition that $n_{me\ H} = n_{me\ HAP}$. We will determine the change of idling rpm at altitudes when the fuel feed to the engine is maintained constant by means of the low-pressure valve with the ECL in the idling position. For these flight altitudes, as for flight altitudes before automatic operation of the governor, we may write

$$\frac{G_{f.re\ H2}}{G_{f.re\ H3}}=\frac{n_{re\ H2}-n'''}{n_{re\ H3}-n'''} \tag{16.8}$$

or

$$\frac{G_{fme\ H2}\frac{760}{p_{H2}}\sqrt{\frac{288}{T^*_{H2}}}}{G_{fme\ H3}\frac{760}{p^*_{H3}}\sqrt{\frac{288}{T^*_{H3}}}}=\frac{n_{me\ H2}\sqrt{\frac{288}{T^*_{H2}}}-n'''}{n_{me\ H3}\sqrt{\frac{288}{T^*_{H3}}}-n'''}, \tag{16.9}$$

where $G_{f.re\ H3}$ and $n_{re\ H3}$ are the reduced measured fuel flow rate and rpm at idle on segment III;

p^*_{H3} and T^*_{H3} are the pressure and absolute temperature of the air in stagnant flow at altitudes and velocities at which the idle rpm is determined by adjustment of the low-pressure valve or by the minimum capacity setting;

n''' is the rpm cut on the abscissa axis by straight line DC'' of the function $G_{f.re} = f(n_{re})$.

Since $G_{f.me\ H2} = G_{f.me\ H3}$, then after conversions we may write

$$n_{me\,H3}=\frac{p^*_{H2}}{p^*_{H3}}\,n_{me\,H2}+n'''\left(\sqrt{\frac{T^*_{H3}}{288}}-\frac{p^*_{H2}}{p^*_{H3}}\sqrt{\frac{T^*_{H2}}{288}}\right). \qquad (16.10)$$

The values p^*_{H2} and T^*_{H2} entering in equation (16.5) are determined by equation (16.7). Then we may find using equation (16.10) the change of engine rpm for different constant flight speeds with the ECL at the idling position at altitudes of the low-pressure valve operation and can also determine the altitudes at which engine rpm with the ECL in the idling position will be equal to the maximum engine rpm.

For the case when the control system has no low-pressure valve the capacity of the fuel pump, as soon as minimum feed is reached, begins to increase with a further increase of flight altitude, since here the engine rpm and consequently fuel pump rpm increase with the ECL in the idling position. To determine the idling rpm in these cases it is necessary to know the dependence of fuel pump capacity at the minimum feed setting on the pump rotor rpm. This dependence is determined in laboratory tests of the fuel pump on the ground.

Laboratory tests show that the fuel pump capacity at the minimum feed setting increases in proportion to rpm. Therefore the value $G_{f.meH3}$ entering in equation (16.9) can be determined according to the equation

$$G_{f.me\,H3} = G_{f.me\,H2} + \Delta G_f = G_{f.me\,H2} + Ki(n_{me\,H3} - n_{me\,H2}),$$

where K is the proportionality factor determined according to the dependence of fuel pump capacity at the minimum feed setting on engine rotor rpm;

i is the gear ratio between the engine rotor and the fuel pump rotor.

Then equation (16.9) is written in the form

$$\frac{G_{f.me_{H2}}\frac{760}{p^*_{H2}}\sqrt{\frac{288}{T^*_{H2}}}}{[(G_{f.me\,H2}+Ki(n_{me\,H3}-n_{me\,H2})]\frac{760}{p^*_{H3}}\sqrt{\frac{288}{T^*_{H3}}}}=$$

$$=\frac{n_{me\,H2}\sqrt{\frac{288}{T^*_{H2}}}-n'''}{n_{me\,H3}\sqrt{\frac{288}{T^*_{H3}}}-n'''}.$$

From the latter equation we can derive an equation for determining the measured idling rpm on segment III for engines in which the minimum fuel feed to the engine is determined by the minimum capacity setting:

$$n_{me\,H3}=\frac{G_{f.me\,H2}\left(\frac{p^{\bullet}_{H3}}{p^{\bullet}_{H2}}\sqrt{\frac{T^{\bullet}_{H3}}{T^{\bullet}_{H2}}}n^{\prime\prime}+\sqrt{\frac{288}{T^{\bullet}_{H2}}}n_{me.H2}^{-n^{\prime\prime}}\right)}{G_{f.me\,H2}\frac{p^{\bullet}_{H3}}{p^{\bullet}_{H2}}\sqrt{\frac{288}{T^{\bullet}_{H2}}}+Kin^{\prime\prime}-Ki\sqrt{\frac{288}{T^{\bullet}_{H2}}}n_{me\,H2}}+$$
$$+\frac{n_{me\,H2}\left(Kin^{\prime\prime}-Kin_{me\,H2}\sqrt{\frac{288}{T^{\bullet}_{H2}}}\right)}{G_{f.me\,H2}\frac{p^{\bullet}_{H3}}{p^{\bullet}_{H2}}\sqrt{\frac{288}{T^{\bullet}_{H2}}}+Kin^{\prime\prime}-Ki\sqrt{\frac{288}{T^{\bullet}_{H2}}}n_{me\,H2}}. \qquad (16.11)$$

Using equations (16.4), (16.7), (16.10), (16.11) we can find the engine idling rpm at various altitudes at constant flight speeds. Change of idling rpm with flight altitude is shown in Figure 115 for a turbojet engine with an axial compressor. As seen, the engine idling rpm increases as flight altitude increases. First the rpm increases from values close to the on the ground idling rpm to automatic operation rpm (HAP). When the fuel pump reaches minimum capacity the rpm continues to increase beyond HAP. In individual cases, particularly at low flight speeds and when the low-pressure valve or minimum capacity setting are improperly regulated, the idling rpm may reach the maximum rpm of a given engine, or even exceed it at high flight altitudes.

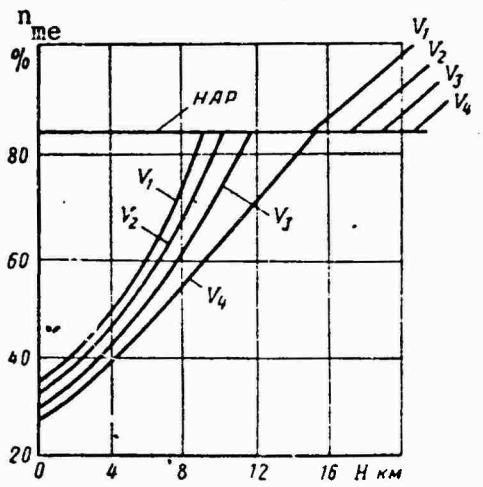

Figure 115. Engine rotor idle rpm as function of flight altitude: $V_1 < V_2 < V_3 < V_4$.

As seen in Figure 116 the range of change of engine rotor rpm during in-flight starting of the engine depends between autorotation and idling on the flight altitude and velocity at which the engine is started. At altitudes where automatic operation begins, the difference between the idling rpm and autorotation rpm is greatest. At high altitudes this difference between the idling rpm and autorotation rpm diminishes considerably at high flight speeds.

If the character of change of idling rpm is known, the measured value of any engine parameter in the idling regime can be determined with the reduction equations. The change of air and flow rates in the idling regime is shown in Figures 117 and 118 for various flight speeds as a function of altitude.

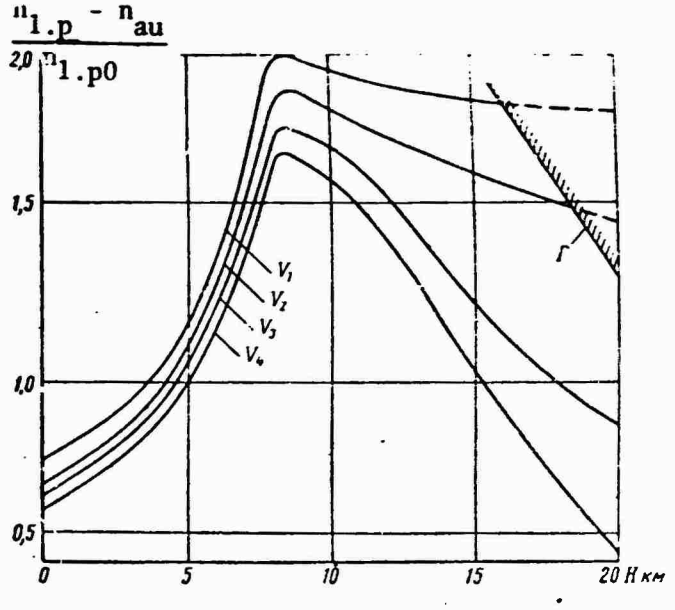

Figure 116. Change of engine rpm during in-flight starting as function of flight altitude and speed: Г -- boundary of altitudes at which idling rpm is equal to maximum rpm: $V_1 < V_2 < V_3 < V_4$.

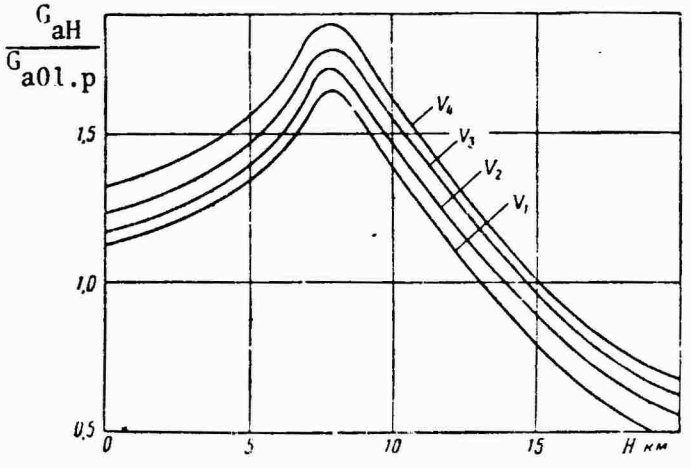

Figure 117. Actual air flow rate through engine during operation in the idling regime as function of flight altitude: $V_1 < V_2 < V_3 < V_4$.

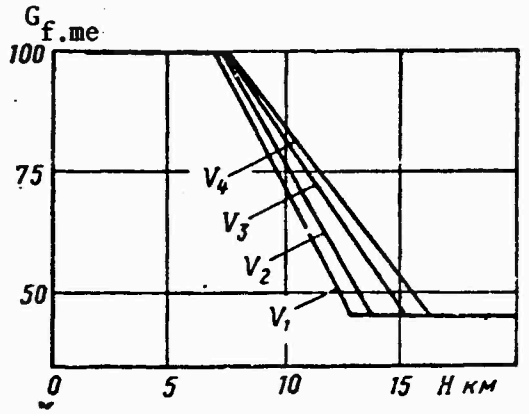

Figure 118. Actual fuel flow rate at idling rpm as function of flight altitude: $V_1 < V_2 < V_3 < V_4$.

Using the character of change of engine parameters that we have found in the autorotation and idling modes as a function of flight altitude and speed we will examine the features of the starting process of a turbojet engine in flight in the same phases characterizing on the ground starting of the engine (with the exception of the phase of preliminary engine rotor acceleration by an external power source).

CHAPTER 17. ENGINE CHARACTERISTICS AND PARAMETERS IN TRANSITION TO LOW RPM REGIME

§39. Features of Initial Ignition

To ensure in-flight starting of an engine, like on the ground starting, it is essential first of all to create an effective flame center for ignition of the fuel-air mixture in the combustion chambers. This flame center is formed during on the ground starting at the initial moment at low air velocities in the combustion chambers. During in-flight starting the initial flame center is formed in the autorotation regime, when combustion chamber conditions can differ substantially from those on the ground at the moment of formation of the initial flame center.

The operation of flame type starters depends on the fuel-air mixture parameters in the ignition chamber and the energy discharged in the spark gap of the plugs. The fuel-air mixture parameters (mixture composition, its pressure, temperature and velocity) depend on the air parameters and the amount of starter fuel injected into the starter igniter chamber.

Until now air gathered from the engine combustion chambers has been used for the starter igniters. Consequently the air parameters in the starter igniter chamber will be the same as in the engine combustion chambers in the autorotation regime. The amount of fuel entering the starter igniter chamber does not depend on flight conditions and remains practically the same as during on the ground start-up. Consequently all parameters of the fuel-air mixture in the starter igniters will vary as the flight speed and altitude change. As seen in Figure 119 the fuel-air mixture in the starter igniters is richer during flight in the autorotation regime than during on the ground starting. The mixture may become especially rich at high altitudes and flight speeds close to minimum.

As flight speed increases, the fuel-air mixture in the starter igniters becomes impoverished. Enrichment of the fuel-air mixture in the starter igniters during flight in the autorotation mode leads to poor ignition and reduction of the flame temperature discharged from the starter igniter.

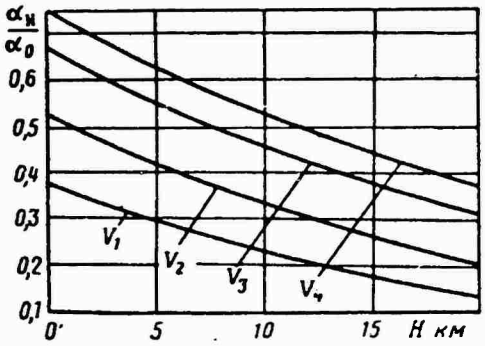

Figure 119. Ratio of excess air coefficient in flight to excess air coefficient on the ground in starter igniters as function of flight altitude: $V_1 < V_2 < V_3 < V_4$.

The pressure and velocity of the mixture have a great effect on the ignition and combustion stability of the fuel-air mixture in the starter igniters. As the pressure drops, ignition and combustion stability of the mixture get worse and at some completely determined pressure the mixture fails to ignite. This effect of pressure on mixture ignition can be explained by the fact that as the pressure drops, the thermal width of the flame front increases, and consequently the ratio of the mass of combustion products in the initial combustion center to the mass of the mixture that must be ignited decreases.

As the pressure decreases, the volume of the initial combustion center increases approximately in proportion to the density of the medium. Furthermore a slight drop in pressure lowers the combustion temperature of the mixture in the initial center due to an increase in the degree of dissociation of the combustion products.

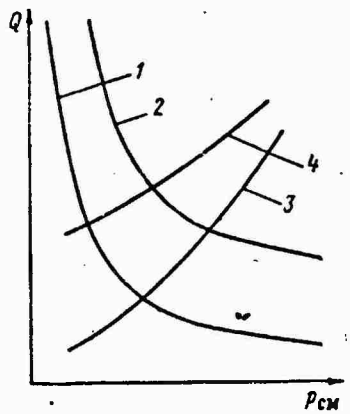

Figure 120. Energy required for formation of combustion center as function of mixture pressure in combustion zone: 1 -- energy required for formation of initial combustion center; 2 -- energy required for mixture ignition in combustion chamber; 3 -- energy provided by ordinary ignition system; 4 -- energy provided by improved ignition system.

The energy discharged in the spark gap of the starter igniter plugs depends primarily on the type of ignition system installed in the engine. In high-voltage ignition systems, sometimes used for gas turbine engines, this energy decreases as the pressure decreases and mixture velocity increases. As the pressure drops, the voltage on the plug electrodes required for spark discharge decreases and consequently less energy is discharged.

An increase in mixture velocity narrows its ignition range and, starting at some mixture velocity the mixture cannot be ignited by the given spark, since the heat losses from the initial combustion center increase, and consequently its temperature drops.

We know at the same time that the spark energy required to ignite the fuel-air mixture in the starter igniters should increase as the

flight altitude and velocity increase. As this energy increases, naturally, the fuel-air mixture can be ignited at lower mixture pressures (Figure 120), i.e., at higher flight altitudes.

High-voltage ignition systems increase the spark energy, for instance, by increasing the gap between the spark plug electrodes. Here, however, ignition system reliability is lowered, since all its components begin to operate at high voltage.

Electrode form also has an influence on the ignition capacity of the spark. Plugs with sharp pointed electrodes provide wider ignition boundaries. The stated discrepancy between the required and available energy in high-voltage ignition systems prompted the development of new types of ignition systems, ensuring a powerful discharge between spark plug electrodes at all working altitudes and flight speeds. Considerable expansion of the ignition boundary is achieved by using an arc discharge system that produces additional evaporation of the mixture.

Thus as the pressure and temperature decrease and mixture velocity increases, the energy and ignition capacity of the initial flame center created by the flame type igniters decrease, regardless of the character of the ignition source, since here the heat release rate is lowered. For each type of starter igniter there are limiting flight speeds and altitudes that limit mixture ignition possibilities.

The possibility of regulating the parameters that influence ignition conditions in starter igniters is extremely limited. Sometimes this can be done by changing the mixture composition in the starter igniter by periodically turning on and off the starter fuel feed. In this case the mixture composition changes as a result of change of the starter fuel pressure (flow rate). Maximum starter flame intensity is reached as soon as the relations of the parameters most favorable for igniting the fuel-air mixture are established.

The boundary of mixture ignition in the starter igniter depends both on its design features and on the properties of the fuel used and heat release conditions. If a fuel whose viscosity increases as temperature falls is used as the starter fuel, then ignition and stable combustion of the mixture in the starter igniters are possible at lower flight altitudes and speeds.

Flame type starter igniters in which air is delivered into the combustion zone from a special source have better characteristics with respect to ignition and combustion of the fuel-air mixture, since the formation and development of the flame are practically independent of the air flow parameters in the combustion chamber.

Feeding the starter igniter with oxygen can be employed to improve heat release conditions (Figure 121). Here the boundary of stable starter igniter operation is expanded with respect to flight speed and altitude.

As the oxygen concentration in the air increases, the energy required for ignition of the mixture decreases. It only takes a slight enrichment of air with oxygen to substantially improve mixture ignition conditions.

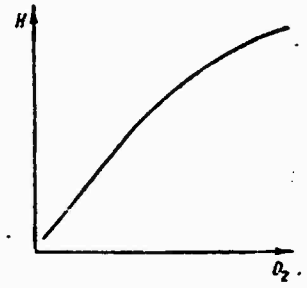

Figure 121. Altitude of stable starter igniter operation as function of oxygen concentration in the air.

§40. Features of Main Fuel Ignition by Flame from Initial Center

The flame from the starter igniter ignites the fuel-air mixture in the combustion chambers. Reliable ignition of this mixture requires that the flame of the starter igniter penetrate into the countercurrent zone.

Ignition of the fuel-air mixture in the combustion chambers depends both on the power of the flame produced by the starter igniter and on the characteristics of the mixture itself (pressure, velocity, temperature and mixture composition) at the instant of its ignition. The mixture characteristics are determined by the previously discussed air parameters behind the compressor in the autorotation mode and by the amount of fuel delivered to the engine by the fuel system in the autorotation mode. One possible dependence of maximum possible fuel feed to the engine in the autorotation mode on flight altitude and speed is shown in Figure 122. In accordance with increasing engine rotor rpm in the autorotation mode with increasing flight speed and altitude, the fuel pump increases the fuel feed to the engine to a value equal to the capacity of the fuel pump in the idling position. Then the engine's fuel system ensures constant quantity of fuel to the engine.

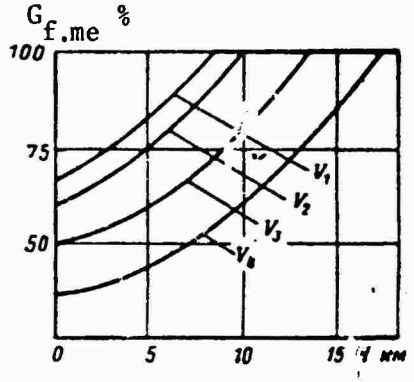

Figure 122. Fuel feed to combustion chambers in autorotation mode as function of flight altitude at various flight speeds: $V_1 > V_2 > V_3 > V_4$.

As seen in Figure 123, the fuel-air mixture in the combustion chambers is enriched at all flight speeds in the autorotation mode as flight altitude increases.

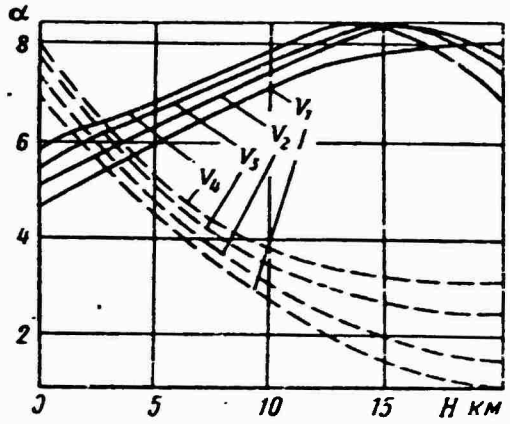

Figure 123. Excess air coefficient as function of flight altitude (continuous curves show change of α in steady state regime after ignition of fuel and broken curves -- during autorotation): $V_1 < V_2 < V_3 < V_4$.

As the flight speed and altitude change in the autorotation mode, all characteristics of the fuel-air mixture in the combustion chambers also change. Flight altitude has the greatest effect on this change. As flight altitude increases, the ignitability of the fuel-air mixture in the combustion chambers decreases because of lower pressure, temperature and excess air coefficient, and also because of the increased velocity of the fuel-air mixture. As flight altitude increases, the limits of combustion with respect to the composition of the fuel-air mixture narrow and the combustion process is adversely affected. At low air pressures the combustion process is weak, the gases in the central part of the combustion chamber have a low temperature and therefore the zone in which most of the fuel should ignite is displaced to the region of intensive intake of cold air.

A lowering of the air pressure in the combustion chamber is accompanied by a displacement of the outer ignition boundary toward the axis of the flame tube. The mixture composition in the center of the circulation zone remains favorable for ignition and combustion in a broad range of pressure change. As the air pressure decreases, the maximum flow velocity at which ignition of the mixture is still possible decreases and all starting characteristics are displaced to the region of smaller values of summary excess air coefficient (Figure 124). The maximum velocity decreases due to reduction of the ignition capacity of the initial combustion center because of a lowering of its temperature.

As the pressure drops, the width of the combustion zone (distance to which the fuel burns completely) increases considerably. This impoverishes the fuel-air mixture in the combustion zone and lowers the gas temperature in the countercurrent region of the circulation zone. Here the preparation of the mixture for combustion and flame stabilization progressively worsens, which leads in turn to retardation of the combustion process.

As flight altitude is increased, the process of the fuel-air mixture combustion in the combustion chambers slows down and combustion completeness decreases. Combustion completeness changes differently as flight altitude is increased for combustion chambers with different combustion designs. Even when the other fuel-air mixture parameters remain constant a lowering of the mixture pressure below 0.6 atm sharply reduces mixture combustion completeness.

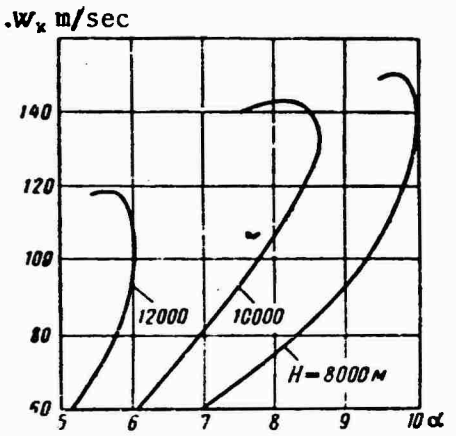

Figure 124. Effect of flight altitude on lower boundary of ignition of fuel mixture in combustion chamber.

Cooling or heating of the air changes primarily its density and viscosity, on which depends the quality of atomization and the trajectory of the droplets. Furthermore the rate of evaporation of the fuel and conditions of cooling of the initial combustion center depend on the air temperature.

The chief effect of cooling of the air amounts to retardation of evaporation of the droplets due to cooling of the fuel on the surfaces of the droplets and to retardation of the diffusion of vapor from the surfaces of the droplets into the surrounding environment. The fuel concentration around the droplets becomes lower and the conditions of transfer of the flame from droplet to droplet worsen. Furthermore, as the air cools, the rate of development of the initial combustion center decreases.

The negative effect of cooling of the air on starting characteristics can be eliminated to a known extent by increasing somewhat the fuel flow rate or by increasing the power of the ignition system. For homogeneous mixture the ignition energy is inversely proportional to the cube of the absolute temperature. This relation is obviously also valid for an inhomogeneous mixture.

As flight altitude increases, the velocity of the flow in the combustion chamber increases at constant air speed. At some altitude, obviously, at minimum flight speed the flow velocity in the combustion chamber becomes maximum. This altitude will be the boundary, above which, for a given aircraft, transfer of the flame through the flame tubes and, consequently, engine start-up are impossible.

The ignition of the fuel-air mixture in the combustion chambers is adversely affected with increasing flight velocity in the autorotation mode only by increasing the velocity of the mixture in the combustion chambers. The other parameters of the fuel-air mixture change in such a way that the conditions for ignition of the fuel-air mixture are improved.

The position of the combustion zone in the flame tube depends on the velocity of the mixture in the combustion chambers. At low speeds the mixture burns in the countercurrent zone, which has a favorable effect on fuel combustion completeness and gas temperature in the combustion zone. At high mixture velocities the combustion zone, displaced downflow from the nozzles, may spill over into the direct current zone, which changes the temperature in the combustion zone.

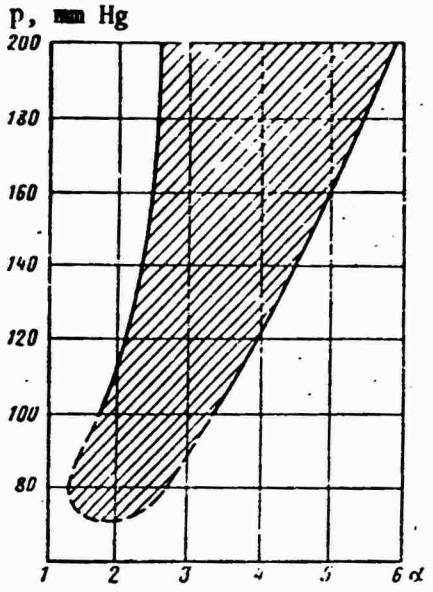

Figure 125. Region of stable chamber operation for W_k = = 50 m/sec; t_k = 22°C.

The possibility of in-flight engine starting is limited also by fuel combustion stability in the combustion chamber. The pressure at which stable combustion in the combustion chamber cannot be maintained can be reached in any combustion chamber velocity operating regime (Figure 125).

The difference in the regions of stable chamber operation are determined for ordinary fossil fuels by evaporability and also by the quality of atomization. In principle a more volatile fuel may lead to the formation of local zones of relatively homogeneous mixture, which will be too lean or rich for combustion. As the quality of fuel atomization improves, the combustion process approaches, in terms of its character, the process of combustion of a homogeneous mixture, and this in turn narrows the range of stable chamber operation.

Thus the fuel-air mixture parameters in the combustion chambers change sharply as flight speed and altitude change. There is always a boundary of possible ignition and combustion of the fuel mixture in the combustion chambers for each type of engine with respect to flight speed and altitude in the autorotation regime.

§41. Features of Flame Propagation in Combustion Chambers

After ignition of the fuel in the combustion chambers by the starting igniters the flame should spread into the other combustion chambers of the engine.

In an engine with individual combustion chambers or with individual flame tubes housed in a common shell the flame spreads through the connective branch pipes between the combustion chambers.

The combustion of fuel in the combustion chambers with starter igniters makes the pressure in these chambers higher compared to adjacent chambers, where the fuel has not yet started to burn. Under the influence of the developing pressure drop between the chambers the gases begin to escape along with the flame from the chambers with higher pressure into the chambers with lower pressure through the connective branch pipe. For this reason the fuel-air mixture is ignited in the chambers where the combustion process has not yet started. The connective branch pipes between the combustion chambers are arranged so as to ensure the most favorable character of flow of the gases with the flame.

The possibility of igniting the fuel-air mixture in the combustion chambers depends both on the mixture parameters in them and especially on the ignition capacity of the flames discharged from the connective branch pipes. The igniting capacity of the flame is governed by its temperature, kinetic energy and geometric dimensions.

The flame temperature depends on mixture composition, fuel combustion completeness, relative location of the transition branch pipe and flame front in the flame tube. Well atomized fuel and good mixing, improving combustion completeness, elevate the temperature of the flame escaping from the branch pipes.

The kinetic energy of the igniting flame depends entirely on the pressure drop between the combustion chambers; the greater and more completely the fuel is burned in the combustion chamber, the greater the kinetic energy will be.

The geometric dimensions of the igniting flame with constant pressure drop between the chambers depend on the passage cross section of the connective branch pipes. The larger this passage cross section, naturally, the greater will be the dimensions of the igniting flame emerging from the connective branch pipes.

As flight altitude increases, the conditions of flame propagation through the combustion chambers worsens. This is explained by the smaller pressure drop between the combustion chambers and consequently by a reduction of the igniting capacity of the flames flowing from the connective branch pipes. Furthermore, due to displacement of the combustion zone toward the rear of the combustion chamber and separation of this zone from the connective branch pipes as flight altitude increases, the temperature of the igniting flames drops. Therefore, by measure of increasing flight altitude the flame can spread through the combustion chambers only at lower fuel-air mixture velocities.

As seen in Figure 126, as flight altitude increases, the flow velocity in the combustion chambers at constant air speed increases. Therefore the flame can spread through the combustion chambers at a given flight speed only up to a certain altitude. At higher altitudes under given conditions it becomes impossible to start the engine (see Figure 126,

zone A). With a flame of higher igniting capacity (increased, for instance, by making the cross section of the connective branch pipes larger), naturally, spreading of the flame becomes possible at higher altitudes (see Figure 126, zone B).

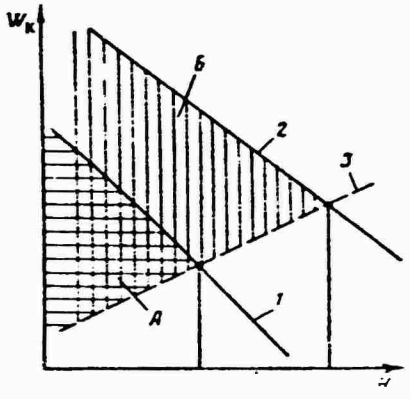

Figure 126. Air velocity behind compressor at which flame can spread through combustion chambers during in-flight starting of engine as function of flight altitude: 1 -- maximum velocity at combustion chamber intake, at which the flame can spread through the connective branch pipes of normal cross section; 2 -- likewise through branch pipes of enlarged cross section; 3 -- velocity at combustion chamber intake corresponding to minimum flight speed; A -- region of stable spreading of flame through branch pipes of normal cross section; B -- likewise through branch pipes of enlarged cross section.

As flight increases, the possibility of the flame spreading through the chambers lessens. Only vaporized fuel, as we know, enters into the combustion process. Evaporation of fuel droplets requires some time, depending on the dimensions of the droplets and their relative velocity. Therefore when the combustion chambers operate in a high-speed regime the boundary at which the time of residence of most of the fuel droplets in the circulation zone becomes equal to the time required for their evaporation is inevitably reached. Consequently at some flight speed the limiting conditions under which the flame can spread through the combustion chambers are reached at each altitude.

§42. Features of Engine Rotor Acceleration to Idling Rpm

After ignition of the fuel-air mixture in the combustion chambers the engine rotor should be accelerated to the idling rpm. This acceleration begins, however, only if the engine turbine develops more power than required for turning the compressor.

We will examine the conditions required for accelerating the rotor with the engine turbine. At the first instant of in-flight engine starting (i.e., after ignition of the fuel-air mixture in the combustion chambers), the engine changes at the same rpm from the autorotation regime to that characteristic of the gas turbine engine. Knowing the character of change of engine rotor rpm in the autorotation mode with altitude and speed, and also the characteristics of change of all engine parameters by rpm in the steady state modes of operation on the earth, we can determine these

parameters at steady state rpm in flight, equal to the rpm in the autorotation regime, using the similarity equations. Certain engine parameters that ensure stable operation at the rpm equal to rotor speed in the autorotation regime are presented in Figures 127 and 128. With the parameters indicated in Figures 127 and 128, naturally, the engine rotor will not be accelerated.

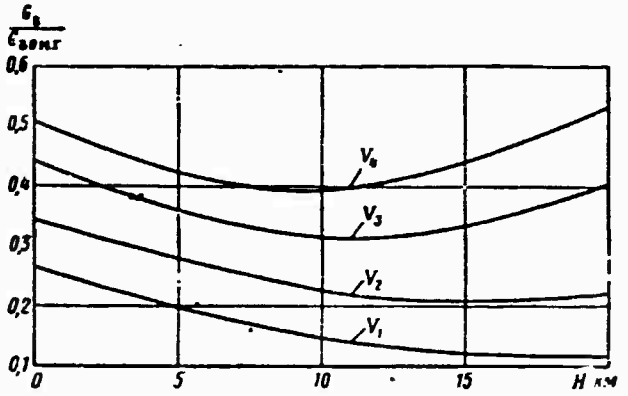

Figure 127. Change of actual air flow rate through engine at which stable engine operation is ensured after ignition of fuel mixture at rpm equal to the rpm in the autorotation mode, as function of flight altitude: $V_1 < V_2 < V_3 < V_4$.

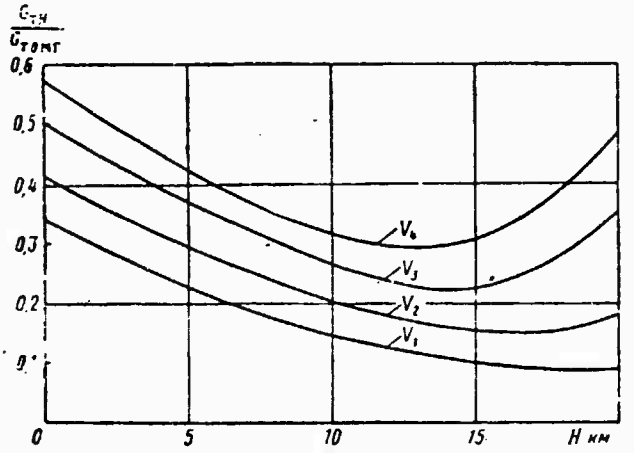

Figure 128. Change of actual fuel flow rate through engine during stable engine operation after ignition of fuel mixture at rpm equal to the rpm in the autorotation mode, as function of flight altitude: $V_1 < V_2 < V_3 < V_4$.

Ignition of the fuel-air mixture in the combustion chambers, as we see, leads to instantaneous change of air parameters through the engine duct. The air flow rate through the engine in the steady state engine operating modes at rpm equal to that in the autorotation regime is usually less than the air flow rate in the autorotation regime. Only at very high altitudes (H > 17 km in Figure 127) and high flight speeds does the air flow rate through the engine after ignition of the fuel mixture in the combustion chambers during in-flight engine starting exceed the air flow rate in the autorotation regime. The fuel flow rate required for stable engine operation at rpm equal to the autorotation rpm is substantially less than the fuel feed to the engine provided by the fuel system during autorotation.

Turbine gas temperatures required for stable engine operation at rpm equivalent to the autorotation regime are plotted in Figure 129 against altitude. At altitudes above 3,000 meters these temperatures must fall between 650-400°C. To ensure engine acceleration during in-flight starting by surplus gas turbine power, the heating of the air in the combustion chambers, naturally, should be such that the gas temperature behind the turbine will be higher than the temperatures given in Figure 129 for the corresponding flight altitudes and speeds. This is the fundamental condition ensuring engine rotor acceleration after ignition of the fuel-air mixture in the combustion chambers.

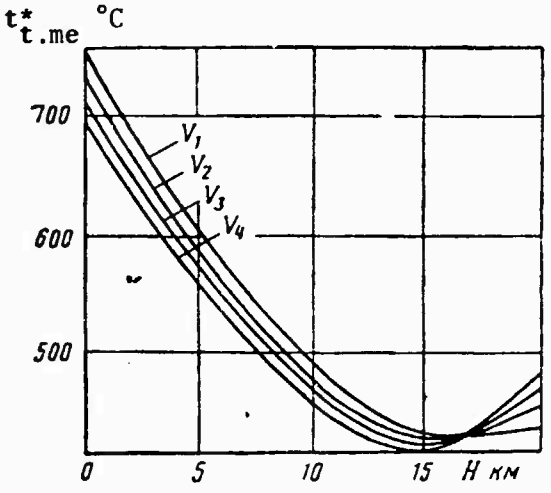

Figure 129. Character of change of turbine gas temperature at which engine operates stably after ignition of fuel mixture at rpm equivalent to autorotation: $V_1 < V_2 < V_3 < V_4$.

If the turbine gas temperature is equal to or less than the temperatures indicated in Figure 129, then the engine rotor will not accelerate and the so-called "cold hovering" of the engine rotor will occur (i.e., the rpm will not increase at low turbine gas temperatures). An additional condition for

acceleration of certain types of engines is heating of the air in the combustion chamber so that the compressor of the engine will not fall into the unstable zone. In this case engine rotor rpm also does not increase, but the turbine gas temperature rises rapidly (the so-called "hot hovering" of engine rotor rpm occurs).

As soon as the engine rotor begins to accelerate from the rpm equivalent to autorotation the in-flight starting reliability of a gas turbine engine is determined in the final analysis by the character of acceleration of the rotor to the idling rpm. This process should not last too long, and the gas temperature should not exceed the tolerable levels.

The character of engine rotor acceleration during in-flight start-up depends basically on gas turbine efficiency in the starting regimes and this depends, in turn, on the air compression ratio in the compressor, air flow rate and heating of the air in the combustion chambers. The air compression ratio in the compressor of an operating engine and the air flow rate in the starting regime are determined by the amount of heating of the air in the combustion chambers. Therefore engine rotor acceleration to idling rpm in flight also depends chiefly on the turbine gas temperature.

The excess air coefficient in the fuel-air mixture and fuel combustion completeness in the combustion chambers have an influence on the turbine gas temperature during in-flight start-up. From the standpoint of ensuring minimum rotor cranking time to idling rpm the excess air coefficient in the fuel-air mixture in the starting regime depends on the amount of fuel injected into the combustion chambers by the fuel system.

The character of change of engine rotor rpm with altitude is shown in Figure 130. As engine rotor rpm increases beyond the boundaries indicated in Figure 130 for the corresponding altitudes and speeds, the engine fuel feed will be constant, equal to the fuel flow rate during idling on the ground.

As seen in Figure 130 the starter fuel system limits fuel feed to the combustion chambers during in-flight starting only during the initial starting phase. This limitation is in force in approximately an rpm range at least 1/5 of the total range of engine rotor acceleration during in-flight starting.

Such automatic starter fuel system operation naturally leads to over-enrichment of the air-fuel mixture in the combustion chambers, particularly during starts at high flight altitudes. The combustion chambers at certain reduced air pressures cannot provide high-temperature gases in front of the turbine because of the low fuel combustion completeness. Here the maximum possible gas temperature in front of the turbine is substantially reduced, and the range of stable combustion with respect to the excess air coefficient is extremely limited.

Reduction of fuel-air mixture combustion efficiency with a reduction

of pressure can be attributed to poorer mixing, poor combustion or to both simultaneously.

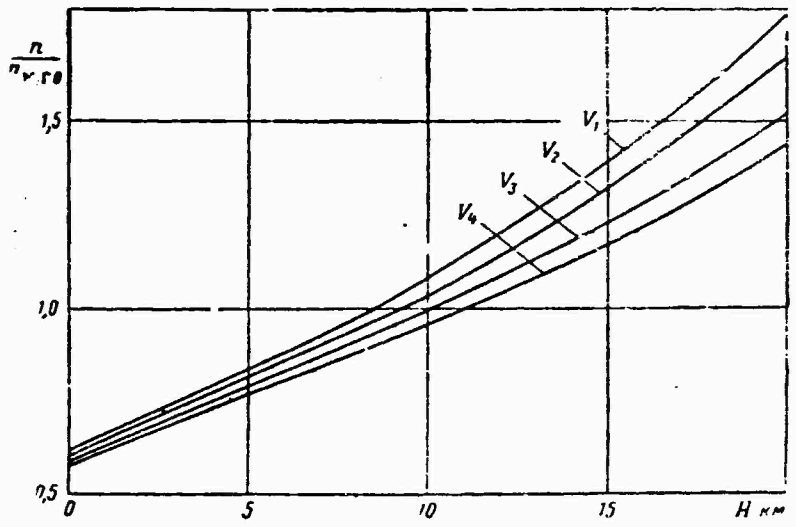

Figure 130. Engine rotor rpm at which starter fuel system shuts down as function of flight altitude: $V_1 < V_2 < V_3 < V_4$.

Over-enrichment of the fuel-air mixture in the combustion chambers after shutdown of the automatic starter fuel system can lead to "hot hovering" of engine rotor rpm during in-flight starting. This hovering occurs either as a result of unstable compressor operation or as a result of reduction of the gas temperature in front of the turbine. The latter occurs with extreme over-enrichment of the fuel-air mixture. In the given case, despite the low gas temperature ahead of the turbine, the gas temperature behind the turbine may become quite high due to afterburning of the fuel.

In cases of "hot hovering" of rpm during engine start-up the rotor can be accelerated by regulating the amount of fuel fed to the combustion chambers, by moving the engine control lever or by means of a special automatic system (Figure 131). Due to expansion of the aneroid of this apparatus during ascent the amount of fuel diverted to the drain is increased, and accordingly the amount of fuel reaching the engine injectors decreases.

The conditions of transition of the engine to idling rpm during in-flight starting change principally as a function of flight altitude, since here the rpm range between autorotation and idling is greatly expanded. Due to the expansion of the rpm range during acceleration, worsening of combustion chamber operation and reduction of surplus turbine power in the starting regime the starting process worsens with increasing flight altitude.

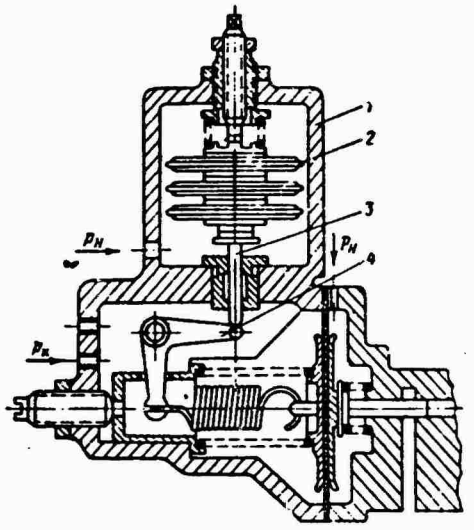

Figure 131. Automatic starter fuel regulator with altitude adjustment: 1 -- body of altitude adjuster; 2 -- membrane; 3 -- plunger; 4 -- two-arm lever.

The time of transition of the engine to idling rpm increases with increasing flight altitude. This is illustrated in Figure 132. Engine acceleration occurs, as a rule, with high gas temperature behind the turbine.

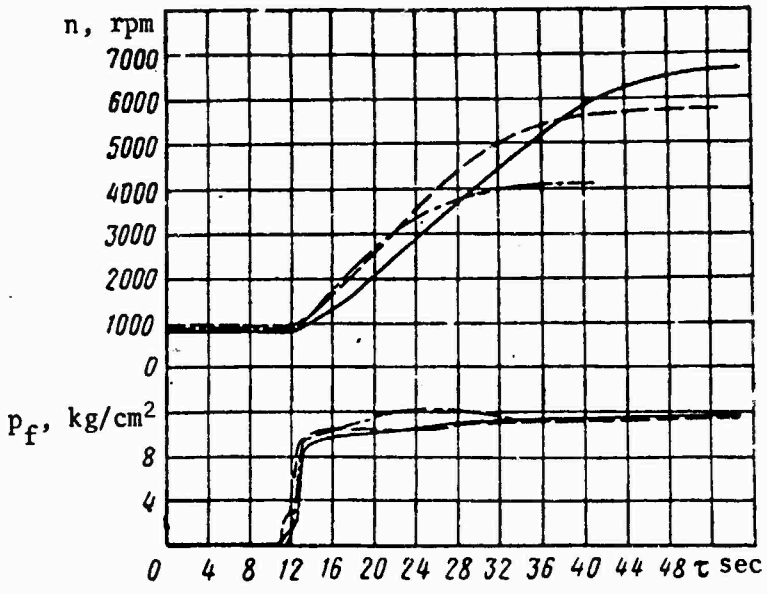

Figure 132. Change of rotor rpm and fuel pressure in front of working injectors with time during starting of VK-1A engine at different altitudes (continuous curve represents character of change of parameters at 10,000 m, broken curve -- at 8,000 m and dot-dash curve -- at 4,000 m).

During acceleration of the engine at high altitudes there may also be a step-by-step increase of rpm. In these cases transition of the engine to idling rpm is prolonged, overheating of the turbine and exhaust system is possible due to afterburning of the fuel.

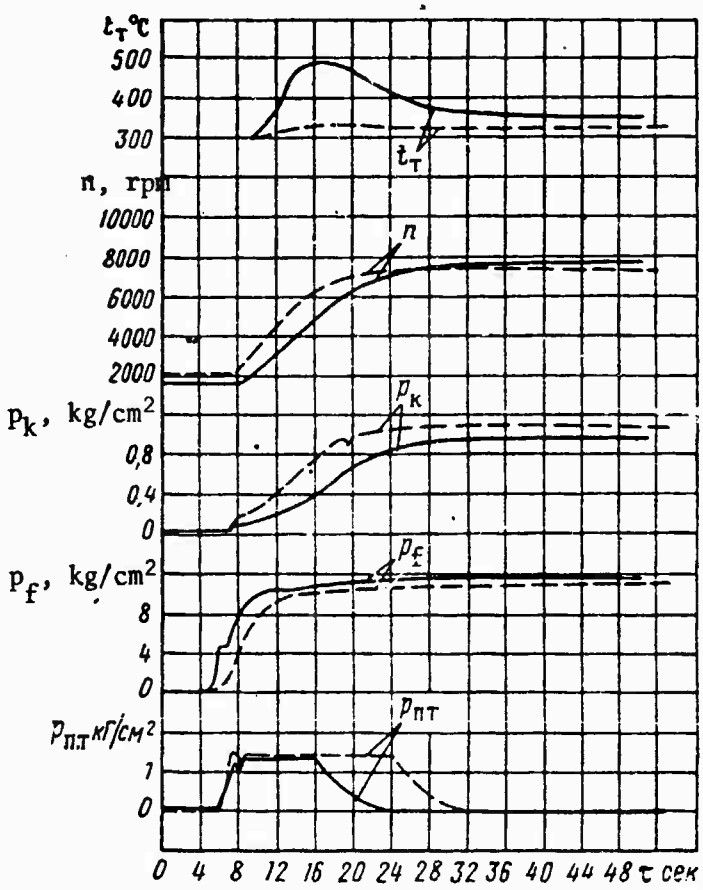

Figure 133. Change of parameters of VK-1A engine during starting process (continuous curves indicate changes of parameters at H = 6,000 m and V_{re} = 320 km/hr, and the broken curves -- H = 6,000 m and V_{re} = 420 km/hr).

As flight speed changes (up to speeds at which both the starting and main fuel ignite and burn) the autorotation rpm at which starting is initiated changes and so does surplus turbine power during the starting process. For this reason engine starting quality improves, i.e., the time required for reaching the idling regime and the gas temperature behind the turbine during starting decrease (Figure 133) as flight speed is increased at all altitudes. Therefore, for purposes of faster engine rotor acceleration to the idling rpm the engine should be started at the highest possible flight speeds. This speed is limited only by the possibility of ignition and combustion of the starter and main fuels.

As flight altitude increases, the conditions of transition of the engine to the idling regime worsen, since here surplus turbine power decreases and the rpm required for turning the rotor during starting increases.

CHAPTER 18. RELIABILITY LIMITS OF IN-FLIGHT STARTING

§43. Starting Limit Determined by Fuel Ignition Reliability and Compressor Stability

It is clear from what we have examined above that flight speed and altitude have a substantial influence on in-flight engine starting reliability and govern the possibility of starting at certain values.

Change of flight speed and altitude influences the formation of the initial flame center, ignition and stable combustion of the main fuel, spreading of the flame through the combustion chambers and also acceleration of the engine to idling rpm.

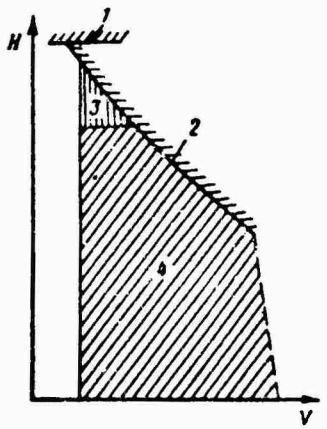

Figure 134. Typical boundary of in-flight starting of turbojet engine: 1 -- boundary of starter fuel ignition; 2 -- boundary of main fuel ignition; 3 -- region of altitudes and speeds where transition of the engine to idling rpm is difficult; 4 -- region of altitudes and speeds of reliable starting.

The reliability boundary of in-flight starting in terms of flight altitude and speed is determined experimentally for each engine.

The starting limit with decreasing flight speed is determined, on the one hand, by the tolerable minimum flight speed of the aircraft and, on the other hand, by the possibility of accelerating the engine from low autorotation rpm (Figure 134). At high flight altitudes the transition of the engine to the low rpm regime is possible only beginning at a certain autorotation rpm. At lower autorotation rpm, the engine rpm does not increase, even though the main fuel ignites -- the engine hovers at a certain rpm.

The starting boundary with increasing flight speed is determined by the possibility of formation of the initial flame center,

ignition and stable combustion of the fuel mixture in the combustion chambers. Since the actual flight speed of an aircraft increases with increasing altitude at the same air speed (consequently the velocity of the air in the combustion chambers increases), the range of air speeds at which in-flight engine starting is possible decreases with altitude. Finally at some altitude it is possible to start the engine only at the minimum tolerable air speed or at the speed at which normal engine acceleration is possible. This speed is the starting reliability limit of the engine.

§44. Influence of Ambient Air Temperature and Fuel Grade on Starting Limit

The following factors in addition to flight speed and altitude influence the starting reliability limit of an engine: a) ambient air temperature at altitude of start; b) individual features of each engine; c) features of joint operation of combustion chamber and starter igniter; d) operating features of starter automatic fuel regulator.

As seen in Figure 135 the effect of the ambient air temperature on the in-flight starting reliability limit increases as flight speed increases (an consequently as the air velocity increases in the combustion chamber intake) at the moment of start-up. With an accuracy sufficient for practical purposes the dependence of the altitudes of reliable in-flight starting on ambient air temperature t_a^* at starting altitude can be approximated by the equation

$$\overline{H} = \sqrt[5]{\frac{t_a^*}{51{,}2} + 1}.$$

The effect of inversion of the ambient air temperature on the altitude of reliable starting can be evaluated by means of the dependence obtained. Thus, an 18°C drop in the ambient air temperature at the start-up altitude compared to standard temperature can lower the altitude of reliable starting approximately 1-1.5 km (Figure 136).

§45. Determination of Reliable Starting Boundaries

The boundaries of reliable starting of five engines are show in Figure 137 by way of example, and the possible scattering of reliable starting altitude, corresponding to a certain set of engines of a given type is illustrated in Figure 138. As seen, for each specific engine of a given make starter igniter efficiency, fuel-air mixture composition and air flow parameters in the main combustion chambers in the autorotation regime differ. All this has an effect on the starting reliability boundary of each engine. The width of the zone of reliable starting of a certain set of engines is influenced by the number of igniters, air velocity in the combustion chamber in the autorotation regime, etc. The width of the reliable starting zone of certain engines with respect to altitude may reach approximately 15% of the reliable starting altitude.

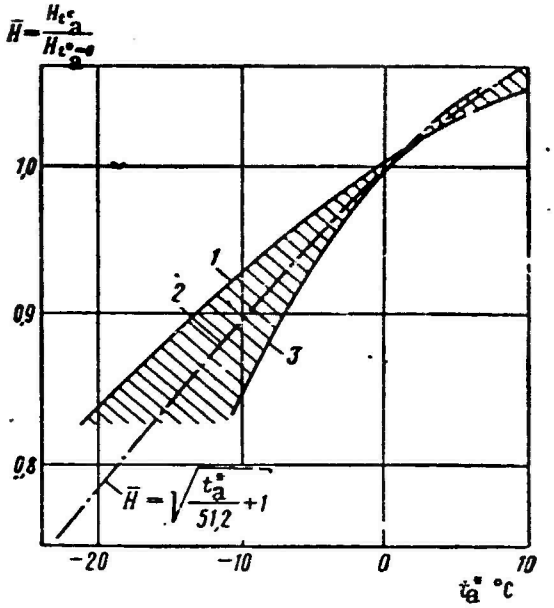

Figure 135. Effect of air temperature in front of engine compressor on in-flight starting boundary: 1 -- $n_{re.au}$ = 1,000 rpm; 2 -- $n_{re.au}$ = 1,500 rpm; 3 -- $n_{re.au}$ = 2,000 rpm.

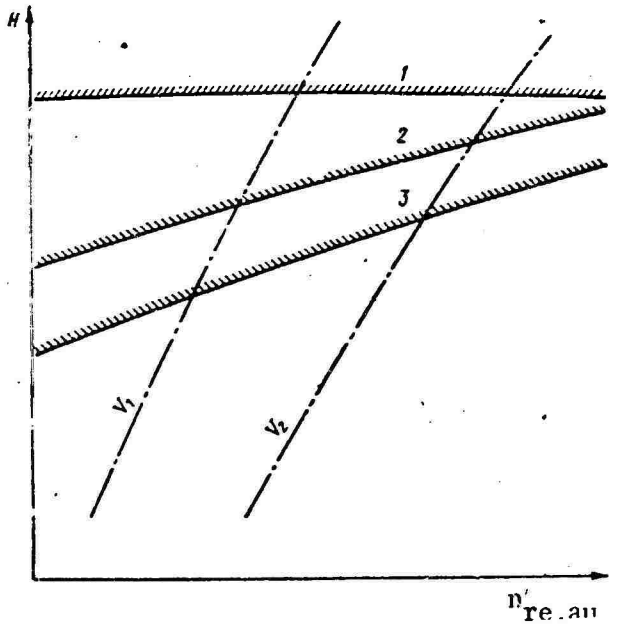

Figure 136. Boundaries of high-altitude starting at different ambient air temperatures ($V_1 < V_2$): 1 -- $t_a^* = 12°C$; 2 -- $t_a^* = f(H; M)$ at t_H according to MSA; 3 -- $t_a^* = f(H; M)$ at t_H according to MSA with inversion (-18°C).

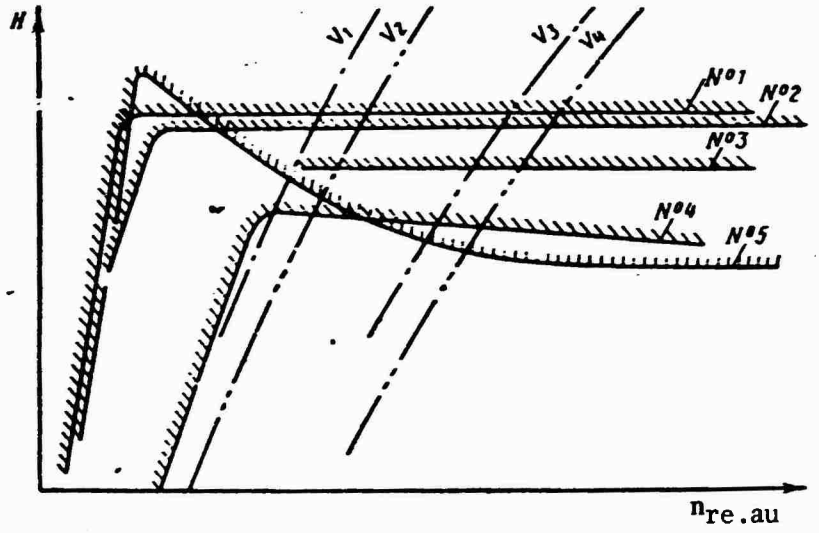

Figure 137. Starting boundaries of different engines of the same make: $V_1 < V_2 < V_3 < V_4$.

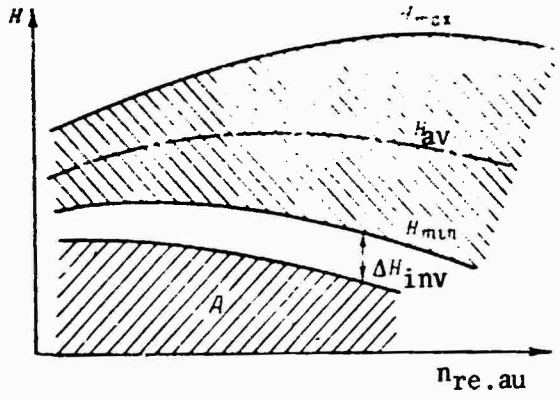

Figure 138. Limits of high-altitude starting for a series of engines: A -- region of reliable starting with confidence level $\gamma = 0.99$.

Depending on the matching of combustion chamber and starter igniter characteristics, starting characteristics may differ (Figure 139). Considering that in many cases it is quite sufficient to ensure starting in some specific region of flight regimes, it can be seen that there is a certain optimal form of starting characteristics. In particular, characteristics of the form $p_k/\lambda_k = \text{const}$ are clearly not optimal, since the minimum starting altitude is obtained in the range of working air speeds, and at low Mach numbers, where starting altitude is highest, it may not be achieved due to deficient compressor stability reserves, etc. Furthermore, if a certain type of starting characteristic is achieved, then the scattering

of the boundaries may be insignificant in some region of flight regimes most suitable for engine starting.

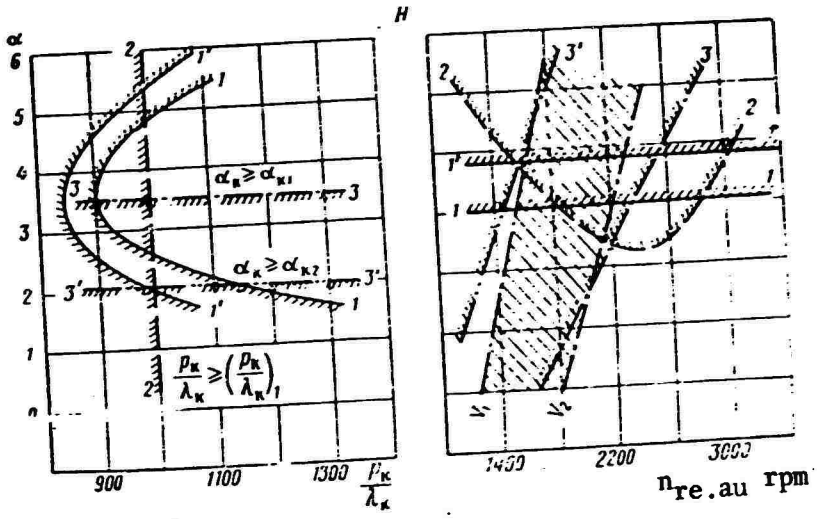

Figure 139. Relation between starting characteristics of igniter and high-altitude starting limit (flow velocity $V_1 < V_2$).

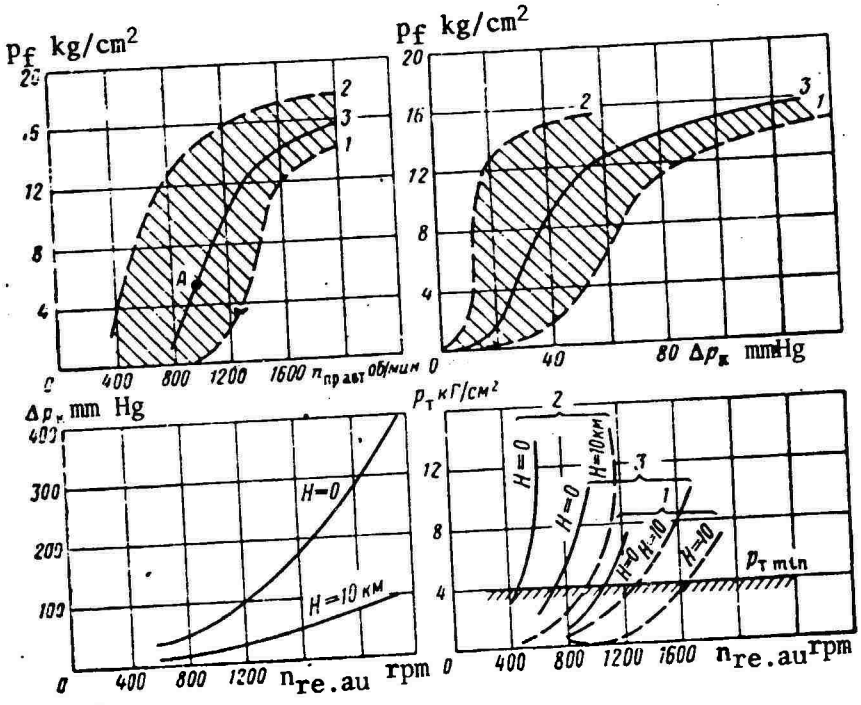

Figure 140. Starter fuel regulator characteristics.

Depending on the automatic starter fuel regulator adjustment, producing a certain relationship between the fuel pressure in front of the working injectors (fuel flow rate through combustion chambers) and pressure drop on the SFR diaphragm during in-flight starting, the result (Figure 140) may be maximum lean 1 and maximum rich 2 characteristics of fuel feed to the combustion chamber during the starting process. Considering that the best conditions for ignition of the fuel-air mixture at a certain flight altitude are created at a certain fuel pressure (flow rate) the high-altitude starting boundary can be determined by means of the graphs presented in Figure 141 for a certain fuel pressure in front of the working injectors.

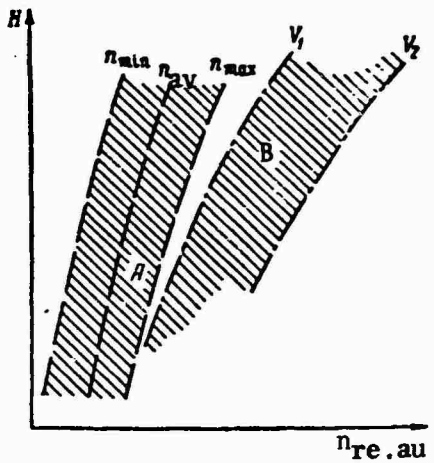

Figure 141. Determination of reliable in-flight starting boundaries: A -- region of lowest autorotation rpm at which ignition of the main fuel is possible; B -- region in which the engine must be started ($V_1 < V_2$).

The starting boundary with lean adjustment of the SFR is most hazardous, since it usually occurs along with the region of flight regimes in which in-flight engine starting is recommended. The stated boundary for rich regulation of the SFR in the region of the stated flight regimes is not reached, since the compressor stability limit is reached first with the regulation system used for the given engine.

The use of measures to intensify the ignition and combustion of fuel-air mixtures in the starter igniters ensures their reliable operation in the entire range of altitudes and flight speeds recommended for engine starting. In this case starting reliability depends only on compressor and combustion chamber stability.

The following sequence is recommended for starting the engine:

1) the flight altitude and speed required for reliable starting are selected;

2) the fuel pump and the system that forms the initial flame center are turned on,

3) the engine control lever is moved to the "Idle" position.

The engine should independently reach the idling rpm. In some cases it is necessary to organize fuel feed to the combustion chambers by means of the engine control lever only at altitudes close to maximum. In the event of an unsuccessful start another attempt is made to start the engine after the corresponding blowing of the engine at lower altitude.

CHAPTER 19. IN-FLIGHT COUNTER-STARTING FEATURES OF ENGINE

In certain cases the engine can be started before it reaches the steady state autorotation regime, i.e., during running up from the rpm at which the engine flamed out to the beginning of the autorotation regime. Starting under such conditions is called counter-starting. Counter-starting has the following advantages over starting from steady autorotation rpm: the engine can be started almost immediately after flame-out, and in a wider range of flight altitudes and speeds; it is easier to organize the combustion of fuel in the combustion chamber; the problem of fuel delivery is simplified.

The character of change of pressure behind the compressor and air flow rate through the engine as the engine runs down is very important in terms of the possibility of counter-starting. The ignition and stable combustion of the fuel in the combustion chambers depend on these parameters.

At the moment of fuel feed shut-off the air pressure behind the compressor drops sharply due to the disappearance of the heat head behind it, formed by the combustion of fuel in the combustion chambers. The reduction of the air pressure behind the compressor is approximately equal to the square root of the ratio of the temperatures at the end of the combustion chambers during combustion and without combustion.

Eventually the air pressure behind the compressor drops practically at constant air temperature at the end of the combustion chamber, and the degree of pressure decrease is determined by the character of change of rpm during run-down. The air pressure behind the compressor during run-down is less at the same rpm than during the combustion of fuel in the combustion chambers by a magnitude equal to the ratio of the temperatures in the combustion chambers with combustion and without combustion. Finally the air pressure behind the compressor drops to the values characteristic of steady state autorotation.

The air flow rate through the engine during run-down can be determined from the equation of the air flow rate through the first nozzle for conditions of run-down and fuel combustion in the combustion chambers:

air flow rate during combustion of fuel will be

$$G_g = m_g F_{c.a} \frac{p_g^*}{\sqrt{T_g^*}} q(\lambda_{c.a});$$

air flow rate in run-down regime will be

$$G_a' = m_g' F_{c.a}' \frac{p_g^{*\prime}}{\sqrt{T_g^{*\prime}}} q(\lambda_{c.a}').$$

From the ratio of these air flow rates we obtain

$$\frac{G_a}{G_a'} = \frac{m_g F_{c.a} p_g^* q(\lambda_{c.a})}{m_g' F_{c.a}' p_g' q(\lambda_{c.a}')} \sqrt{\frac{T_g^{*\prime}}{T_g^*}}.$$

Considering $q(\lambda_{c.a}) = q(\lambda'_{c.a})$ and $T_g^* = \tau_k \tau_{k.c} T_{in}^*$, we obtain

$$\left(\frac{G_a}{G_a'}\right)^2 = \frac{\tau_k' \tau_{k.c}'}{\tau_k \tau_{k.c}} \left(\frac{m_g}{m_g'}\right)^2.$$

When $\eta_k = \eta_k'$ the air flow rate will be $G_a' = G_a \sqrt{\tau_{k.c}} \frac{m_g'}{m_g}$.

At constant rotor rpm the pressure ratio in the combustion chambers with combustion and without combustion can be found from the equation

$$\frac{p_k'}{p_k^{*\prime}} = \sqrt{\tau_{k.c}}.$$

The ratio of air velocities behind the compressor in the above-examined regimes will be

$$\frac{W_k'}{W_k} = \frac{G_a'}{G_a} \frac{p_k}{p_k'} \frac{T_k'}{T_k}.$$

To determine the current air parameters behind the compressor during run-down it is necessary to find the dependence of these values on time. For this purpose it is necessary to know the function n = f(t).

From the expression for the power balance during run-down we obtain

$$\frac{dn}{dt} = \frac{900}{\pi^2 J_0 n'} \frac{G_a' T_{in}^*}{A} \left[\tau_k' \left(1 - \frac{1}{\tau_\tau'}\right) \eta_M' - (\tau_k' - 1)\right] c_{pa}'.$$

For determination of dn/dt during run-down it is necessary to know τ_t' and η_m'.

We will assume that at identical compression ratios and constant Mach number the heat drop on the turbine and the mechanical efficiency during run-down with combustion in the combustion chambers remain constant. This will enable us with consideration of the existing relations of compressor and turbine parameters with fuel combustion in the combustion chambers to obtain the following equations:

with air bypass strip from the compressor closed

$$\left(\frac{dn}{dt}\right)_{re} = \frac{900T_{in}^{*}}{\pi^2 J_0 A} \frac{G_{a.re}'}{n_{re}'}\left[(\tau_k - 1)\left(\frac{G_a}{G_a'}\right)^2 - (\tau_k' - 1)\right] c_{pa};$$

with air bypass strip from the compressor open

$$\left(\frac{dn}{dt}\right)_{re} = \frac{900T_{in}^{*}}{\pi^2 J_0 A} \frac{G_{a.re}'}{n_{re}'}\left\{\left[(\tau_k' - 1) + \frac{1+g_a}{g_a}(\tau_{by} - 1)\right]\left(\frac{G_a}{G_a'}\right)^2 - \right.$$
$$\left. - (\tau_k' - 1) + \frac{1-g_a'}{g_a'}(\tau_{by}' - 1)\right\} c_{pa}'$$

where g_a is the ratio of the air flow rate at compressor exhaust to the air flow rate at compressor intake;

τ_{by} is the ratio of the temperature of the air at the outlet from the bypass ports to the temperature of the air at compressor intake.

The operating conditions of the starter igniter during counter-starting differ substantially from those during starting from steady-state autorotation rpm. From the equation of the air flow rate through the compressor we have

$$G_a' = G_{a.au}\left(\frac{p_k' W_k'}{T_k'}\right)\left(\frac{T_k}{p_k W_k}\right)_{au}.$$

Under identical conditions $p_k' : p_{k.au}$ = 2.5-3 and $W_k' : W_{k.au}$ = 1.5-2.0. Hence it follows that the air flow rate through the starter igniter during counter-starting is 4-6 times greater than in the steady-state autorotation regime. In this connection normal operation of the starter igniters during counter-starting requires that more fuel be fed into them.

To achieve counter-starting a special ignition system is required. During starting from steady-state autorotation regimes all components of the spark plug and wiring are under identical pressures and air densities. Under these conditions the required discharge voltages are usually 2.0-2.5 times less than the breakthrough voltages. In counter-starting the spark

gap is under higher pressure and air density compared to the shielding of the spark plug and wires. Therefore under certain flight conditions the required discharge voltages exceed the breakthrough voltage on the shield, which greatly limits the possibility of using spark discharge systems. Low-voltage ignition systems satisfy the requirements of counter-starting.

CHAPTER 20. STARTING FEATURES OF TURBOPROP ENGINES

The in-flight starting of turboprop engines differs from the in-flight starting of turbojet engines because of the presence of propellers, which under the influence of the oncoming flow can create additional rotor acceleration. By changing the pitch of the propeller blades it is possible at any altitude and speed to make the engine autorotate in a wide range: from zero to maximum. The engine parameters also change in a wide range, and this is reflected in the reliability of ignition and combustion of the starter and main fuels, and also in the operation of the gas turbines during the starting process.

Depending on the pitch of the propeller blades the following cases of combined propeller and engine operation are possible in the autorotation regime:

1. Surplus power on the engine shaft and propeller power are equal to zero (the propellers are partially defeathered). This case is possible at a given altitude and speed only at one propeller blade pitch and is analogous to autorotation of the rotor of a turbojet engine.

2. If the pitch of the propeller blades is less than in the former case, then the autorotation rpm of the engine rotor will increase, since it will also be accelerated by the surplus power of the propellers, produced by their interaction with the dynamic energy of the air stream.

3. If the propeller blades are feathered or are nearly feathered, then the engine will create surplus power on the shaft due to the action of the dynamic energy of the air stream within it, which is absorbed by the propellers.

The ability to change substantially engine rotor rpm by changing the pitch of the propeller blades can be used in the very process of engine starting. Here, depending on the phase of the starting process, the excess power from the propellers is used, and different variations of bringing a turboprop engine up to the low rpm mode in flight are possible. The feed of starter and main fuels for engine starting can be initiated at different times during the starting process:

1. At the initial moment of defeathering of the props. In this case the most unfavorable conditions for the ignition and combustion of the fuel are created, especially at high altitudes.

2. As soon as the engine reaches the idling rpm only by defeathering the propellers. In this way the air pressure at combustion chamber intake is more favorable for the ignition and combustion of the fuels. Due to the high velocities at the combustion chamber intake, however, flame breakaway is possible.

3. As soon as the engine rotor rpm (with the propellers defeathered) reaches the value at which the air flow parameters at the combustion chamber intake ensure reliable ignition and combustion of the starter and main fuels.

In-flight starting of a turboprop engine begins with defeathering of the propeller blades, which must be done after engine shutdown to reduce drag. By virtue of this the engine makes a transition to intermediate rpm, at which the starter and main fuels can ignite and burn. As the starting process proceeds, the rotor is turned by the combined action of the moments from the propeller and the engine turbine.

The propellers create a large torque, greatly exceeding the moment imparted to the rotor of a turbojet engine during start-up. Therefore the time required for transition of a turboprop engine to the in-flight idling regime is much shorter than required for a turbojet engine. The approximate change of engine rotor rpm and torques imparted to it from the propeller and turbine during in-flight starting of turbojet and turboprop engines is depicted in Figure 142. The torques from the propeller increase as the rate of defeathering of the propellers is increased. Therefore, during in-flight starting of a turboprop engine with rapid defeathering of the propellers large negative propeller thrusts may develop, capable of causing sudden deceleration of the aircraft.

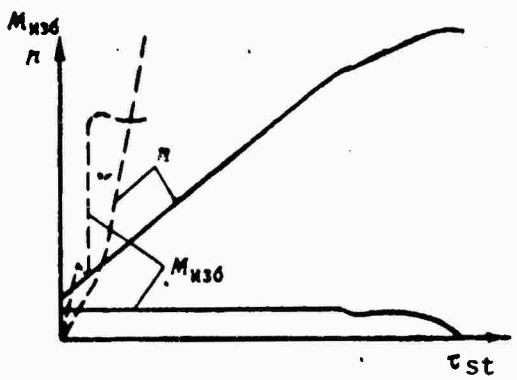

Figure 142. Change of rotor rpm and surplus torque during in-flight starting of turbojet (continuous curves) and turboprop (broken curves) engines.

The in-flight starting process of a turboprop engine can be described as follows.

After establishing the required flight speed (essentially close to the minimum speed) and turning on the "In-flight starter" button or tumbler, partial defeathering of the propellers is done in short pulses to the rpm at which the fuel-air mixture ignites in the combustion chambers. Ignition of the mixture is controlled according to the rise of the gas temperature behind the turbine. Then the "In-flight starter" button or tumbler is turned off and further acceleration of the engine rotor to the idling rpm is provided by additional defeathering of the propellers.

Additional defeathering is particularly essential in those cases when the gas temperature behind the turbine increases sharply after ignition of the fuel-air mixture in the combustion chamber and the rate of engine rotor rotation increases only slightly.

Thus the following basic phases of in-flight starting of turboprop engines are:

1) preliminary changing of propellers from feathered position (this ensures formation of the flames of the starter igniters);

2) termination of change of propellers from feathered position and ignition of fuel-air mixture in combustion chamber;

3) further acceleration of engine rotor to idling rpm.

By way of example we will examine the in-flight starting of the AI-20 engine.

After in-flight engine shutdown the propeller is feathered and the stopcock is placed in the "Closed" position. After the operating cycle of the automatic feathering system is complete the "In-flight starting" switch is turned on. After heating of the spark plugs (8-10 sec) the propeller is defeathered so that rotor rpm reaches 15-17% (according to the instrument readings). At this rpm the most favorable conditions are created for the ignition of the fuel-air mixture in the combustion chambers.

After ignition of the mixture defeathering of the propeller is continued, increasing the rpm to 20-25%. Eventually the engine will continue the starting process automatically.

After the engine reaches working rpm the "In-flight start" button is turned off and the control lever is placed in the position required for continuation of flight. If at 15-17% rpm the fuel does not ignite, the stopcock is placed in the "Closed" position and the propeller is feathered after 3-4 sec. In cases when ignition of the fuel cannot be achieved at rpm exceeding 15-17% the propeller is returned to the feathered position (the stopcock remains closed) and engine starting is repeated after 1-1.5 min.

BIBLIOGRAPHY

1. Abiants, V. Kh., *Aviatsionnyye Gazovyye Turbiny* (Aviation Gas Turbines), Oborongiz [State Scientific and Technical Publishing House of Literature on Defense], 1958.

2. Abramovich, G. N., *Prikladnaya Gazovaya Dinamika* (Applied Gas Dynamics), Oborongiz, 1951.

3. Zhiritskiy, G. S., et al, *Gazovyye Turbiny Aviatsionnykh Dvigateley* (Gas Turbines of Aviation Engines), Oborongiz, 1963.

4. Kirillov, I. I., *Gazovyye Turbiny i Gazoturbinnyye Ustanovki* (Gas Turbines and Gas Turbine Power Plants), Mashgiz [State Scientific and Technical Publishing House of Literature on Machinery Manufacture], 1956.

5. Klochkov, S. A., "On the Calculation of the Starting Regimes of the Turbocompressor Unit of a Gas Turbine Power Plant," *Sudostroyeniye* (Ship Building), No. 12, 1956.

6. Kotlyar, I. V., *Peremennyy Reshim Raboty Gazoturbinnykh Ustanovok* (Variable Mode of Gas Turbine Power Plant Operation), Mashgiz, 1961.

7. Kulebakin, V. S. and V. D. Nagorskiy, *Elektroprivod Samoletnykh Agregatov i Mekhanizmov* (Electric Drive of Aviation Accessories and Mechanisms), Oborongiz, 1958.

8. Stechkin, B. S., P. K. Kazandzhan, L. P. Alekseyev, A. N. Govorov, Yu. N. Nechayev and R. M. Redorov, *Teoriya Reaktivnykh Dvigateley* (Theory of Jet Engines), Oborongiz, 1956-58.

9. Cherkez, A. Ya., *Primeneniye Metoda Malykh Otkloneniy v Teorii i Raschete Aviatsionnykh TRD* (Application of Small Deviations Method in Theory and Design of Aviation Turbojet Engines), Oborongiz, 1953.

10. Cherkasov, B. A., *Avtomatika i Regulirovaniye Vozdushno-Reaktivnykh Dvigateley* (Automation and Control of Jet Engines), Mashgiz, 1957.

11. Shtoda, A. V., S. P. Aleshchenko, A. D. Ivanov, V. S. Krasavtsev, F. N. Morozov, V. A. Sekistov and A. T. Shiukov, *Konstruktsiya Aviatsionnykh Gazoturbinnykh Dvigateley* (Design of Aviation Gas Turbine Engines), Voyenizdat [Military Publishing House of the Ministry of Defense, USSR], 1961.

12. *Reaktivnyye Dvigateli* (Jet Engines), edited by O. E. Lancaster, Voyenizdat, 1962.

13. Shevyakov, A. A., *Avtomatika Aviatsionnykh Silovykh Ustanovok* (Automation of Aviation Power Plants), Oborongiz, 1960.

14. Sherlygin, N. A., *Zapusk GTD* (Starting of Gas Turbine Engines) (textbook), VAU [Voyennoye aviatsionnoye uchilishche; Military Aviation School] GA [Gosudarstvennyy arkhiv; State archives], 1965.

15. Schmider, H. R. and J. H. Ferguson, "A Study of Self-Contained Starting Systems for Turbojet and Turboprop Engines," *SAE Preprint*, No. 48T, 1959.

16. Stein, P. G., "The Modern Gas Turbine Auxiliary Power Plant -- Characteristics and Applications," *SAE Preprint*, No. 535, 1959.

17. Woodall, R. H., "Some Trends in the Development of Aircraft Electrical and Starting Systems," *JRAeS*, Vol. 59, No. 537, 1955.

18. "Factors That Affect Operational Reliability of Turbojet Engines," *Technical Report R-54*, NASA, 1960.

19. Casamassa, Jack V. and Ralph D. Bent, *Jet Aircraft Power Systems*, 1966.